Pipeline & Hazardous Materials Safety Administration

Pipeline Inspection Technologies Demonstration Report

Pipeline Safety Research & Development Program

Final

EXECUTIVE SUMMARY

The pipeline infrastructure is a critical element in the energy delivery system across the United States. Its failure can affect both public health and safety directly and indirectly through impacts on the energy supply. The pipeline infrastructure is aging, while at the same time Research & Development (R&D) funding from the pipeline industry to develop technologies to assure its integrity is experiencing budgetary constraints. Total R&D funding is being further reduced through the elimination of programs resulting from restructuring within the government and energy industry.

The Pipeline & Hazardous Materials Safety Administration (PHMSA), Pipeline Safety R&D Program mission is to ensure the safe, reliable & environmentally sound operation of the nation's pipeline transportation system. With passage of the Pipeline Safety Improvement Act (PSIA) in 2002, industry is now required to invest significantly more capital to inspect and maintain their systems. The PSIA requires enhanced maintenance programs and continuing integrity inspection of all pipelines located within "high consequence areas" where a pipeline failure could threaten public safety, property and the environment. According to the Interstate Natural Gas Association of America (INGAA) the cost to industry to implement the PSIA in the first ten years will exceed $2 billion.

The focus of the PHMSA Pipeline Safety R&D Program is to sponsor research and development projects intended on providing near-term solutions that will improve the safety, reduce environmental impact, and enhance the reliability of the nation's pipeline transportation system. Conducting in-field technology demonstration test to facilitate technology transfer from government funded R&D programs strengthens communication and coordination with industry stakeholders

The keys to enhanced pipeline safety are understanding the risks, focusing on the problems, imagining solutions, and applying our ingenuity—

Ted Willke.

The PHMSA Pipeline Safety R&D Program role in technology development and innovation has increased with the passage of the Pipeline Safety Improvement Act of 2002[1]. The implementation of the Integrity Management Program for natural gas and hazardous liquids has focused efforts on proactively finding and fixing safety-related problems.

For several years the PHMSA Pipeline Safety R&D Program along with the DOE/NETL, Gas Delivery Reliability Program have funded the development of advanced in-line inspection (ILI) technologies to detect mechanical damage, corrosion and other threats to pipeline integrity. Several projects have matured to a stage where demonstrations of their detection capability are now warranted. During the week of January 9th, 2006, the PHMSA Pipeline Safety R&D Program and the DOE/NETL, Gas Delivery Reliability Program co-sponsored a demonstration of six innovative technologies.

[1] http://www.eia.doe.gov/oil_gas/natural_gas/analysis_publications/ngmajorleg/pubsafety.html

The demonstrations were conducted at Battelle West Jefferson's Pipeline Simulation Facility (PSF) near Columbus, Ohio. The pipes used in the demonstration were prepared by Battelle at the PSF and each was pre-calibrated to establish baseline defect measurements. Each technology performed a series of pipeline inspection runs to determine their capability to detect and size mechanical damage, corrosion, stress corrosion cracking or plastic pipe defects. Overall, each technology performed well in their assessment category.

BACKGROUND

Information regarding inspection technology advances needs to be disseminated and understood by many stakeholders in the pipeline industry. While research reports, review meetings and conference presentations are commonly used to disseminate information, live demonstrations can provide additional information on the current state and future potential of each development. Demonstrations are challenging to technology developers because newly developed technologies must be sufficiently reliable to obtain results in a fixed time frame. There is not the opportunity to return to the laboratory to confirm results or change parameters. While the pressure to demonstrate the best capability of their technology advances is enormous, the developers understand these events are needed to bolster support for continued development. The results of demonstrations can be difficult to directly compare since each implementation can be at a different stage of development. No direct comparisons were made in this report. At this demonstration, representatives from the pipeline industry, industry trade associations, and pipeline service providers were able to witness the performance of six new technologies and interact with technology developers to clarify the current and potential capability of these new developments. The participation of these groups was an essential element of the demonstration.

This is the second benchmark of emerging pipeline inspection technologies performed by Battelle for DOT PHMSA Pipeline Safety R&D Program and DOE NETL. Information on the pipe defect sets, pipe preparation, demonstration facility layout, and demonstration procedures from the first test can be can be found in the final report, *Benchmarking Emerging Pipeline Inspection Technologies*[2], prepared by Battelle. The results from the first benchmarking can be found in the *Pipeline Inspection Technologies - Demonstration Report*[3], prepared by NETL.

Purpose

This report provides a brief summary assessment of the demonstration benchmark results. The purpose of this assessment is to help identify promising inspection technologies best suited for further development as part of an integrated teaming effort between robotic platform and sensor developers. This report is not intended to provide a detailed analysis of each technology's performance or to rate their performance relative to one another.

[2] http://primis.rspa.dot.gov/matrix/FilGet.rdm?fil=718
[3] http://www.netl.doe.gov/technologies/oil-gas/publications/td/Battelle%20Inspection%20Demo%20Final%20Report_111804.pdf

The Technologies

Six innovative sensor technologies were demonstrated at Battelle's Pipeline Simulation Facility (PSF) the week of January 9, 2006. The different technologies demonstrated their ability to detect pipeline corrosion, mechanical defects, stress corrosion cracking, or plastic pipe defects. Additional information on each technology may be found in both Appendix B and Appendix C. The technologies were:

ORNL Shear Horizontal Electromagnetic Acoustic Transducer (EMAT) – Oak Ridge National Laboratory (ORNL) has developed an EMAT system that uses shear horizontal waves to detect flaws on natural gas pipelines. A wavelet-based analysis of ultrasonic sensor signals is used for detecting physical flaws (e.g., SCC, circumferential and axial flaws, and corrosion) in the walls of gas pipelines. Using an in-line non-contact EMAT transmitter-receiver pair, flaws can be detected on the walls of the pipe that the current magnetic flux leakage (MFL) technology has problems detecting. One EMAT is used as a transmitter, exciting an ultrasonic impulse into the pipe wall while the second EMAT located a few inches away from the first is used as a receiving transducer. ORNL's technology is depicted in Figure 1.

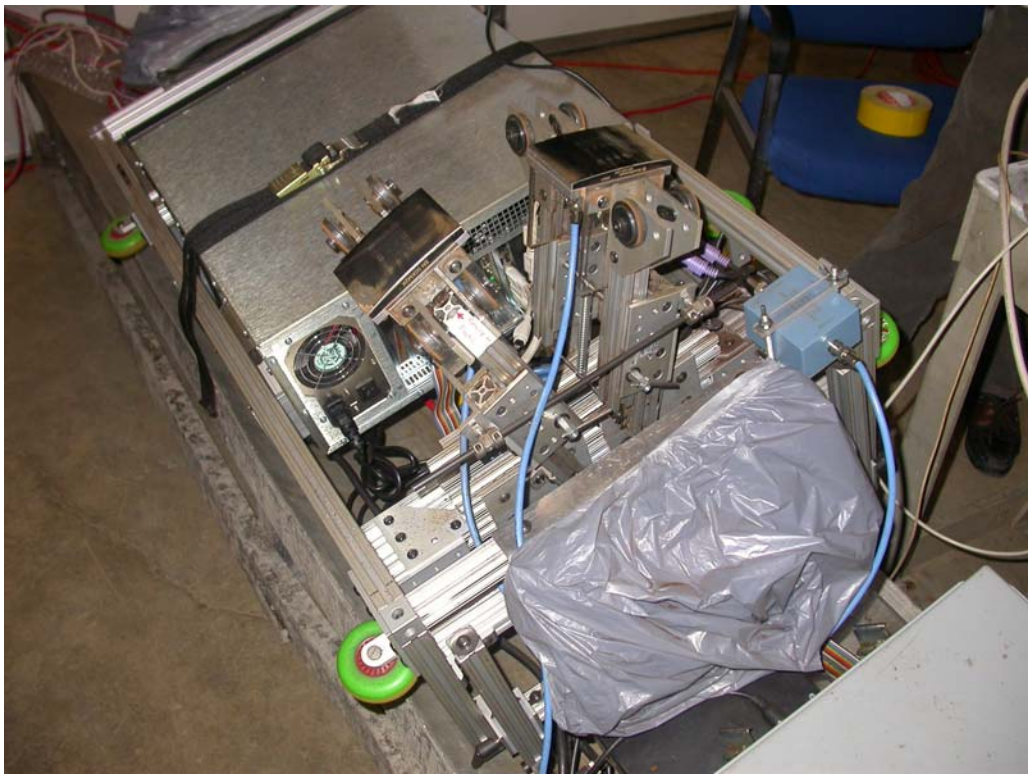

Figure 1. ORNL Shear Horizontal EMAT

GTI Remote Field Eddy Current (RFEC) – The Gas Technology Institute (GTI) has developed a RFEC inspection technique to inspect pipelines with multiple diameters, valve and bore restrictions, and tight or miter bends. This electromagnetic technique uses a simple exciter coil that can be less than on third of the pipe diameter and is driven by a low-frequency sinusoidal current to generate an oscillating electromagnetic field that small sensor coils can detect. The oscillating field propagates along two paths; a direct axial path and an indirect or remote path.

The direct field attenuates rapidly because the pipe acts as a waveguide that will only allow frequencies in the gigahertz range and above to propagate. It becomes negligible after 2 to 3 pipe diameters. Thus after 2 to 3 pipe diameters, the only signal left is that from the remote field, which propagates out through the pipe wall, along its exterior and then re-enters the pipe 2 to 3 pipe diameters from the exciter coil. This is exactly what is needed for defect detection since the electromagnetic waves must now pass directly through metal loss defect regions and other flaws. Changes from nominal values of the amplitude and phase of the remote field detect defects in the pipe wall and measure their severity. GTI's technology is depicted in Figure 2.

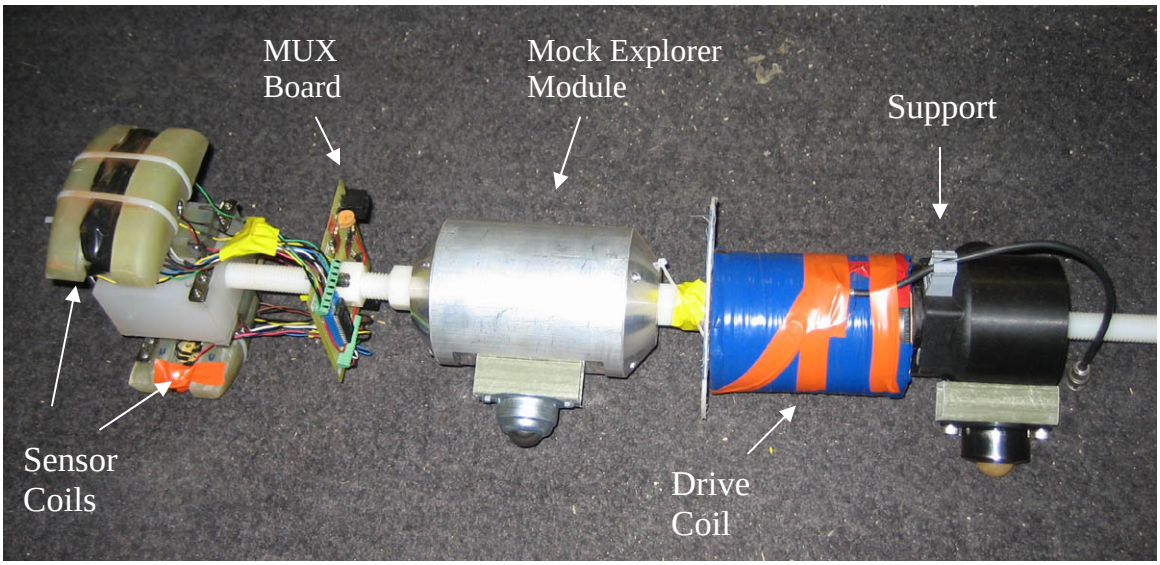

Figure 2. GTI Remote Field Eddy Current

SwRI Remote Field Eddy Current (RFEC) – Through funding support from PHMSA/OPS, Southwest Research Institute® has developed a remote-field eddy current (RFEC) technology to be used in unpiggable lines. The SwRI RFEC tool is capable of detecting corrosion on the inside or outside pipe surface. Since a large percentage of pipelines cannot be inspected using "smart pig" techniques because of diameter restrictions, pipe bends, and valves, a concept for a collapsible excitation coil was developed but found unnecessary for the pipe sizes and materials of interest in this demonstration. A breadboard system that meets the size, power, and communication requirements for integration into the Carnegie Mellon Explorer II robot was developed and used in the demonstration tests. This system is shown in Figure 3. The demonstration system incorporates eight detectors, and data from all eight channels are acquired and processed simultaneously as the system is scanned along the pipe at speeds up to 4 inch/sec. All of the instrumentation, except for a DC power supply and a laptop computer (used for storage of the processed data), is located on the tool. The RFEC system can expand to inspect 6- or 8-inch-diameter pipe and can retract to 4 inches to pass through obstructions.

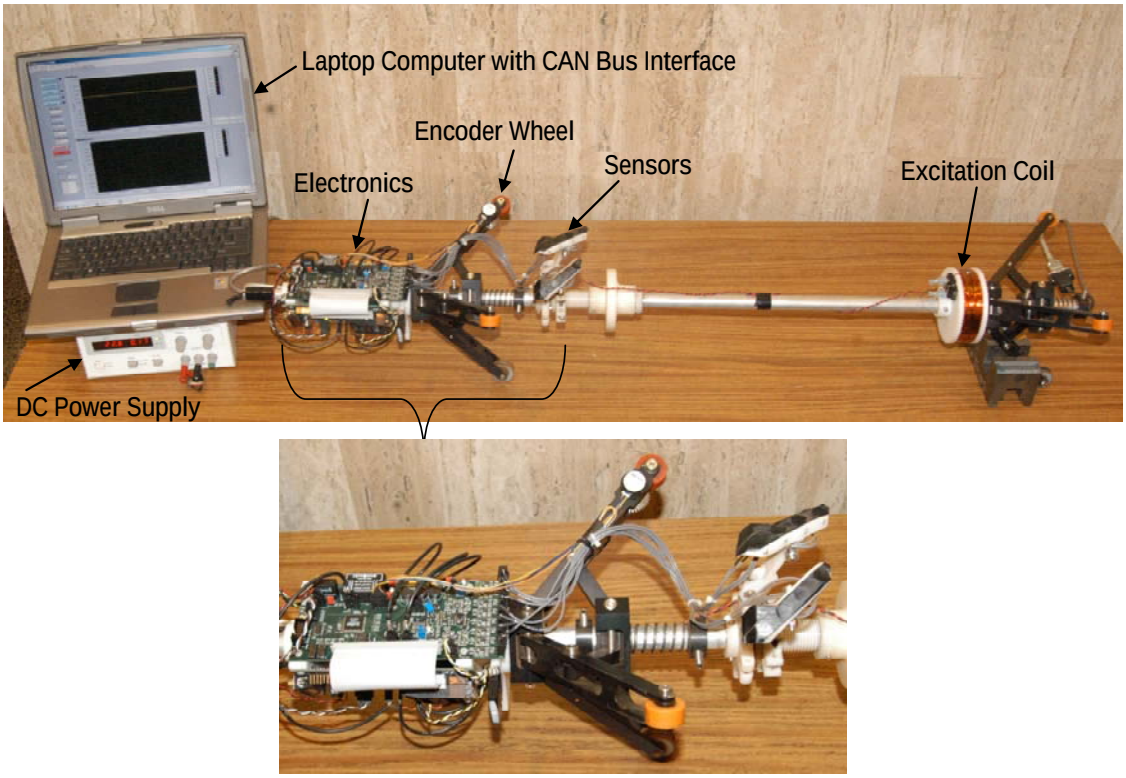

Figure 3. SwRI Remote Field Eddy Current

PNNL Ultrasonic Strain Measurement – Pacific Northwest National Laboratory (PNNL) has developed an ultrasonic sensor system capable of detecting pipeline stress and strain caused by mechanical damage i.e., dents and gouges. PNNL has established the relationship between residual strain and the change in ultrasonic response (shear wave birefringence) under a uniaxial load. Initial measurements on samples in both axial and biaxial states have shown excellent correlation between shear birefringence measurements. The demonstration focused on refining the methodology, particularly under circumstances when the damage is more complex than a simple uniaxial deformation. PNNL's technology is depicted in Figure 4.

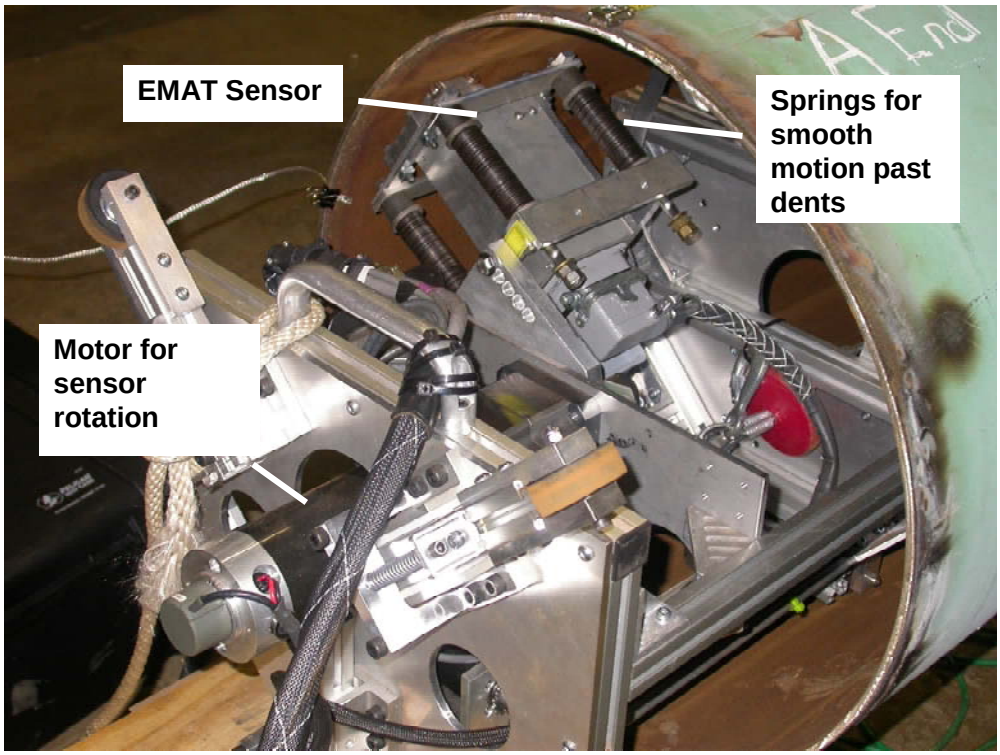

Figure 4. PNNL Ultrasonic Strain Measurement

Rotating Permanent Magnet – Battelle is developing a rotating permanent magnet inspection system where pairs of permanent magnets are rotated around the central axis. This alternative to the more common concentric coil method can be used to induce high current densities in the pipe. Along the pipe away from the magnets in either direction, the currents flow in the circumferential direction. Anomalies and wall thickness variations are detected with an array of sensors that measure local changes in the magnetic field produced by the current flowing in the pipe. The inspection methodology can be configured to pass tight restrictions and narrow openings such as plug valves. The separation between the magnets and the pipe wall is on the order of an inch (2.5cm). The strength of circumferential current produces signals on the order of a few gauss, which can be detected by hall effect sensors positioned between 8 and 40 inches (10 and 100 cm) away from the rotating magnets. This evolving inspection methodology was first demonstrated in summer of 2004. Battelle's technology is depicted in Figure 5.

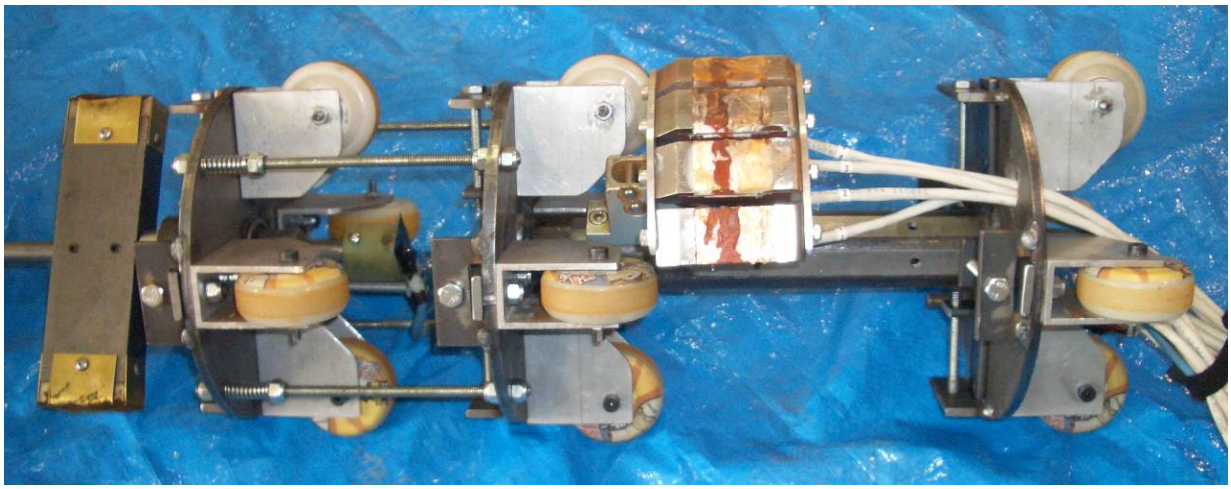

Figure 5. Battelle Rotating Permanent Magnet

Capacitive Sensor for Polyethylene Pipe Inspection – The National Energy Technology Laboratory (NETL) has developed a capacitive probe to resolve defects in plastic natural gas pipelines. This new technology uses a non-destructive and non-hazardous projected electric field to map voids and other anomalies. The probe can function autonomously and is intended for use in conjunction with existing "pigs" or on its own platform. NETL's technology is depicted in Figure 6.

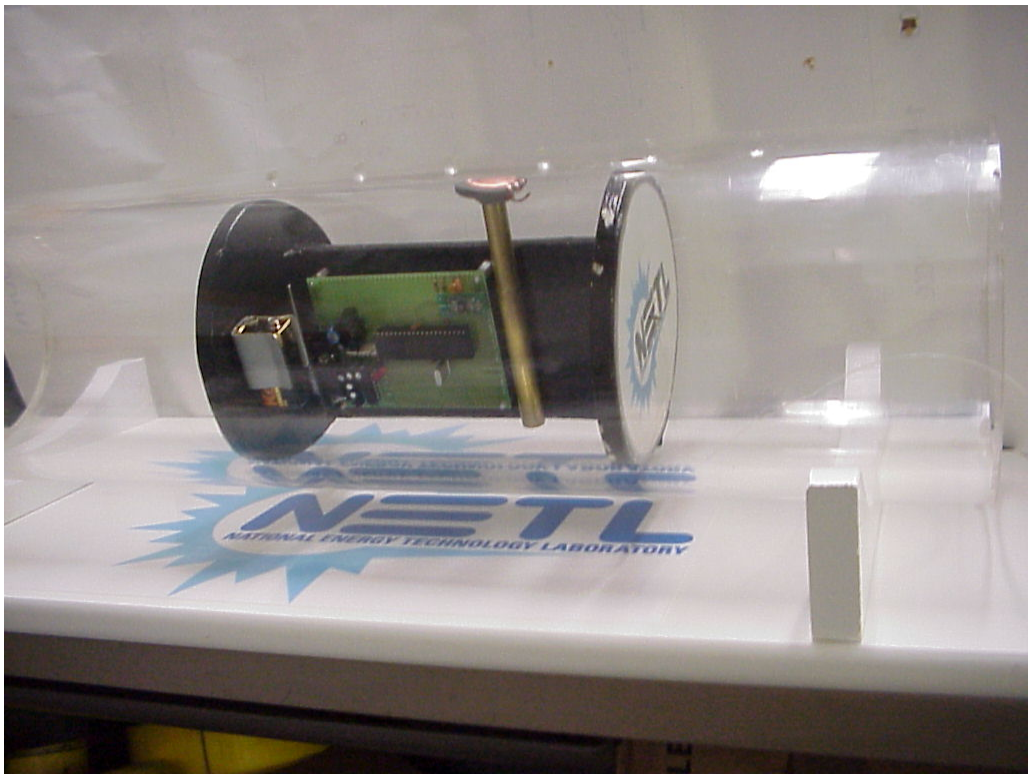

Figure 6. NETL Capacitive Sensor

Demonstration Configuration

The emerging inspection technologies were tested within a 40 by 100 foot high-bay area at Battelle's PSF. Pipes selected for these tests had various types of natural and machined defects. A black tarp and bubble wrap covered the pipes to hide defect locations. Figure 7 shows the configuration of the pipes during the demonstration. These pipes included:

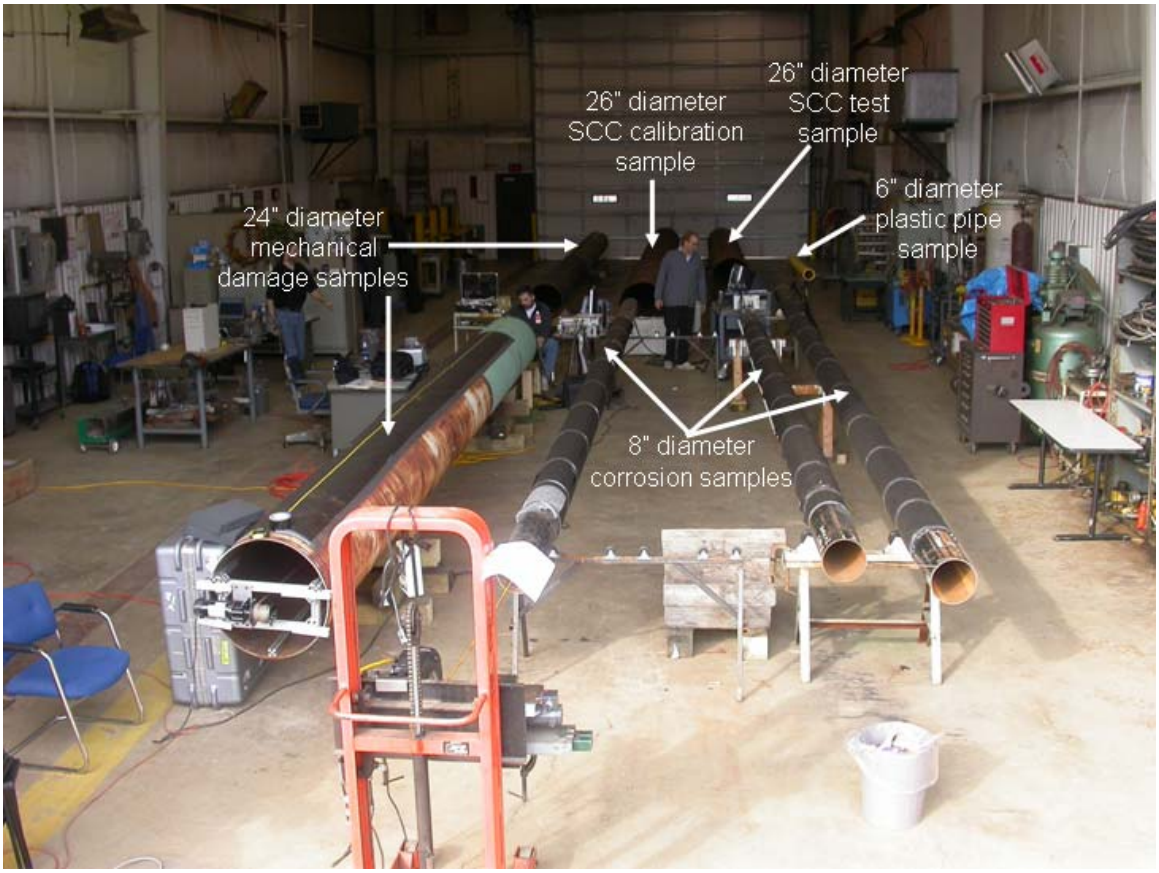

Figure 7. High-bay Looking North

Detection of Metal Loss

- One 8-inch diameter ERW seam welded pipe measuring 30-feet in length (0.188 inch wall thickness). The pipe sample contained two rows of simulated corrosion defects spaced 180° apart.
- One 8-inch diameter ERW seam welded pipe measuring 35-feet in length (0.188 inch wall thickness). The pipe sample contained two rows of simulated corrosion defects spaced 180° apart. This sample also included a 5-foot section of natural corrosion from a pipe pulled from service.
- One 8-inch diameter ERW seam welded pipe measuring 40-feet in length (0.188 inch wall thickness). The pipe sample contained two rows of simulated corrosion defects spaced 180° apart.

Detection of Mechanical Damage

- One 24-inch diameter pipe measuring approximately 28-feet in length (0.292 inch wall thickness) comprised of two separate pipes welded together with mechanical damage defects. Three rows of mechanical damage defects were located on this pipe sample spaced 120° apart but only one row with track hoe defects were used in the benchmarking.
- One 24-inch diameter pipe measuring approximately 40 feet in length (0.292 inch wall thickness) with plain (or smooth) dent defects along one row.

Detection of Stress Corrosion Cracking (SCC)

- One 26-inch diameter pipe measuring approximately 26 feet in length (0.281 inch wall thickness) with natural stress corrosion cracking. A separate 26-inch diameter SCC pipe sample was provided for calibration.

Detection of Plastic Pipe Defects

- One 6-inch diameter polyethylene pipe measuring 13 feet in length (0.5 inch wall thickness) with cylindrical drill holes and saw cut defects along one row on the exterior of the pipe.

Additional information on the pipe defect sets, pipe preparation, demonstration facility layout, and demonstration procedures can be found in the final benchmarking report, Pipe and Anomaly Configuration for the Phase II Benchmarking of Emerging Pipeline Inspection Technologies prepared by Battelle and included in Appendix D.

DEMONSTRATION RESULTS

This section provides an assessment of the test data relative to the benchmark data developed at the Battelle Pipeline Simulation Facility (PSF). The benchmark data is provided as Appendix A of this document and test results for the individual technologies, as prepared and submitted by the technology developers, can be found in Appendix B.

Metal Loss Corrosion Assessment

The three corrosion assessment technologies were demonstrated in an 8-inch diameter pipe[4]. This diameter was chosen to match a specific crawler implementation, Explorer, being separately developed under NETL DOE and Northeast Gas Association (NGA) funding[5]. The untethered platform is designed to traverse pipelines ranging from 6 to 8 inches inside diameter. The inspection technology developers were asked to include as many of the configuration and interface requirements of this platform as practical.

Three 8-inch diameter pipes were inspected by each technology for corrosion. The first pipe (Pipe Sample 1) was a seam-welded pipe measuring approximately 35 feet in length. This sample consisted of three pipe sections welded together (two circumferential welds) and

[4] In the first demonstration these technologies were demonstrated in 12-inch diameter pipe.
[5] http://www.netl.doe.gov/technologies/oil-gas/publications/td/41155_Final.PDF

contained simulated corrosion defects set along two test lines 180° apart. The simulated corrosion was created using electrochemical etching techniques, an example of which is shown in Figure 8. A 5 foot section of Pipe Sample 1 also contained natural corrosion from a pipe recently pulled from service.

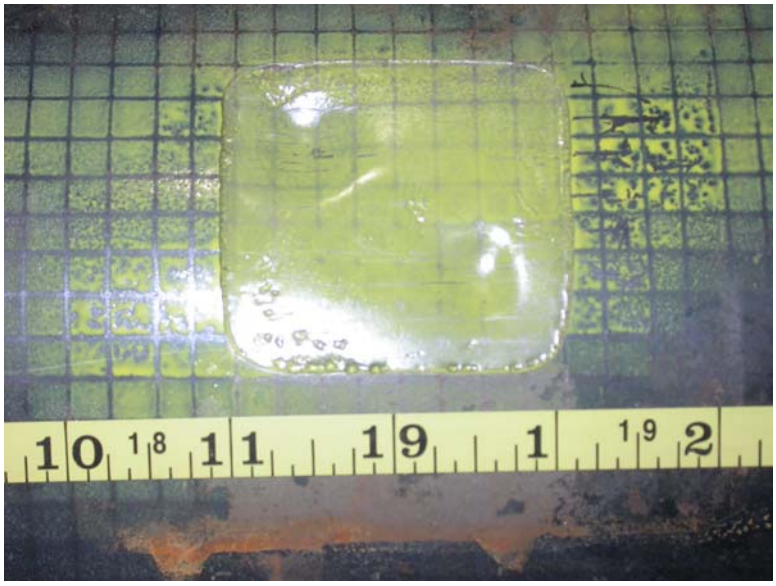

Figure 8. Example Simulated Corrosion Defect using Electrochemical Etching Techniques

The donated natural corrosion pipe sample had a field girth weld with corrosion on both sides of the weld. The weld drop through was too large for the inspection tool specifications and as such the pipe was trimmed to include roughly 2 feet of corrosion on one end, 3 feet of full thickness pipe at the other end, and no field welds. The pipe was then sandblasted and welded between two new pipes to comprise Pipe Sample 1. When the pipe was being fully characterized, an additional weld was found in the middle of the corrosion area (see Figure 9). This weld was very fine and did not have a significant crown. The natural corrosion defects were intended to be a "stretch goal" of these emerging inspection technologies. While the natural corrosion sample represents a real world problem, this additional weld adds a complex scenario that is most likely new to the technology developers. As such, these search areas are reported but are not included in the results evaluation.

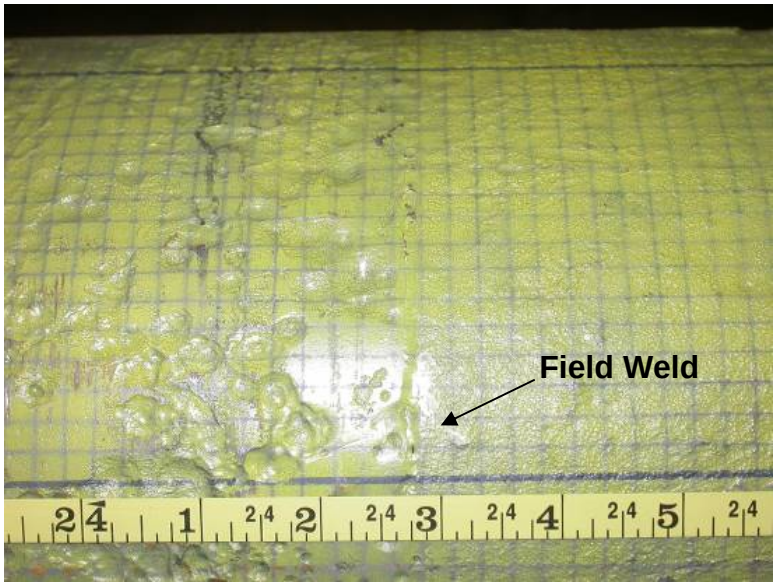

Figure 9. Fine, Field Weld in Natural Corrosion Pipe Segment

The second pipe (Pipe Sample 2) was a seam-welded pipe measuring approximately 30 feet in length. This sample consisted of two pipe sections welded together (one circumferential weld) and contained simulated corrosion defects set along two test lines 180° apart. The third pipe (Pipe Sample 3) was a seam-welded pipe measuring approximately 40 feet in length. This sample consisted of two pipe sections welded together (one circumferential weld) and contained simulated corrosion defects along two test lines 180° apart.

All three technologies detected one false positive signal; however, none of the technologies had a false positive in the same location. None of the technologies failed to identify a defect and were fairly accurate in predicting the locations. These results are summarized in Table 1. In addition, the corrosion sizing results were plotted in a manner commonly used by pipeline inspection vendors to demonstrate commercial in-line inspection technology capabilities. For these graphs, benchmark data is plotted against the values reported by the technology developers. Care must be taken in interpreting these graphs since:

- Error in the benchmark measurements is not zero
- Only the maximum depth is compared while the corrosion pit depth varied throughout the defect; many corrosion areas had more than one area of local thinning.
- Length and width were measured at the surface; however other measures can also be used that still accurately describe the anomaly.

Overall these graphs show the results predicted by each technology correlated well with the benchmark data.

Table 1. Detection Rates for the Corrosion Technologies

Technology	Detection Rate	False Positive Rate	False Negative Rate	Mean Difference in Location of Defect	Standard Deviation of Defect Location
SwRI – RFEC	100% (32 of 32)	3.3% (1 of 30) – Defect P2-8 called as a repeatable signal, but does not have typical flaw signal characteristics; 0.17" deep, 1.38" long and 1.06" wide	0% (0 of 32)	0.33	1.71
GTI – RFEC	100% (32 of 32)	3.3% (1 of 30) – Defect P1-2 called as an unknown feature resembling metal loss; 0.008" deep, <1" long, and >4" wide	0% (0 of 32)	0.08	1.18
Battelle – Rotating Permanent Magnet	100% (32 of 32)	3.3% (1 of 30) – Defect P1-17 called as a small single pit 0.02" deep, 0.7" long, and 0.75" wide	0% (0 of 32)	-0.31	2.05

SwRI Results

SwRI began testing the morning of Monday, January 9, 2006, and completed testing by mid-day Thursday, January 12, 2006. The SwRI RFEC tool acquired, processed, and displayed data in real time as it was continuously pulled through each pipe sample. Each scan took approximately 5 minutes to complete with selected higher speed runs taking approximately one to two minutes to complete. A circumferential region of 60 degrees was inspected in each scan, and two scans were made along each defect line to ensure complete coverage of all defects.

The SwRI *RFEC* technology detection rate was 100%, detecting all defect sites on Pipe Sample 1, Pipe Sample 2, and Pipe Sample 3. On average, SwRI located anomalies slightly past the actual start of the defect location with a standard deviation of 1.71 inches. The SwRI *RFEC* technology detected one false positive signal on Test Line 1 of Pipe Sample 2. The false positive signal was identified as a repeatable signal without typical flaw signal characteristics with a depth of nearly 90% of the wall thickness and approximately 1 5/8 -inch in length. SwRI's sizing accuracy is depicted in Figures 10 through 12 in which the predicted and measured anomaly depths, lengths, and widths are presented.

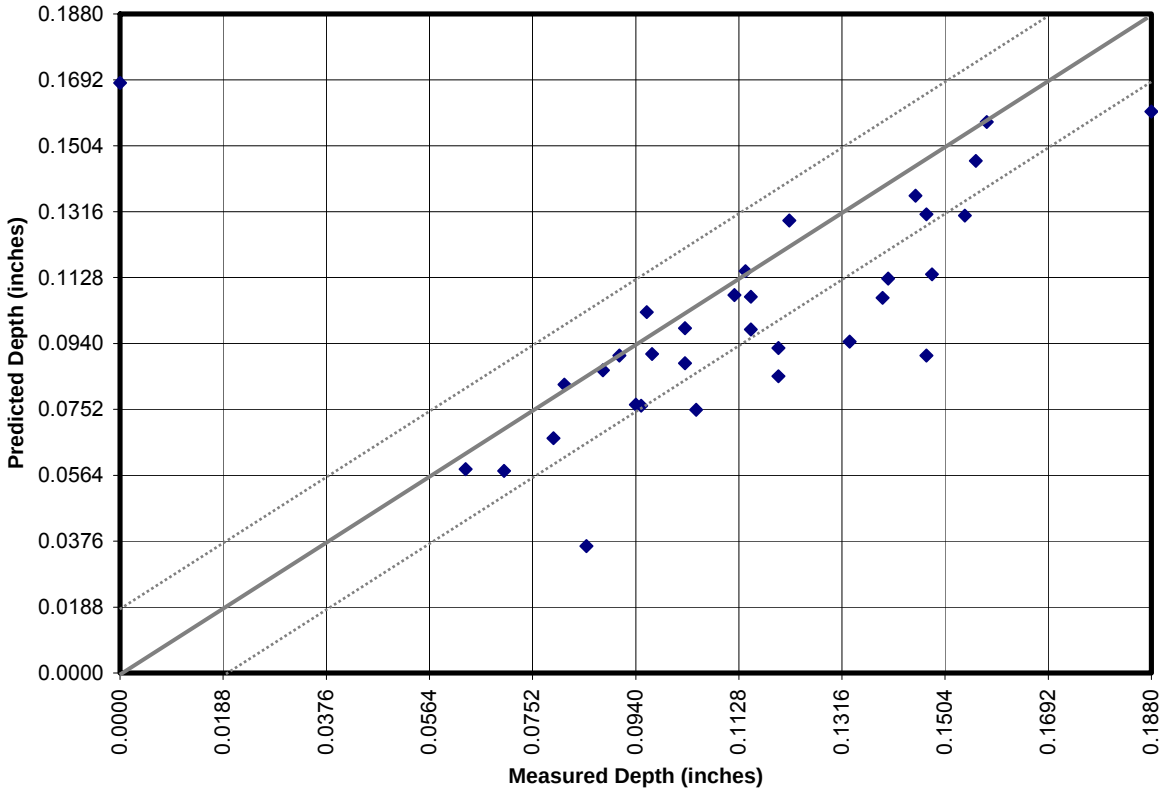

Figure 10. Measured Depth vs. Predicted Depth for the SwRI *RFEC*

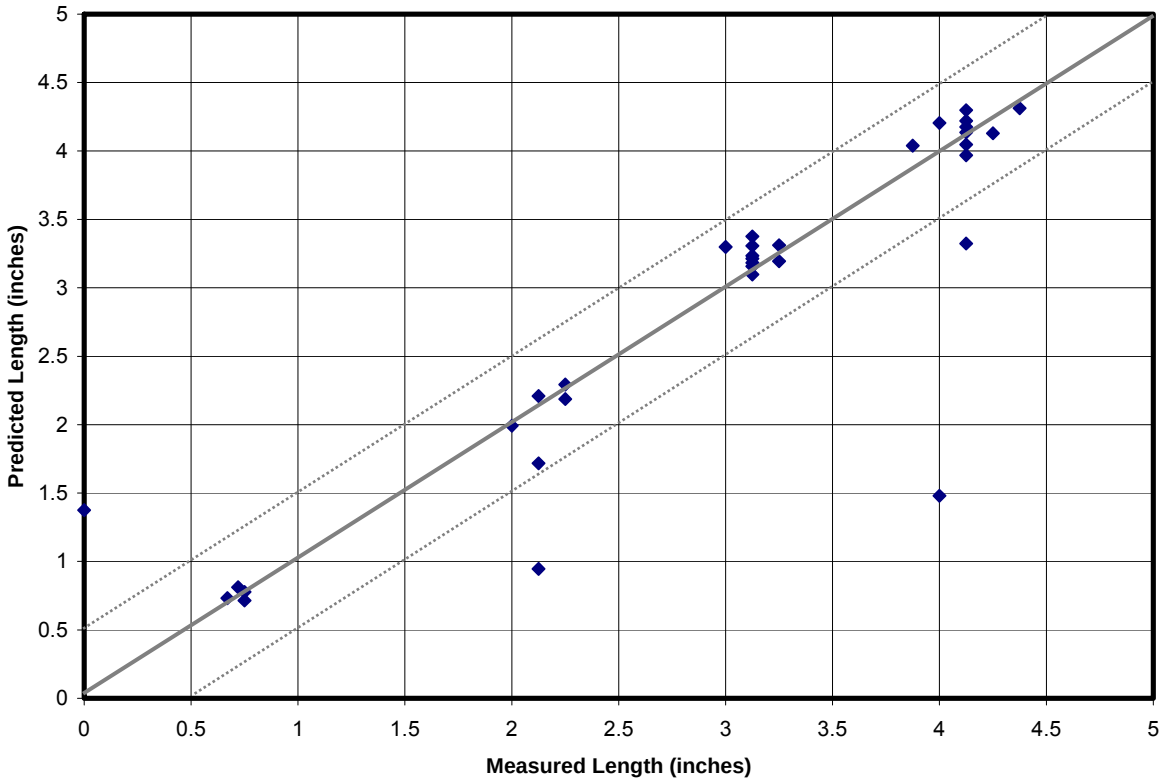

Figure 11. Measured Length vs. Predicted Length for the SwRI *RFEC*

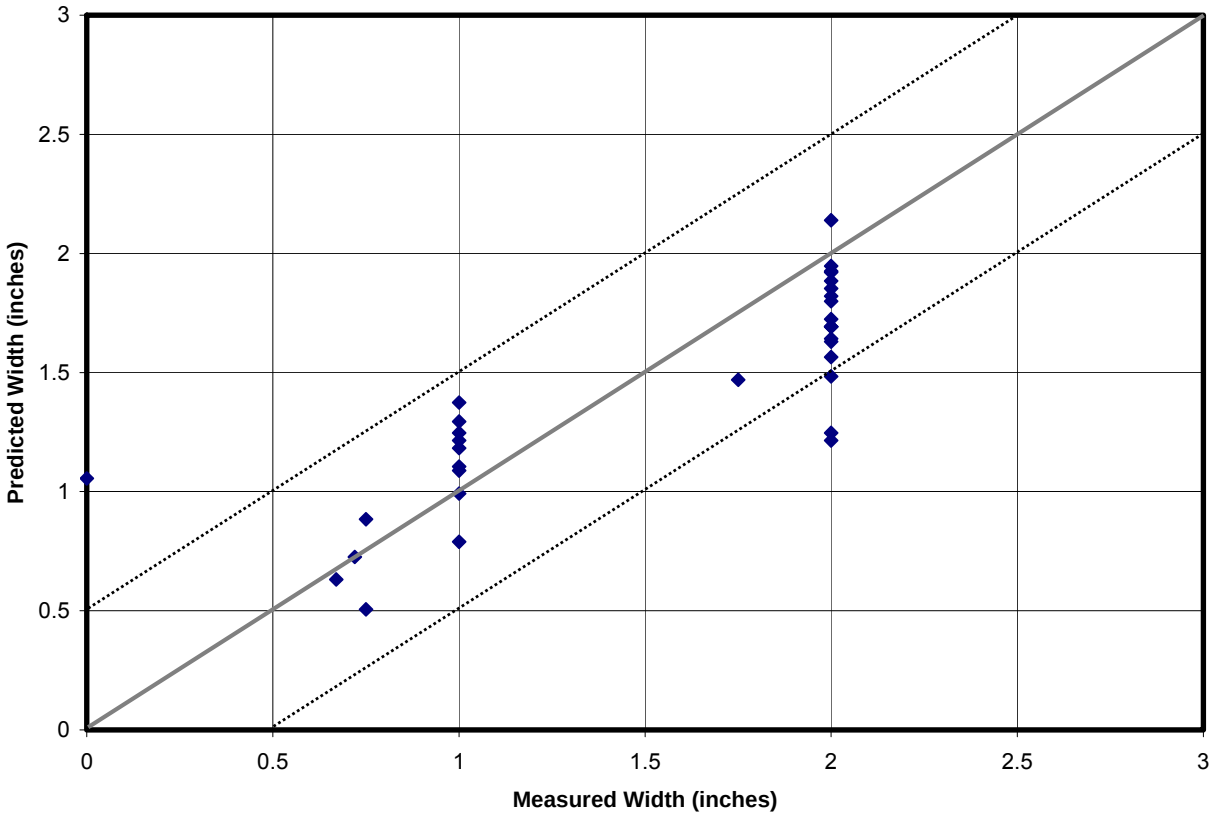

Figure 12. Measured Width vs. Predicted Width for the SwRI *RFEC*

GTI Results

GTI began testing on the morning of Monday January 9, 2006 and completed testing by the evening of Thursday January 12, 2006. The GTI *RFEC* sensor technology collected data by indexing through each defect region in 0.25 inch steps. The GTI *RFEC* technology was able to scan both test lines in each pipe sample at the same time but because of the small incremental data collection each pipe sample required a full day to collect data. GTI did attempt a continuous scan with the results of this scan provided in Appendix C.

The GTI *RFEC* technology detection rate was 100%, detecting all defect sites on Pipe Sample 1, Pipe Sample 2, and Pipe Sample 3. On average, GTI located anomalies slightly past the actual start of the defect location with a standard deviation of 1.18 inches. The GTI *RFEC* technology detected one false positive signal on Test Line 1 of Pipe Sample 1 but identified the anomaly as a small unknown feature with a depth of only 4% of the wall thickness and approximately 1-inch in length. GTI's sizing accuracy is depicted in Figures 13 through 15 in which the predicted and measured anomaly depths, lengths, and widths are presented.

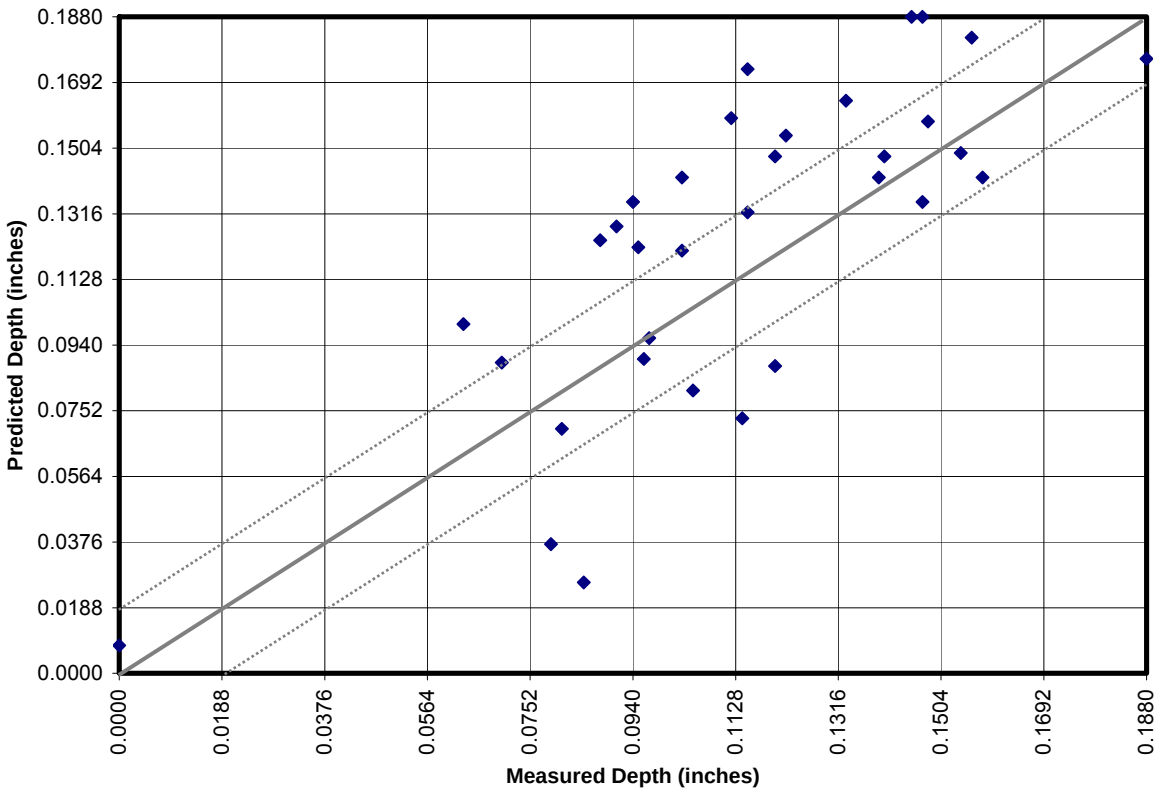

Figure 13. Measured Depth vs. Predicted Depth for the GTI *RFEC*

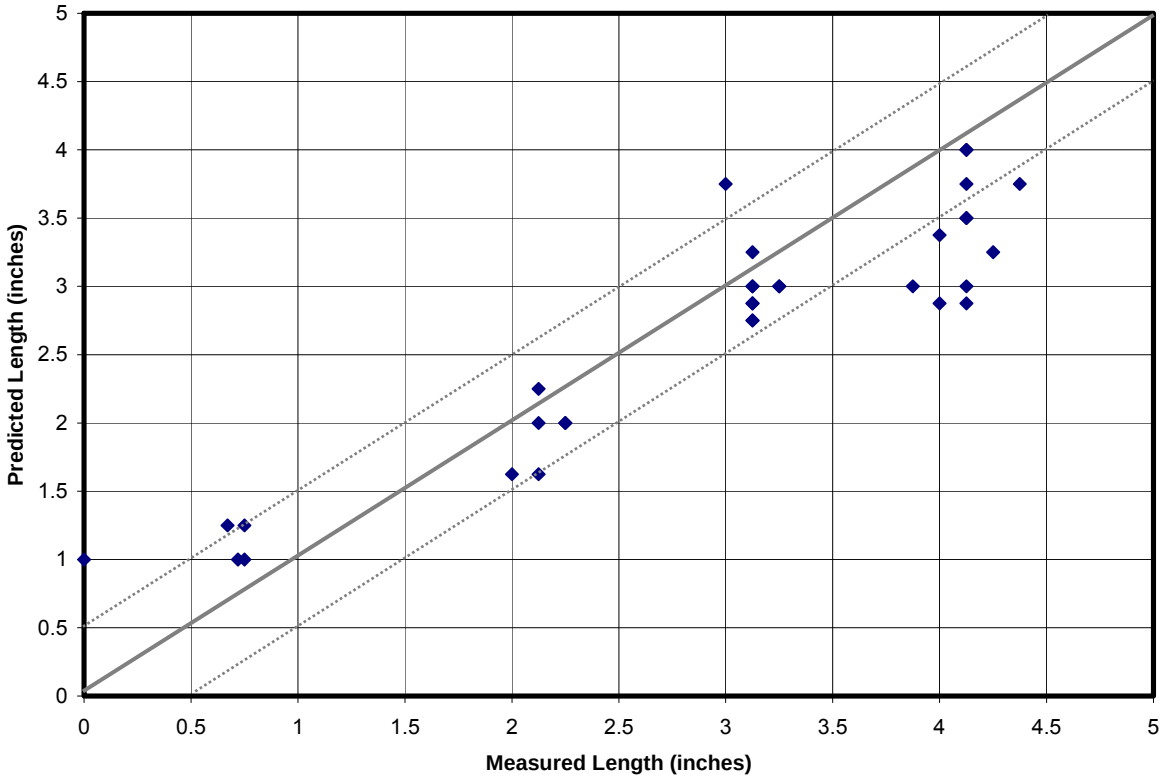

Figure 14. Measured Length vs. Predicted Length for the GTI *RFEC*

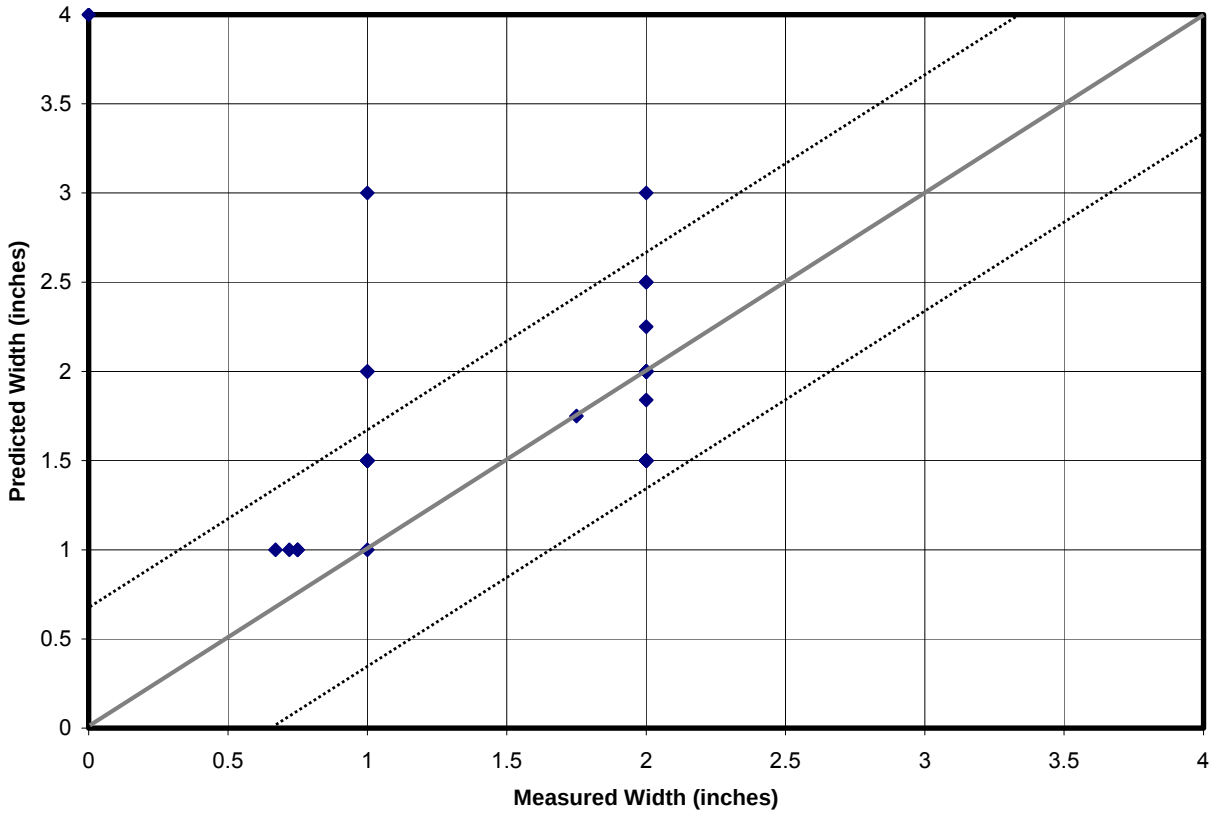

Figure 15. Measured Width vs. Predicted Width for the GTI *RFEC*

Battelle Results

Battelle began testing the afternoon of Tuesday January 10, 2006 and completed testing by the afternoon of Friday January 13, 2006. Battelle's testing was periodically interrupted due to concerns from the other corrosion inspection technology developers that the permanent magnet was causing interference with their systems. The Battelle *Rotating Permanent Magnet* technology was able to continuously acquire data through each pipe sample taking approximately 10 to 15 minutes to scan one test line. During the demonstration Battelle processed signals and displayed inspection results in real-time.

The Battelle *Rotating Permanent Magnet* technology detection rate was 100%, detecting all defect sites on Pipe Sample 1, Pipe Sample 2, and Pipe Sample 3. On average, Battelle located anomalies shy of the actual start of the defect location with a standard deviation of 2.05 inches. The Battelle *Rotating Permanent Magnet* technology detected one false positive signal on Test Line 2 of Pipe Sample 1 but identified the anomaly as a small single pit with a depth of only 11% of the wall thickness and approximately 3/4-inch in length. Battelle's sizing accuracy is depicted in Figures 16 through 18 in which the predicted and measured anomaly depths, lengths, and widths are presented.

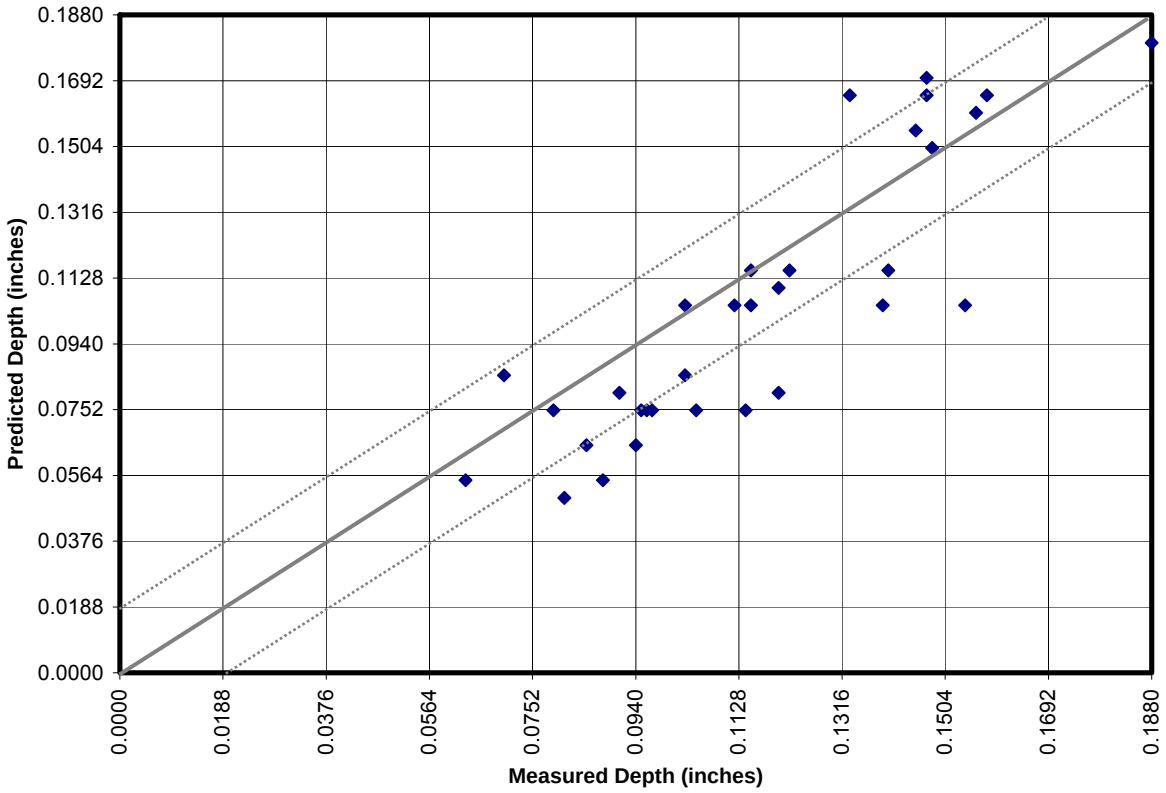

Figure 16. Measured Depth vs. Predicted Depth for the Battelle *Rotating Permanent Magnet*

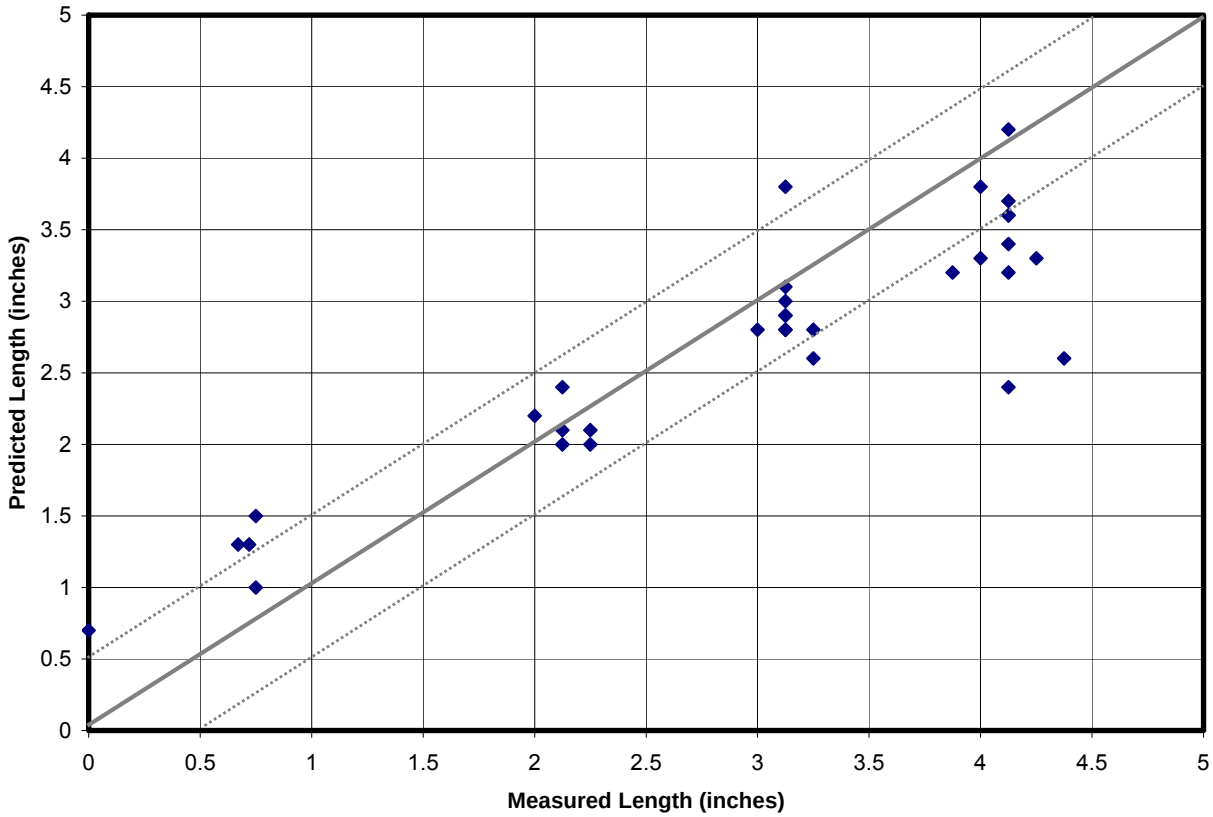

Figure 17. Measured Length vs. Predicted Length for the Battelle *Rotating Permanent Magnet*

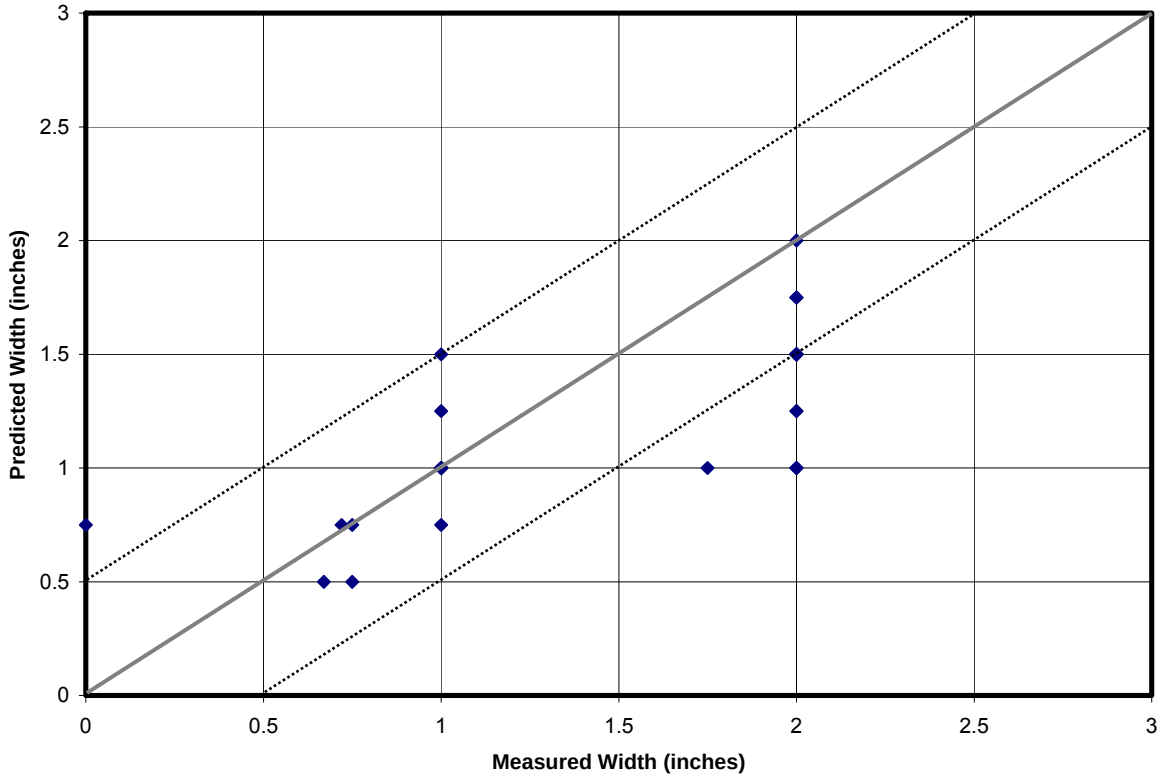

Figure 18. Measured Width vs. Predicted Width for the Battelle *Rotating Permanent Magnet*

The benchmark data and test results for the three technologies that tested for metal loss on Pipe Samples 1, 2, and 3 are shown in Table 2 through Table 7.

This page intentionally blank.

Table 2. Benchmark Data vs. Results for Corrosion Pipe Sample 1; Test Line 1

Simulated Corrosion Pipe Sample 1 Test Line 1												
Defect Number	P1-1	P1-2	P1-3	P1-4	P1-5	P1-6	P1-7	P1-8	P1-9	P1-10	P1-11	P1-12
Search Region (from End B)	328" to 340"	304" to 316"	280" to 292"	256" to 268"	232" to 244"	208" to 220"	184" to 196"	160" to 172"	120" to 144"	100" to 112"	76" to 88"	52" to 64"
Start and End of Defect (inches)5												
Benchmark Data	Blank	Blank	287.75 290.875	259.625 263.625	232.75 235.75	Blank	190.625 192.75	Blank	120" 140.25"	Blank	Blank	56.75 60.875
SwRI –RFEC			282.6 285.8	254.5 258.7	227.7 231.0		188.8 189.7	160.0 172.0	a=120.0 122.3 b=128.5 129.3			56.9 60.2
GTI – RFEC		~311.25 ~314.25	~281.75 ~285.5	~260.5 ~264.75	~232 ~236.5		~191.25 ~193.75		~120 ~134.25			~56.75 ~60.5
Battelle – Rotating Permanent Magnet			288 292.8	260.1 264.9	233.2 237		188.8 192.2		120 132			58.1 62.3
Defect Length (inches)												
Benchmark Data	Blank	Blank	3.125	4	3	Blank	2.125	Blank	20.25	Blank	Blank	4.125
SwRI –RFEC			3.16	4.20	3.30		0.95	12	a=2.25 b=0.77			3.32
GTI – RFEC		< 1	2.875	3.375	3.75		1.625		14.25			2.875
Battelle – Rotating Permanent Magnet			3.8	3.8	2.8		2.4		12			3.2
Defect Width (inches)												
Benchmark Data	Blank	Blank	2	2	1	Blank	2	Blank	Full Circ.	Blank	Blank	2
SwRI –RFEC			1.25	1.95	1.09		1.92	Full Circ.	a=1.82 b=Full Circ.			1.63
GTI – RFEC		> 4	1.5	~3	> 3		1.5		>4			1.84
Battelle – Rotating Permanent Magnet			1.0	1.5	1.0		1.5		32			1.75
Maximum Defect Depth (inches)												
Benchmark Data	Blank	Blank	0.096	0.063	0.081	Blank	0.147	Blank	0.146	Blank	Blank	0.122
SwRI –RFEC			0.10	0.06	0.08		0.09	0.18	a=0.066 b=0.83			0.13
GTI – RFEC		0.008	0.090 0.064	0.100 0.075	0.07		0.135 0.133		~0.141			0.154 0.142
Battelle – Rotating Permanent Magnet			0.075	0.055	0.050		0.165		Various up to 0.150			0.115
Comments												
SwRI –RFEC					defect signal outside stated region			appears to be large region of general wall thinning that extends out of the designated region. Signal patterns not characteristic of calibration defects.	two defects in region, designated a and b.			
GTI – RFEC		unknown feature resembling metal loss, 4%	2 axially aligned pits, 48% and 34%	2 axially aligned pits, 53% and 40%	2 pits, deepest 37%. Additional features observed attributed to through hole of defect 18 sitting over drive coil		2 pits offset diagonally, 72% and 71%		deepest pit was a single small slit ~75%			2 axially aligned pits, 82% and 75.5%
Battelle – Rotating Permanent Magnet			corrosion patch, multiple pits of different depths	corrosion patch, multiple pits of different depths	corrosion patch, multiple pits of different depths		corrosion patch, multiple pits of different depths	a slow change in signal in all sensor throughout the region indicates a material property change	large area of general corrosion of variable depth that spans the entire sensor width. The corrosion is close to the weld, altering both signals. A large wide corrosion area at 128"			corrosion patch, multiple pits of different depths

Table 3. Benchmark Data vs. Results for Corrosion Pipe Sample 1; Test Line 2

Simulated Corrosion Pipe Sample 1 Test Line 2											
Defect Number	P1-13	P1-14	P1-15	P1-16	P1-17	P1-18	P1-19	P1-20	P1-21	P1-22	P1-23
Search Region (from End B)	330" to 342"	306" to 318"	282" to 294"	258" to 270"	234" to 246"	210" to 222"	186" to 198"	160" to 172"	120" to 144"	98" to 110"	74" to 86"
Start and End of Defect (inches)											
Benchmark Data	335.75 339.625	308.875 312	Blank	Blank	Blank	213.625 217.875	Blank	Blank	120 140.75	108 110	79.75 83.75
SwRI –RFEC	335.8 339.9	309.5 312.8				214.0 218.1		160.0 172.0	128.9 129.7	108.1 110.1	79.9 81.4
GTI – RFEC	~336.375 ~340.25	~309 ~312.75				214.75 218.875			~120 ~134.25	~108.5 ~111	~79.75 ~83.5
Battelle – Rotating Permanent Magnet	334.2 338.4	306.9 310.8			241.1 241.8	212.5 216.8			126.0 138.0	103.1 106.3	74.8 79.1
Defect Length (inches)											
Benchmark Data	3.875	3.125	Blank	Blank	Blank	4.25	Blank	Blank	20.75	2	4
SwRI –RFEC	4.04	3.31				4.13		12	0.79	1.99	1.48
GTI – RFEC	3	2.875				3.25			14.25	1.625	2.875
Battelle – Rotating Permanent Magnet	3.2	2.9			0.7	3.3			12	2.2	3.3
Defect Width (inches)											
Benchmark Data	1.75	1	Blank	Blank	Blank	2	Blank	Blank	Full Circ.	2	2
SwRI –RFEC	1.47	1.37				1.69		Full Circ.	Full Circ.	1.82	1.72
GTI – RFEC	1.75	1.5				2			> 4	1.5	2.25
Battelle – Rotating Permanent Magnet	1.0	1.25			0.75	2.0			> 5	1.75	1.0
Maximum Defect Depth (inches)											
Benchmark Data	0.095	0.115	Blank	Blank	Blank	0.145	Blank	Blank	0.127	0.12	0.097
SwRI –RFEC	0.08	0.11				0.14		0.18	0.06	0.08	0.09
GTI – RFEC	0.122 0.070	0.113 0.132				0.188 0.111			0.113 0.122	0.088	0.096
Battelle – Rotating Permanent Magnet	0.075	0.115			0.020	0.155			Various up to 0.150	0.110	0.075
Comments											
SwRI –RFEC								appears to be large region of general wall thinning that extends out of the designated region. Signal patterns not characteristic of calibration defects.			
GTI – RFEC	2 axially aligned pits, 65% and 37%	2 axially aligned pits, 70% and 60%				2 pits, through hole and 59%			general corrosion, deepest 60% and 65%	diagonal feature, 47%	51%
Battelle – Rotating Permanent Magnet	corrosion patch, multiple pits of different depths	corrosion patch, multiple pits of different depths			small single pit	corrosion patch, multiple pits of different depths		a slow change in signal in all sensor throughout the region indicates a material property change	area of general corrosion of variable depth that spans most sensors. A large wide corrosion area at 128"	corrosion patch, multiple pits of different depths	corrosion patch, multiple pits of different depths

Table 4. Benchmark Data vs. Results for Corrosion Pipe Sample 2; Test Line 1

Simulated Corrosion Pipe Sample 2 Test Line 1											
Defect Number	P2-1	P2-2	P2-3	P2-4	P2-5	P2-6	P2-7	P2-8	P2-9	P2-10	P2-11
Search Region (from End B)	294" to 306"	270" to 282"	246" to 258"	222" to 234"	198" to 210"	174" to 186"	150" to 162"	126" to 138"	102" to 114"	78" to 90"	54" to 66"
Start and End of Defect (inches)											
Benchmark Data	Blank	Blank	Blank	227.25 229.375	Blank	180.25 183.375	153.125 156.375	Blank	108.125 112.25	80.125 84.5	Blank
SwRI – RFEC				227.6 229.8		180.2 183.5	153.4 156.7	129.8 131.1	108.2 112.3	80.0 84.3	
GTI – RFEC				227.25 229.5		179.75 183	152.75 155.75		107.75 111.75	80.25 84	
Battelle – Rotating Permanent Magnet				228.9 232.0		181.1 184.9	153.8 157.6		108.6 112.0	80.0 83.6	
Defect Length (inches)											
Benchmark Data	Blank	Blank	Blank	2.125	Blank	3.125	3.25	Blank	4.125	4.375	Blank
SwRI –RFEC				2.21		3.23	3.31	1.38	4.05	4.31	
GTI – RFEC				2.25		3.25	3		4	3.75	
Battelle – Rotating Permanent Magnet				2.1		2.8	2.8		2.4	2.6	
Defect Width (inches)											
Benchmark Data	Blank	Blank	Blank	2	Blank	1	1	Blank	2	2	Blank
SwRI –RFEC				1.57		0.99	1.18	1.06	2.14	1.88	
GTI – RFEC				2		1	2		1.5	2.5	
Battelle – Rotating Permanent Magnet				1.0		1.0	1.0		1.5	1.5	
Maximum Defect Depth (inches)											
Benchmark Data	Blank	Blank	Blank	0.079	Blank	0.114	0.085	Blank	0.158	0.147	Blank
SwRI –RFEC				0.07		0.11	0.04	0.17	0.16	0.13	
GTI – RFEC				0.037		0.073	0.026		0.142	0.188	
Battelle – Rotating Permanent Magnet				0.075		0.075	0.065		0.165	0.170	
Comments											
SwRI –RFEC								Repeatable signal, but does not have typical flaw signal characteristics.			
GTI – RFEC											
Battelle – Rotating Permanent Magnet				Corrosion patch, with multiple pits of different depths		Corrosion patch, with multiple pits of different depths	Corrosion patch, with multiple pits of different depths		Corrosion patch, with large multiple pits of different depths	Corrosion patch, with large multiple pits of different depths	

Table 5. Benchmark Data vs. Results for Corrosion Pipe Sample 2; Test Line 2

Simulated Corrosion Pipe Sample 2 Test Line 2												
Defect Number	P2-12	P2-13	P2-14	P2-15	P2-16	P2-17	P2-18	P2-19	P2-20			
Search Region (from End B)	246" to 258"	222" to 234"	198" to 210"	174" to 186"	150" to 162"	126" to 138"	102" to 114"	78" to 90"	54" to 66"			
Start and End of Defect (inches)												
Benchmark Data	248.125 250.25	Blank	202.625 205.75	Blank	Blank	130 134.125	Blank	Blank	57.75 60.875			
SwRI –RFEC	248.1 249.8		202.3 205.4			129.1 133.2			56.3 59.7			
GTI – RFEC	249 251		201 204			129.5 133.5			57.5 60.5			
Battelle – Rotating Permanent Magnet	250.0 253.0		204.9 209.0			132.8 137.4			59.4 63.2			
Defect Length (inches)												
Benchmark Data	2.125	Blank	3.125	Blank	Blank	4.125	Blank	Blank	3.125			
SwRI –RFEC	1.72		3.10			4.14			3.37			
GTI – RFEC	2		3			4			3			
Battelle – Rotating Permanent Magnet	2.0		3.1			3.6			2.8			
Defect Width (inches)												
Benchmark Data	2	Blank	1	Blank	Blank	2	Blank	Blank	1			
SwRI –RFEC	1.21		1.21			1.69			1.25			
GTI – RFEC	1.5		1.5			2			1.5			
Battelle – Rotating Permanent Magnet	1.5		0.75			1.5			1.0			
Maximum Defect Depth (inches)												
Benchmark Data	0.14	Blank	0.105	Blank	Blank	0.112	Blank	Blank	0.188			
SwRI –RFEC	0.11		0.08			0.11			0.16			
GTI – RFEC	0.148		0.081			0.159			0.176			
Battelle – Rotating Permanent Magnet	0.115		0.075			0.105			0.180			
Comments												
SwRI –RFEC												
GTI – RFEC												
Battelle – Rotating Permanent Magnet	Corrosion patch, with multiple pits of different depths		Corrosion patch, with multiple pits of different depths			Corrosion patch, with multiple pits of different depths			Corrosion patch, with multiple pits of different depths, One pit may be through hole			

Table 6. Benchmark Data vs. Results for Corrosion Pipe Sample 3; Test Line 1

Simulated Corrosion Pipe Sample 3 Test Line 1												
Defect Number	P3-1	P3-2	P3-3	P3-4	P3-5	P3-6	P3-7	P3-8	P3-9	P3-10	P3-11	
Search Region (from End B)	384" to 396"	360" to 372"	330" to 342"	300" to 312"	270" to 282"	222" to 234"	186" to 198"	162" to 174"	138" to 150"	102" to 114"	66" to 78"	
Start and End of Defect (inches)												
Benchmark Data	Blank	Blank	335 337.25	305.625 306.375	275 277.25	Blank	189.875 194	Blank	143.665 144.335	106.375 109.625	Blank	
SwRI –RFEC			336.3 338.5	306.8 307.6	276.0 278.3		190.5 194.8		144.1 144.8	106.7 109.9		
GTI – RFEC			335 337	306.5 307.75	275.75 277.75		190 193.5		143.5 144.75	106 109		
Battelle – Rotating Permanent Magnet			338.0 341.0	307.8 309.3	276.4 279.5		187.8 193.0		144.2 145.5	108.8 112.4		
Defect Length (inches)												
Benchmark Data	Blank	Blank	2.25	0.75	2.25	Blank	4.125	Blank	0.67	3.25	Blank	
SwRI –RFEC			2.19	0.78	2.29		4.22		0.73	3.19		
GTI – RFEC			2	1.25	2		3.5		1.25	3		
Battelle – Rotating Permanent Magnet			2.0	1.5	2.1		4.2		1.3	2.6		
Defect Width (inches)												
Benchmark Data	Blank	Blank	2	0.75	2	Blank	2	Blank	0.67	1	Blank	
SwRI –RFEC			1.8	0.88	1.93		1.64		0.63	1.29		
GTI – RFEC			1.5	1	2		2		1	2		
Battelle – Rotating Permanent Magnet			1.75	0.75	1.5		1.5		0.5	1.5		
Maximum Defect Depth (inches)												
Benchmark Data	Blank	Blank	0.133	0.148	0.103	Blank	0.115	Blank	0.120	0.156	Blank	
SwRI –RFEC			0.09	0.11	0.09		0.10		0.09	0.15		
GTI – RFEC			0.164	0.158	0.142 0.119		0.173		0.148 0.112	0.182 0.176		
Battelle – Rotating Permanent Magnet			0.165	0.150	0.105		0.105		0.080	0.160		
Comments												
SwRI –RFEC												
GTI – RFEC					Three pits					Three pits	Two pits axially aligned	
Battelle – Rotating Permanent Magnet			Corrosion patch, with multiple pits of different depths	Single Pit	Corrosion patch, with multiple pits of different depths		Corrosion patch, with multiple pits of different depths		Single Pit	Corrosion patch, with multiple pits of different depths		

Table 7. Benchmark Data vs. Results for Corrosion Pipe Sample 3; Test Line 2

Simulated Corrosion Pipe Sample 3 Test Line 2												
Defect Number	P3-12	P3-13	P3-14	P3-15	P3-16	P3-17	P3-18	P3-19	P3-20	P3-21	P3-22	P3-23
Search Region (from End B)	390" to 402"	356" to 368"	330" to 342"	306" to 318"	282" to 294"	248" to 260"	210" to 222"	180" to 192"	156" to 168"	126" to 138"	102" to 114"	66" to 78"
Start and End of Defect (inches)												
Benchmark Data	392.25 396.375	Blank	335.875 336.625	Blank	Blank	250.625 253.75	214.5 217.625	185.765 186.485	Blank	130 134.125	Blank	69.5 73.625
SwRI –RFEC	392.5 396.6		336.9 337.7			251.6 254.8	215.2 218.4	186.4 187.2		130.5 134.5		69.5 73.8
GTI – RFEC	393 396		335.75 336.75			251.25 254	214.5 217.25	185.75 186.75		130.25 133.75		70.25 74
Battelle – Rotating Permanent Magnet	392.4 397.0		337.1 338.0			250.5 254.4	214.1 218.1	184.9 186.2		128.3 132.7		65.9 70.6
Defect Length (inches)												
Benchmark Data	4.125	Blank	0.75	Blank	Blank	3.125	3.125	0.72	Blank	4.125	Blank	4.125
SwRI –RFEC	4.18		0.72			3.21	3.18	0.81		3.97		4.3
GTI – RFEC	3		1			2.75	2.75	1		3.5		3.75
Battelle – Rotating Permanent Magnet	3.6		0.9			2.9	3.0	1.3		3.4		3.7
Defect Width (inches)												
Benchmark Data	2	Blank	0.75	Blank	Blank	1	1	0.72	Blank	2	Blank	2
SwRI –RFEC	1.69		0.51			0.79	1.10	0.73		1.48		1.85
GTI – RFEC	2.5		1			1.5	1.5	1		2		2
Battelle – Rotating Permanent Magnet	1.25		0.5			1.0	1.0	0.75		1.25		1.5
Maximum Defect Depth (inches)												
Benchmark Data	0.094	Blank	0.154	Blank	Blank	0.07	0.091	0.139	Blank	0.103	Blank	0.088
SwRI –RFEC	0.08		0.13			0.06	0.09	0.11		0.10		0.09
GTI – RFEC	0.135 0.102		0.149 0.145			0.089 0.066	0.128 0.094	0.142 0.124		0.121 0.114		0.124 0.009
Battelle – Rotating Permanent Magnet	0.065		0.105			0.085	0.080	0.105		0.085		0.055
Comments												
SwRI –RFEC												
GTI – RFEC	Two pits axially aligned			There was an increase in amplitude in this region. We concluded that the increase in the field was caused by the drive coil being located at P3-14. An actual defect may be "buried" in the field but it is not obvious.		Two pits axially aligned	Two pits axially aligned			Two pits	Reflection from defect 10	Two features
Battelle – Rotating Permanent Magnet	Corrosion patch, with multiple pits of different depths		Single Pit			Corrosion patch, with multiple pits of different depths	Corrosion patch, with multiple pits of different depths	Single Pit		Corrosion patch, with multiple pits of different depths		Corrosion patch, with multiple pits of different depths

Mechanical Damage Assessment

Only one technology, the PNNL *Ultrasonic Strain Measurement* technology, was tested for assessment of mechanical damage. Two 24-inch diameter pipes were inspected by PNNL for mechanical damage. The first pipe (Pipe Sample 1) consisted of two pipes welded together with mechanical damage defects along three rows separated by 120° and measured approximately 28-feet in length. The test line on Pipe Sample 1 consisted of mechanical damage created using a 50-ton track hoe. An example mechanical damage defect from Pipe Sample 1 is shown in Figure 19. The second pipe (Pipe Sample 2) measured approximately 40 feet in length with plain (or smooth) dent defects along one test line. An example mechanical damage defect from Pipe Sample 2 is shown in Figure 20.

Figure 19. Example Mechanical Damage Defect from Pipe Sample 1

Figure 20. Example Mechanical Damage Defect from Pipe Sample 2

The benchmark data and test results for PNNL's *PNNL Ultrasonic Strain Measurement* technology are shown in Table 8 and Table 9.

Table 8. Benchmark vs. Test Results for Mechanical Damage Pipe Sample 1

PIPE SAMPLE 1				
Defect Number	Search Region (from End A)	Dent Severity 0 = No damage 1 = Least Severe 2 = Moderately Severe 3 = Severe 4 = Most Severe		Comments
		Benchmark	PNNL	
D1	64.5"	2	4	dent start at 63.5" end at 66.5", length 3"
D2	68.5"	2	2	dent start at 67" end at 70", length 3"
D3	77.5"	2	1	dent start at 77.3" end at 78.1", length 0.9"
D4	105"	2	2.5	long dent along the axis dent start at 99.9" end at 110.4", length 10.5"
D5	114"	1	2.5	long dent along the axis dent start at 113.8" end at 119.9", length 6.1"
D6	162"	Not Part of Benchmark		detected, damage looks as significant as a 3 or 4, length approximately 6 inches long or two dents approximately 2 inches long separated by 1 inch
	195.5"			damage detected; damage looks as significant as a 3, (1 defect approximately 7 inches long or 2 defects, one 4 inches long and a second 2 inches long separated by approximately 1 inch)
D7	230"	2	3	dent start at 228.1" end at 234.7", length 6.7"
D8	240"	1	2	dent start at 236.4" end at 242.1 length 5.7"
D9	246"	1	0.5	dent start at 245.7" end at 246.2", length 0.5"
D10	267.5"	4	4	similar to calibration defects dent start at 264" end at 270.1", length 6.1"
D11	274"	2	4	similar to calibration defects dent start at 271" end at 276.1 length 5.1"
D12	280.5"	3	4	similar to calibration defects dent start at 277.3" end at 282.6", length 5.3"
D13	305.5"	4	NR	out of scan range
D14	310"	4	NR	out of scan range
D15	313"	3	NR	out of scan range

Table 9. Benchmark vs. Test Results for Mechanical Damage Pipe Sample 2

PIPE SAMPLE 2				
Defect Number	Search Region (from End A)	Dent Severity 0 = No damage 1 = Least Severe 2 = Moderately Severe 3 = Most Severe		Comments
		Benchmark	PNNL	
R03	109.25"	1	1	small degree of damage, start of dent 107" end 110" length 3"
R04	144"	3	2	moderate damage, start of dent 140.25" end 147.5", length 7.25"
R05	183"	2	3	significant damage, start of dent 178.75" end 187.25, length 8.5
R06	217"	1	1	small degree of localized damage, start of dent 215.5" end 220, length 4.5"
R07	253"	2	2	moderate damage, start of dent 250.5" end 258.5, length 8"
R08	289.5"	3	3	significant damage, start of dent 286.75 end 295.25, length 8.5"
R09	325"	2	2	moderate damage, start of dent 323" end 331", length 8"
R10	360.5"	3	3	significant damage, start of dent 359" end 367", length 8"
R11	397"	0	0	no dent

The term "dent severity" is used in this report to describe relative severity of dents within a specific pipe sample. The absolute severity of each dent is not known. Determining the severity of mechanical damage is difficult since there are no standards such as those used for corrosion anomalies. The criteria used to establish the benchmark severity ratings could differ from PNNL's severity criteria and as such may have led to the discrepancies.

PNNL began testing the afternoon of Monday January 10, 2006 and completed testing by the afternoon of Friday January 13, 2006. The PNNL U*ltrasonic Strain Measurement t*echnology only assesses the relative severity of mechanical damage defects. Location of dents is more practically performed by caliper tools and as such was not part of the evaluation criteria for this technology. Additionally, because PNNL was only required to identify dent severity at a specific location the scan speed was also not assessed.

PNNL's technology performed well on the mechanical damage sample with plain dents (Pipe Sample 2). There was discrepancy between the PNNL data and the benchmark at defect sites R04 and R05 on Pipe Sample 2; however the remaining defect locations correlated well.

There were a number of differences between the benchmark data and the PNNL data for Pipe Sample 1. PNNL noted that the multiple dents and the non-circular nature of the pipe from the three rows of dent defects on Pipe Sample 1 created a significant amount of background deformation and thus stress and strain within the pipe sample. Due to these factors, the PNNL U*ltrasonic Strain Measurement* technology was not optimized for the degree of background deformation and is possibly the reason for the discrepancies between the benchmark data and PNNL's results. PNNL indicated that additional tests would be desirable to help classify the dent severity for Pipe Sample 1.

Stress Corrosion Cracking

Only one technology, the ORNL *Shear Horizontal EMAT*, was tested for detection of stress corrosion cracking. ORNL began testing the afternoon of Tuesday January 10, 2006 and completed testing by mid-day Thursday January 12, 2006. The ORNL Shear Horizontal EMAT technology acquired data as their inspection tool was continuously pulled through the pipe sample at the rate of about an inch per second. ORNL took multiple scans through each line to assess the consistency of the signal. Results were not displayed in real time; rather ORNL post processes the captured data to develop final results. ORNL claims post processing is minimal and could easily be performed during data acquisition with current generation computing power.

As shown in Table 10 the technology ran three lines on a 26-inch diameter pipe with natural stress corrosion cracking. The EMAT technology detected one false positive signal on each test line. The configuration of the SCC defects could have contributed to the false positive readings. Because the EMAT configuration scans a minimum of 9-inches of the pipe's circumference, some of the false positives could be the result of other cracks located in close proximity to the SCC defects under evaluation.

Only one defect site (SCC2) provided no discernable signal; however magnetic particle analysis showed that these cracks are small and difficult to detect. Additionally, the location of the crack colony listed as SCC3 is off by a couple of inches. This is possibly due to defect (18), not considered as part of the test and located approximately 3-inches away in the circumferential direction, which may have been detected over the smaller SCC colony in SCC3. The most significant cracks (SCC8, SCC9, and SCC10) in the test sample were detected by the ORNL *Shear Horizontal EMAT* technology. An example SCC defect is shown in Figure 21. The benchmark data and test results for ORNL's *Shear Horizontal EMAT* technology are shown in Table 10.

Figure 21. Example SCC Defect

Table 10. Benchmark vs. ORNL Test Results; SCC Testing

Defect Number	Search Region (from End B)	Benchmark			ORNL		
		Start of Crack Region (from End B)	End of Crack Region (from End B)	Type of SCC	Start of Crack Region (from End B)	End of Crack Region (from End B)	Type of SCC
Test Line 1							
SCC1	242" to 254"	Blank					
SCC2 (5 & 4)	226" to 242"	225.25	238.25	Isolated			
SCC3 (8)	210" to 222"	209.25	212.25	Colony	214	216	Isolated
SCC4	175" to 187"	Blank					
SCC5	140" to 152"	Blank			145	148	Colony; another isolated at 142
Test Line 2							
SCC6	246" to 258"	Blank					
SCC7	234" to 246"	Blank			236	237	Isolated
SCC8 (6)	210" to 222"	210.75	213.5	Colony	210	211	Isolated
SCC9 (7)	188" to 200"	189.25	193.5	Colony	194	196	Colony
SCC10 (9)	140" to 152"	141.5	145.5	Colony	144	149	Colony; looks like gap in the middle; may be 2 sets separated by 1-inch.
Test Line 3							
SCC11 (16)	225" to 245"	224.25	241.25	Colony	237	239	Isolated; After scanning, we documented large dirt patches along line 3 We believe EMATs lifted off the surface due to dirt inside pipe. Reliability of data in this area is low
SCC12	210" to 222"	Blank					
SCC13	188" to 200"	Blank					
SCC14	140" to 152"	Blank			139	141	Isolated

Polyethylene Pipe Defects

Only one technology, the NETL *Capacitive Sensor for Polyethylene Pipe Inspection*, was tested for detection of plastic pipe defects. This technology inspects for small volumetric anomalies with an NETL specified detection threshold of approximately 0.015 cubic inches. The measurement technology is localized and therefore anomalies in close proximity and pipe end effects do not influence its detection capabilities.

A measure of defect significance was established based on the calibration defect which was 3/8-inch in diameter and 50% deep (0.028 cubic inches). The volume of the calibration defect was set at a significance of one. The significance of all other defects was based on the volume of the

calibration defect. An example defect is shown in Figure 22. This defect was calculated to have a volume of 0.04 cubic inches which equals a significance of 1.43. As shown in Table 11, the technology ran one test line on a 6-inch diameter polyethylene pipe sample.

Figure 22. Example Plastic Pipe Defect

Table 11. Benchmark vs. NETL Test Results; Plastic Pipe Testing

Defect Number	Search Region	Benchmark				NETL			Comments
		Defect Location from Side A (to center)	Significance of Defect (volume ratio from calibration defect)	Defect Volume	Defect Diameter	Defect Location from Side A (to center)	Significance of Defect (volume ratio from calibration defect)	Defect Volume	
	inches	inches	ratio	in^3	inches	inches	ratio	in^3	
D1	21" to 27"	25”	1.57	0.044	0.375”	25.06”	1.38	0.039	For significance: defect calibration hole @ 18” = 1 Vol @ 18” = 0.028, Vol @ 25.06 = 0.039
D2	28" to 34"	Blank				None			
D3	35" to 41"	Blank				None			
D4	42" to 48"	46”	0.79	0.022	0.25”	45.62”	0.99	0.028	Volume = 0.028
D5	49" to 55"	53”	0.89	0.025	1/8” wide 1” long saw cut	52.55”	1.31	0.037	Volume = 0.037
D6	56" to 62"	Blank				None			
D7	62" to 70"	67”	1.57	0.044	0.375”	66.36”	1.15	0.033	Volume = 0.033
D8	70" to 76"	Blank				None			
D9	77" to 83"	Blank				None			
D10	84" to 90"	88”	0.61	0.017	0.25”	87.15”	0.43	0.012	Volume = 0.012
D11	91" to 97"	Blank				None			
D12	98" to 104"	102”	1.43	0.04	1/8” wide 1” long saw cut	101.03”	1.61	0.045	Volume = 0.045
D13	105" to 111"	109”	1.43	0.04	0.75”	107.84”	0.71	0.02	Volume = 0.020
D14	112" to 118"	116”	0.54	0.015	0.375”	114.75”	0.57	0.16	Volume = 0.016
D15	119" to 125"	123” and 123.5”	0.61 (each)	0.017 (each)	0.25” (each)	121.89”	0.74	0.74	Volume = 0.021
D16	126" to 132"	Blank				None?			Indications that a consistent amount of material may have been removed along entire length
D17	132" to 138"	Blank				None?			Indications that a consistent amount of material may have been removed along entire length
D18	138" to 144"	140”	1.25	0.035	0.75”	138.3”	1.13	0.032	Volume = 0.032
D19	144" to 150"	148”	1.11	0.031	0.75”	146.76”	0.71	0.020	Volume = 0.020

Not part of the benchmarking demonstration

This page intentionally blank.

While this was the second demonstration for all other technology developers, this demonstration was the first for the NETL *Capacitive Sensor* technology and should be taken into consideration when evaluating the results. During the demonstration, the NETL *Capacitive Sensor* technology collected data at a frequency of 1-hertz but has the capability to collect data up to a frequency of 45-hertz.

NETL's accuracy in assessing defect severity is depicted in Figure 23. The NETL *Capacitive Sensor* technology detection was excellent detecting all defect sites to within 1% of the actual centerline location and did not report any false positive signals. The percentage difference in defect significance was approximately 25%.

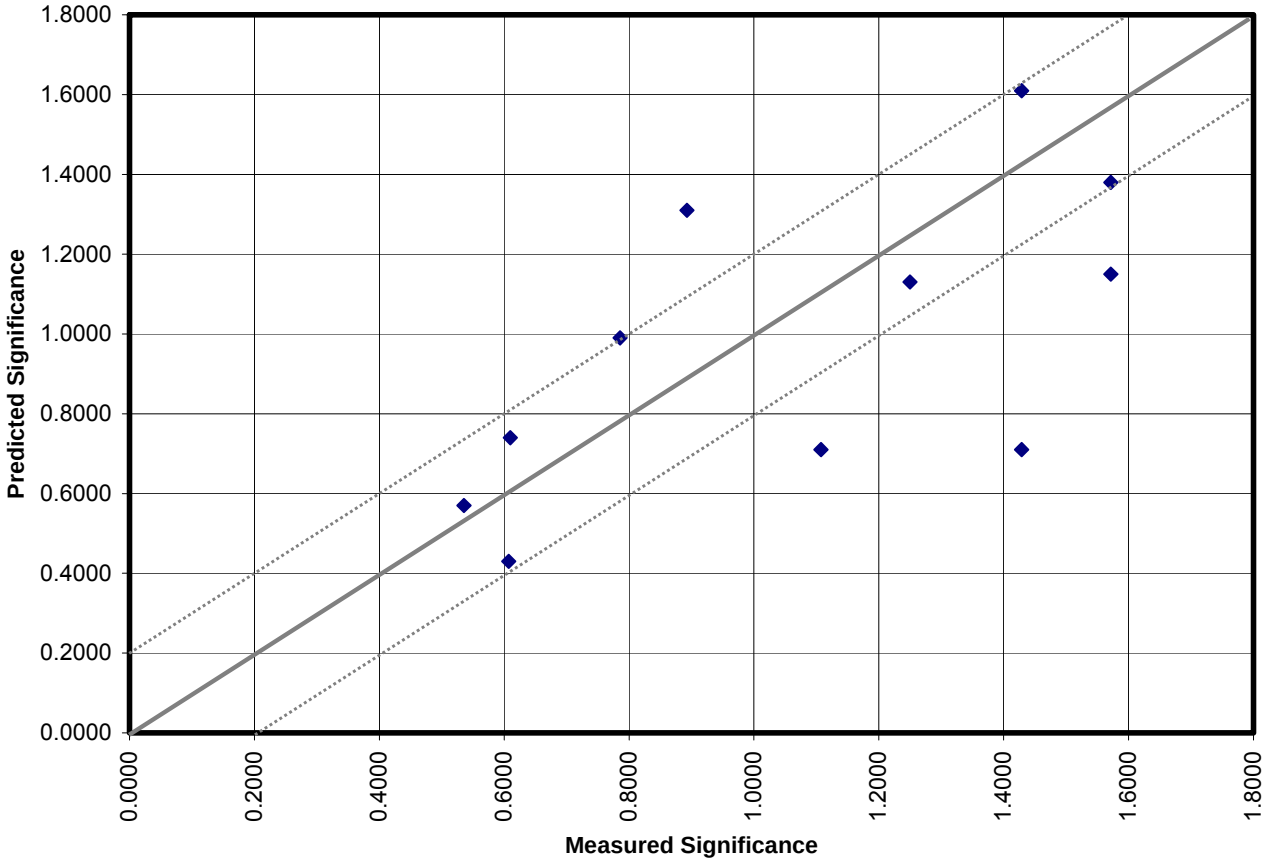

Figure 23. Measured Severity vs. Predicted Severity for the NETL *Capacitive Sensor*

SUMMARY

Four pipeline anomaly conditions were evaluated by six different sensor technology developers. Three technologies assessed corrosion anomalies while individual technologies assessed mechanical damage, SCC, and plastic pipe material loss.

The corrosion detection techniques demonstrated significant promise for inspection of unpiggable pipelines. Accurate detection and sizing of natural corrosion appears to be reachable

but additional development may be required to refine sizing algorithms especially when pipe material properties are unknown and calibration defects are not available. Additional data processing for some of the technologies and collection of larger natural corrosion defect libraries to conduct repeatable testing needs to be established. Future collection of data towards target corrosion on pipe samples pulled from service will improve system capabilities. In addition, the speed at which data is collected could be improved for all of the technologies. The usability of these technologies will rely on their ability to collect data for long pipeline segments in a relatively short amount of time as well as their ability to meet the design and power requirements of the Explorer robotic platform.

PNNL's mechanical damage detection technique also achieved reasonably good results especially in the pipe sample containing only plain dents. Considering the uniqueness of Pipe Sample 1 (multiple dents in close proximity), more accurately assessing the dent severity for this type of pipe sample would be a future goal for PNNL's technology. In-service pipelines with the amount of denting evident on Pipe Sample 1 is highly unlikely and does not represent a realistic pipeline operating scenario. Track hoe defects; however, would be typical of third party damage evident on operating pipelines.

The ORNL EMAT system also performed well detecting natural stress corrosion cracks that formed while the pipeline was in-service. The ORNL EMAT technology did detect some false positives on each test line but was also able to detect the most significant SCC locations. Given the nature of SCC, it is difficult to accurately size crack depths. Some of the cracks used in the benchmarking program may have been too small to clearly detect. Collection of additional SCC defect libraries and crack sizing would be a valuable addition to this benchmarking program.

The NETL *Capacitive Sensor* was quite accurate in identifying defect locations. Sizing of plastic pipe defects is reachable but will require additional research to develop defect sizing algorithms. While this was a successful demonstration of the inspection sensor technology, inspection variables need to be considered in future evaluations.

Following the submittal of their test data, the technology developers were sent the benchmark data. They were given an opportunity to comment on their results and to provide their perspective on their technology's performance relative to the benchmark data. Appendix C contains the developer's comments. Overall, the technologies performed well and the results are encouraging. As the development of these technologies progresses and future testing takes place, it is envisioned that improvements in the technology and data analysis techniques will continue to improve the false positive rate and enhance the precision and accuracy of the defect signals.

PATH FORWARD

As noted, PHMSA Pipeline Safety R&D Program goals are to understand the gaps between existing technologies and those needed to resolve the key pipeline issues. One recognized path forward is to integrate successfully demonstrated sensor technologies into a robotic platform/sensor system that can be deployed remotely as part of an integrated package. This effort is driven in large part by new PSIA regulations which require inspection of gas

transmission pipelines and distribution mains in high-consequence areas. A large percentage of these pipes cannot be inspected using typical “smart-pig” techniques because of diameter restrictions, pipe bends and valves. In addition, pressure differentials and flow can be too low to push a pig through some pipes. To help solve these problems, the PHMSA Pipeline Safety R&D Program has established an aggressive schedule to develop a prototype remote system which includes continued co-funding with industry partners. It is anticipated that upon completion of the prototype systems, they will be able to traverse all pipes (including unpiggable lines) of various diameters while providing continuous, real-time detection of pipe anomalies or defects.

This page intentionally blank.

APPENDIX A – BENCHMARK DATA

Detection of Metal Loss - Page 1

Name:	
Date:	
Company:	
Sensor Design:	

CALIBRATION DATA

Pipe Sample	Calibration Metal Loss Location	Metal Loss Length & Width	Depth of Metal Loss	Measured Length & Width of Defect	Measured Max. Depth of Defect	Comments
	inches from End B to center of defect	inches	inches			
			PIPE SAMPLE 1:			
Calibration P1-1:	361" (59" from End A)	2 x 2	See profile			

TEST DATA

Pipe Sample:	**PIPE SAMPLE 1**
Defect Set:	8" Diameter, 0.188" Wall Thickness Pipe Sample; Schedule 10; Length = 34' 11.75"

TEST LINE 1

Defect Number	Search Region (Distance from End B)	Start of Metal Loss Region from Side B	End of Metal Loss Region from Side B	Total Length of Metal Loss Region	Width of Metal Loss Region	Maximum Depth of Metal Loss Region	Additional Data Attached?	Comments
	inches	inches	inches	inches	inches	inches	Y/N	
P1-12	52" to 64"	**56.75"**	**60.875"**	**4.125"**	**2"**	**0.122"**	**Y**	**Defect 6**
P1-11	76" to 88"	**---**	**---**	**---**	**---**	**---**	**N**	**BLANK 6**
P1-10	100" to 112"	**---**	**---**	**---**	**---**	**---**	**N**	**BLANK 5**
WELD	120"							
P1-9	120" to 144"	**120"**	**140.25"**	**20.25"**	**Full Circumference**	**0.146"**	**Y**	**P1-NC1**
P1-8	160" to 172"	**---**	**---**	**---**	**---**	**---**	**N**	**BLANK 4 (natural corrosion pipe segment)**
WELD	180"							
P1-7	184" to 196"	**190.625"**	**192.75"**	**2.125"**	**2"**	**0.147"**	**Y**	**Defect 5**
P1-6	208" to 220"	**---**	**---**	**---**	**---**	**---**	**N**	**BLANK 3**
P1-5	232" to 244"	**232.75"**	**235.75"**	**3"**	**1"**	**0.081"**	**Y**	**Defect 4**
P1-4	256" to 268"	**259.625"**	**263.625"**	**4"**	**2"**	**0.063"**	**Y**	**Defect 3**
P1-3	280" to 292"	**287.75"**	**290.875"**	**3.125"**	**2"**	**0.096"**	**Y**	**Defect 2**
P1-2	304" to 316"	**---**	**---**	**---**	**---**	**---**	**N**	**BLANK 2**
P1-1	328" to 340"	**---**	**---**	**---**	**---**	**---**	**N**	**BLANK 1**

TEST LINE 2

Defect Number	Search Region (Distance from End B)	Start of Metal Loss Region from Side B	End of Metal Loss Region from Side B	Total Length of Metal Loss Region	Width of Metal Loss Region	Maximum Depth of Metal Loss Region	Additional Data Attached?	Comments
	inches	inches	inches	inches	inches	inches	Y/N	
P1-23	74" to 86"	**79.75"**	**83.75"**	**4"**	**2"**	**0.097"**	**Y**	**Defect 11**
P1-22	98" to 110"	**108"**	**110"**	**2"**	**2"**	**0.12"**	**Y**	**Defect 10**
WELD	120"							
P1-21	120" to 144"	**120"**	**140.75"**	**20.75"**	**Full Circumference**	**0.127"**	**Y**	**P1-NC2**
P1-20	160" to 172"	**---**	**---**	**---**	**---**	**---**	**N**	**BLANK 11 (natural corrosion pipe segment)**
WELD	180"							
P1-19	186" to 198"	**---**	**---**	**---**	**---**	**---**	**N**	**BLANK 10**
P1-18	210" to 222"	**213.625"**	**217.875"**	**4.25"**	**2"**	**0.145"**	**Y**	**Defect 9**
P1-17	234" to 246"	**---**	**---**	**---**	**---**	**---**	**N**	**BLANK 9**
P1-16	258" to 270"	**---**	**---**	**---**	**---**	**---**	**N**	**BLANK 8**
P1-15	282" to 294"	**---**	**---**	**---**	**---**	**---**	**N**	**BLANK 7**
P1-14	306" to 318"	**308.875"**	**312"**	**3.125"**	**1"**	**0.115"**	**Y**	**Defect 8**
P1-13	330" to 342"	**335.75"**	**339.625"**	**3.875"**	**1.75"**	**0.095"**	**Y**	**Defect 7**

Benchmarking of Inspection Technologies
Detection of Metal Loss - Page 2

Name:	
Date:	
Company:	
Sensor Design:	

CALIBRATION DATA

Pipe Sample	Calibration Metal Loss Location	Metal Loss Length & Width	Depth of Metal Loss	Measured Length & Width of Defect	Measured Max. Depth of Defect	Comments
	inches from End B to center of defect	inches	inches			
PIPE SAMPLE 2:						
Calibration P2-1:	301.5" (58.5" from End A)	3 x 1	See profile			
Calibration P2-2:	275" (85" from End A)	2 x 2	See profile			

TEST DATA

Pipe Sample:	**PIPE SAMPLE 2**
Defect Set:	8" Diameter, 0.188" Wall Thickness Pipe Sample; Schedule 10; Length = 30' 0.375"

TEST LINE 1

Defect Number	Search Region (Distance from End B)	Start of Metal Loss Region from Side B	End of Metal Loss Region from Side B	Total Length of Metal Loss Region	Width of Metal Loss Region	Maximum Depth of Metal Loss Region	Additional Data Attached?	Comments
	inches	inches	inches	inches	inches	inches	Y/N	
P2-11	54" to 66"	---	---	---	---	---	N	BLANK 6
P2-10	78" to 90"	80.125"	84.5"	4.375"	2"	0.147"	Y	Defect 5
P2-9	102" to 114"	108.125"	112.25"	4.125"	2"	0.158"	Y	Defect 4
WELD	120"							
P2-8	126" to 138"	---	---	---	---	---	N	BLANK 5
P2-7	150" to 162"	153.125"	156.375"	3.25"	1"	0.085"	Y	Defect 3
P2-6	174" to 186"	180.25"	183.375"	3.125"	1"	0.114"	Y	Defect 2
P2-5	198" to 210"	---	---	---	---	---	N	BLANK 4
P2-4	222" to 234"	227.25"	229.375"	2.125"	2"	0.079"	Y	Defect 1
P2-3	246" to 258"	---	---	---	---	---	N	BLANK 3
P2-2	270" to 282"	---	---	---	---	---	N	BLANK 2
P2-1	294" to 306"	---	---	---	---	---	N	BLANK 1

TEST LINE 2

Defect Number	Search Region (Distance from End B)	Start of Metal Loss Region from Side B	End of Metal Loss Region from Side B	Total Length of Metal Loss Region	Width of Metal Loss Region	Maximum Depth of Metal Loss Region	Additional Data Attached?	Comments
	inches	inches	inches	inches	inches	inches	Y/N	
P2-20	54" to 66"	57.75"	60.875"	3.125"	1"	0.188"	Y	Defect 11; through hole
P2-19	78" to 90"	---	---	---	---	---	N	BLANK 11
P2-18	102" to 114"	---	---	---	---	---	N	BLANK 10
WELD	120"							
P2-17	126" to 138"	130"	134.125"	4.125"	2"	0.112"	Y	Defect 10
P2-16	150" to 162"	---	---	---	---	---	N	BLANK 9
P2-15	174" to 186"	---	---	---	---	---	N	BLANK 8
P2-14	198" to 210"	202.625"	205.75"	3.125"	1"	0.105"	Y	Defect 9
P2-13	222" to 234"	---	---	---	---	---	N	BLANK 7
P2-12	246" to 258"	248.125"	250.25"	2.125"	2"	0.14"	Y	Defect 8

Benchmarking of Inspection Technologies
Detection of Metal Loss - Page 3

Name:	
Date:	
Company:	
Sensor Design:	

CALIBRATION DATA

Pipe Sample	Calibration Metal Loss Location	Metal Loss Length & Width	Depth of Metal Loss	Measured Length & Width of Defect	Measured Max. Depth of Defect	Comments
	inches from End B to center of defect	inches	inches			
			PIPE SAMPLE 3:			
Calibration P3-1:	421" (59" from End A)	2 x 2	See profile			

TEST DATA

Pipe Sample:	**PIPE SAMPLE 3**
Defect Set:	8" Diameter, 0.188" Wall Thickness Pipe Sample; Schedule 10; Length = 40' 0.25"

TEST LINE 1

Defect Number	Search Region (Distance from End B)	Start of Metal Loss Region from Side B	End of Metal Loss Region from Side B	Total Length of Metal Loss Region	Width of Metal Loss Region	Maximum Depth of Metal Loss Region	Additional Data Attached?	Comments
	inches	inches	inches	inches	inches	inches	Y/N	
P3-11	66" to 78"	---	---	---	---	---	N	BLANK 5
P3-10	102" to 114"	106.375"	109.625"	3.25"	1"	0.156"	Y	Defect 7
P3-9	138" to 150"	143.665"	144.335"	0.67"	0.67"	0.120"	N	Defect 6; machined defect
P3-8	162" to 174"	---	---	---	---	---	N	BLANK 4
P3-7	186" to 198"	189.875"	194"	4.125"	2"	0.115"	Y	Defect 5
P3-6	222" to 234"	---	---	---	---	---	N	BLANK 3
WELD	240"							
P3-5	270" to 282"	275"	277.25"	2.25"	2"	0.103"	Y	Defect 4
P3-4	300" to 312"	305.625"	306.375"	0.75"	0.75"	0.148"	N	Defect 3; machined defect
P3-3	330" to 342"	335"	337.25"	2.25"	2"	0.133"	Y	Defect 2
P3-2	360" to 372"	---	---	---	---	---	N	BLANK 2
P3-1	384" to 396"	---	---	---	---	---	N	BLANK 1

TEST LINE 2

Defect Number	Search Region (Distance from End B)	Start of Metal Loss Region from Side B	End of Metal Loss Region from Side B	Total Length of Metal Loss Region	Width of Metal Loss Region	Maximum Depth of Metal Loss Region	Additional Data Attached?	Comments
	inches	inches	inches	inches	inches	inches	Y/N	
P3-23	66" to 78"	69.5"	73.625"	4.125"	2"	0.088"	Y	Defect 14
P3-22	102" to 114"	---	---	---	---	---	N	BLANK 10
P3-21	126" to 138"	130"	134.125"	4.125"	2"	0.103"	Y	Defect 13
P3-20	156" to 168"	---	---	---	---	---	N	BLANK 9
P3-19	180" to 192"	185.765"	186.485"	0.72"	0.72"	0.139"	N	Defect 12; machined defect
P3-18	210" to 222"	214.5"	217.625"	3.125"	1"	0.091"	Y	Defect 11
WELD	240"							
P3-17	248" to 260"	250.625"	253.75"	3.125"	1"	0.07"	Y	Defect 10
P3-16	282" to 294"	---	---	---	---	---	N	BLANK 8
P3-15	306" to 318"	---	---	---	---	---	N	BLANK 7
P3-14	330" to 342"	335.875"	336.625"	0.75"	0.75"	0.154"	N	Defect 9; machined defect
P3-13	356" to 368"	---	---	---	---	---	N	BLANK 6
P3-12	390" to 402"	392.25"	396.375"	4.125"	2"	0.094"	Y	Defect 8

This page intentionally blank.

Benchmarking of Inspection Technologies
Detection of Mechanical Damage - Page 1

Name:	
Date:	
Company:	
Sensor Design:	

CALIBRATION DATA

	Dent Locations	Total Length of Dent Region	Maximum Depth of Dent Region	Relative Dent Severity	Comments
	inches from end A to center of dents	inches	Depth measured with deformation sensor (in)	0 = No damage 1 = Least Severe 2 = Moderately Severe 3 = Severe 4 = Most Severe	Dent severity is relative to the pipe sample being evaluated. Do NOT interpret dent severity between Pipe Sample 1 and Pipe Sample 2; only evaluate the relative severity between dents in the same pipe sample.
Mechanical Damage Pipe SAMPLE 1 (~28 feet)					
Calibration Dent P06dTH1:	1' 8"	20	-.025"	0	
	1' 11"	20	.075"	1	
	2' 2"	20	.325"	3	
	2' 5"	20	.150"	2	
	2' 8"	20	.200"	3	
	2' 11"	20	0	0	
	3' 2"	20	.325"	3	
	3' 5"	20	0.75"	1	
Mechanical Damage Pipe SAMPLE 2 (40' 1.5")					
Calibration Dent R01:	42.25"	3.5	1.2%	1	
Calibration Dent R02:	73.25"	8.5	0.8%	2	

TEST DATA

Pipe Sample:	**SAMPLE 1**
Defect Set:	24" Diameter Pipe with Mechanical Damage; Length =~28'

Defect Number	Search Region (Distance from End A to Center of Dent)	Dent Severity	Commments
	feet & inches	0 = No damage 1 = Least Severe 2 = Moderately Severe 3 = Severe 4 = Most Severe	
D1	5' 4.5"	**2**	**Deformation data indicates max dent depth of 0.225 inches**
D2	5' 8.5"	**2**	**Deformation data indicates max dent depth of 0.24 inches**
D3	6' 5.5"	**2**	
D4	8' 9"	**2**	**Deformation data indicates max dent depth of 0.15 inches**
D5	9' 6"	**1**	**Deformation data indicates max dent depth of 0.075 inches**
WELD	10' 5.5"		
D6	13' 6"	**4**	**GOUGE NOT PART OF DEMONSTRATION; Deformation data indicates max dent depth of 0.42 inches**
D7	19' 2"	**2**	**Deformation data indicates max dent depth of 0.28 inches**
D8	20'	**1**	**Deformation data indicates max dent depth of 0.125 inches**
D9	20' 6"	**1**	**Deformation data indicates max dent depth of 0.10 inches**
D10	22' 3.5"	**4**	**Deformation data indicates max dent depth of 0.48 inches**
D11	22' 10"	**2**	**Deformation data indicates max dent depth of 0.20 inches**
D12	23' 4.5"	**3**	**Deformation data indicates max dent depth of 0.30 inches**
D13	25' 5.5"	**4**	**Deformation data indicates max dent depth of 0.48 inches**
D14	25' 10"	**4**	**Deformation data indicates max dent depth of 0.48 inches**
D15	26' 1"	**3**	**Deformation data indicates max dent depth of 0.30 inches**

This page intentionally blank.

Benchmarking of Inspection Technologies Detection of Mechanical Damage - Page 2	
Name:	
Date:	
Company:	
Sensor Design:	

TEST DATA	
Pipe Sample:	**SAMPLE 2**
Defect Set:	24" Diameter Pipe with Mechanical Damage; Length = 40' 1.5"

Defect Number	Search Region (Distance from End A to Center of Dent)	Dent Severity	Comments
	inches	0 = No damage 1 = Least Severe 2 = Moderate Severity 3 = Most Severe	
R03	109.25"	**1**	**R03 = Calibration Dent R01 = R06**
R04	144"	**3**	**R04 = R08 = R10**
R05	183"	**2**	**R05 = Calibration Dent R02 = R07 = R09**
R06	217"	**1**	**R03 = Calibration Dent R01 = R06**
R07	253"	**2**	**R05 = Calibration Dent R02 = R07 = R09**
R08	289.5"	**3**	**R04 = R08 = R10**
R09	325"	**2**	**R05 = Calibration Dent R02 = R07 = R09**
R10	360.5"	**3**	**R04 = R08 = R10**
R11	397"	**0**	**Blank**

Benchmarking of Inspection Technologies Detection of SCC - Page 1	
Name:	
Date:	
Company:	
Sensor Design:	

CALIBRATION DATA						
Pipe Sample: 993	Calibration Crack Location	Length	Depth	Measured Length	Measured Depth	Comments
	inches from end B	inches	% wall thickness			
1	186.4	2.5				multiple cracks; max = ~3/4"
2	58.7	5				multiple cracks; max = ~1/4"
3	86.4	5				multiple cracks; max = ~3 1/4"
4	82.4	2.5				multiple cracks; max = ~1/2"
5	44.4	3				multiple cracks; max = ~1/2"
Blank Area:						

TEST DATA	
Pipe Sample:	**893**
Defect Set:	26" Diameter Pipe with Stress Corrosion Cracks; Length = 26 feet
	TEST LINE 1

Defect Number	Search Region (Distance from End B)	Start of Crack Region from Side B	End of Crack Region from Side B	Type of SCC	Comments
	inches	inches	inches		
SCC5 (Blank 1)	140" to 152"	---	---	☐ Isolated Crack ☐ Colony of Cracks ☑ **None**	**Blank 1**
SCC4 (Blank 2)	175" to 187"	---	---	☐ Isolated Crack ☐ Colony of Cracks ☑ **None**	**Blank 2**
SCC3 (8)	210" to 222"	**209.25**	**212.25**	☐ Isolated Crack ☑ **Colony of Cracks** ☐ None	**Multiple 1/4" cracks; cracked area 2 3/4" by 2 1/2"**
SCC2 (5 & 4)	226" to 242"	**225.25**	**238.25**	☑ **Isolated Cracks** ☐ Colony of Cracks ☐ None	**Two isolated cracks; cracked area 4" by 1 1/2" with ~2" long crack; cracked area 5 1/4" by 1 1/4" with ~3" long crack**
SCC1 (Blank 3)	242" to 254"	---	---	☐ Isolated Crack ☐ Colony of Cracks ☑ **None**	**Blank 3**

Benchmarking of Inspection Technologies Detection of SCC - Page 2					
Name:					
Date:					
Company:					
Sensor Design:					
TEST DATA					
Pipe Sample:	893				
Defect Set:	26" Diameter Pipe with Stress Corrosion Cracks; Length = 26 feet				
	TEST LINE 2				
Defect Number	Search Region (Distance from End B)	Start of Crack Region from Side B	End of Crack Region from Side B	Type of SCC	Comments
	inches	inches	inches		
SCC10 (9)	140" to 152"	141.5	145.5	☐ Isolated Crack ☑ Colony of Cracks ☐ None	Multiple cracks; max ~1/4" long; cracked area 3 1/2" by 3 1/2"
SCC9 (7)	188" to 200"	189.25	193.5	☐ Isolated Crack ☑ Colony of Cracks ☐ None	Multiple cracks; max ~1/4" long; cracked area 4 1/4" by 3 3/4"
SCC8 (6)	210" to 222"	210.75	213.5	☐ Isolated Crack ☑ Colony of Cracks ☐ None	Multiple cracks; max ~1/2" long; cracked area 3" by 2 1/2"
SCC7 (Blank 4)	234" to 246"	---	---	☐ Isolated Crack ☐ Colony of Cracks ☑ None	Blank
SCC6 (Blank 5)	246" to 258"	---	---	☐ Isolated Crack ☐ Colony of Cracks ☑ None	Blank

Benchmarking of Inspection Technologies Detection of SCC - Page 3					
Name:					
Date:					
Company:					
Sensor Design:					
TEST DATA					
Pipe Sample:	**893**				
Defect Set:	26" Diameter Pipe with Stress Corrosion Cracks; Length = 26 feet				
	TEST LINE 3				
Defect Number	Search Region (Distance from End B)	Start of Crack Region from Side B	End of Crack Region from Side B	Type of SCC	Comments
	inches	inches	inches		
SCC14 **(Blank 6)**	140" to 152"	**---**	**---**	☐ Isolated Crack ☐ Colony of Cracks ☑ **None**	**Blank**
SCC13 **(Blank 7)**	188" to 200"	**---**	**---**	☐ Isolated Crack ☐ Colony of Cracks ☑ **None**	**Blank**
SCC12 **(Blank 8)**	210" to 222"	**---**	**---**	☐ Isolated Crack ☐ Colony of Cracks ☑ **None**	**Blank**
SCC11 **(16)**	225" to 245"	**224.25**	**241.25**	☐ Isolated Crack ☑ **Colony of Cracks** ☐ None	**Multiple cracks; max ~3/4" long; cracked area 17" by 1 3/4"**

Benchmarking of Inspection Technologies
Detection of Plastic Pipe Defects - Page 1

Name:	
Date:	
Company:	
Sensor Design:	

CALIBRATION DATA

Defect	Calibration Defect Location	Volume of Defect	Depth of Defect	Diameter of Defect	Comments
	inches from end A	cubic inches	inches	inches	
C1:	18	0.028	0.25	0.375	

TEST DATA

Pipe Sample:	**PLASTIC PIPE SAMPLE**
Pipe Parameters:	6" Diameter, 0.5" Wall Thickness Pipe Sample, ~13' in length

LINE 1

Defect Number	Search Region (Distance from End A)	Location of Defect Region from Side A	Significance of Defect (based on volume ratio from calibration defect)	Volume of Defect (in^3) (provided to participant after defect signif reported)	Depth of Defect (in) (provided to participant after defect signif reported)	Diameter of Defect (in) (provided to participant after defect signif reported)	Comments
	inches	inches	Calibration Defect = 1 Less Severe <1 More Severe >1	cubic inches	inches	inches	
D1	21" to 27"	**25"**	**1.57**	**0.044**	**0.4**	**0.375**	
D2	28" to 34"	**BLANK**	**0**	**----**	**----**	**----**	
D3	35" to 41"	**BLANK**	**0**	**----**	**----**	**----**	
D4	42" to 48"	**46"**	**0.79**	**0.022**	**0.45**	**0.25**	
D5	49" to 55"	**53"**	**0.89**	**0.025**	**0.2**	**0.125**	**Saw Cut ~1" long and 1/8" wide**
D6	56" to 62"	**BLANK**	**0**	**----**	**----**	**----**	
D7	63" to 69"	**67"**	**1.57**	**0.044**	**0.4**	**0.375**	**Same as D1**
D8	70" to 76"	**BLANK**	**0**	**----**	**----**	**----**	
D9	77" to 83"	**BLANK**	**0**	**----**	**----**	**----**	
D10	84" to 90"	**88"**	**0.61**	**0.017**	**0.35**	**0.25**	
D11	91" to 97"	**BLANK**	**0**	**----**	**----**	**----**	
D12	98" to 104"	**102"**	**1.43**	**0.04**	**0.35**	**0.125**	**Saw Cut ~0.9" long and 1/8" wide**
D13	105" to 111"	**109"**	**1.43**	**0.04**	**0.09**	**0.75**	
D14	112" to 118"	**116"**	**0.54**	**0.015**	**0.14**	**0.375**	
D15	119" to 125"	**123" and 123.5"**	**0.61 (each)**	**0.017 (each)**	**0.35 (each)**	**0.25 (each)**	**Defect consists of two identical holes 1/2" apart**
D16	126" to 132"	**BLANK**	**0**	**----**	**----**	**----**	
D17	132" to 138"	**BLANK**	**0**	**----**	**----**	**----**	
D18	138" to 144"	**140"**	**1.25**	**0.035**	**0.08**	**0.75**	
D19	144" to 150"	**148"**	**1.11**	**0.031**	**0.07**	**0.75**	

This page intentionally blank.

APPENDIX B – DEMONSTRATION TEST DATA

SOUTHWEST RESEARCH INSTITUTE (SWRI)
DEMONSTRATION TEST DATA

This page intentionally blank.

Benchmarking of Inspection Technologies
Detection of Metal Loss - Page 1

Name:	Gary Burkhardt
Date:	27-Jan-06
Company:	Southwest Research Institute
Sensor Design:	RFEC

CALIBRATION DATA

Pipe Sample	Calibration Metal Loss Location	Metal Loss Length & Width	Depth of Metal Loss	Measured Length & Width of Defect	Measured Max. Depth of Defect	Comments
	inches from End B to center of defect	inches	inches			
		PIPE SAMPLE 1:				
Calibration P1-1:	359 (59 from End A)	2 x 2	See profile			
		PIPE SAMPLE 2:				
Calibration P2-1:	298.5 (58.5 from End A)	3 x 1	See profile			
Calibration P2-2:	277 (85 from End A)	2 x 2	See profile			
		PIPE SAMPLE 3:				
Calibration P3-1:	(59 from End A)	2 x 2	See profile			

TEST DATA

Pipe Sample: **PIPE SAMPLE 1**

Defect Set: 8" Diameter, 0.188" Wall Thickness Pipe Sample; Schedule 10; Length = 34' 11.75"

TEST LINE 1

Defect Number	Search Region (Distance from End B)	Start of Metal Loss Region from Side B	End of Metal Loss Region from Side B	Total Length of Metal Loss Region	Width of Metal Loss Region	Maximum Depth of Metal Loss Region	Additional Data Attached?	Comments
	inches	inches	inches	inches	inches	inches	Y/N	
P1-12	52" to 64"	56.9	60.2	3.32	1.63	0.13	N	
P1-11	76" to 88"							No indication
P1-10	100" to 112"							No indication
WELD	120"							
P1-9	120" to 144"	a=120, b=128.5	a=122.3, b=129.3	a=2.25, b=0.77	a=1.82, b=Full Circ.	a=0.066, b=.083	N	Two defects in region, designated a and b.
P1-8	160" to 172"	160.0	172.0	12.00	Full Circ.	0.18	N	Appears to be large region of general wall thinning that extends out of the designated region. Signal patterns are not characteristic of the calibration defects.
WELD	180"							
P1-7	184" to 196"	188.8	189.7	0.95	1.92	0.09	N	
P1-6	208" to 220"							No indication
P1-5	232" to 244"	227.7	231.0	3.30	1.09	0.08	N	Defect type signal outside stated region.
P1-4	256" to 268"	254.5	258.7	4.20	1.95	0.06	N	
P1-3	280" to 292"	282.6	285.8	3.16	1.25	0.10	N	
P1-2	304" to 316"							No indication
P1-1	328" to 340"							No indication

TEST LINE 2

Defect Number	Search Region (Distance from End B)	Start of Metal Loss Region from Side B	End of Metal Loss Region from Side B	Total Length of Metal Loss Region	Width of Metal Loss Region	Maximum Depth of Metal Loss Region	Additional Data Attached?	Comments
	inches	inches	inches	inches	inches	inches	Y/N	
P1-23	74" to 86"	79.9	81.4	1.48	1.72	0.09	N	
P1-22	98" to 110"	108.1	110.1	1.99	1.82	0.08	N	
WELD	120"							
P1-21	120" to 144"	128.9	129.7	0.79	Full Circ.	0.06	N	
P1-20	160" to 172"	160.0	172.0	12.00	Full Circ.	0.18	N	Appears to be large region of general wall thinning that extends out of the designated region. Signal patterns are not characteristic of the calibration defects.
WELD	180"							
P1-19	186" to 198"							No indication
P1-18	210" to 222"	214.0	218.1	4.13	1.69	0.14	N	
P1-17	234" to 246"							No indication
P1-16	258" to 270"							No indication
P1-15	282" to 294"							No indication
P1-14	306" to 318"	309.5	312.8	3.31	1.37	0.11	N	
P1-13	330" to 342"	335.8	339.9	4.04	1.47	0.08	N	

Benchmarking of Inspection Technologies
Detection of Metal Loss - Page 2

Name:	Gary Burkhardt
Date:	27-Jan-06
Company:	Southwest Research Institute
Sensor Design:	RFEC

TEST DATA

Pipe Sample:	**PIPE SAMPLE 2**
Defect Set:	8" Diameter, 0.188" Wall Thickness Pipe Sample; Schedule 10; Length = 30' 0.375"

TEST LINE 1

Defect Number	Search Region (Distance from End B)	Start of Metal Loss Region from Side B	End of Metal Loss Region from Side B	Total Length of Metal Loss Region	Width of Metal Loss Region	Maximum Depth of Metal Loss Region	Additional Data Attached?	Comments
	inches	inches	inches	inches	inches	inches	Y/N	
P2-11	54" to 66"							No indication
P2-10	78" to 90"	80.0	84.3	4.31	1.88	0.13	N	
P2-9	102" to 114"	108.2	112.3	4.05	2.14	0.16	N	
WELD	120"							
P2-8	126" to 138"	129.8	131.1	1.38	1.06	0.17	N	Repeatable signal, but does not have typical flaw signal characteristics
P2-7	150" to 162"	153.4	156.7	3.31	1.18	0.04	N	
P2-6	174" to 186"	180.2	183.5	3.23	0.99	0.11	N	
P2-5	198" to 210"							No indication
P2-4	222" to 234"	227.6	229.8	2.21	1.57	0.07	N	
P2-3	246" to 258"							No indication
P2-2	270" to 282"							No indication
P2-1	294" to 306"							No indication

TEST LINE 2

Defect Number	Search Region (Distance from End B)	Start of Metal Loss Region from Side B	End of Metal Loss Region from Side B	Total Length of Metal Loss Region	Width of Metal Loss Region	Maximum Depth of Metal Loss Region	Additional Data Attached?	Comments
	inches	inches	inches	inches	inches	inches	Y/N	
P2-20	54" to 66"	56.3	59.7	3.37	1.25	0.16	N	
P2-19	78" to 90"							No indication
P2-18	102" to 114"							No indication
WELD	120"							
P2-17	126" to 138"	129.1	133.2	4.14	1.69	0.11	N	
P2-16	150" to 162"							No indication
P2-15	174" to 186"							No indication
P2-14	198" to 210"	202.3	205.4	3.10	1.21	0.08	N	
P2-13	222" to 234"							No indication
P2-12	246" to 258"	248.1	249.8	1.72	1.21	0.11	N	

Benchmarking of Inspection Technologies
Detection of Metal Loss - Page 3

Name:	Gary Burkhardt
Date:	27-Jan-06
Company:	Southwest Research Institute
Sensor Design:	RFEC

TEST DATA

Pipe Sample:	**PIPE SAMPLE 3**
Defect Set:	8" Diameter, 0.188" Wall Thickness Pipe Sample; Schedule 10; Length = 40' 0.25"

TEST LINE 1

Defect Number	Search Region (Distance from End B)	Start of Metal Loss Region from Side B	End of Metal Loss Region from Side B	Total Length of Metal Loss Region	Width of Metal Loss Region	Maximum Depth of Metal Loss Region	Additional Data Attached?	Comments
	inches	inches	inches	inches	inches	inches	Y/N	
P3-11	66" to 78"							No indication
P3-10	102" to 114"	106.7	109.9	3.19	1.29	0.15	N	
P3-9	138" to 150"	144.1	144.8	0.73	0.63	0.09	N	
P3-8	162" to 174"							No indication
P3-7	186" to 198"	190.5	194.8	4.22	1.64	0.10	N	
P3-6	222" to 234"							No indication
WELD	240"							
P3-5	270" to 282"	276.0	278.3	2.29	1.93	0.09	N	
P3-4	300" to 312"	306.8	307.6	0.78	0.88	0.11	N	
P3-3	330" to 342"	336.3	338.5	2.19	1.80	0.09	N	
P3-2	360" to 372"							No indication
P3-1	384" to 396"							No indication

TEST LINE 2

Defect Number	Search Region (Distance from End B)	Start of Metal Loss Region from Side B	End of Metal Loss Region from Side B	Total Length of Metal Loss Region	Width of Metal Loss Region	Maximum Depth of Metal Loss Region	Additional Data Attached?	Comments
	inches	inches	inches	inches	inches	inches	Y/N	
P3-23	66" to 78"	69.5	73.8	4.30	1.85	0.09	N	
P3-22	102" to 114"							No indication
P3-21	126" to 138"	130.5	134.5	3.97	1.48	0.10	N	
P3-20	156" to 168"							No indication
P3-19	180" to 192"	186.4	187.2	0.81	0.73	0.11	N	
P3-18	210" to 222"	215.2	218.4	3.18	1.10	0.09	N	
WELD	240"							
P3-17	248" to 260"	251.6	254.8	3.21	0.79	0.06	N	
P3-16	282" to 294"							No indication
P3-15	306" to 318"							No indication
P3-14	330" to 342"	336.9	337.7	0.72	0.51	0.13	N	
P3-13	356" to 368"							No indication
P3-12	390" to 402"	392.5	396.6	4.18	1.69	0.08	N	

This page intentionally blank.

Comments on Tests Performed During Demonstration at Battelle: "Phase II Benchmarking Emerging Pipeline Inspection Technologies" January 9–13, 2006

APPLICATION OF REMOTE-FIELD EDDY CURRENT (RFEC) TESTING TO INSPECTION OF UNPIGGABLE PIPELINES

OTHER TRANSACTION AGREEMENT DTRS56-02-T-0001
SwRI® PROJECT 14.06162
PIPELINE AND HAZARDOUS MATERIALS SAFETY ADMNISTRATION
U.S. DEPARTMENT OF TRANSPORTATION

SOUTHWEST RESEARCH INSTITUTE®

January 2006

Demonstration tests of the remote-field eddy current (RFEC) method for inspection of 8-inch pipe were performed by Southwest Research Institute® (SwRI®). The target application of the inspection technology is to integrate it with the Explorer II robot under development by Carnegie Mellon University. Therefore, the approach taken by SwRI was to perform the demonstration using a tool that meets the requirements and specifications for the Explorer II robot. All of the instrumentation (except for external power, which will be supplied by the robot), including excitation signal generation, amplification, filtering, multiplexing, analog-to-digital conversion, and digital signal processing (to provide phase-sensitive signal detection), was located on the RFEC tool. Total power required was less than half of the power budget available from the robot. Communication of commands and transfer of the processed signal data to an external computer were accomplished using a CAN bus—the same bus that will be used on the robot. Although the tool incorporated 8 channels (coverage of 60 degrees circumferentially) instead of the 48 channels intended for the robot tool (to achieve 360 degrees coverage), the circuitry is readily scalable to the full number of channels. Data were acquired by all 8 channels simultaneously during a single scan. The scans were made at a velocity of 1.5 inches/sec, and it was demonstrated that 4 inches/sec (the maximum scan speed of the robot) was possible. The data were post-processed for analysis to determine defect characteristics (length, width, and depth) using software that is readily adaptable to field inspections

The development of hardware that meets constraints associated with factors such as scan speed, power, and size always results in compromises that are not factors if, for example, laboratory instrumentation is used and if scan speeds are very slow. For example, slow scan speeds mean that significantly greater noise-reduction filtering can be used because time constants can be very long compared to those necessitated by fast scan speeds. Laboratory instrumentation can incorporate additional filtering and signal processing that cannot readily be performed by circuitry that must meet size and power constraints. Since the SwRI tool met the robot constraints, it can be expected that results similar to those achieved in these tests can be expected from the final integrated hardware.

It should be noted that defect characterization has a strong subjective element. In this demonstration, we were working with a brand new system, looking at defect types we had not seen before. That meant we had to use our best judgment and understanding of the RFEC method to interpret the indications. After the system has been used more extensively, experience will allow the operator to know quickly what type of defect is being detected based on the signal characteristics. The quantitative interpretation of the signals will then be improved over the present level. For example, the natural corrosion region in the demonstration pipes gave a signal unlike any of the calibration defects in our lab or supplied by Battelle. Furthermore, the signal extended beyond the designated region. As a result, we used our best judgment and reported the wall loss indicated by our depth algorithms. Magnetic field effects or the simple nature of RFEC response to very large area defects could cause our estimate to be in error. Familiarity with this type defect over a period of time would assure us of making a quicker and potentially more accurate appraisal of the corrosion.

GAS TECHNOLOGY INSTITUTE (GTI)

Demonstration Test Da

Benchmarking of Inspection Technologies Detection of Metal Loss - Page 2	
Name:	
Date:	
Company:	
Sensor Design:	

TEST DATA

Pipe Sample:	**PIPE SAMPLE 2**
Defect Set:	8" Diameter, 0.188" Wall Thickness Pipe Sample; Schedule 10; Length = 30' 0.375"

TEST LINE 1

Defect Number	Search Region (Distance from End B)	Start of Metal Loss Region from Side B	End of Metal Loss Region from Side B	Total Length of Metal Loss Region	Width of Metal Loss Region	Maximum Depth of Metal Loss Region	Additional Data Attached?	Comments
	inches	inches	inches	inches	inches	inches	Y/N	
P2-11	54" to 66"							None
P2-10	78" to 90"	80.25	84	3.75	2.5	0.188		
P2-9	102" to 114"	107.75	111.75	4	1.5	0.142		
WELD	120"							
P2-8	126" to 138"							None
P2-7	150" to 162"	152.75	155.75	3	2	0.026		
P2-6	174" to 186"	179.75	183	3.25	1	0.073		
P2-5	198" to 210"							None
P2-4	222" to 234"	227.25	229.5	2.25	2	0.037		
P2-3	246" to 258"							None
P2-2	270" to 282"							None
P2-1	294" to 306"							None

TEST LINE 2

Defect Number	Search Region (Distance from End B)	Start of Metal Loss Region from Side B	End of Metal Loss Region from Side B	Total Length of Metal Loss Region	Width of Metal Loss Region	Maximum Depth of Metal Loss Region	Additional Data Attached?	Comments
	inches	inches	inches	inches	inches	inches	Y/N	
P2-20	54" to 66"	57.5	60.5	3	1.5	0.176		
P2-19	78" to 90"							None
P2-18	102" to 114"							None
WELD	120"							
P2-17	126" to 138"	129.5	133.5	4	2	0.159		
P2-16	150" to 162"							None
P2-15	174" to 186"							None
P2-14	198" to 210"	201	204	3	1.5	0.081		
P2-13	222" to 234"							None
P2-12	246" to 258"	249	251	2	1.5	0.148		

Benchmarking of Inspection Technologies
Detection of Metal Loss - Page 3

Name:	
Date:	
Company:	GTI
Sensor Design:	RFEC

TEST DATA

Pipe Sample:	**PIPE SAMPLE 3**
Defect Set:	8" Diameter, 0.188" Wall Thickness Pipe Sample; Schedule 10; Length = 40' 0.25"

TEST LINE 1

Defect Number	Search Region (Distance from End B)	Start of Metal Loss Region from Side B	End of Metal Loss Region from Side B	Total Length of Metal Loss Region	Width of Metal Loss Region	Maximum Depth of Metal Loss Region	Additional Data Attached?	Comments
	inches	inches	inches	inches	inches	inches	Y/N	
P3-11	66" to 78"	X	X	X	X	X	N	
P3-10	102" to 114"	106	109	3	2	0.182 & 0.176	Y	Two pits axially aligned
P3-9	138" to 150"	143.5	144.75	1.25	1	0.148 & 0.112	Y	Three pits
P3-8	162" to 174"	X	X	X	X	X	N	
P3-7	186" to 198"	190	193.5	3.5	2	0.173	Y	
P3-6	222" to 234"	X	X	X	X	X	N	
WELD	240"							
P3-5	270" to 282"	275.75	277.75	2	2	0.142 & 0.119	Y	Three pits
P3-4	300" to 312"	306.5	307.75	1.25	1	0.158	Y	
P3-3	330" to 342"	335	337	2	1.5	0.164	Y	
P3-2	360" to 372"	X	X	X	X	X	N	
P3-1	384" to 396"	X	X	X	X	X	N	ly, P3-12 was detected in the same axial location on Line 2. P3-12 is a

TEST LINE 2

Defect Number	Search Region (Distance from End B)	Start of Metal Loss Region from Side B	End of Metal Loss Region from Side B	Total Length of Metal Loss Region	Width of Metal Loss Region	Maximum Depth of Metal Loss Region	Additional Data Attached?	Comments
	inches	inches	inches	inches	inches	inches	Y/N	
P3-23	66" to 78"	70.25	74	3.75	2	0.124 & 0.009	Y	Two features
P3-22	102" to 114"	X	X	X	X	X	N	Reflection fron defect 10
P3-21	126" to 138"	130.25	133.75	3.5	2	0.121 & .114	Y	Two pits
P3-20	156" to 168"	X	X	X	X	X	N	
P3-19	180" to 192"	185.75	186.75	1	1	0.142 & 0.124	Y	
P3-18	210" to 222"	214.5	217.25	2.75	1.5	0.128 & 0.094	Y	Two pits axially aligned
WELD	240"							
P3-17	248" to 260"	251.25	254	2.75	1.5	0.089 & 0.066	Y	Two pits axially aligned
P3-16	282" to 294"	X	X	X	X	X	N	
P3-15	306" to 318"	X	X	X	X	X	N	he increase in the field was caused by the drive coil being located at P
P3-14	330" to 342"	335.75	336.75	1	1	0.149 & 0.145	Y	
P3-13	356" to 368"	X	X	X	X	X	N	
P3-12	390" to 402"	393	396	3	2.5	0.135 & 0.102	Y	Two pits axially aligned

Analysis of Sensor Benchmarking Tests

Remote Field Eddy Current Technique

Prepared by:
Julie Maupin, Albert Teitsma, Paul Shuttleworth
Gas Technology Institute
1700 S. Mount Prospect Road
Des Plaines, Illinois 60018

27 January 2006

Abstract
During the week of 9 January 2006, GTI staff travelled to the Battelle Lab's West Jefferson facility in Columbus, OH to test a prototype RFEC inspection vehicle in 3 samples of 8" pipe. We report briefly on the apparatus and its design, the electronic readout and data acquisition, and the analysis of the data. Where appropriate, we have discussed effects which lead to uncertainties in the location and size of reported defects. We also discuss uncertainties which may affect whether a defect would have been observable by our apparatus.

Introduction
The remote field eddy current (RFEC) technique is an electromagnetic, through-wall inspection technique for detecting defects and wall thinning in pipe walls. A simple exciter coil can be driven with a low frequency sinusoidal current to generate an oscillating magnetic field that small sensor coils can detect. This low frequency (10's of Hz) oscillating field will propagate via two paths. It will propagate directly down the pipe a short distance. It will also propagate out through the wall, along the exterior of the pipe, and will re-enter the pipe --- the so-called indirect field. At axial distances of 2-3 pipe diameters from the exciter coil, the indirect field re-entering the interior of the pipe is much larger than the direct field coming from the exciter coil. Since it passes through the pipe wall, the indirect field contains information regarding the condition of the pipe. Changes from nominal value of the amplitude and phase of the indirect field indicate defects in the wall.

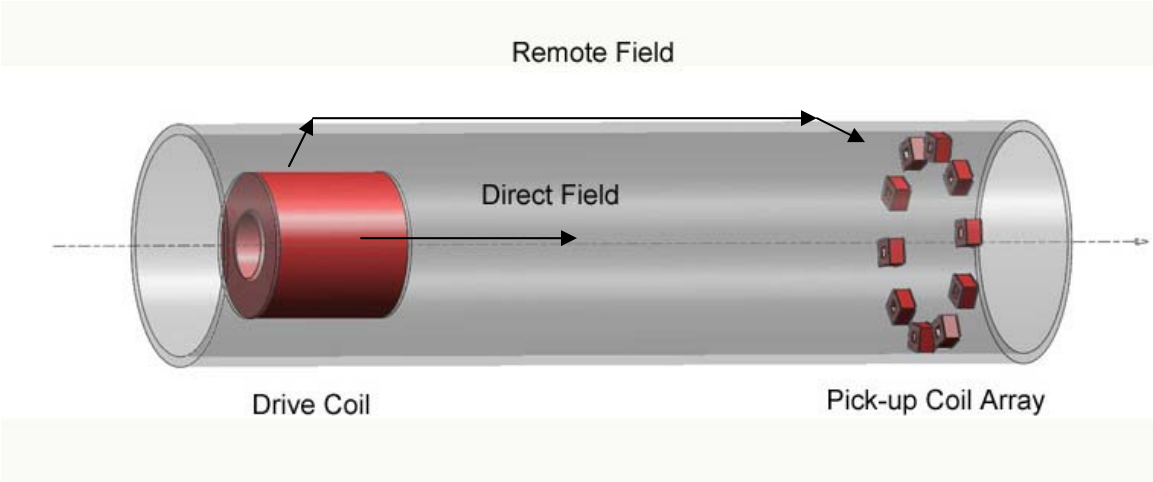

Figure 1: Paths of Energy Flow in the RFEC Technique. The remote field re-entering the pipe is the one containing the information regarding the condition of the pipe wall.

We constructed a vehicle ("jig") for carrying the RFEC apparatus. Near its front end it carried a solenoidal exciter coil, approximately 4" in diameter and 5" in length. It was comprised of1300 windings of 26 gauge wire. The sensor coils are located at distances of approximately 17" upstream of the exciter coil. They are ¾" in diameter, 3/8" in width, and contain approximately 20K windings of 50 gauge wire. Configured on the jig as two sets of 8 sensor coils, each set covered an angle of approximately 60º circumferentially at ¼" spacing.

Mechanical Design
The RFEC vehicle was composed of three parts, front support, rear support, and the center body. The front and rear supports had steering mechanisms on the wheels that helped keep the device upright and prevented any major rotation of the vehicle. The supports were coupled to

the center body, which contained all the equipment necessary to the RFEC technique. A picture of the center body is shown in Figure 2.

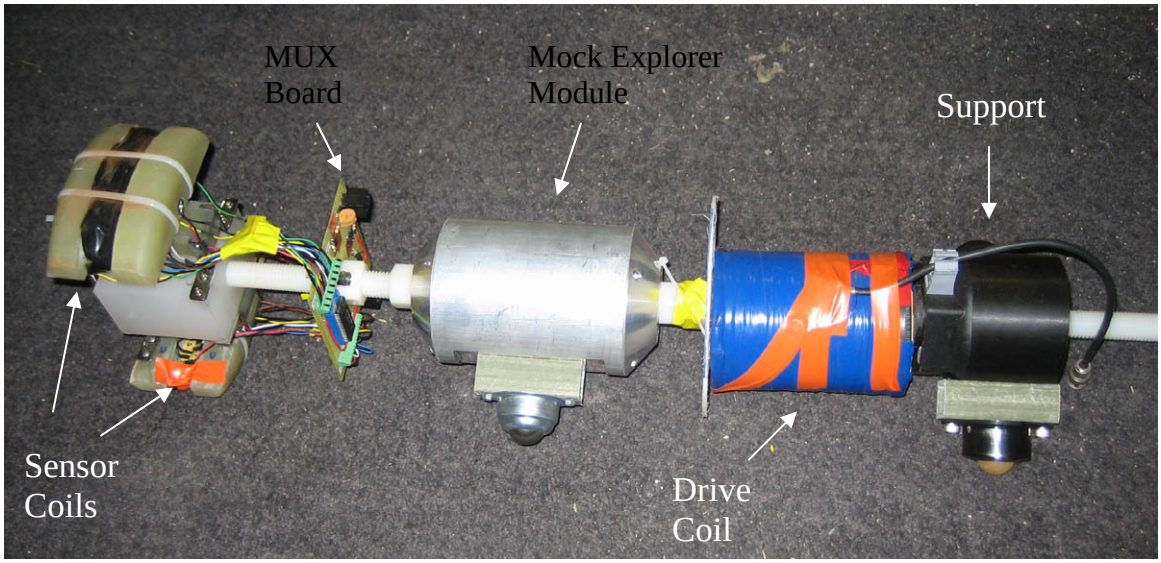

Figure 2: Center body of RFEC vehicle.

GTI used two sets of 8 sensor coils to measure two defect lines simultaneously. The coils were mounted on shafts that served as pegs to attach the coils to plastic guides as shown in Figure 3. The guides were rounded to match the circumference of the pipe and routed on the leading edge to avoid jamming the welds. The guides were held against the pipe wall by spring-loaded, parallelogram configured arms. An end view of the sensor coil mounts is shown in Figure 4.

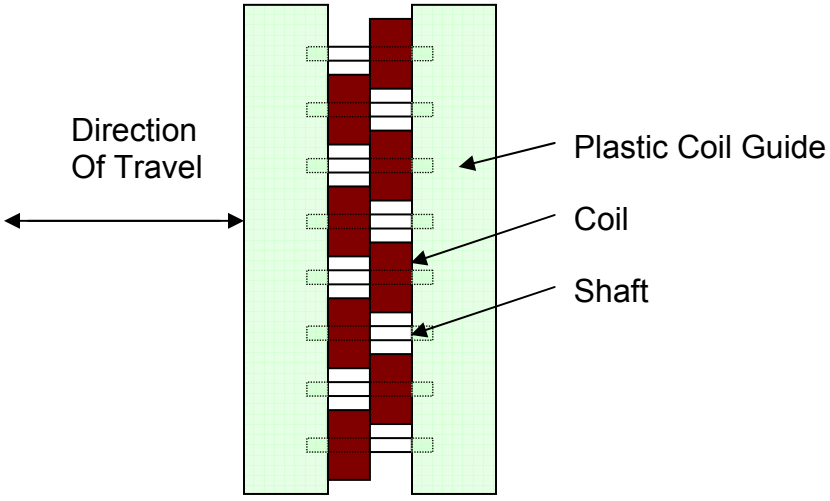

Figure 3: Diagram of sensor coils mounted to plastic guides.

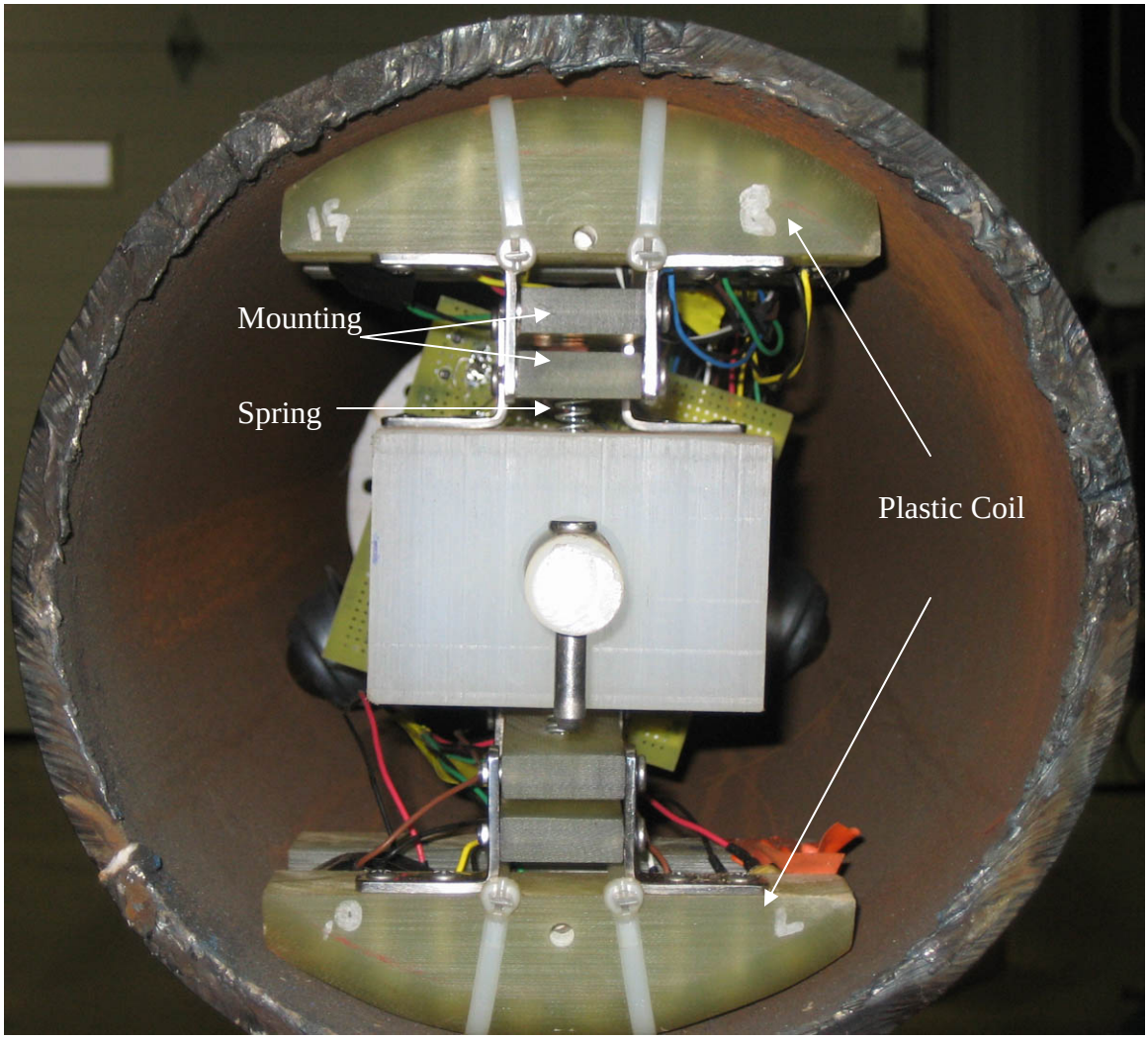

Figure 4: Sensor coil mounts inside an 8” pipe.

The drive coil has been placed between two support modules, one having been built to imitate a module on the Explorer II robot. These support modules were important to keeping the drive coil centered in the pipe.

GTI used an automatic winch system to pull the vehicle through the pipe. A tether line was attached to the front end of the vehicle. The tether wraps once around an encoder and then is wound onto a motor. The system is mounted directly onto the pipe and is controlled by LabVIEW to move the vehicle in ¼” steps.

Uncertainties Related to Mechanics

The jig suffered from some rotation inside the pipe. Each coil could have experienced rotations of up to ±10°. There were some encoder losses. After traveling 25’ in the pipe, we were measuring about 5” short of the actual location of the sensor coils. We eventually attached a fiberglass tape measure to the back end of the vehicle so we could always double check the encoder readings. In order to get good wall coverage from the coils, they had to be staggered, meaning half were closer to the drive coil than the other half. We have made provisions to correct the offset in the data analysis but there will still likely be an effect on the results.

Electronics and Data Acquisition (DAQ) System
GTI's embodiment of a Remote Field Eddy Current inspection system is as follows: Signal Recovery 7265 DSP lock-in amplifier, Kepco BOP36-6M excitation coil driver, ADG407 16 channel multiplexer, Ni GPIB+ Gpib board and Ni PCI-6601 Counter Timer board. The preceding hardware is controlled by a Dell Pentium 4 workstation running at 2.99MHz with 1Gb of main memory and executing Lab View 7.1 under Windows XP Professional operating system. A general schematic of the DAQ system is shown in Figure 7.

Channel addressing and distance gauging is accomplished using a Ni 6601 time/counter PCI circuit board. Distance measurements are made using a relative incremental encoder having a resolution of 1/16".

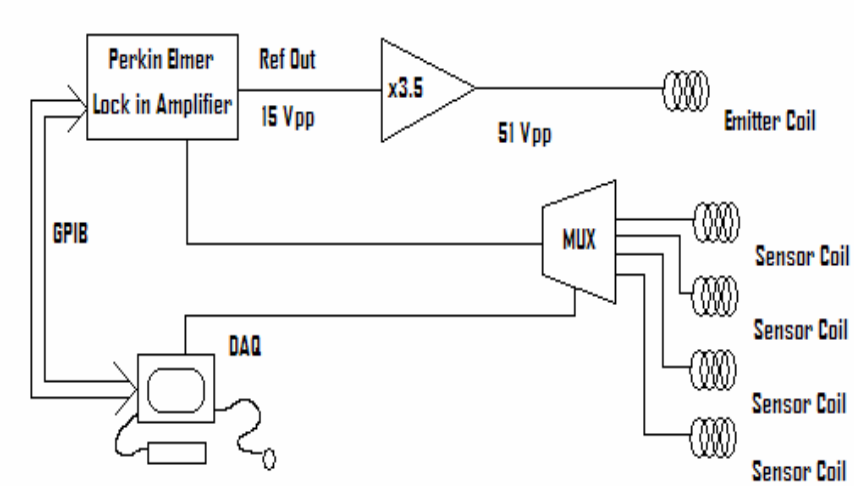

Figure 5: Schematic of DAQ System. This figure schematically shows a 4-channel system. The system we operated at Battelle was a 16-channel version of this schematic.

GTI's RFEC machine is using a 100 count per revolution quadrature encoder. The encoder is interfaced to the system using a National Instrument PCI-6601 counter/timer circuit board. This circuit board supports 5 encoders; the encoder interface is done in hardware. The counter chip used in the NI circuit board has 32 bit registers giving a counting range of 268,435,453 inch.

Data Collection
Three LabView programs were used to collect data from the instrumentation on the jig. One read the encoder, one controlled the motor, and the other controlled the lock-in amplifier and acquired data from the coils. Acquiring the phase angle and magnitude of each coil was achieved by using a sequence of binary addressing to the multiplexer board. The program cycles through each coil sequentially. Once the data has been acquired for all 16 coil channels, the motor program fires the motor until the encoder program realizes it has traveled to the next ¼" step. Once the motor stops, the coils are again read and the phase and magnitude data is recorded to Excel. The process repeats.

The lock-in amplifier has a programmable time constant for the low pass filter at its output. The program was written so that the operator could set the number of time constants that the program would wait at each coil address. Having a wait of multiple time constants ensured that

unsettled data would be flushed out and the readings would be accurate. The drawback to waiting for a certain number of time constants is slower acquisition time. It takes a significantly longer time to obtain data for 16 coils making overall inspection speed slow. No problems were encountered with LabVIEW.

Analysis

Pipe Sample 3

Analysis of defect depth on Pipe Sample 3 was primarily done using Russell NDE Systems Inc.'s Adept Pro program. This program is the result of decades of research and focuses on the Voltage Plane for analysis. The display produced by the program is shown for Defect Line1 in Figure 6.

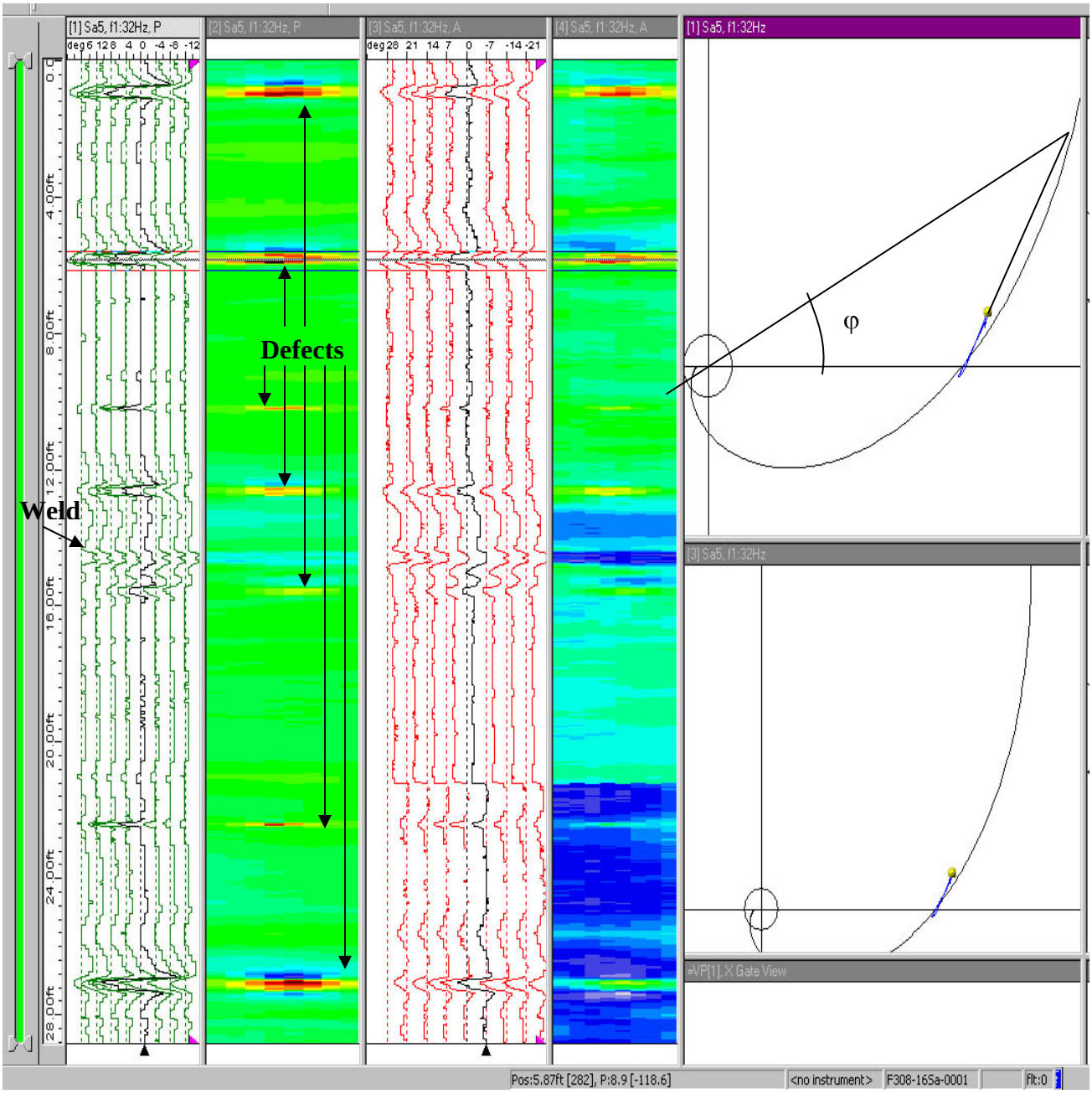

Figure 6: Adept Pro display of Defect Line 1 from Pipe Sample 3.

The display shows a strip chart of the phase angle on the left, followed by a C-Scan of the phase. Although the C-Scan provides a good overview of the defects, often as in this case, the strip chart is better for seeing the smaller defects. The magnitude information (strip chart and C-scan) is displayed to the right of the phase information. The top right hand panel shows the Voltage Plane. The black spiral is the attenuation spiral: as the wall thickness increases, the remote filed eddy current signal strength decreases while the phase also decreases, resulting in a spiral polar plot. The blue curve on the plot is the signal from the defect at the horizontal marker that runs across the strip charts and C-scans. The two red lines on either side of the marker delimit the range of data analyzed.

If the blue line is extended to intersect the wall-thinning spiral, the vector from the origin of the polar plot to the intersection point makes an angle φ with the x-axis. Angle φ is used to determine the depth of the defect. The length of the blue line is used to find the circumferential extent of the defect. As in Figure 6, Figure 7 shows the analysis of Line 2 of Pipe 3.

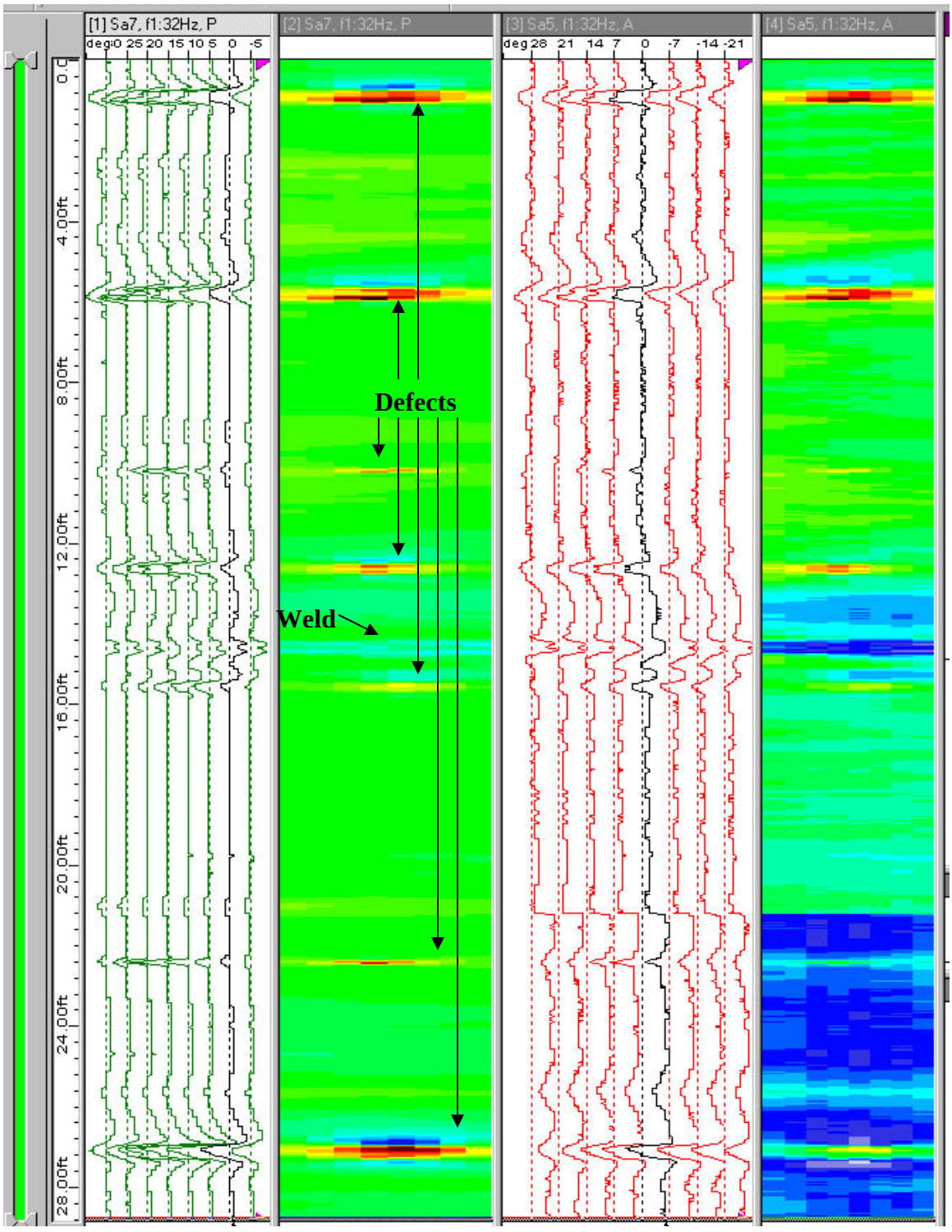

Figure 9: Adept Pro Display of Defect Line 2.

Adept Pro's function is primarily to determine defect depth. Defect length and width are best obtained from axial and circumferential scans across the defect. Remote field eddy current signals spread in both the axial and the circumferential directions. To get length and width

requires corrections for the spread. Axial lengths estimated from the data should be reasonable. However, the combination of much greater spread in the circumferential direction combined with sensor separation means circumferential precision is poor.

Pipe 2 was analyzed with an internally written MATLAB program. The fundamental equations are the same as used by Russell‘s Adept Pro software but there are some differences in the calibration. This can lead to small differences in the results for this pipe. This approach was used because Pipe 2 has two calibration defects with different depths. We expect the new calibration to give better results over a wide range of defect depths.

Table 1: C-scan Plots of defects found on Pipe 3 Test Line 1.

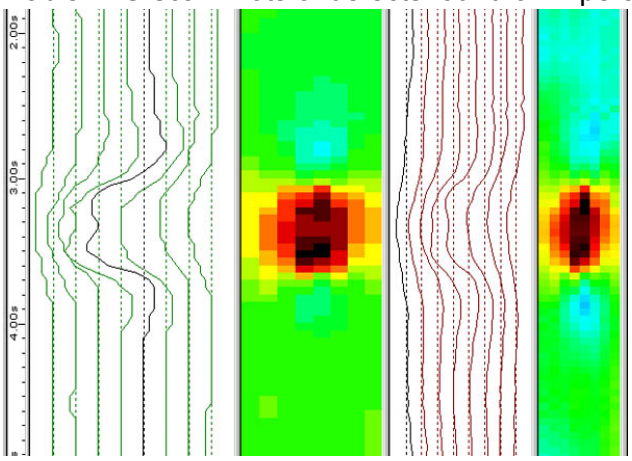

P3-10

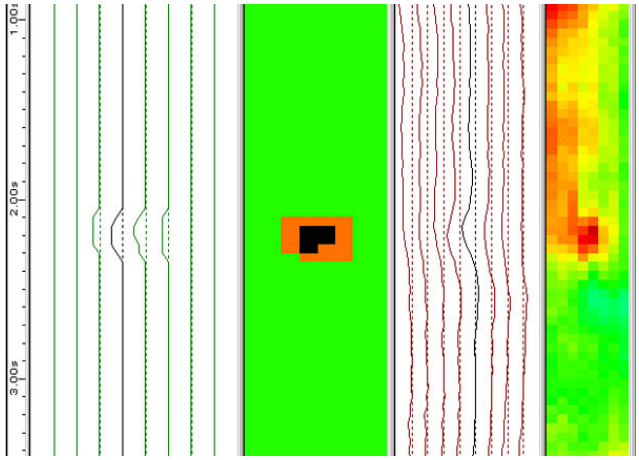

P3-09

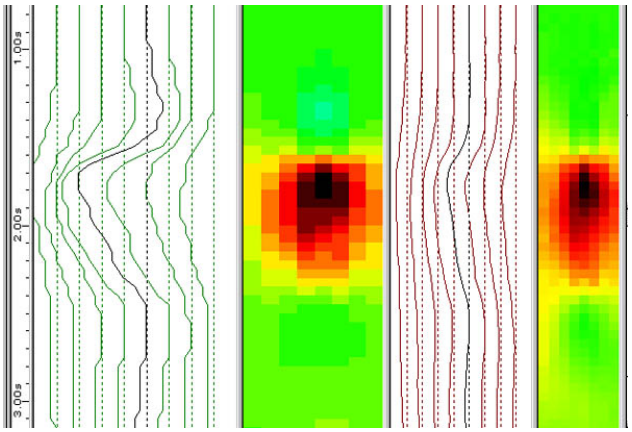

P3-07

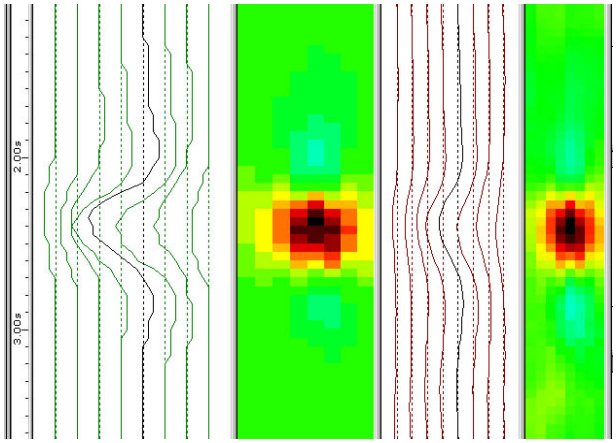

P3-05

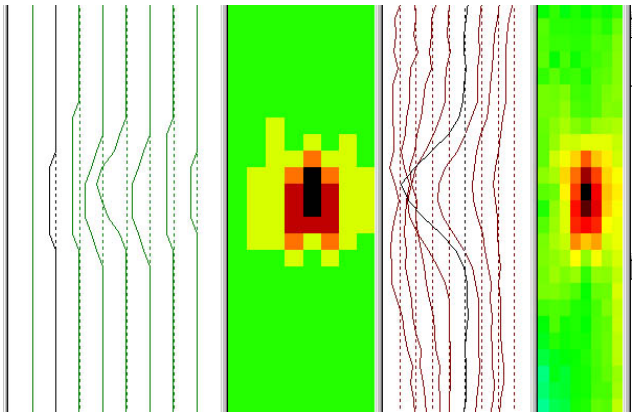

P3-04

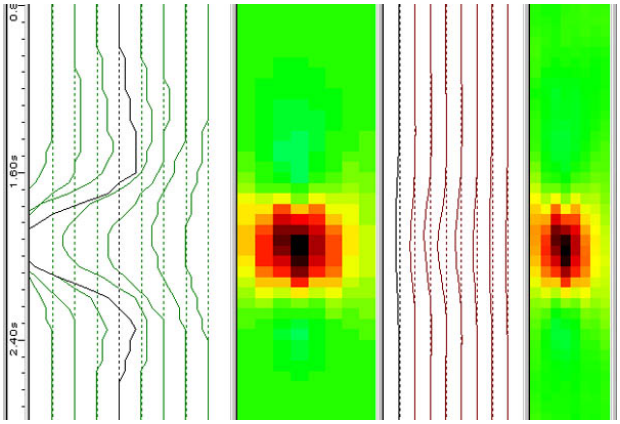

P3-03

Table 2: Line 1 Defects

Defect Location	Max Depth (% of wall thick.)	Defect Length	Defect Width
106”	96%	3”	2”
143.5”	78%	1.25”	1”
190”	92%	3.5”	2”
275.75”	75%	2”	2”
306.5”	84%	1.25”	1”
335”	87%	2”	1.5”

C-Scan plots

The C-scan plots for all found defects are attached as a separate document. The tables containing Pipe 1 defects show the strip chart and C-scan for the phase only. The tables containing Pipe 2 defects show the C-scan for the phase only. Finally, the tables containing Pipe 3 defect information show the strip chart and C-scan for both the phase and magnitude.

Summary Results Table

The Excel spreadsheet summarizing the results is attached as a separate document. Pipe 2 data was only analyzed for the deepest pit. Data from Pipes 1 and 3 that showed dual pits are recorded in the spreadsheet as two measurements representing the maximum depth of each pit.

Table 1: C-scan Plots of defects found on Pipe 1 Test Line 1.

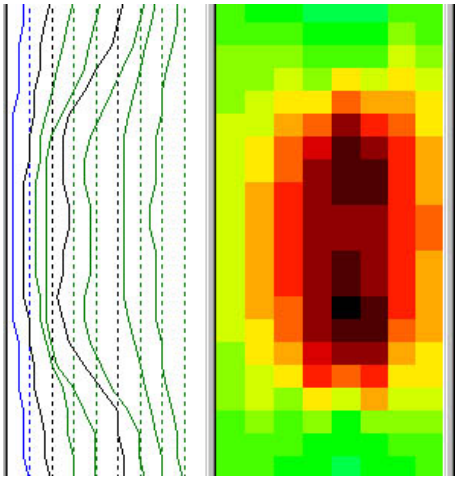

P1-12

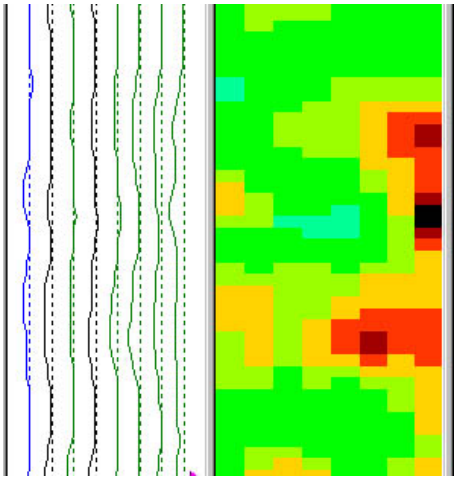

P1-09

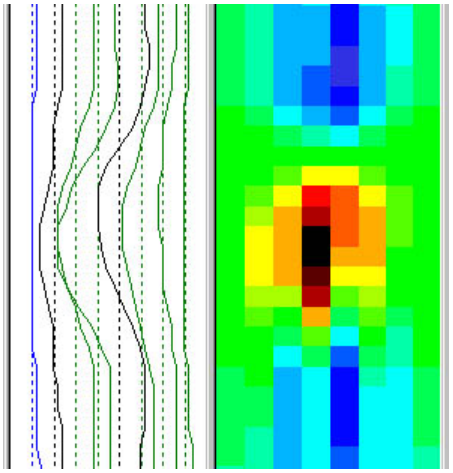

P1-07

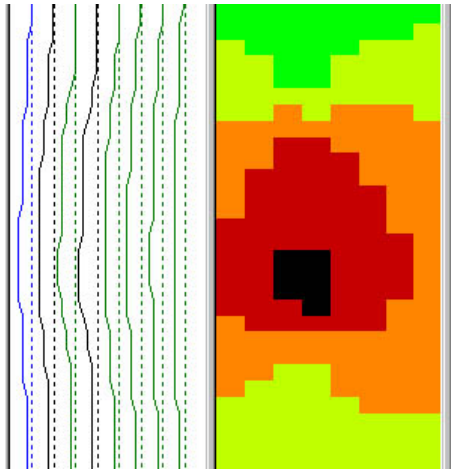

P1-05

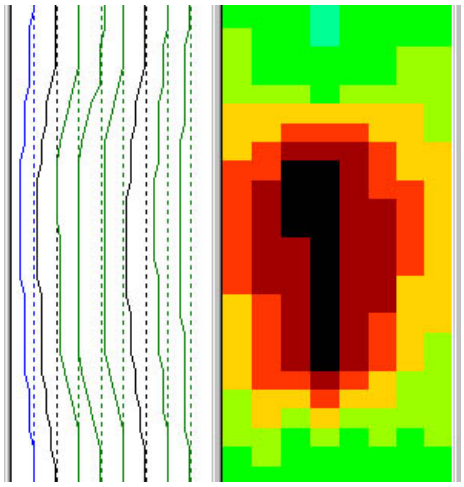

P1-04

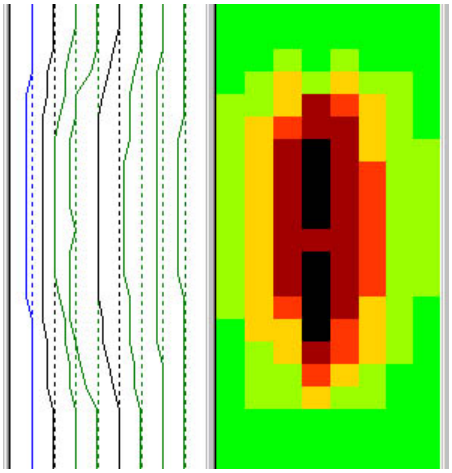

P1-03

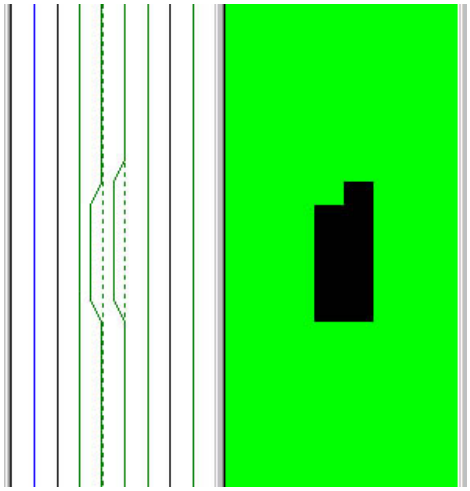

P1-02

Table 2: C-scan Plots of defects found on Pipe 1 Test Line 2.

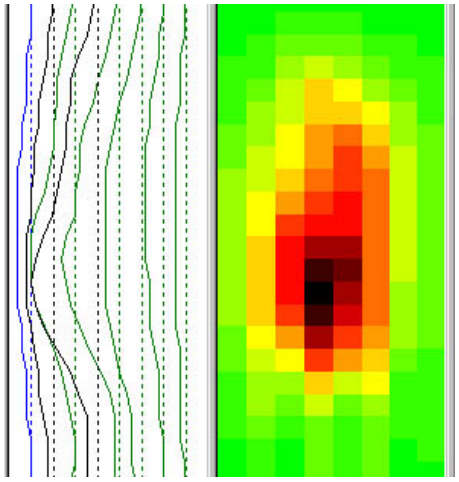

P1-23

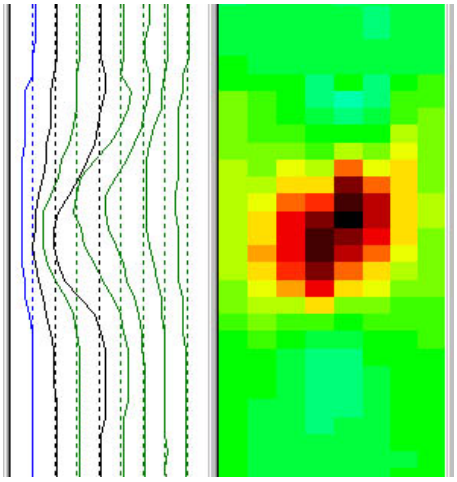

P1-22

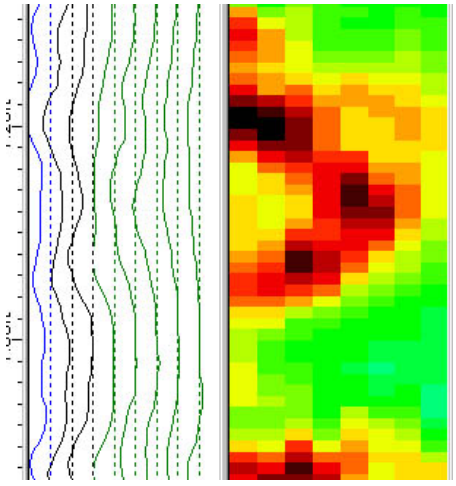

P1-21

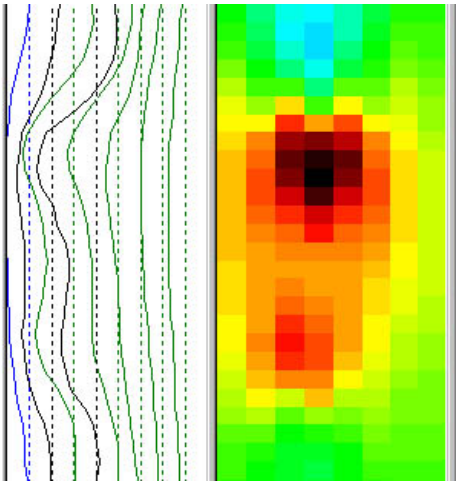

P1-18

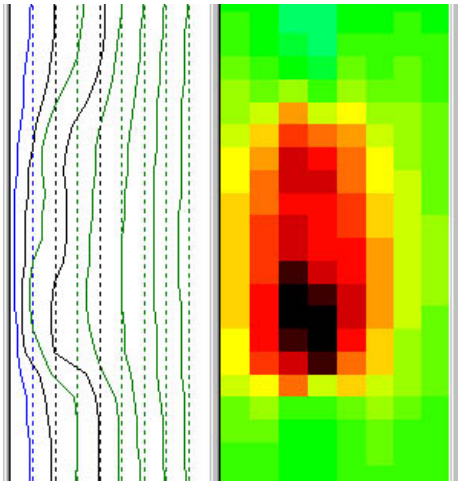

P1-14

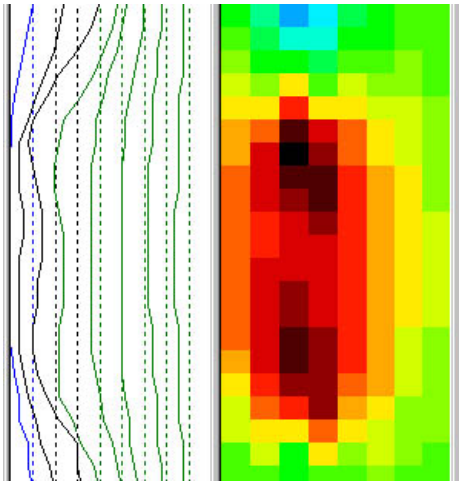

P1-13

Table 3: C-scan Plots of defects found on Pipe 2 Test Line 1.

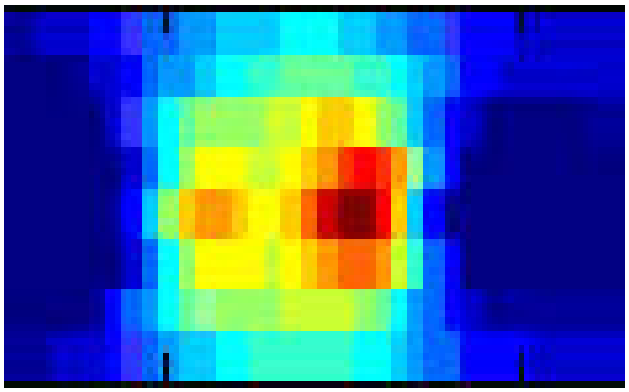

P2-10

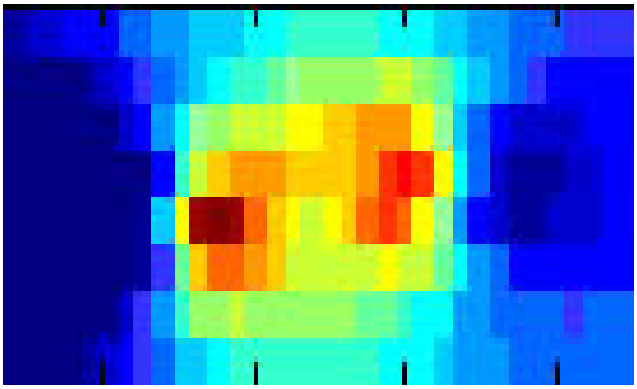

P2-09

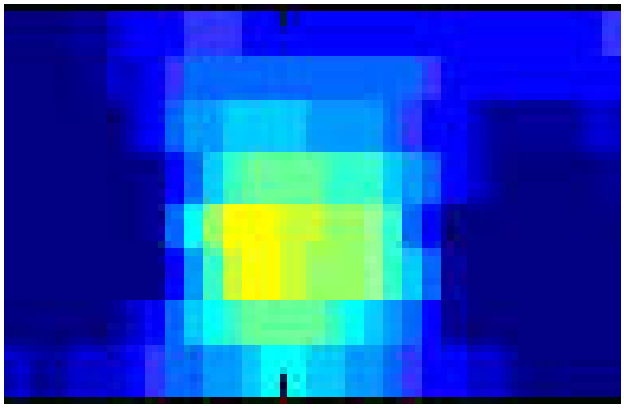

P2-07

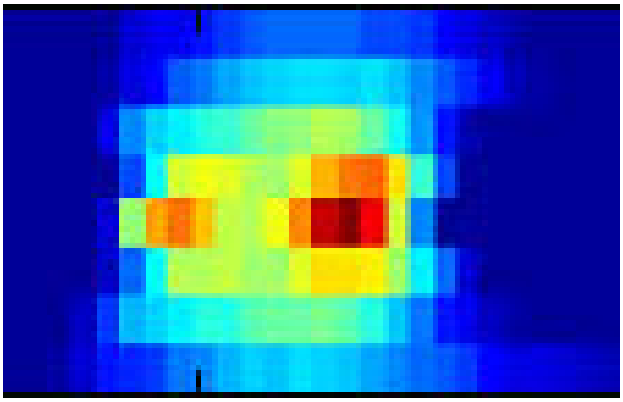

P2-06

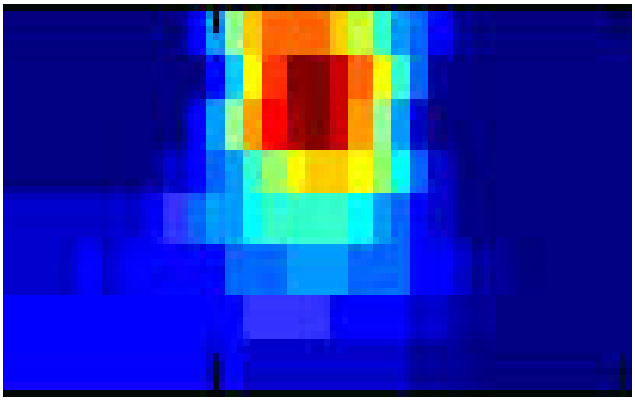

P2-04

Table 4: C-scan Plots of defects found on Pipe 2 Test Line 2.

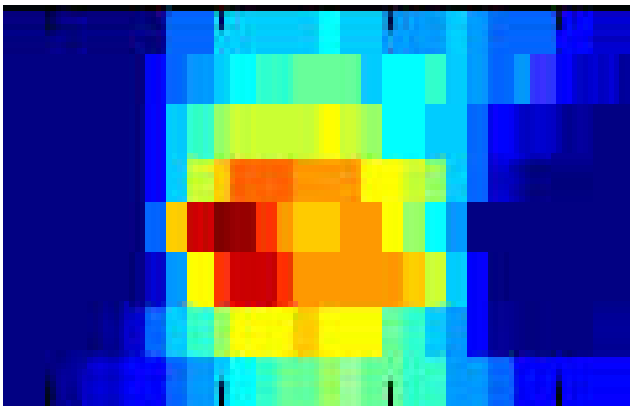

P2-20

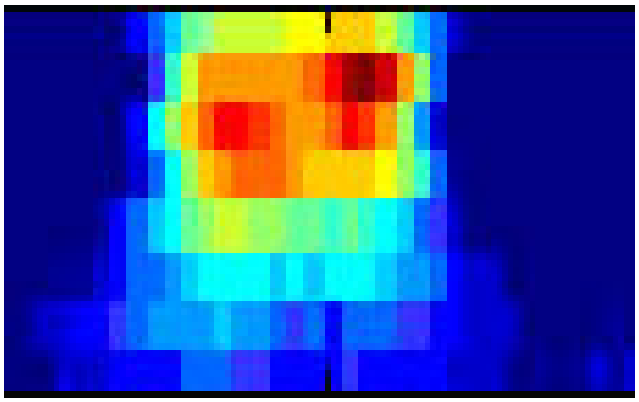

P2-17

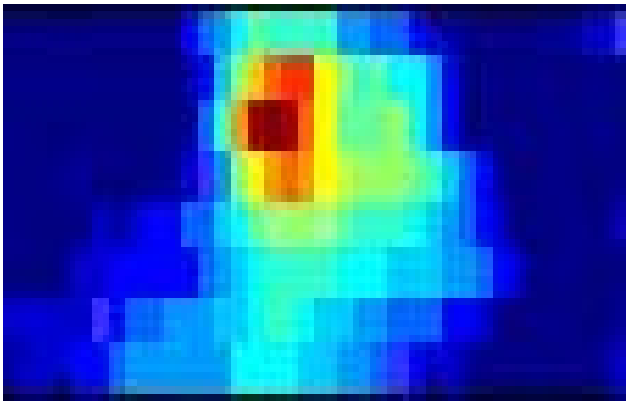

P2-14

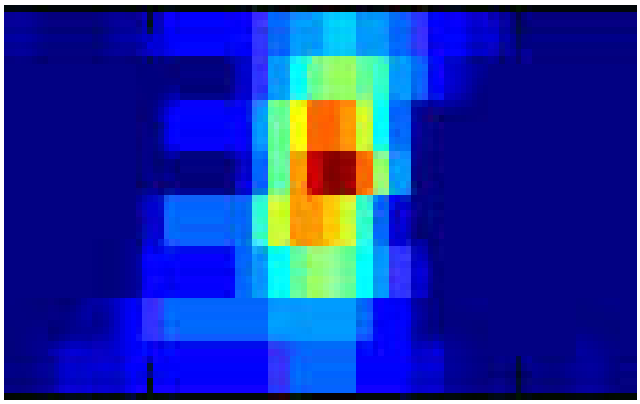

P2-12

Table 5: C-scan Plots of defects found on Pipe 3 Test Line 1.

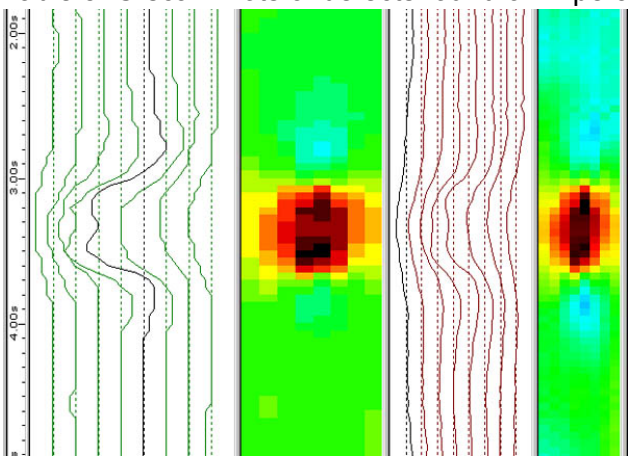

P3-10

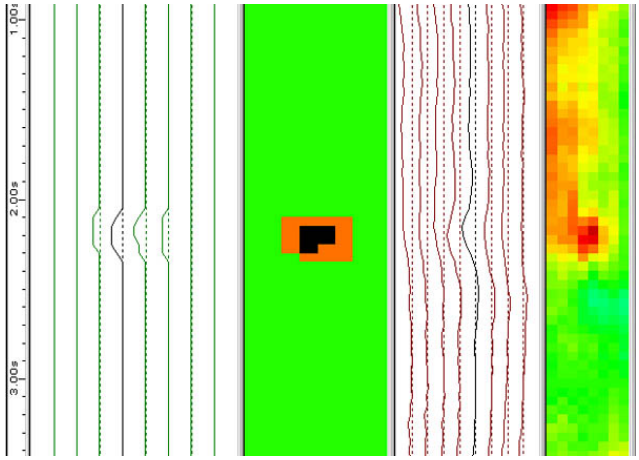

P3-09

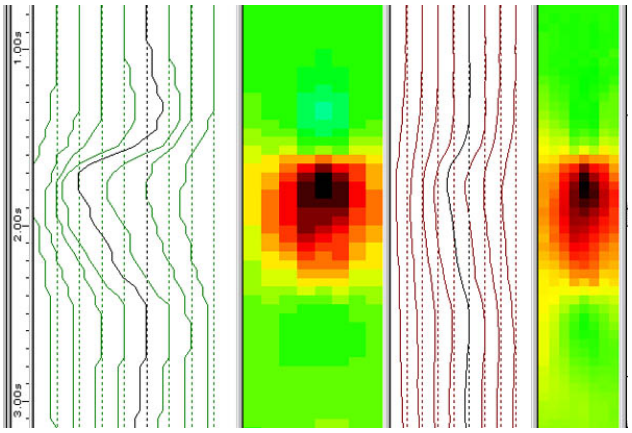

P3-07

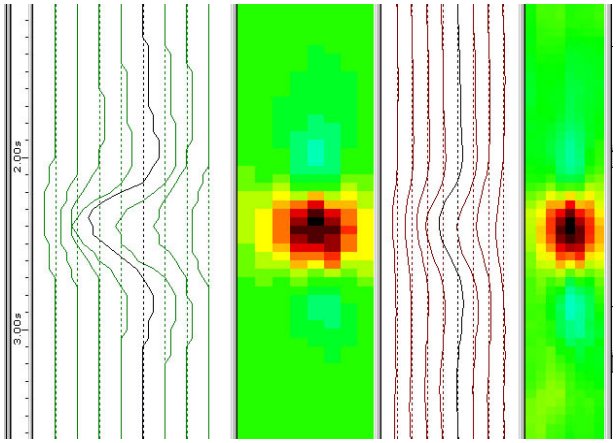

P3-05

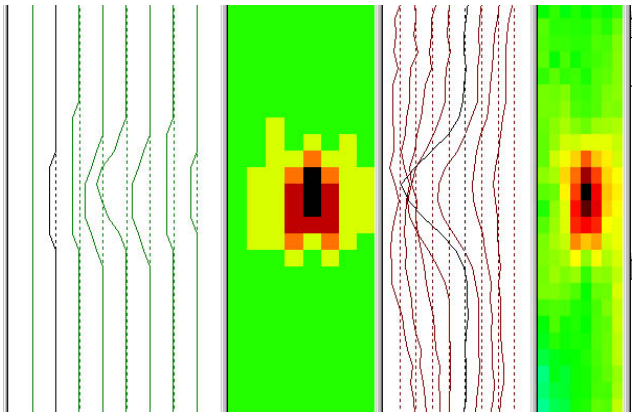

P3-04

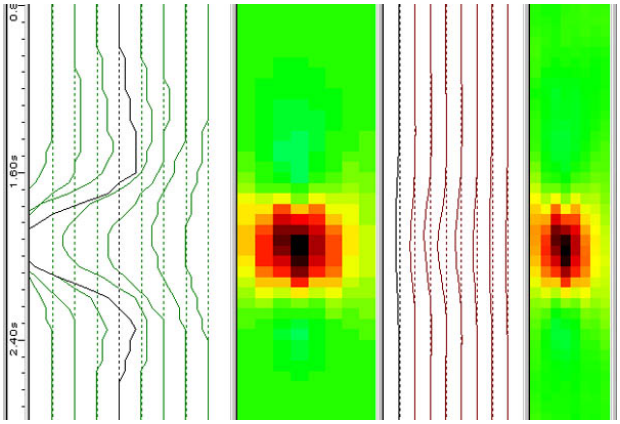

P3-03

Table 6: C-scan Plots of defects found on Pipe 3 Test Line 2.

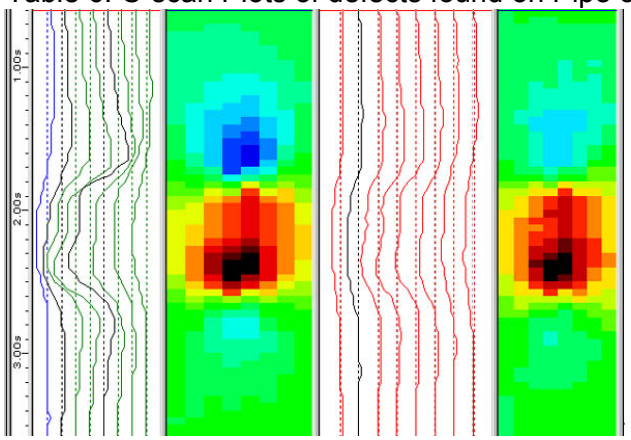

P3-23

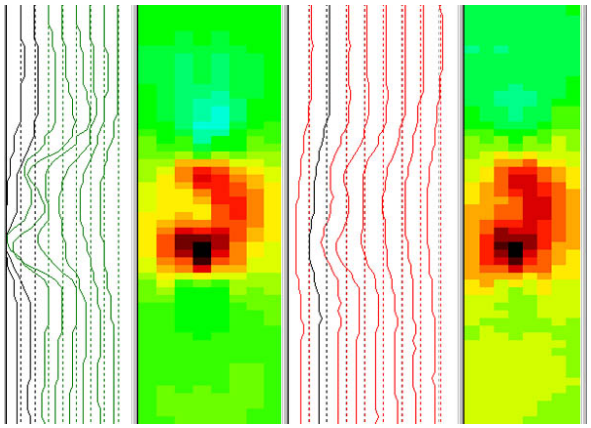

P3-21

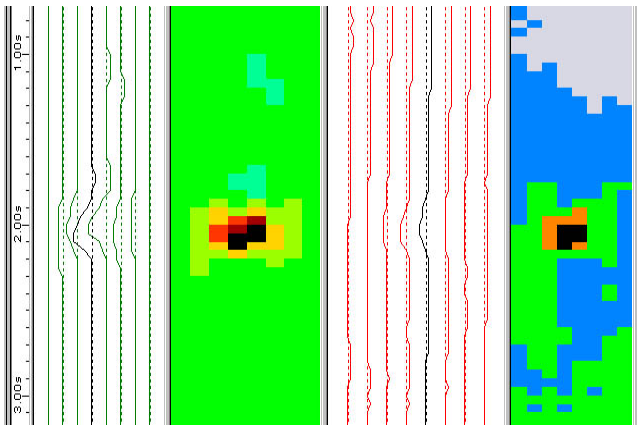

P3-19

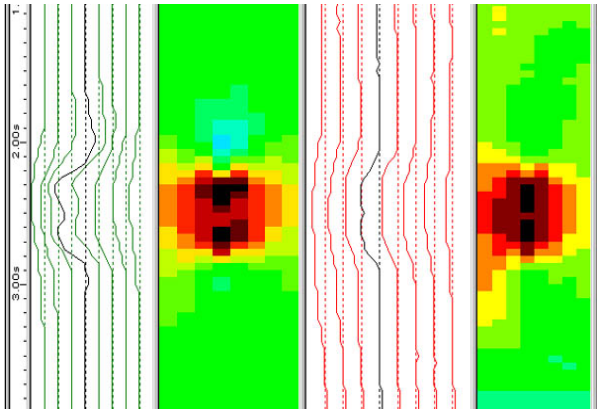

P3-18

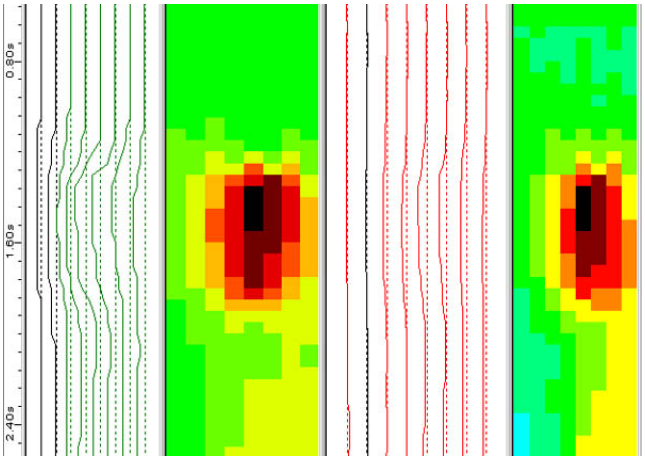

P3-17

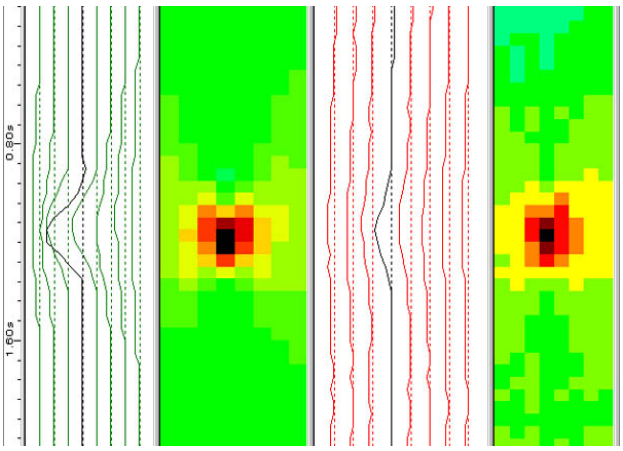

P3-14

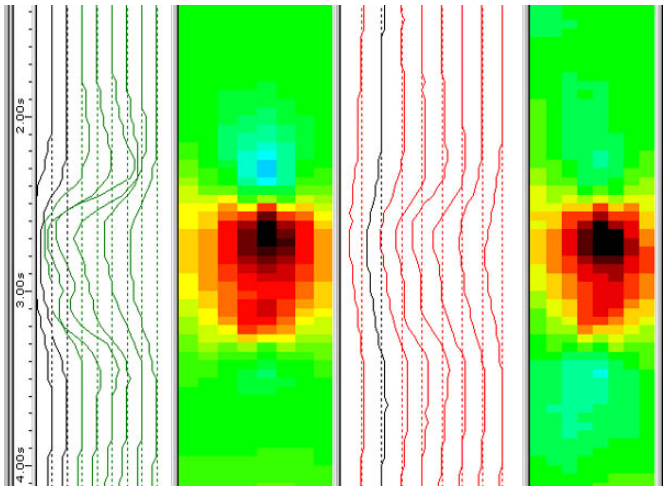

P3-12

BATTELLE
DEMONSTRATION TEST DATA

This page intentionally blank.

Benchmarking of Inspection Technologies
Detection of Metal Loss - Page 1

Name:	Bruce Nestleroth
Date:	January 26,2006
Company:	Battelle
Sensor Design:	Rotating Permanent Magnet Eddy Current Inspection System

TEST DATA

Pipe Sample:	**PIPE SAMPLE 1**
Defect Set:	8" Diameter, 0.188" Wall Thickness Pipe Sample; Schedule 10; Length = 34' 11.75"

TEST LINE 1

Defect Number	Search Region (Distance from End B)	Start of Metal Loss Region from Side B	End of Metal Loss Region from Side B	Total Length of Metal Loss Region	Width of Metal Loss Region	Maximum Depth of Metal Loss Region	Additional Data Attached?	Comments
	inches	inches	inches	inches	inches	inches	Y/N	
P1-12	52" to 64"	**58.1**	**62.3**	**3.2**	**1.75**	**0.115**	Yes. Raw Signals	Corrosion patch, with multiple pits of different depths
P1-11	76" to 88"	**No Metal Loss Detected**					Yes. Raw Signals	
P1-10	100" to 112"	**No Metal Loss Detected**					Yes. Raw Signals	
WELD	120"							
P1-9	120" to 144"	**120.0**	**132.0**	**12.0**	**32.0**	**Various depths up to 0.150 inches**	Yes. Raw Signals	A large area of general corrosion of variable depth that spans the entire sensor width. The corrosion is close to the weld, altering both signals. A large wide corrosion area at 128"
P1-8	160" to 172"	**No Metal Loss Detected**					Yes. Raw Signals	A slow change in signal in all sensors throughout the region indicates a material property change
WELD	180"							
P1-7	184" to 196"	**188.8**	**192.2**	**2.4**	**1.5**	**0.165**	Yes. Raw Signals	Corrosion patch, with multiple pits of different depths
P1-6	208" to 220"	**No Metal Loss Detected**					Yes. Raw Signals	
P1-5	232" to 244"	**233.2**	**237.0**	**2.8**	**1.0**	**0.050**	Yes. Raw Signals	Corrosion patch, with multiple pits of different depths
P1-4	256" to 268"	**260.1**	**264.9**	**3.8**	**1.5**	**0.055**	Yes. Raw Signals	Corrosion patch, with multiple pits of different depths
P1-3	280" to 292"	**288.0**	**292.8**	**3.8**	**1.0**	**0.075**	Yes. Raw Signals	Corrosion patch, with multiple pits of different depths
P1-2	304" to 316"	**No Metal Loss Detected**					Yes. Raw Signals	
P1-1	328" to 340"	**No Metal Loss Detected**					Yes. Raw Signals	

TEST LINE 2

Defect Number	Search Region (Distance from End B)	Start of Metal Loss Region from Side B	End of Metal Loss Region from Side B	Total Length of Metal Loss Region	Width of Metal Loss Region	Maximum Depth of Metal Loss Region	Additional Data Attached?	Comments
	inches	inches	inches	inches	inches	inches	Y/N	
P1-23	74" to 86"	**74.8**	**79.1**	**3.3**	**1.0**	**0.075**	Yes. Raw Signals	Corrosion patch, with multiple pits of different depths
P1-22	98" to 110"	**103.1**	**106.3**	**2.2**	**1.75**	**0.110**	Yes. Raw Signals	Corrosion patch, with multiple pits of different depths
WELD	120"							
P1-21	120" to 144"	**126.0**	**138.0**	**12.0**	**Greater than 5 inches**	**Various depths up to 0.150 inches**	Yes. Raw Signals	A area of general corrosion of variable depth that spans most sensors. A large wide corrosion area at 128".
P1-20	160" to 172"	**No Metal Loss Detected**					Yes. Raw Signals	A slow change in signal in all sensors throughout the region indicates a material property change
WELD	180"							
P1-19	186" to 198"	**No Metal Loss Detected**					Yes. Raw Signals	
P1-18	210" to 222"	**212.5**	**216.8**	**3.3**	**2.0**	**0.155**	Yes. Raw Signals	Corrosion patch, with multiple pits of different depths
P1-17	234" to 246"	**241.1**	**241.8**	**0.7**	**0.75**	**0.020**	Yes. Raw Signals	Small single pit
P1-16	258" to 270"	**No Metal Loss Detected**					Yes. Raw Signals	
P1-15	282" to 294"	**No Metal Loss Detected**					Yes. Raw Signals	
P1-14	306" to 318"	**306.9**	**310.8**	**2.9**	**1.25**	**0.115**	Yes. Raw Signals	Corrosion patch, with multiple pits of different depths
P1-13	330" to 342"	**334.2**	**338.4**	**3.2**	**1.0**	**0.075**	Yes. Raw Signals	Corrosion patch, with multiple pits of different depths

Benchmarking of Inspection Technologies
Detection of Metal Loss - Page 2

Name:	Bruce Nestleroth
Date:	January 26,2006
Company:	Battelle
Sensor Design:	Bruce Nestleroth

TEST DATA

Pipe Sample:	**PIPE SAMPLE 2**
Defect Set:	8" Diameter, 0.188" Wall Thickness Pipe Sample; Schedule 10; Length = 30' 0.375"

TEST LINE 1

Defect Number	Search Region (Distance from End B)	Start of Metal Loss Region from Side B	End of Metal Loss Region from Side B	Total Length of Metal Loss Region	Width of Metal Loss Region	Maximum Depth of Metal Loss Region	Additional Data Attached?	Comments
	inches	inches	inches	inches	inches	inches	Y/N	
P2-11	54" to 66"	**No Metal Loss Detected**					Yes. Raw Signals	
P2-10	78" to 90"	**80.0**	**83.6**	**2.6**	**1.5**	**0.170**	Yes. Raw Signals	Corrosion patch, with large multiple pits of different depths
P2-9	102" to 114"	**108.6**	**112.0**	**2.4**	**1.5**	**0.165**	Yes. Raw Signals	Corrosion patch, with large multiple pits of different depths
WELD	120"						Yes. Raw Signals	
P2-8	126" to 138"	**No Metal Loss Detected**					Yes. Raw Signals	
P2-7	150" to 162"	**153.8**	**157.6**	**2.8**	**1.0**	**0.065**	Yes. Raw Signals	Corrosion patch, with multiple pits of different depths
P2-6	174" to 186"	**181.1**	**184.9**	**2.8**	**1.0**	**0.075**	Yes. Raw Signals	Corrosion patch, with multiple pits of different depths
P2-5	198" to 210"	**No Metal Loss Detected**					Yes. Raw Signals	
P2-4	222" to 234"	**228.9**	**232.0**	**2.1**	**1.0**	**0.075**	Yes. Raw Signals	Corrosion patch, with multiple pits of different depths
P2-3	246" to 258"	**No Metal Loss Detected**					Yes. Raw Signals	
P2-2	270" to 282"	**No Metal Loss Detected**					Yes. Raw Signals	
P2-1	294" to 306"	**No Metal Loss Detected**					Yes. Raw Signals	

TEST LINE 2

Defect Number	Search Region (Distance from End B)	Start of Metal Loss Region from Side B	End of Metal Loss Region from Side B	Total Length of Metal Loss Region	Width of Metal Loss Region	Maximum Depth of Metal Loss Region	Additional Data Attached?	Comments
	inches	inches	inches	inches	inches	inches	Y/N	
P2-20	54" to 66"	**59.4**	**63.2**	**2.8**	**1.0**	**0.180**	Yes. Raw Signals	Corrosion patch, with multiple pits of different depths, One pit may be through hole
P2-19	78" to 90"	**No Metal Loss Detected**					Yes. Raw Signals	
P2-18	102" to 114"	**No Metal Loss Detected**					Yes. Raw Signals	
WELD	120"							
P2-17	126" to 138"	**132.8**	**137.4**	**3.6**	**1.5**	**0.105**	Yes. Raw Signals	Corrosion patch, with multiple pits of different depths
P2-16	150" to 162"	**No Metal Loss Detected**					Yes. Raw Signals	
P2-15	174" to 186"	**No Metal Loss Detected**					Yes. Raw Signals	
P2-14	198" to 210"	**204.9**	**209.0**	**3.1**	**0.75**	**0.075**	Yes. Raw Signals	Corrosion patch, with multiple pits of different depths
P2-13	222" to 234"	**No Metal Loss Detected**					Yes. Raw Signals	
P2-12	246" to 258"	**250.0**	**253.0**	**2.0**	**1.5**	**0.115**	Yes. Raw Signals	Corrosion patch, with multiple pits of different depths

Benchmarking of Inspection Technologies
Detection of Metal Loss - Page 3

Name:	Bruce Nestleroth
Date:	January 26,2006
Company:	Battelle
Sensor Design:	Rotating Permanent Magnet Eddy Current Inspection System

TEST DATA

Pipe Sample:	**PIPE SAMPLE 3**
Defect Set:	8" Diameter, 0.188" Wall Thickness Pipe Sample; Schedule 10; Length = 40' 0.25"

TEST LINE 1

Defect Number	Search Region (Distance from End B)	Start of Metal Loss Region from Side B	End of Metal Loss Region from Side B	Total Length of Metal Loss Region	Width of Metal Loss Region	Maximum Depth of Metal Loss Region	Additional Data Attached?	Comments
	inches	inches	inches	inches	inches	inches	Y/N	
P3-11	66" to 78"	**No Metal Loss Detected**					Yes. Raw Signals	
P3-10	102" to 114"	**108.8**	**112.4**	**2.6**	**1.5**	**0.160**	Yes. Raw Signals	Corrosion patch, with multiple pits of different depths
P3-9	138" to 150"	**144.2**	**145.5**	**1.3**	**0.5**	**0.080**	Yes. Raw Signals	Single Pit
P3-8	162" to 174"	**No Metal Loss Detected**					Yes. Raw Signals	
P3-7	186" to 198"	**187.8**	**193.0**	**4.2**	**1.5**	**0.105**	Yes. Raw Signals	Corrosion patch, with multiple pits of different depths
P3-6	222" to 234"	**No Metal Loss Detected**					Yes. Raw Signals	
WELD	240"						Yes. Raw Signals	
P3-5	270" to 282"	**276.4**	**279.5**	**2.1**	**1.5**	**0.105**	Yes. Raw Signals	Corrosion patch, with multiple pits of different depths
P3-4	300" to 312"	**307.8**	**309.3**	**1.5**	**0.75**	**0.150**	Yes. Raw Signals	Single Pit
P3-3	330" to 342"	**338.0**	**341.0**	**2.0**	**1.75**	**0.165**	Yes. Raw Signals	Corrosion patch, with multiple pits of different depths
P3-2	360" to 372"	**No Metal Loss Detected**					Yes. Raw Signals	
P3-1	384" to 396"	**No Metal Loss Detected**					Yes. Raw Signals	

TEST LINE 2

Defect Number	Search Region (Distance from End B)	Start of Metal Loss Region from Side B	End of Metal Loss Region from Side B	Total Length of Metal Loss Region	Width of Metal Loss Region	Maximum Depth of Metal Loss Region	Additional Data Attached?	Comments
	inches	inches	inches	inches	inches	inches	Y/N	
P3-23	66" to 78"	**65.9**	**70.6**	**3.7**	**1.5**	**0.055**	Yes. Raw Signals	Corrosion patch, with multiple pits of different depths
P3-22	102" to 114"	**No Metal Loss Detected**					Yes. Raw Signals	
P3-21	126" to 138"	**128.3**	**132.7**	**3.4**	**1.25**	**0.085**	Yes. Raw Signals	Corrosion patch, with multiple pits of different depths
P3-20	156" to 168"	**No Metal Loss Detected**					Yes. Raw Signals	
P3-19	180" to 192"	**184.9**	**186.2**	**1.3**	**0.75**	**0.105**	Yes. Raw Signals	Single Pit
P3-18	210" to 222"	**214.1**	**218.1**	**3.0**	**1.0**	**0.080**	Yes. Raw Signals	Corrosion patch, with multiple pits of different depths
WELD	240"						Yes. Raw Signals	
P3-17	248" to 260"	**250.5**	**254.4**	**2.9**	**1.0**	**0.085**	Yes. Raw Signals	Corrosion patch, with multiple pits of different depths
P3-16	282" to 294"	**No Metal Loss Detected**					Yes. Raw Signals	
P3-15	306" to 318"	**No Metal Loss Detected**					Yes. Raw Signals	
P3-14	330" to 342"	**337.1**	**338.0**	**0.9**	**0.5**	**0.105**	Yes. Raw Signals	Single Pit
P3-13	356" to 368"	**No Metal Loss Detected**					Yes. Raw Signals	
P3-12	390" to 402"	**392.4**	**397.0**	**3.6**	**1.25**	**0.065**	Yes. Raw Signals	Corrosion patch, with multiple pits of different depths

This page intentionally blank.

Pipe 1

Raw data output on same scale
420 inches, 2 welds @ 120 and 180 inches

Extra data for noise assessment	**Search Region**	Extra data for noise assessment

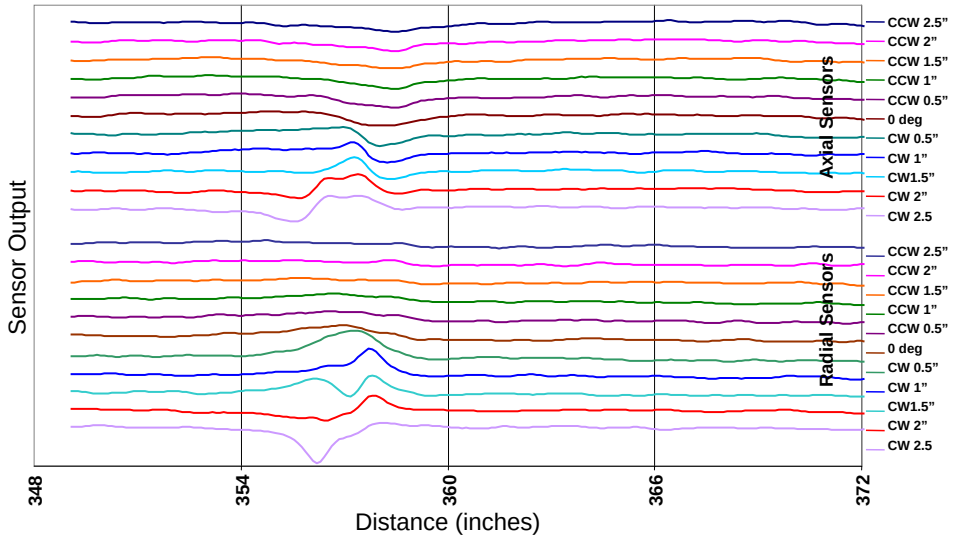

Cal 1-1

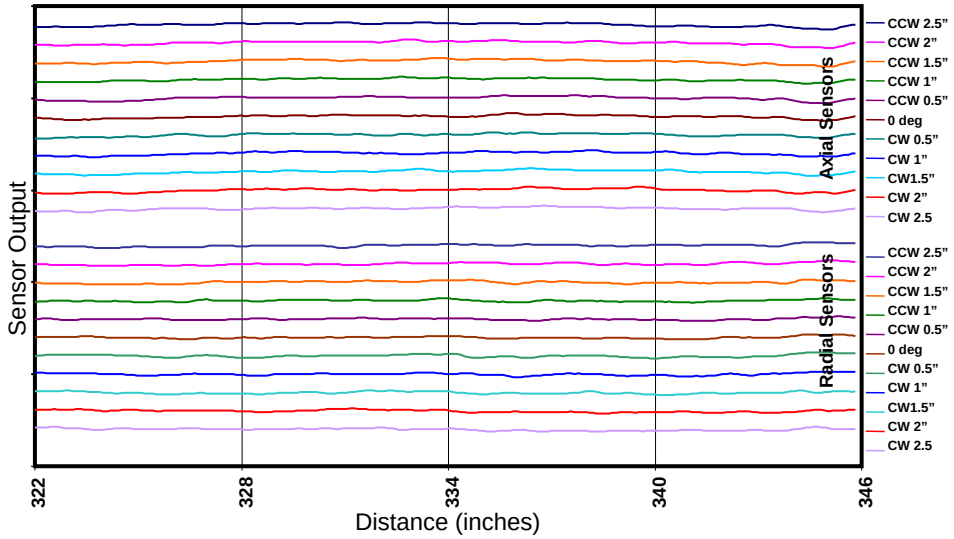
Sensor Output
Distance (inches)
322
328
334
340
346
Axial Sensors
Radial Sensors
CCW 2.5”
CCW 2”
CCW 1.5”
CCW 1”
CCW 0.5”
0 deg
CW 0.5”
CW 1”
CW1.5”
CW 2”
CW 2.5

P1-1

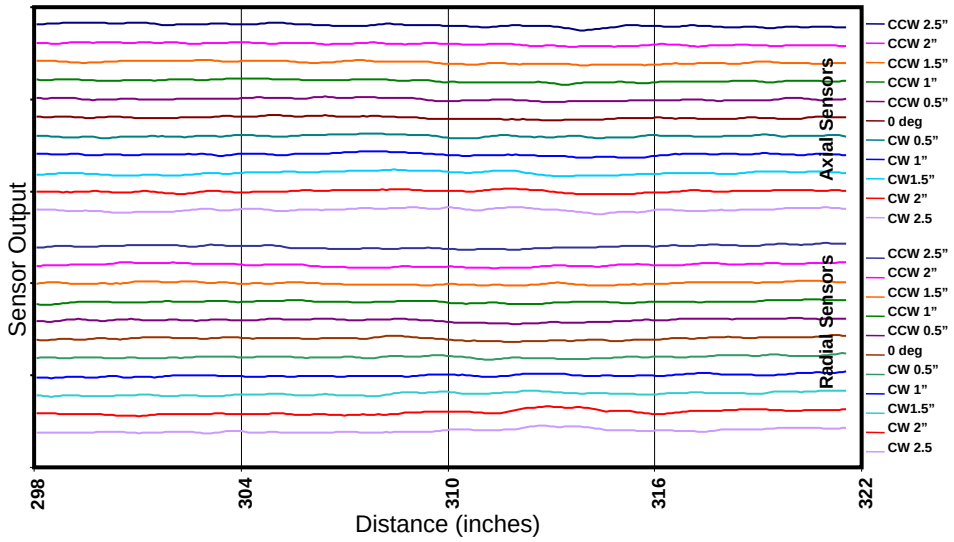
Sensor Output
Distance (inches)
298
304
310
316
322
Axial Sensors
Radial Sensors
CCW 2.5”
CCW 2”
CCW 1.5”
CCW 1”
CCW 0.5”
0 deg
CW 0.5”
CW 1”
CW1.5”
CW 2”
CW 2.5

P1-2

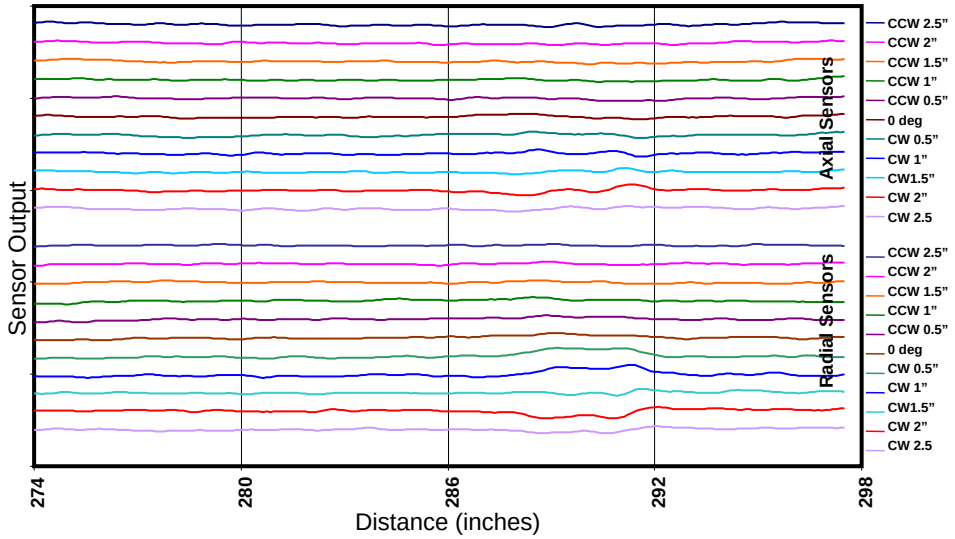
Sensor Output
Distance (inches)
274
280
286
292
298
Axial Sensors
Radial Sensors
CCW 2.5”
CCW 2”
CCW 1.5”
CCW 1”
CCW 0.5”
0 deg
CW 0.5”
CW 1”
CW1.5”
CW 2”
CW 2.5

P1-3

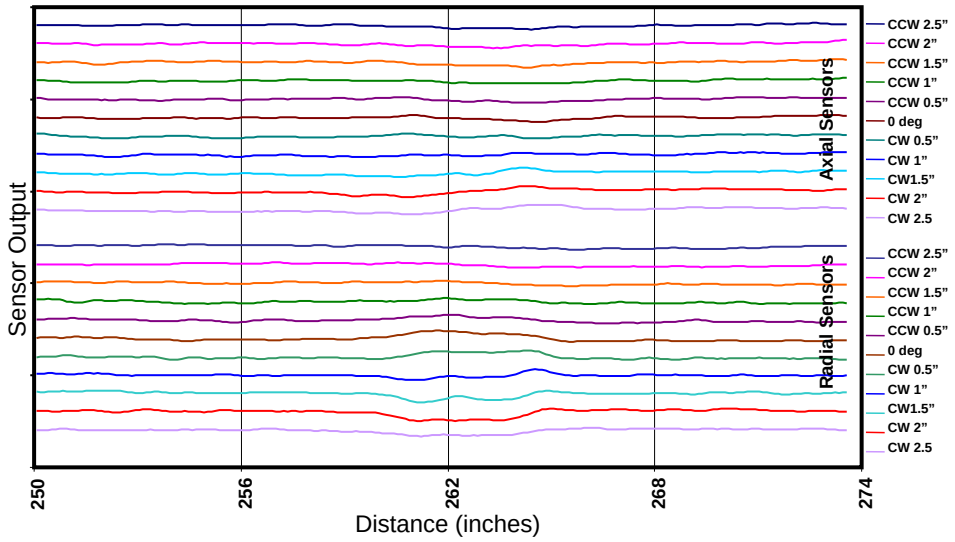
Sensor Output
Distance (inches)
250
256
262
268
274
Axial Sensors
Radial Sensors
CCW 2.5”
CCW 2”
CCW 1.5”
CCW 1”
CCW 0.5”
0 deg
CW 0.5”
CW 1”
CW1.5”
CW 2”
CW 2.5

P1-4

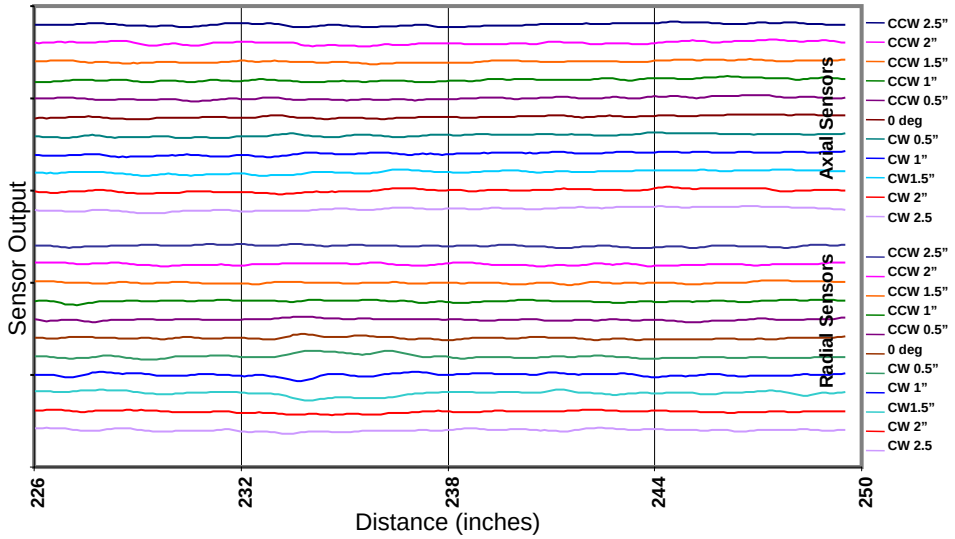
Sensor Output
Distance (inches)
226
232
238
244
250
Axial Sensors
Radial Sensors
CCW 2.5”
CCW 2”
CCW 1.5”
CCW 1”
CCW 0.5”
0 deg
CW 0.5”
CW 1”
CW1.5”
CW 2”
CW 2.5

P1-5

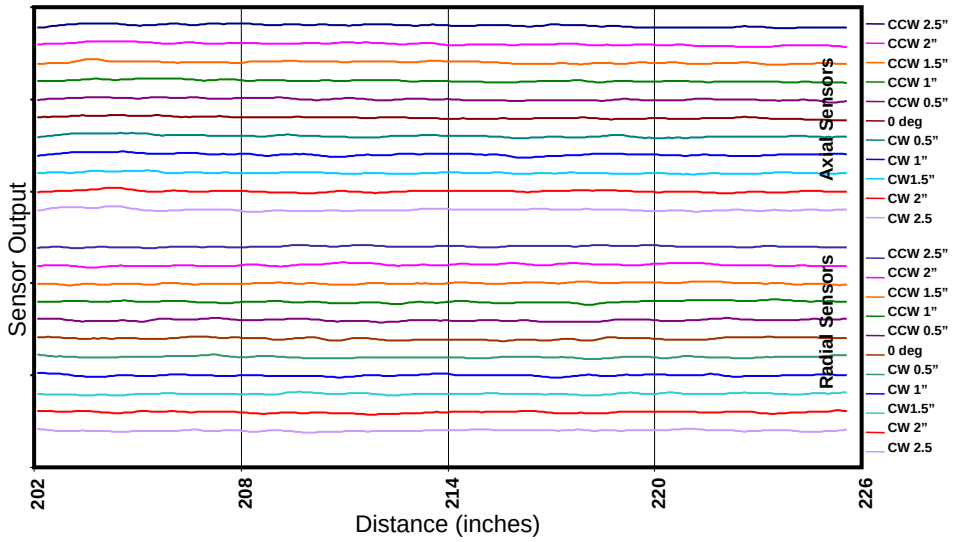
Sensor Output
Distance (inches)
202
208
214
220
226
Axial Sensors
Radial Sensors
CCW 2.5”
CCW 2”
CCW 1.5”
CCW 1”
CCW 0.5”
0 deg
CW 0.5”
CW 1”
CW1.5”
CW 2”
CW 2.5

P1-6

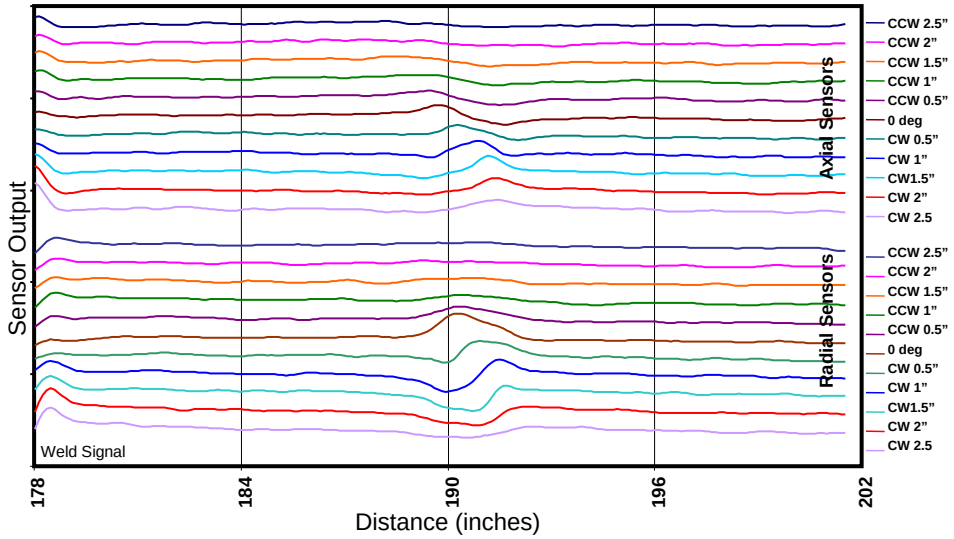
Sensor Output
Distance (inches)
178
184
190
196
202
Weld Signal
Axial Sensors
Radial Sensors
CCW 2.5”
CCW 2”
CCW 1.5”
CCW 1”
CCW 0.5”
0 deg
CW 0.5”
CW 1”
CW1.5”
CW 2”
CW 2.5

P1-7

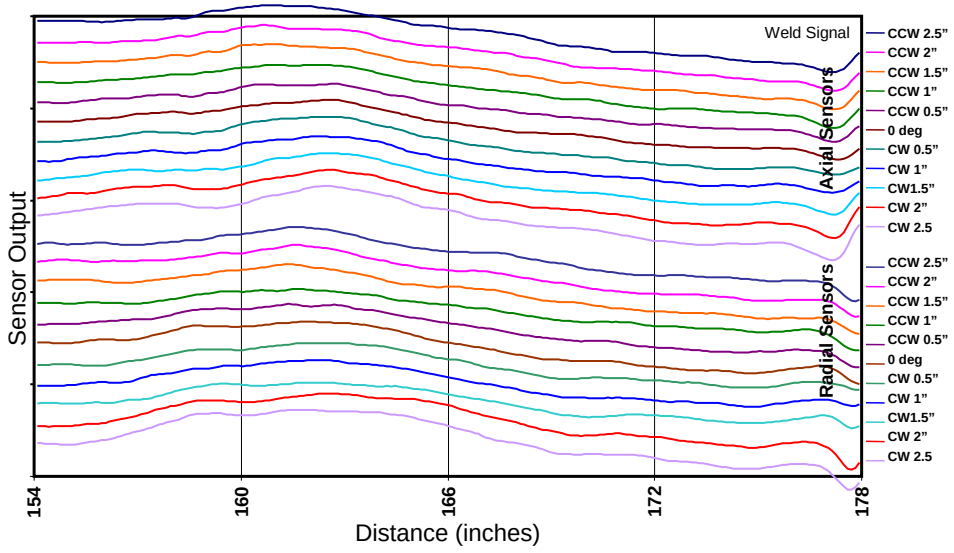
Sensor Output
Distance (inches)
154
160
166
172
178
Weld Signal
Axial Sensors
Radial Sensors
CCW 2.5”
CCW 2”
CCW 1.5”
CCW 1”
CCW 0.5”
0 deg
CW 0.5”
CW 1”
CW1.5”
CW 2”
CW 2.5

P1-8

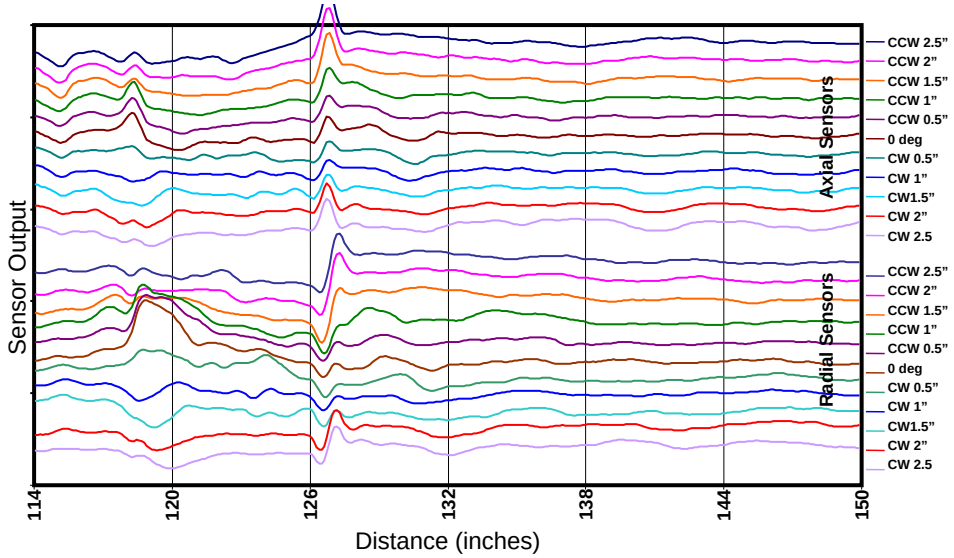

P1-9 note reporting area larger, 120 to 144 inches

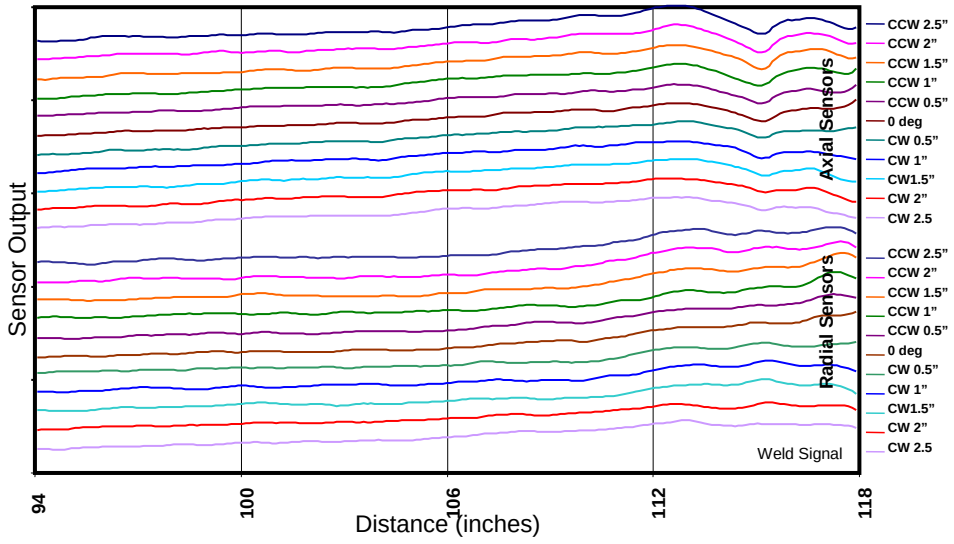

P1-10

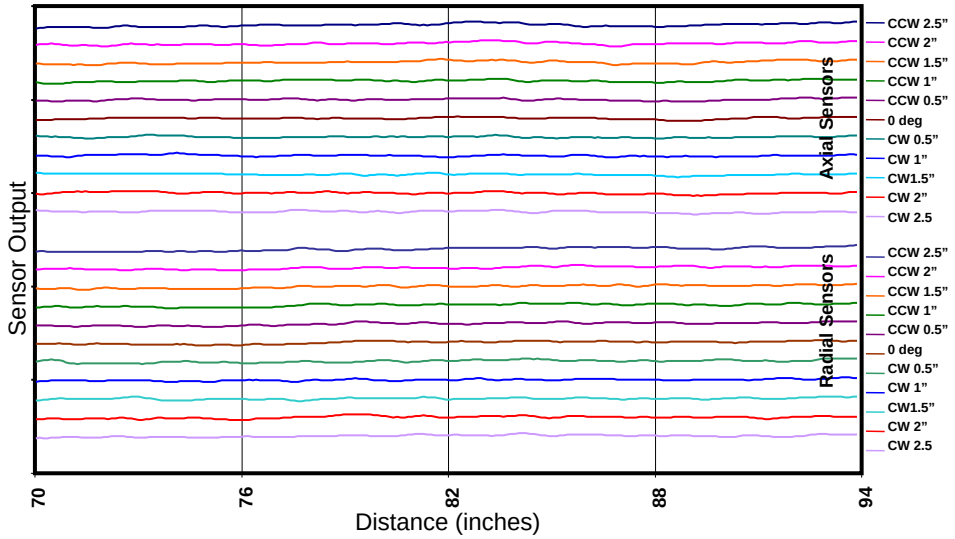
Sensor Output
70
76
82
88
94
Distance (inches)
Axial Sensors
Radial Sensors
CCW 2.5”
CCW 2”
CCW 1.5”
CCW 1”
CCW 0.5”
0 deg
CW 0.5”
CW 1”
CW1.5”
CW 2”
CW 2.5

P1-11

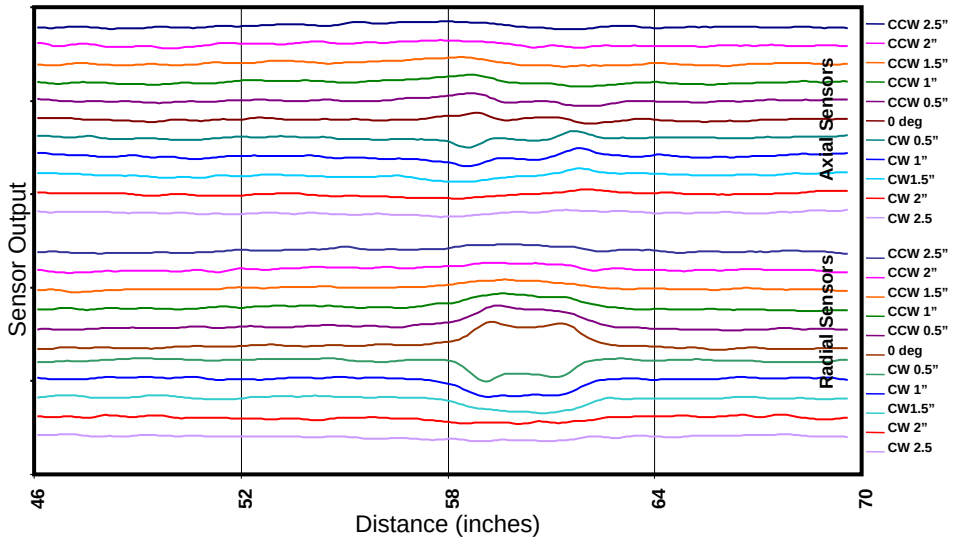
Sensor Output
46
52
58
64
70
Distance (inches)
Axial Sensors
Radial Sensors
CCW 2.5”
CCW 2”
CCW 1.5”
CCW 1”
CCW 0.5”
0 deg
CW 0.5”
CW 1”
CW1.5”
CW 2”
CW 2.5

P1-12

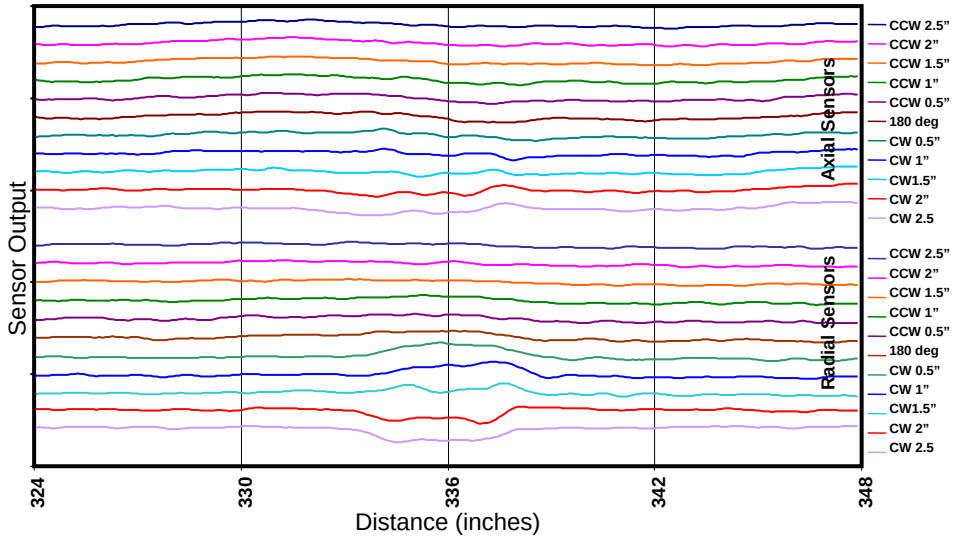
Sensor Output
Distance (inches)
324
330
336
342
348
Axial Sensors
Radial Sensors
CCW 2.5”
CCW 2”
CCW 1.5”
CCW 1”
CCW 0.5”
180 deg
CW 0.5”
CW 1”
CW1.5”
CW 2”
CW 2.5

P1-13

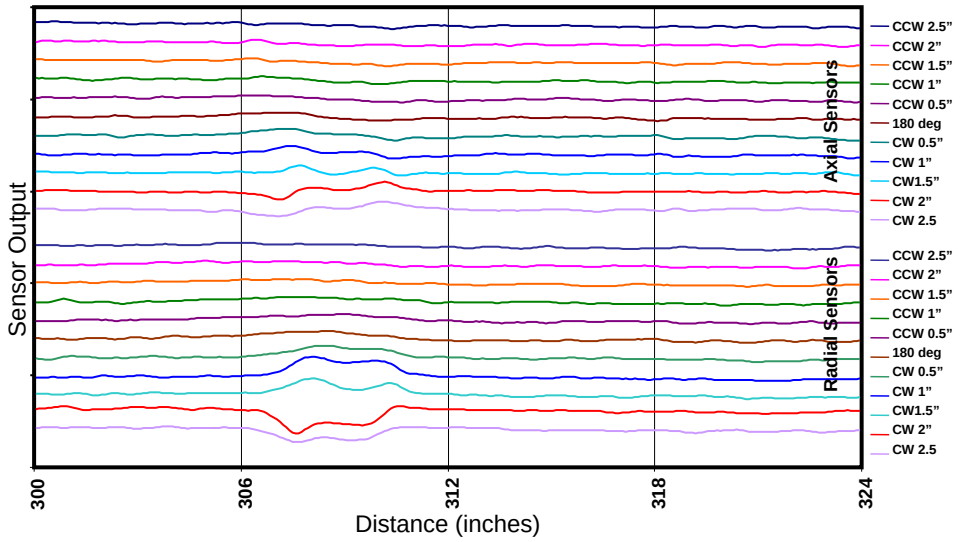
Sensor Output
Distance (inches)
300
306
312
318
324
Axial Sensors
Radial Sensors
CCW 2.5”
CCW 2”
CCW 1.5”
CCW 1”
CCW 0.5”
180 deg
CW 0.5”
CW 1”
CW1.5”
CW 2”
CW 2.5

P1-14

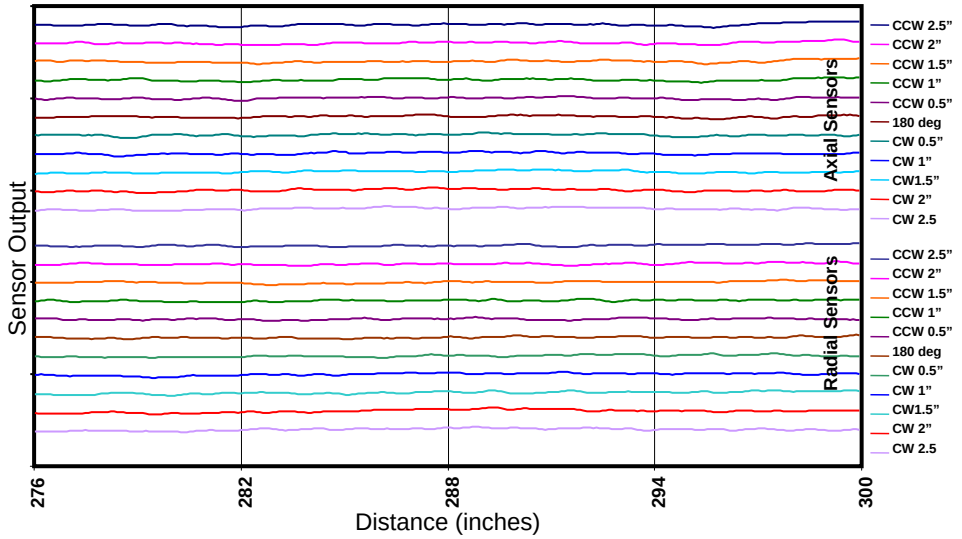
Sensor Output
Distance (inches)
276
282
288
294
300
Axial Sensors
Radial Sensors
CCW 2.5”
CCW 2”
CCW 1.5”
CCW 1”
CCW 0.5”
180 deg
CW 0.5”
CW 1”
CW1.5”
CW 2”
CW 2.5

P1-15

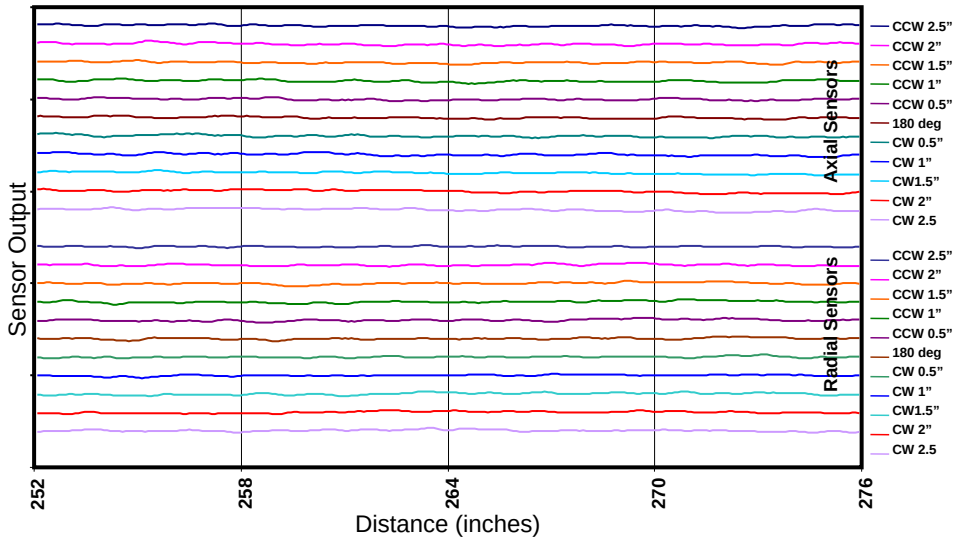
Sensor Output
Distance (inches)
252
258
264
270
276
Axial Sensors
Radial Sensors
CCW 2.5”
CCW 2”
CCW 1.5”
CCW 1”
CCW 0.5”
180 deg
CW 0.5”
CW 1”
CW1.5”
CW 2”
CW 2.5

P1-16

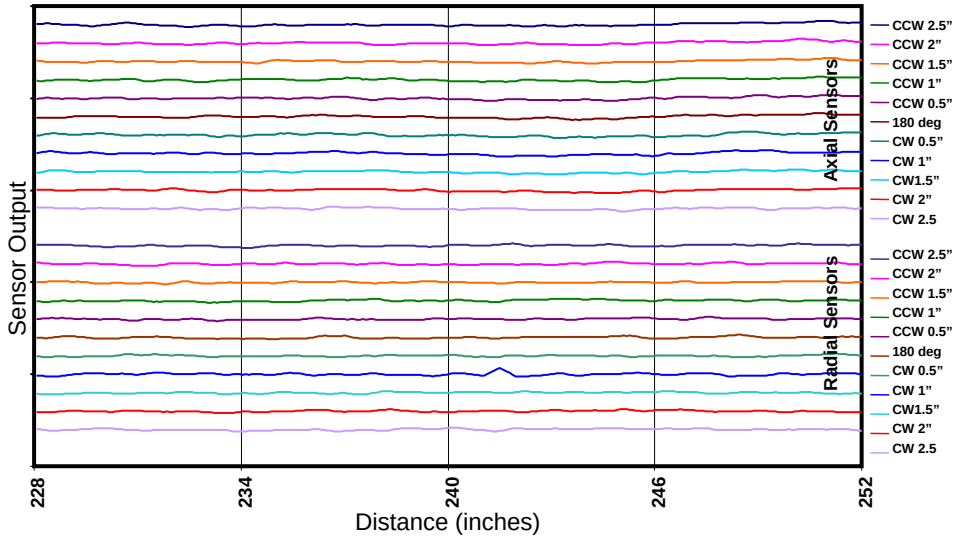
Sensor Output
Distance (inches)
228
234
240
246
252
Axial Sensors
Radial Sensors
CCW 2.5”
CCW 2”
CCW 1.5”
CCW 1”
CCW 0.5”
180 deg
CW 0.5”
CW 1”
CW1.5”
CW 2”
CW 2.5

P1-17

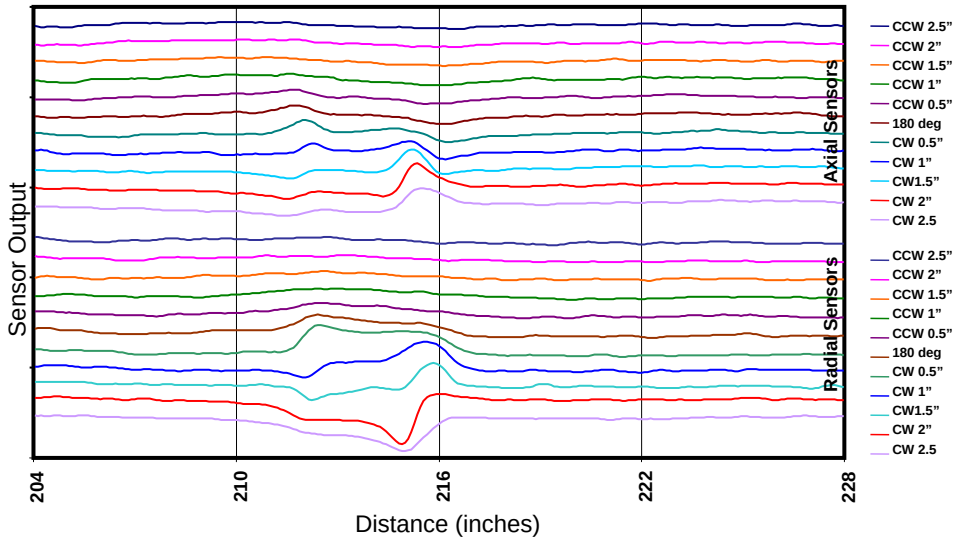
Sensor Output
Distance (inches)
204
210
216
222
228
Axial Sensors
Radial Sensors
CCW 2.5”
CCW 2”
CCW 1.5”
CCW 1”
CCW 0.5”
180 deg
CW 0.5”
CW 1”
CW1.5”
CW 2”
CW 2.5

P1-18

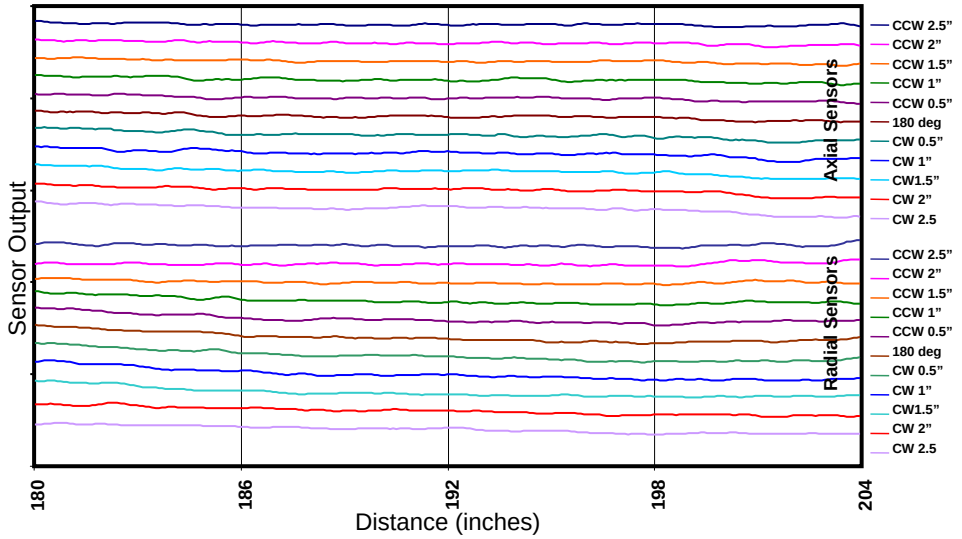
Sensor Output
Distance (inches)
180
186
192
198
204
Axial Sensors
Radial Sensors
CCW 2.5”
CCW 2”
CCW 1.5”
CCW 1”
CCW 0.5”
180 deg
CW 0.5”
CW 1”
CW1.5”
CW 2”
CW 2.5

P1-19

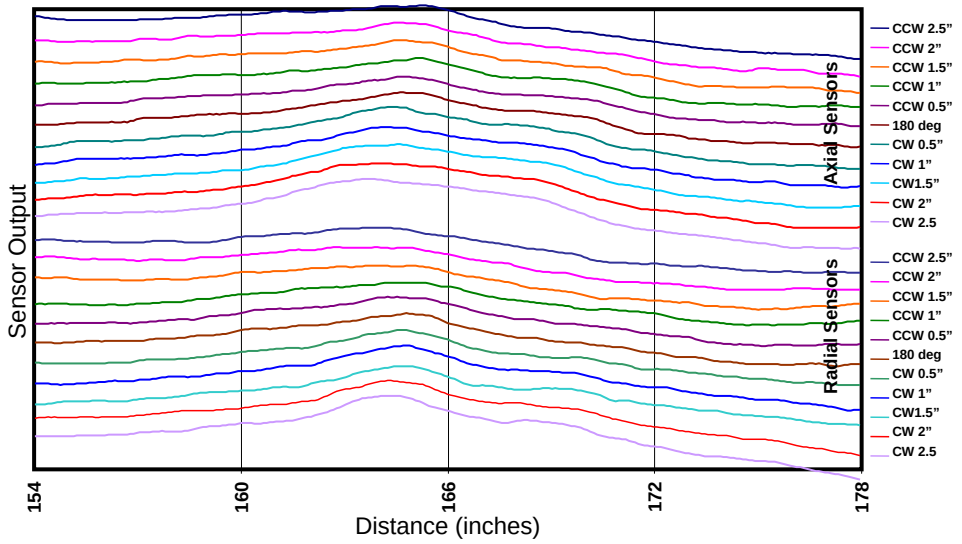
Sensor Output
Distance (inches)
154
160
166
172
178
Axial Sensors
Radial Sensors
CCW 2.5”
CCW 2”
CCW 1.5”
CCW 1”
CCW 0.5”
180 deg
CW 0.5”
CW 1”
CW1.5”
CW 2”
CW 2.5

P1-20

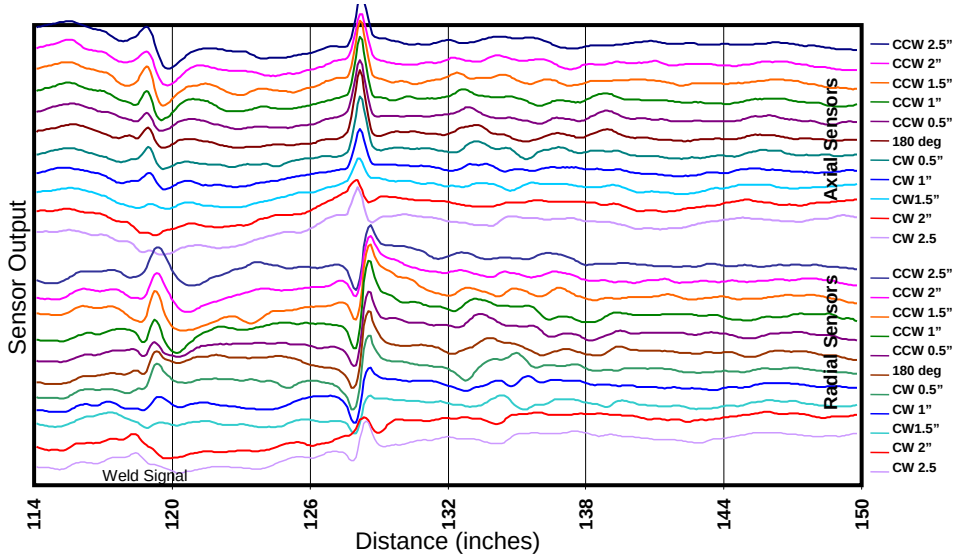

P1-21 note reporting area larger, 120 to 144 inches

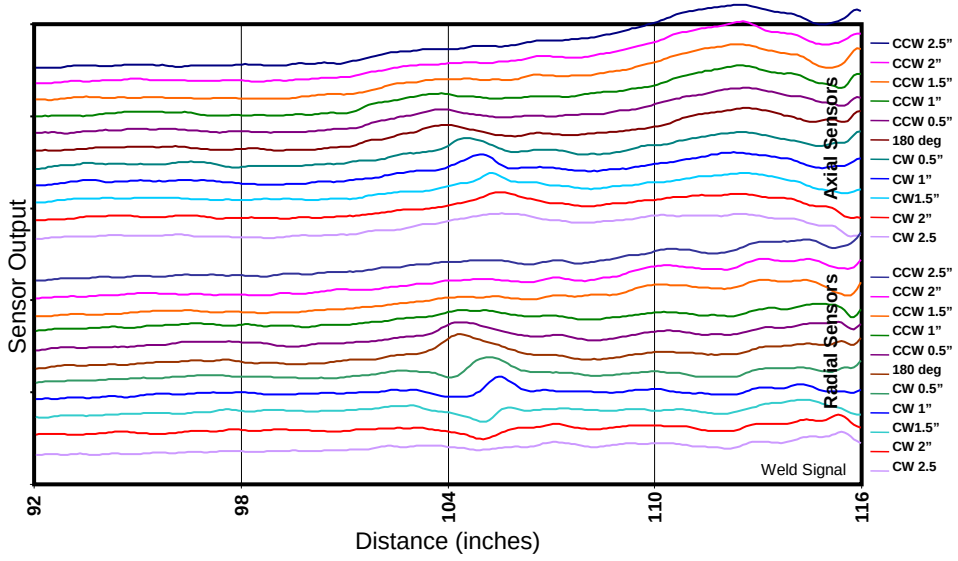

P1-22

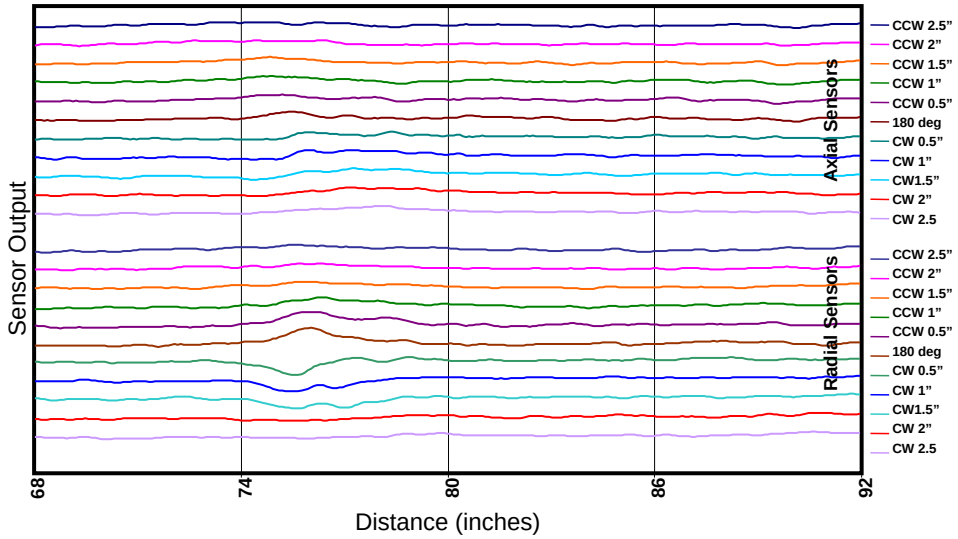
Sensor Output
Distance (inches)
68
74
80
86
92
Axial Sensors
CCW 2.5”
CCW 2”
CCW 1.5”
CCW 1”
CCW 0.5”
180 deg
CW 0.5”
CW 1”
CW1.5”
CW 2”
CW 2.5
Radial Sensors
CCW 2.5”
CCW 2”
CCW 1.5”
CCW 1”
CCW 0.5”
180 deg
CW 0.5”
CW 1”
CW1.5”
CW 2”
CW 2.5

P1-23

Pipe 2

Raw data output on same scale
360 inches,1 weld @120 inches

Extra data for noise assessment	**Search Region**	Extra data for noise assessment

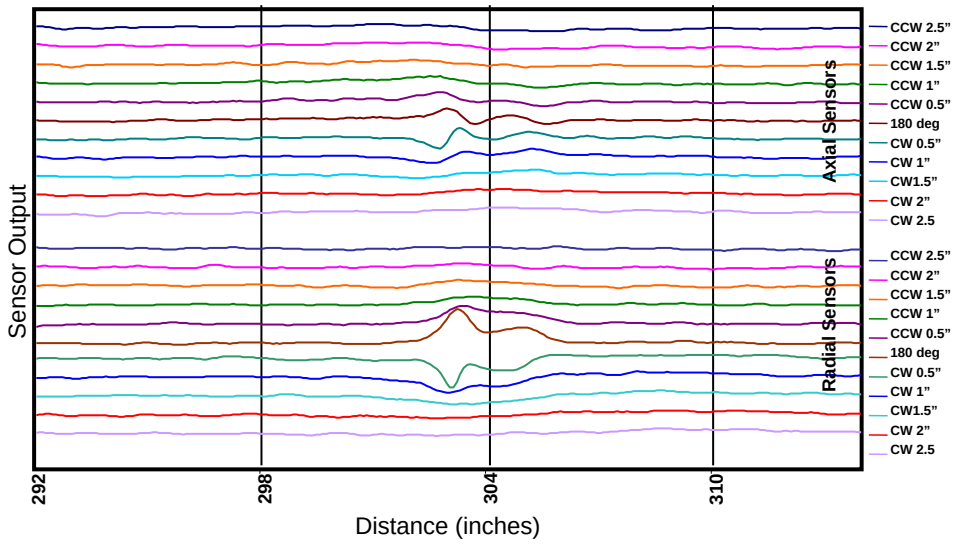

Cal 2-1

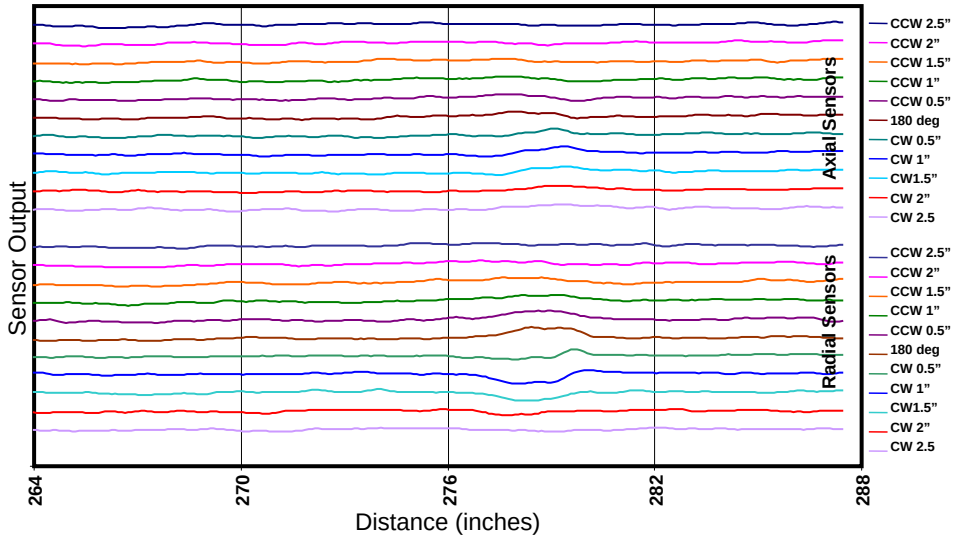
Sensor Output
Distance (inches)
264
270
276
282
288
Axial Sensors
Radial Sensors
CCW 2.5”
CCW 2”
CCW 1.5”
CCW 1”
CCW 0.5”
180 deg
CW 0.5”
CW 1”
CW1.5”
CW 2”
CW 2.5

Cal 2-2

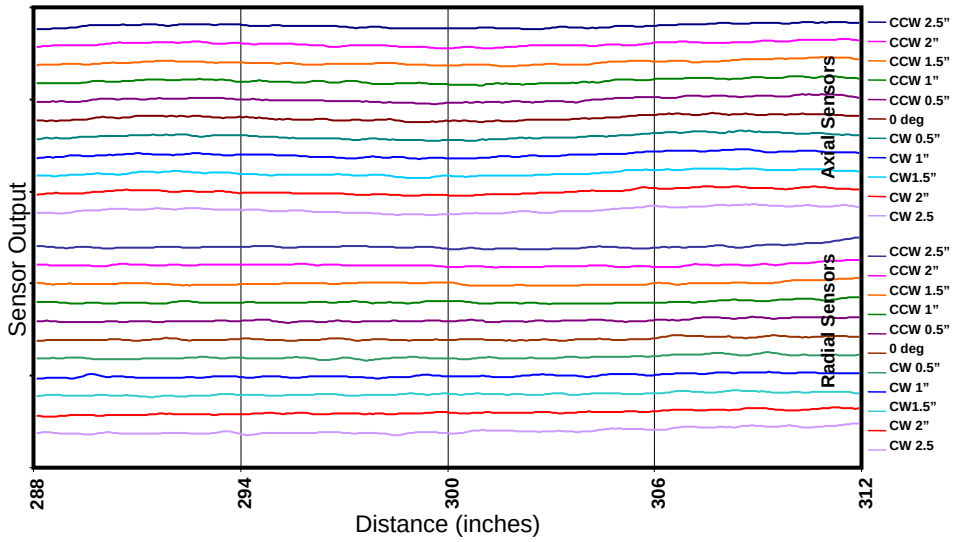
Sensor Output
Distance (inches)
288
294
300
306
312
Axial Sensors
Radial Sensors
CCW 2.5”
CCW 2”
CCW 1.5”
CCW 1”
CCW 0.5”
0 deg
CW 0.5”
CW 1”
CW1.5”
CW 2”
CW 2.5

P2-1

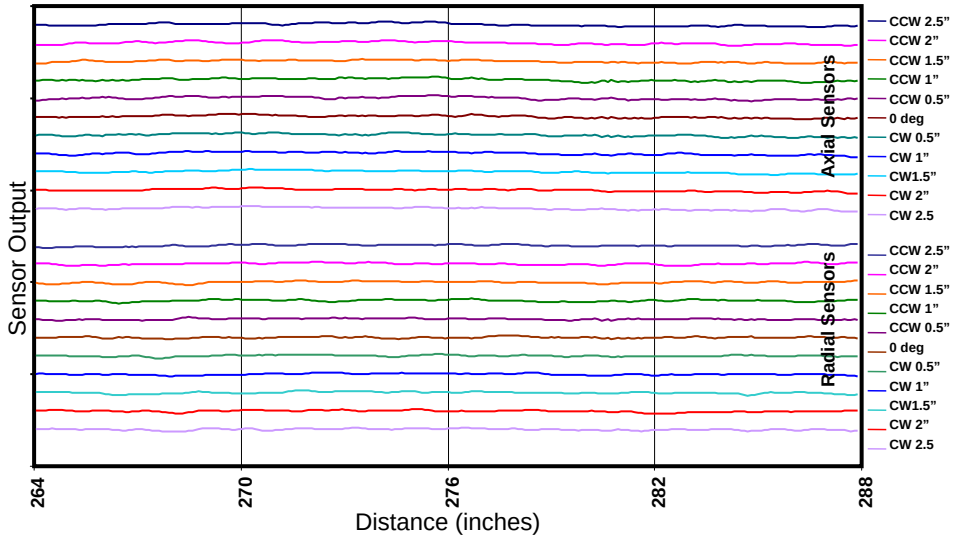
Sensor Output
264
270
276
282
288
Distance (inches)
Axial Sensors
Radial Sensors
CCW 2.5”
CCW 2”
CCW 1.5”
CCW 1”
CCW 0.5”
0 deg
CW 0.5”
CW 1”
CW1.5”
CW 2”
CW 2.5

P2-2

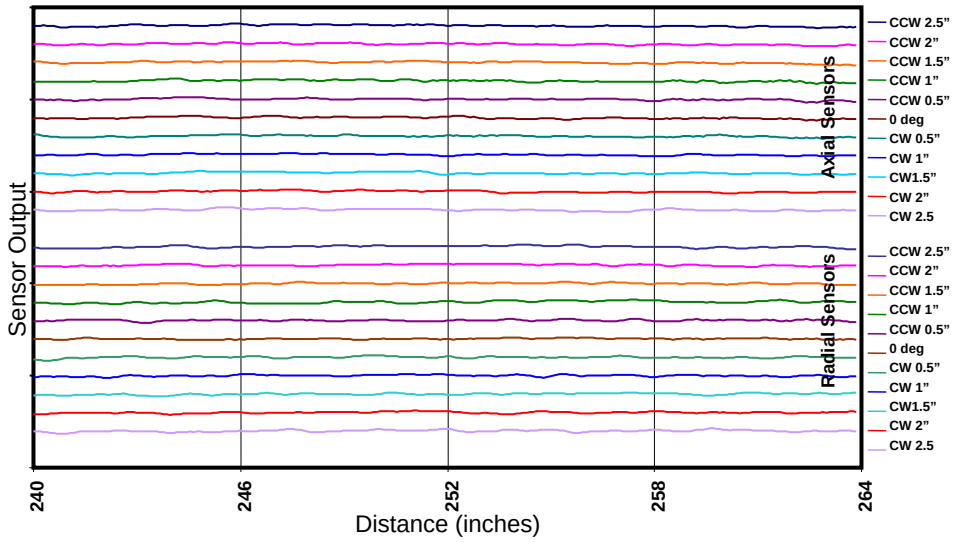
Sensor Output
240
246
252
258
264
Distance (inches)
Axial Sensors
Radial Sensors
CCW 2.5”
CCW 2”
CCW 1.5”
CCW 1”
CCW 0.5”
0 deg
CW 0.5”
CW 1”
CW1.5”
CW 2”
CW 2.5

P2-3

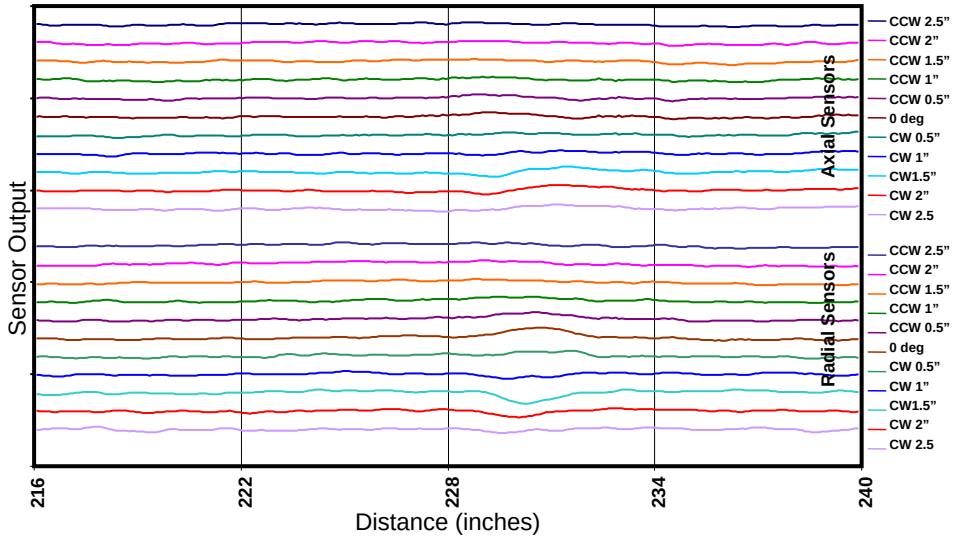
Sensor Output
Distance (inches)
216
222
228
234
240
Axial Sensors
Radial Sensors
CCW 2.5”
CCW 2”
CCW 1.5”
CCW 1”
CCW 0.5”
0 deg
CW 0.5”
CW 1”
CW1.5”
CW 2”
CW 2.5

P2-4

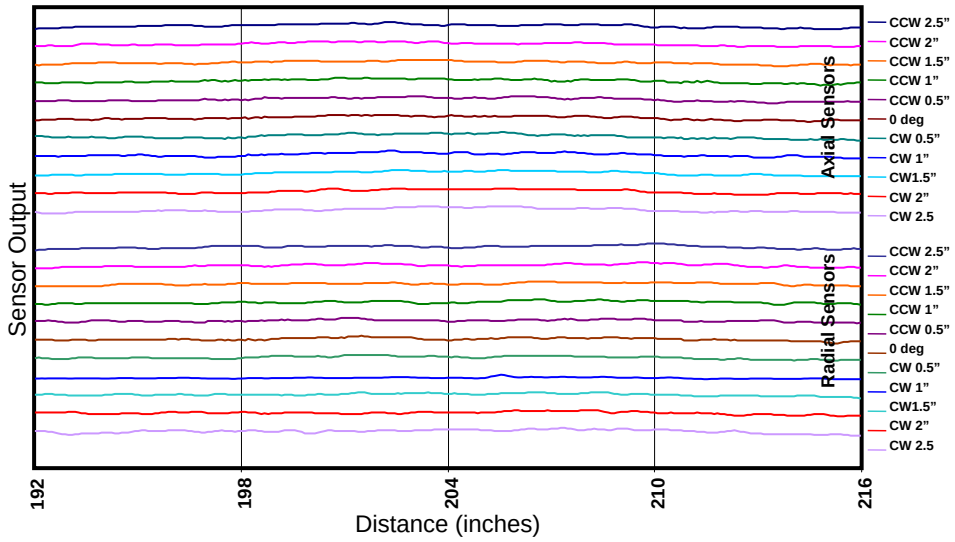
Sensor Output
Distance (inches)
192
198
204
210
216
Axial Sensors
Radial Sensors
CCW 2.5”
CCW 2”
CCW 1.5”
CCW 1”
CCW 0.5”
0 deg
CW 0.5”
CW 1”
CW1.5”
CW 2”
CW 2.5

P2-5

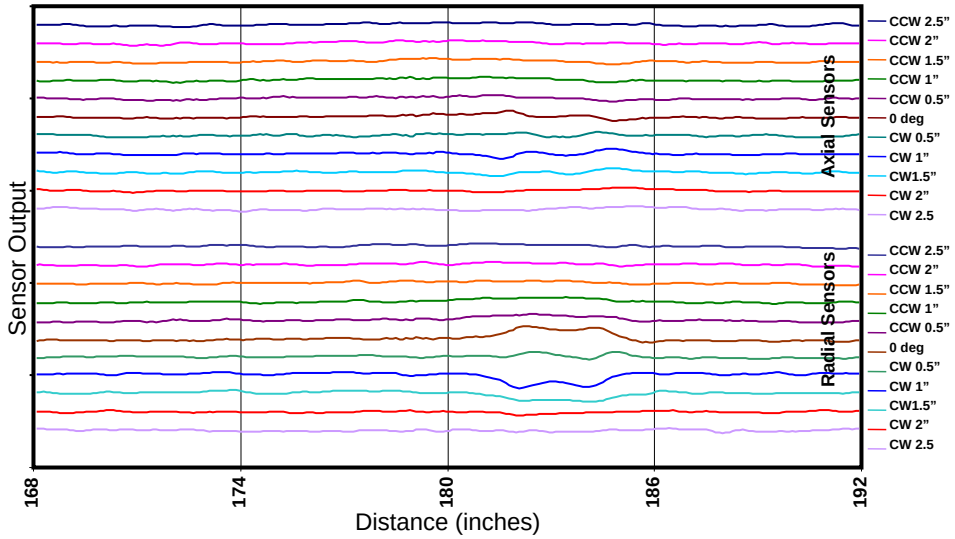
Sensor Output
Distance (inches)
168
174
180
186
192
Axial Sensors
Radial Sensors
CCW 2.5”
CCW 2”
CCW 1.5”
CCW 1”
CCW 0.5”
0 deg
CW 0.5”
CW 1”
CW1.5”
CW 2”
CW 2.5

P2-6

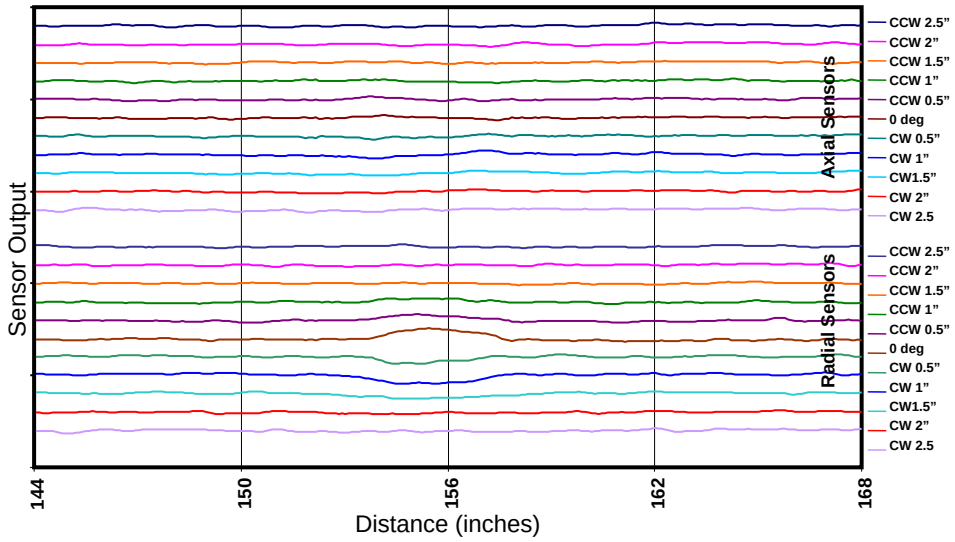
Sensor Output
Distance (inches)
144
150
156
162
168
Axial Sensors
Radial Sensors
CCW 2.5”
CCW 2”
CCW 1.5”
CCW 1”
CCW 0.5”
0 deg
CW 0.5”
CW 1”
CW1.5”
CW 2”
CW 2.5

P2-7

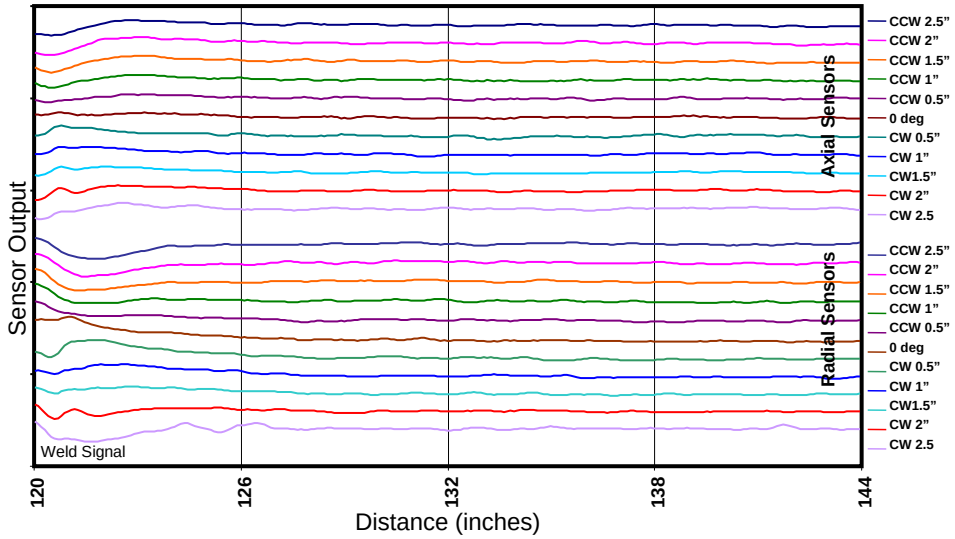
Sensor Output
Weld Signal
Axial Sensors
Radial Sensors
CCW 2.5”
CCW 2”
CCW 1.5”
CCW 1”
CCW 0.5”
0 deg
CW 0.5”
CW 1”
CW1.5”
CW 2”
CW 2.5
120
126
132
138
144
Distance (inches)

P2-8

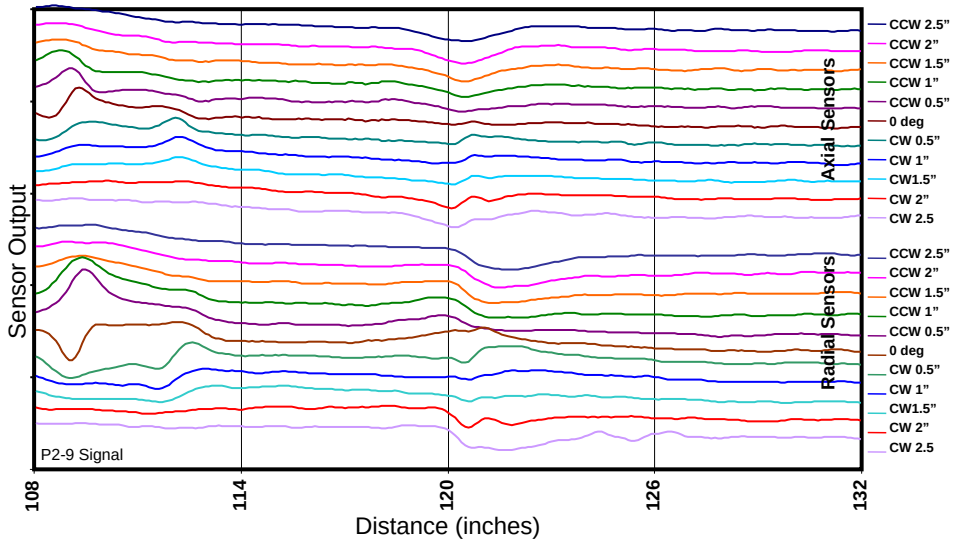
Sensor Output
P2-9 Signal
Axial Sensors
Radial Sensors
CCW 2.5”
CCW 2”
CCW 1.5”
CCW 1”
CCW 0.5”
0 deg
CW 0.5”
CW 1”
CW1.5”
CW 2”
CW 2.5
108
114
120
126
132
Distance (inches)

P2-Weld

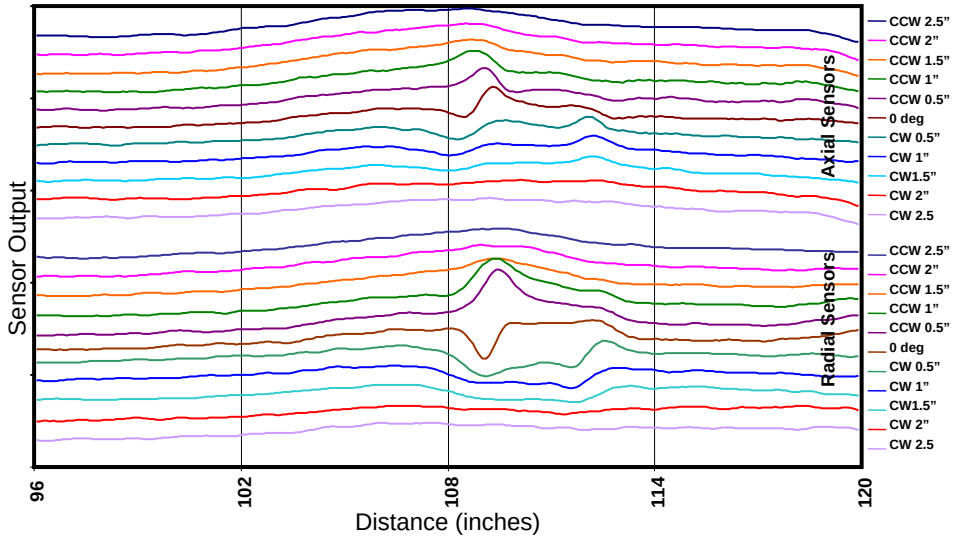
Sensor Output
Distance (inches)
96
102
108
114
120
Axial Sensors
Radial Sensors
CCW 2.5”
CCW 2”
CCW 1.5”
CCW 1”
CCW 0.5”
0 deg
CW 0.5”
CW 1”
CW1.5”
CW 2”
CW 2.5

P2-9

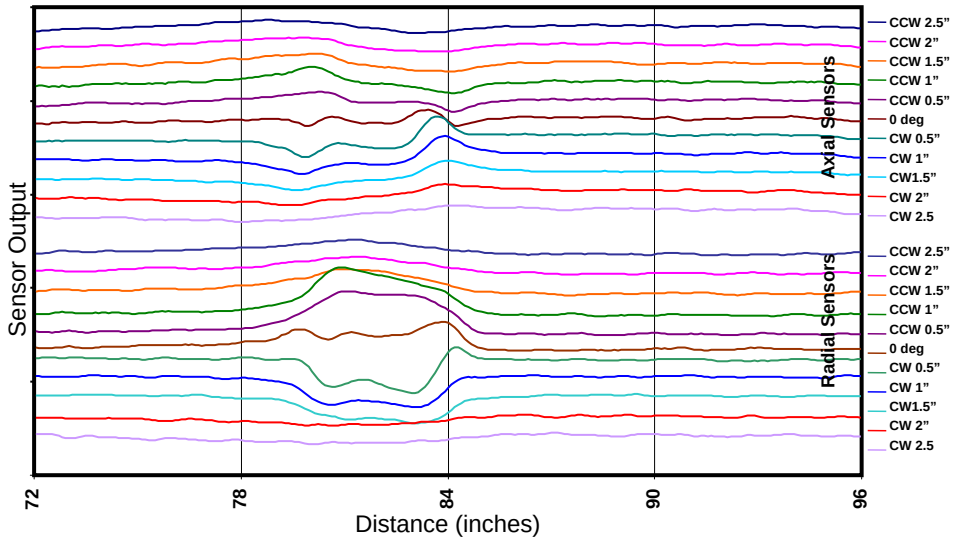
Sensor Output
Distance (inches)
72
78
84
90
96
Axial Sensors
Radial Sensors
CCW 2.5”
CCW 2”
CCW 1.5”
CCW 1”
CCW 0.5”
0 deg
CW 0.5”
CW 1”
CW1.5”
CW 2”
CW 2.5

P2-10

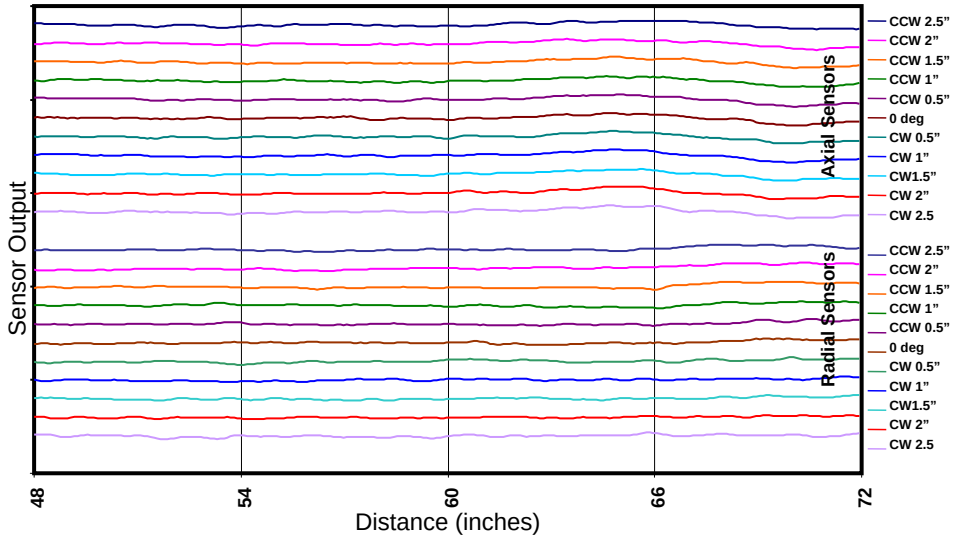
Sensor Output
Distance (inches)
48
54
60
66
72
Axial Sensors
Radial Sensors
CCW 2.5”
CCW 2”
CCW 1.5”
CCW 1”
CCW 0.5”
0 deg
CW 0.5”
CW 1”
CW1.5”
CW 2”
CW 2.5

P2-11

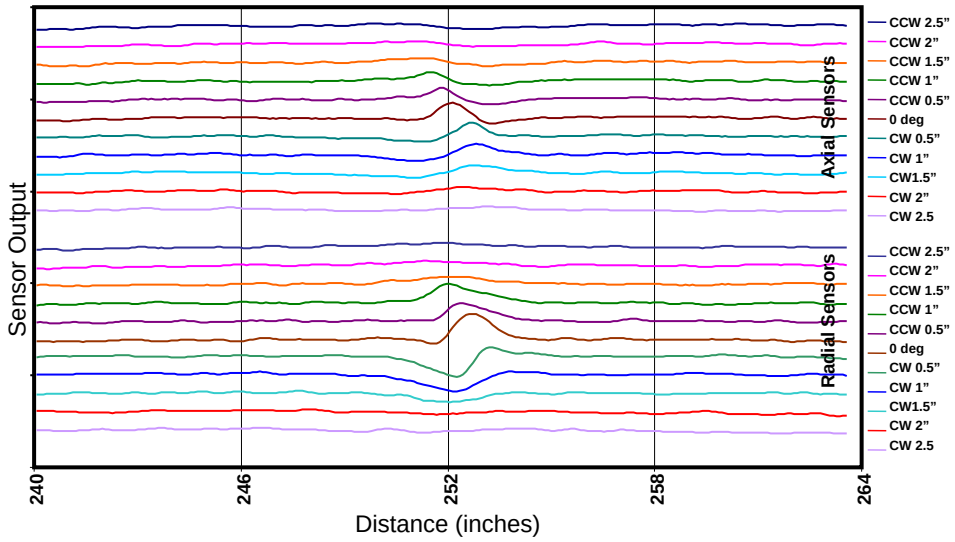
Sensor Output
Distance (inches)
240
246
252
258
264
Axial Sensors
Radial Sensors
CCW 2.5”
CCW 2”
CCW 1.5”
CCW 1”
CCW 0.5”
0 deg
CW 0.5”
CW 1”
CW1.5”
CW 2”
CW 2.5

P2-12

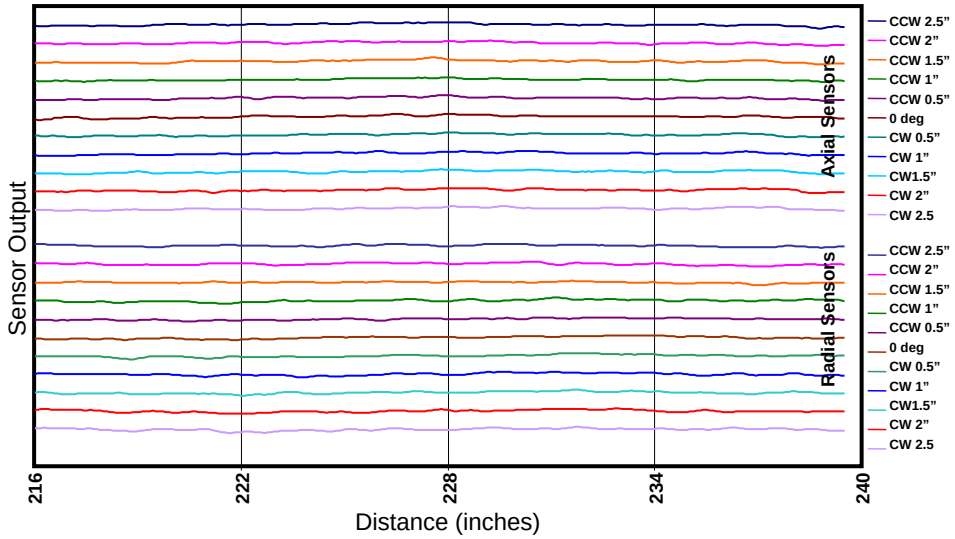
Sensor Output
Distance (inches)
216
222
228
234
240
Axial Sensors
Radial Sensors
CCW 2.5”
CCW 2”
CCW 1.5”
CCW 1”
CCW 0.5”
0 deg
CW 0.5”
CW 1”
CW1.5”
CW 2”
CW 2.5

P2-13

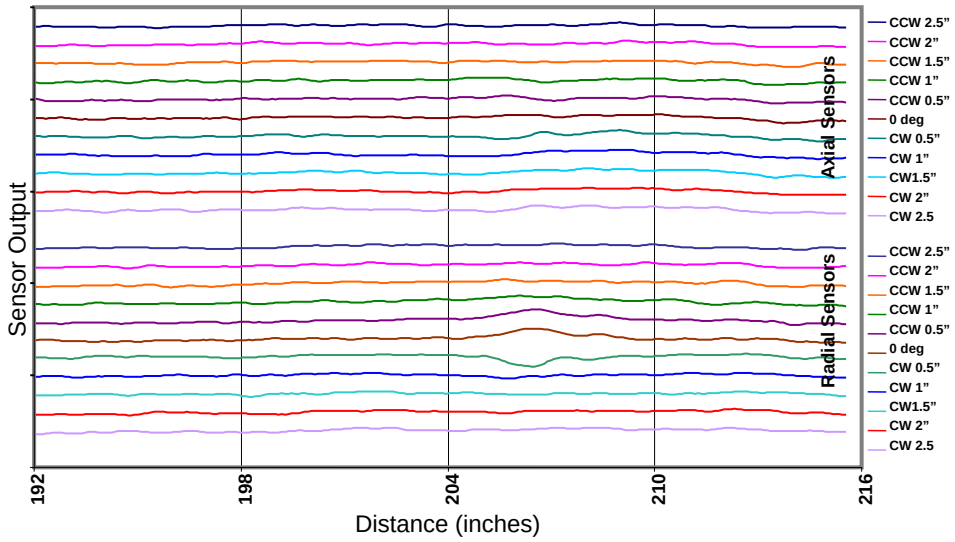
Sensor Output
Distance (inches)
192
198
204
210
216
Axial Sensors
Radial Sensors
CCW 2.5”
CCW 2”
CCW 1.5”
CCW 1”
CCW 0.5”
0 deg
CW 0.5”
CW 1”
CW1.5”
CW 2”
CW 2.5

P2-14

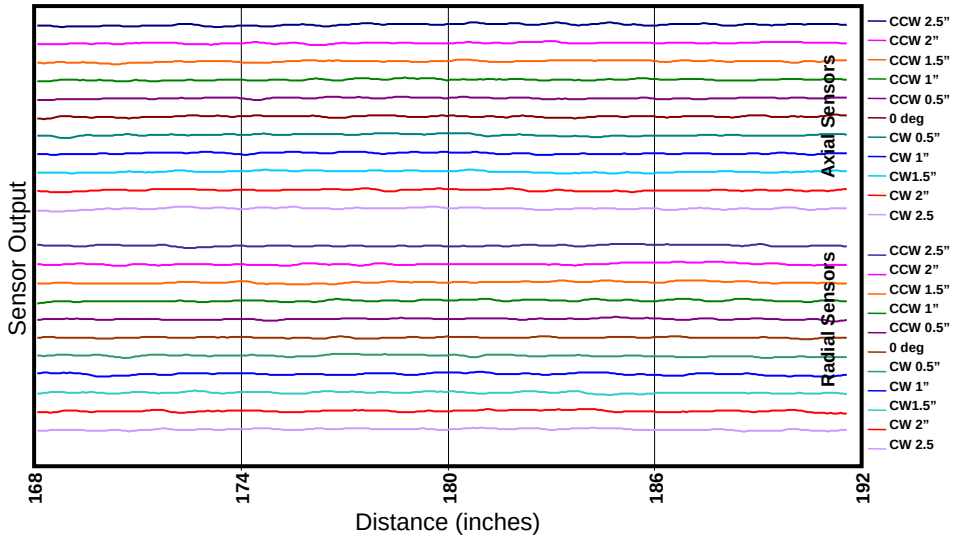
Sensor Output
Distance (inches)
168
174
180
186
192
Axial Sensors
Radial Sensors
CCW 2.5”
CCW 2”
CCW 1.5”
CCW 1”
CCW 0.5”
0 deg
CW 0.5”
CW 1”
CW1.5”
CW 2”
CW 2.5

P2-15

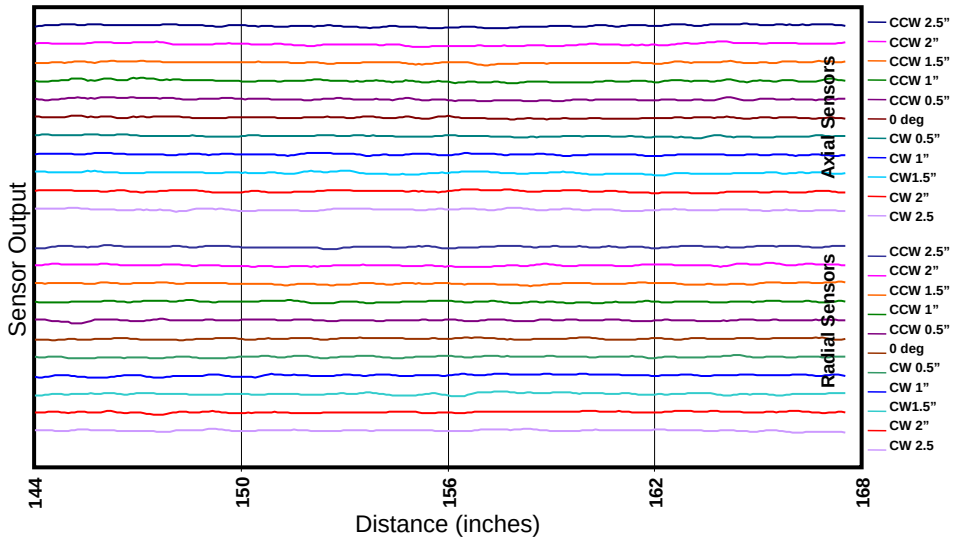
Sensor Output
Distance (inches)
144
150
156
162
168
Axial Sensors
Radial Sensors
CCW 2.5”
CCW 2”
CCW 1.5”
CCW 1”
CCW 0.5”
0 deg
CW 0.5”
CW 1”
CW1.5”
CW 2”
CW 2.5

P2-16

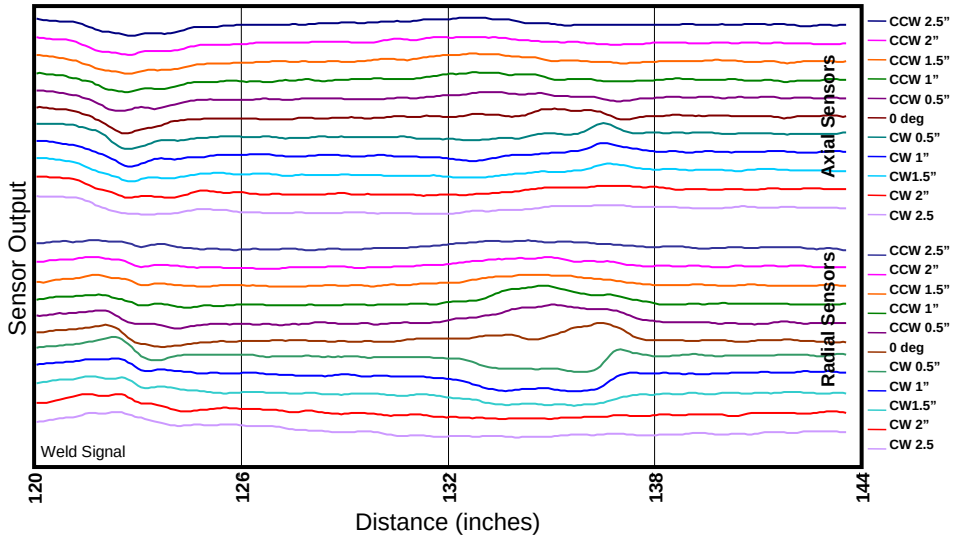
Sensor Output
Distance (inches)
120
126
132
138
144
Weld Signal
Axial Sensors
Radial Sensors
CCW 2.5”
CCW 2”
CCW 1.5”
CCW 1”
CCW 0.5”
0 deg
CW 0.5”
CW 1”
CW1.5”
CW 2”
CW 2.5

P2-17

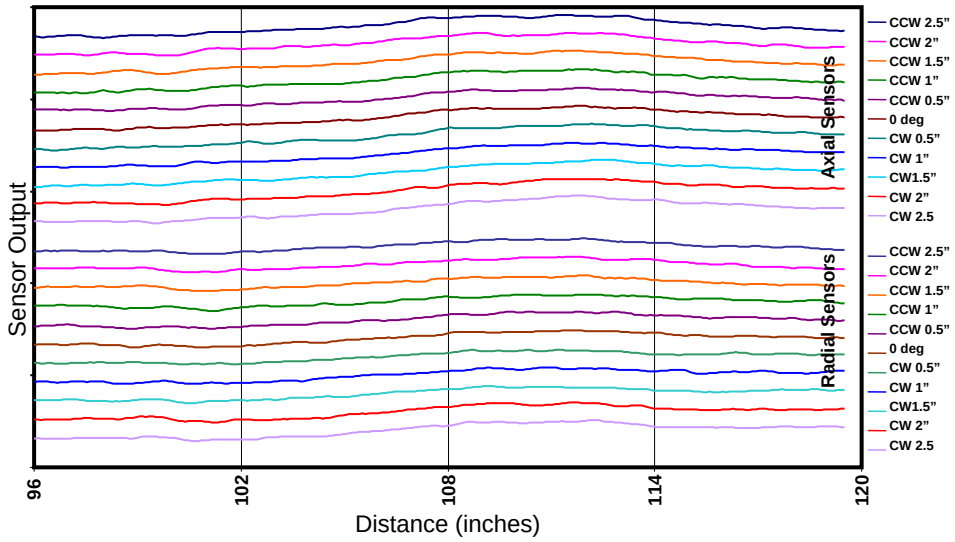
Sensor Output
Distance (inches)
96
102
108
114
120
Axial Sensors
Radial Sensors
CCW 2.5”
CCW 2”
CCW 1.5”
CCW 1”
CCW 0.5”
0 deg
CW 0.5”
CW 1”
CW1.5”
CW 2”
CW 2.5

P2-18

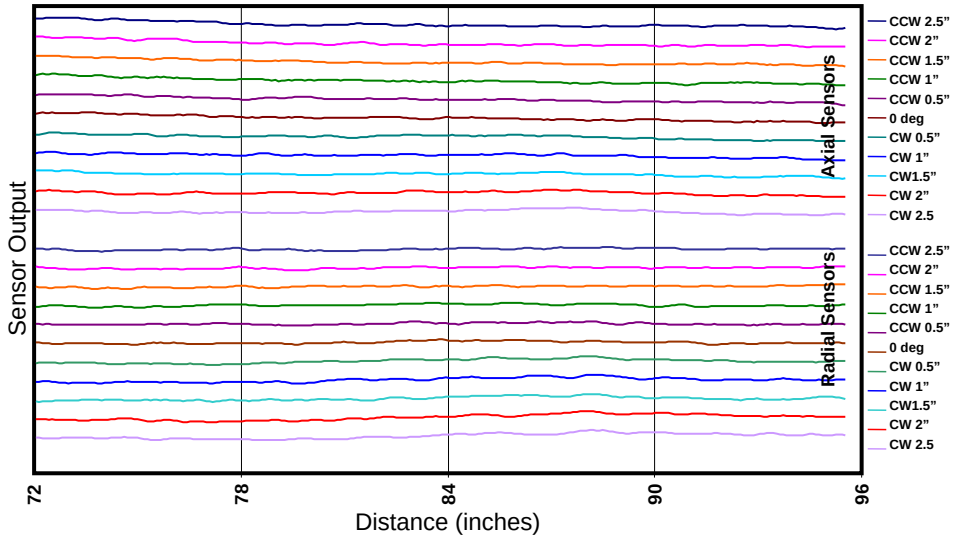
Sensor Output
Distance (inches)
72
78
84
90
96
Axial Sensors
Radial Sensors
CCW 2.5”
CCW 2”
CCW 1.5”
CCW 1”
CCW 0.5”
0 deg
CW 0.5”
CW 1”
CW1.5”
CW 2”
CW 2.5

P2-19

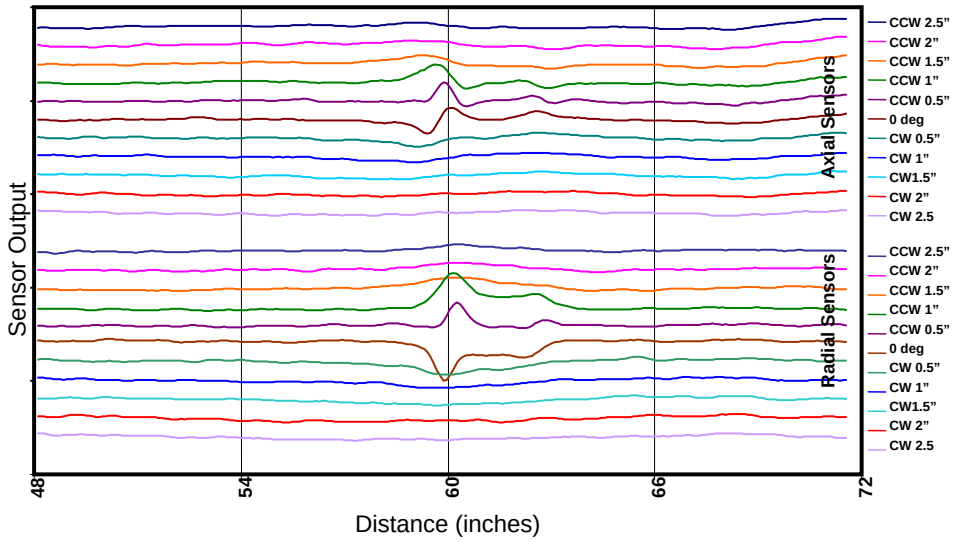
Sensor Output
Distance (inches)
48
54
60
66
72
Axial Sensors
Radial Sensors
CCW 2.5”
CCW 2”
CCW 1.5”
CCW 1”
CCW 0.5”
0 deg
CW 0.5”
CW 1”
CW1.5”
CW 2”
CW 2.5

P2-20

Pipe 3

Raw data output on same scale
480 inches, 1 weld @ 240 inches

Extra data for noise assessment	**Search Region**	Extra data for noise assessment

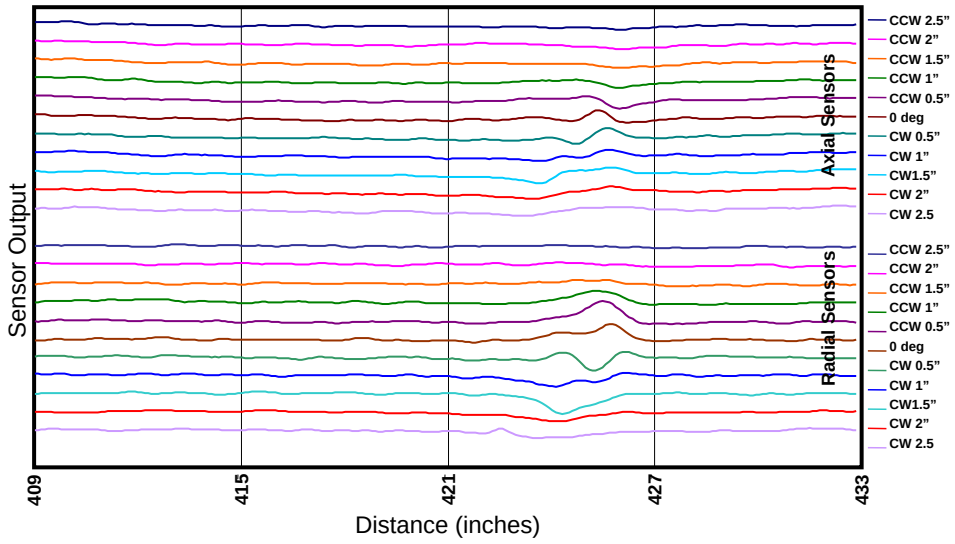

Cal 3-1

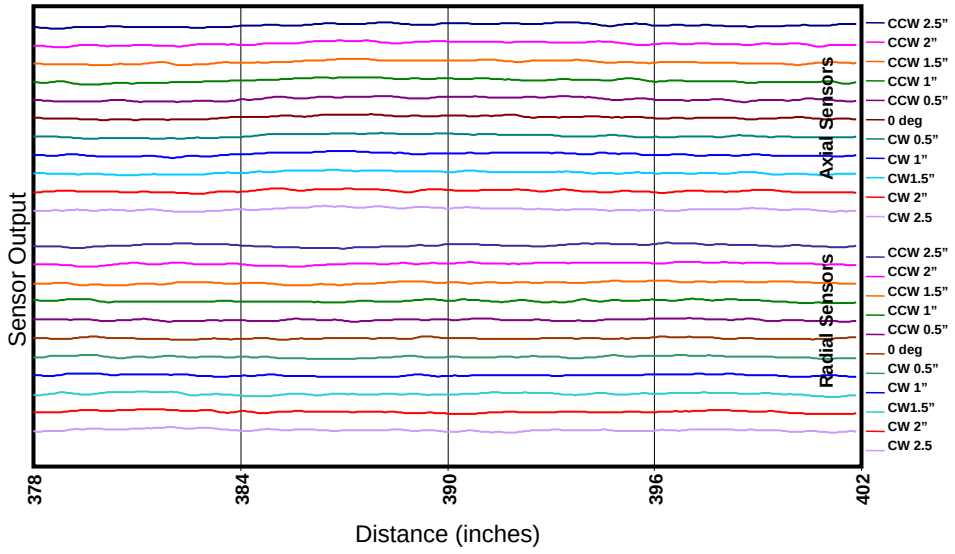
Sensor Output
Distance (inches)
378
384
390
396
402
Axial Sensors
Radial Sensors
CCW 2.5”
CCW 2”
CCW 1.5”
CCW 1”
CCW 0.5”
0 deg
CW 0.5”
CW 1”
CW1.5”
CW 2”
CW 2.5

P3-1

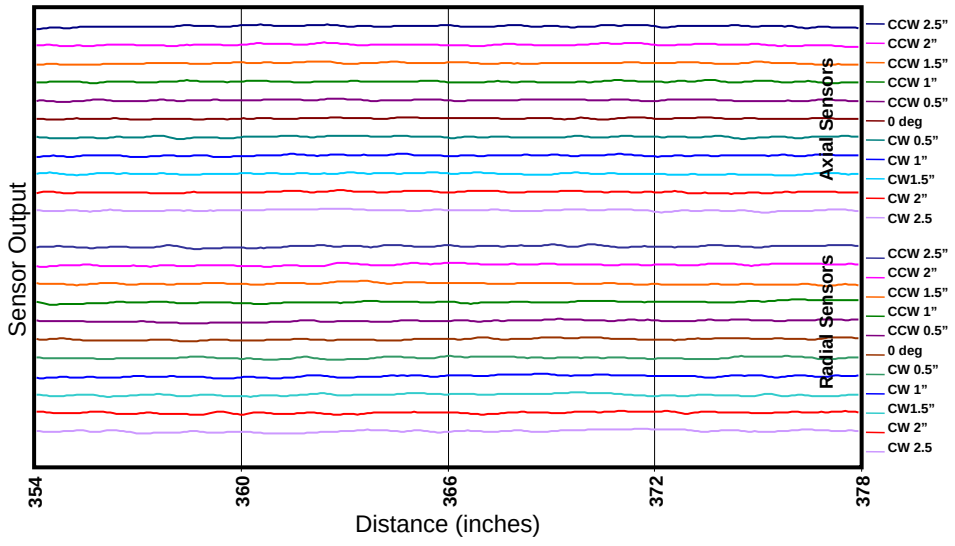
Sensor Output
Distance (inches)
354
360
366
372
378
Axial Sensors
Radial Sensors
CCW 2.5”
CCW 2”
CCW 1.5”
CCW 1”
CCW 0.5”
0 deg
CW 0.5”
CW 1”
CW1.5”
CW 2”
CW 2.5

P3-2

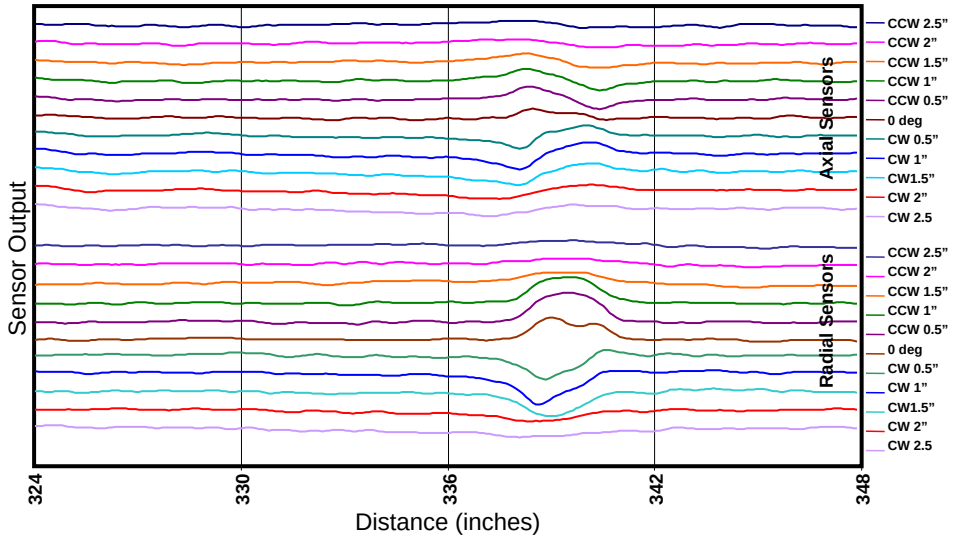
Sensor Output
Distance (inches)
324
330
336
342
348
Axial Sensors
Radial Sensors
CCW 2.5”
CCW 2”
CCW 1.5”
CCW 1”
CCW 0.5”
0 deg
CW 0.5”
CW 1”
CW1.5”
CW 2”
CW 2.5

P3-3

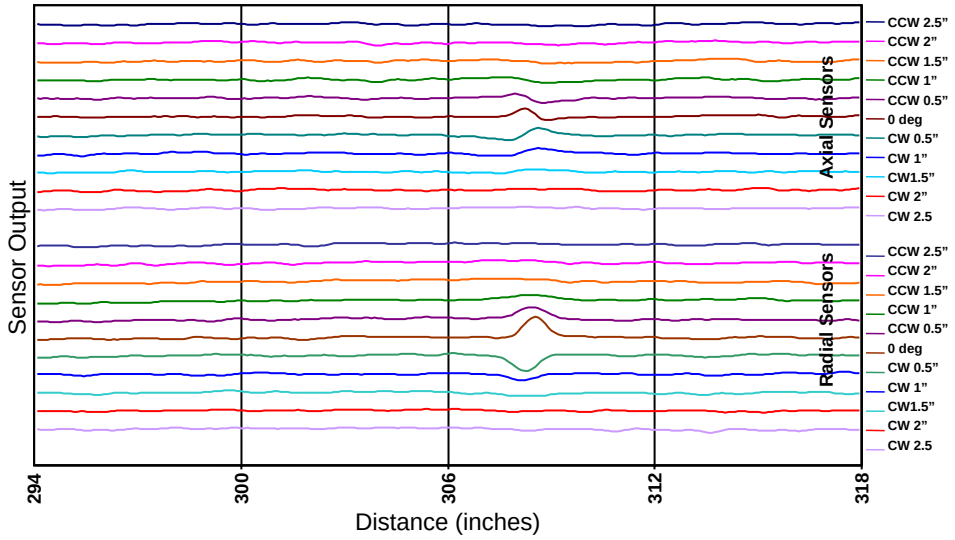
Sensor Output
Distance (inches)
294
300
306
312
318
Axial Sensors
Radial Sensors
CCW 2.5”
CCW 2”
CCW 1.5”
CCW 1”
CCW 0.5”
0 deg
CW 0.5”
CW 1”
CW1.5”
CW 2”
CW 2.5

P3-4

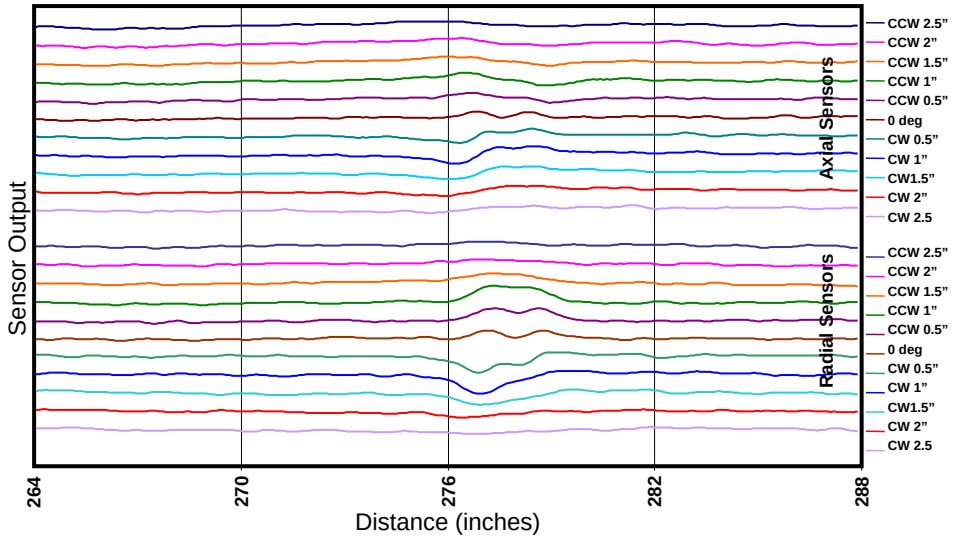
Sensor Output
264
270
276
282
288
Distance (inches)
Axial Sensors
Radial Sensors
CCW 2.5”
CCW 2”
CCW 1.5”
CCW 1”
CCW 0.5”
0 deg
CW 0.5”
CW 1”
CW1.5”
CW 2”
CW 2.5

P3-5

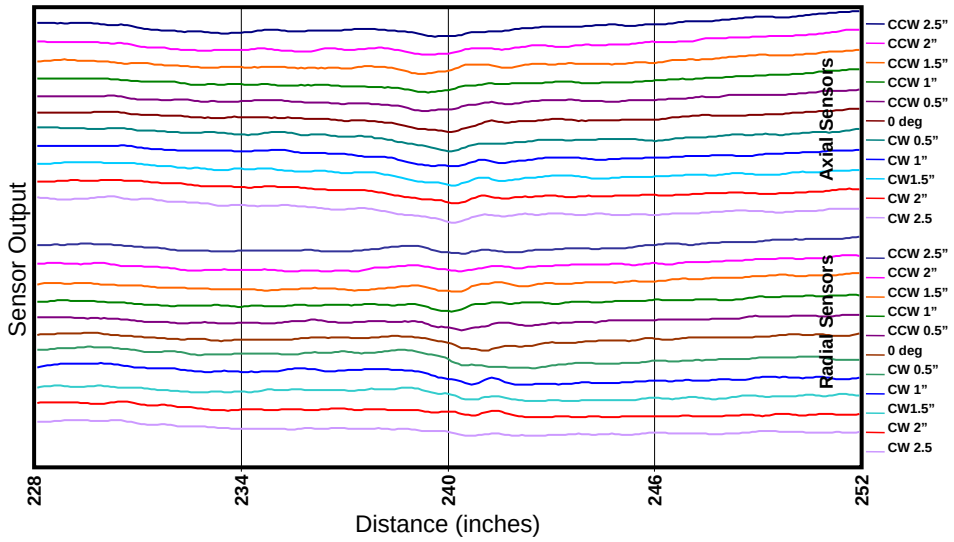
Sensor Output
228
234
240
246
252
Distance (inches)
Axial Sensors
Radial Sensors
CCW 2.5”
CCW 2”
CCW 1.5”
CCW 1”
CCW 0.5”
0 deg
CW 0.5”
CW 1”
CW1.5”
CW 2”
CW 2.5

P3-Weld

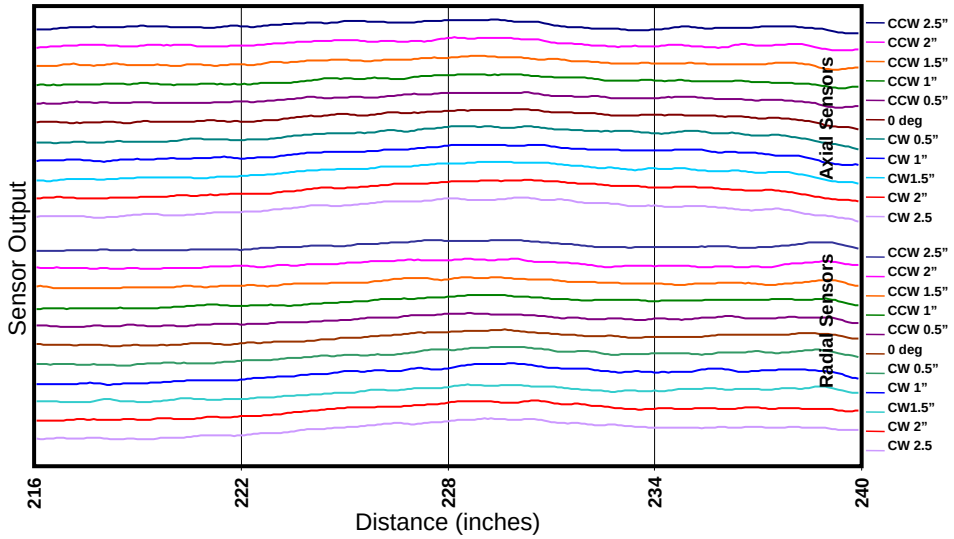
Sensor Output
Distance (inches)
216
222
228
234
240
Axial Sensors
Radial Sensors
CCW 2.5”
CCW 2”
CCW 1.5”
CCW 1”
CCW 0.5”
0 deg
CW 0.5”
CW 1”
CW1.5”
CW 2”
CW 2.5

P3-6

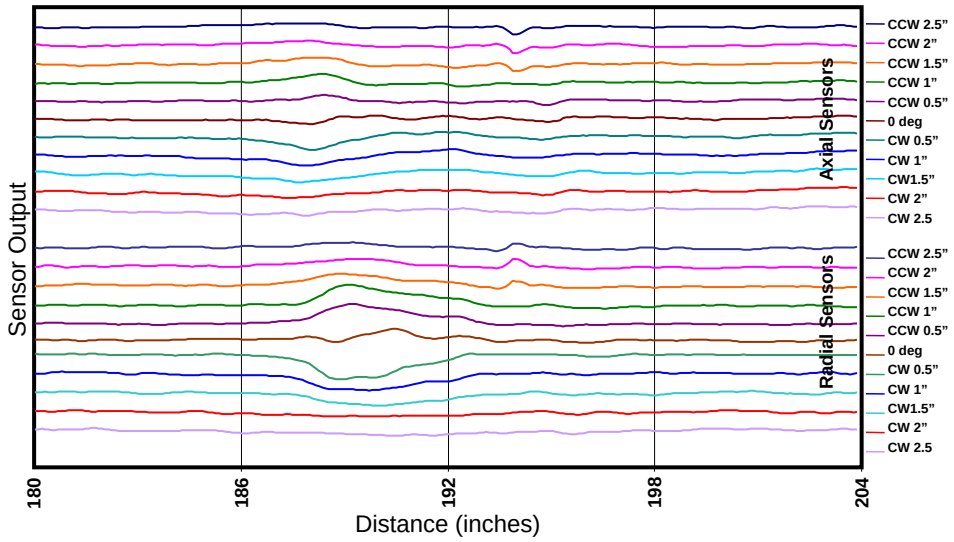
Sensor Output
Distance (inches)
180
186
192
198
204
Axial Sensors
Radial Sensors
CCW 2.5”
CCW 2”
CCW 1.5”
CCW 1”
CCW 0.5”
0 deg
CW 0.5”
CW 1”
CW1.5”
CW 2”
CW 2.5

P3-7

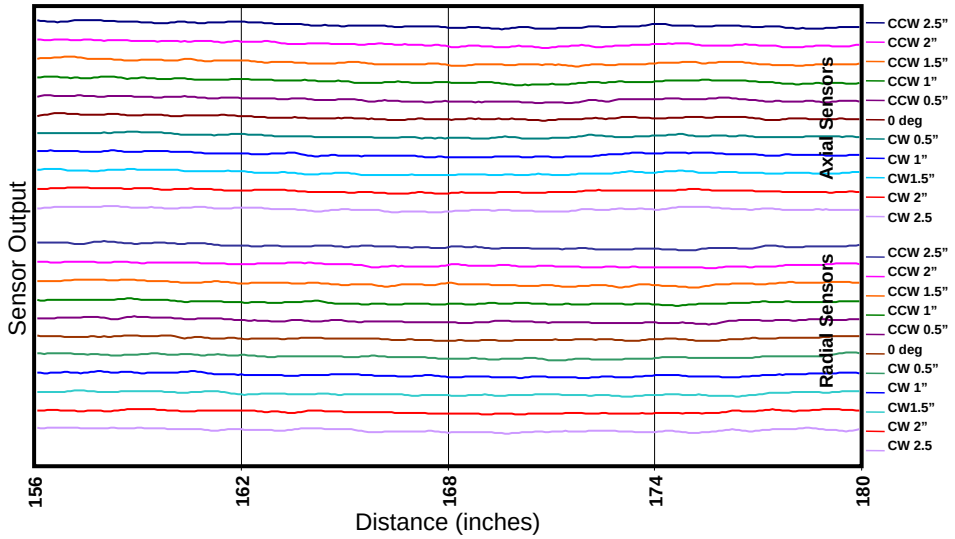
Sensor Output
Distance (inches)
156
162
168
174
180
Axial Sensors
Radial Sensors
CCW 2.5”
CCW 2”
CCW 1.5”
CCW 1”
CCW 0.5”
0 deg
CW 0.5”
CW 1”
CW1.5”
CW 2”
CW 2.5

P3-8

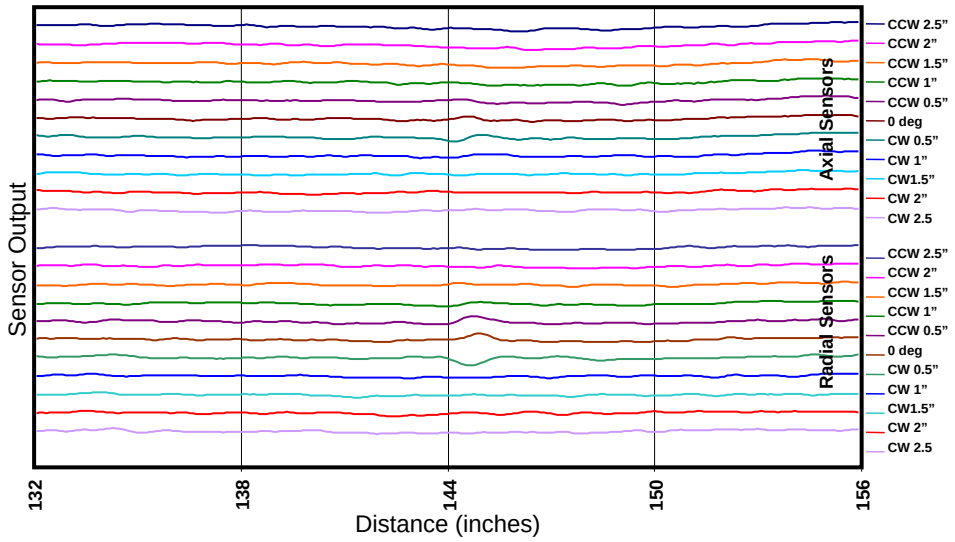
Sensor Output
Distance (inches)
132
138
144
150
156
Axial Sensors
Radial Sensors
CCW 2.5”
CCW 2”
CCW 1.5”
CCW 1”
CCW 0.5”
0 deg
CW 0.5”
CW 1”
CW1.5”
CW 2”
CW 2.5

P3-9

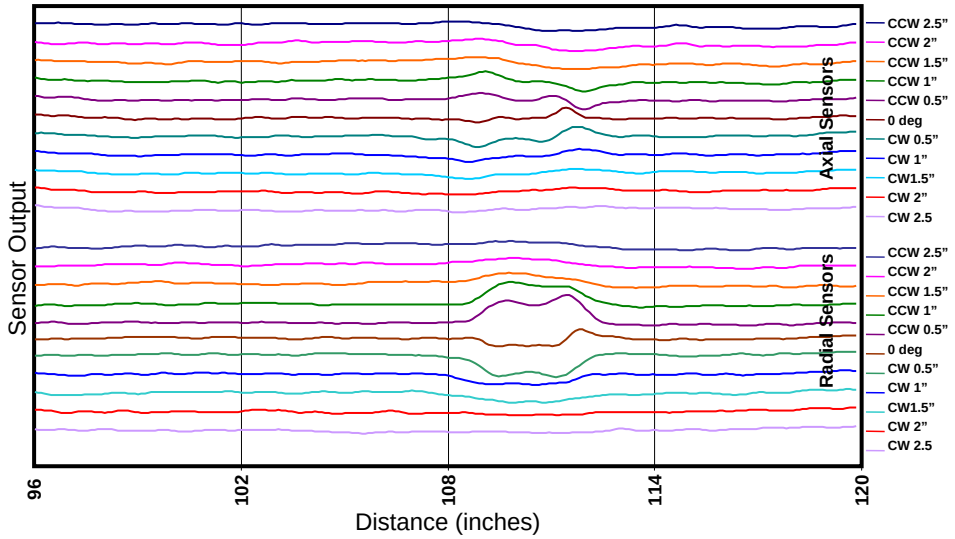
Sensor Output
Distance (inches)
96
102
108
114
120
Axial Sensors
Radial Sensors
CCW 2.5”
CCW 2”
CCW 1.5”
CCW 1”
CCW 0.5”
0 deg
CW 0.5”
CW 1”
CW1.5”
CW 2”
CW 2.5

P3-10

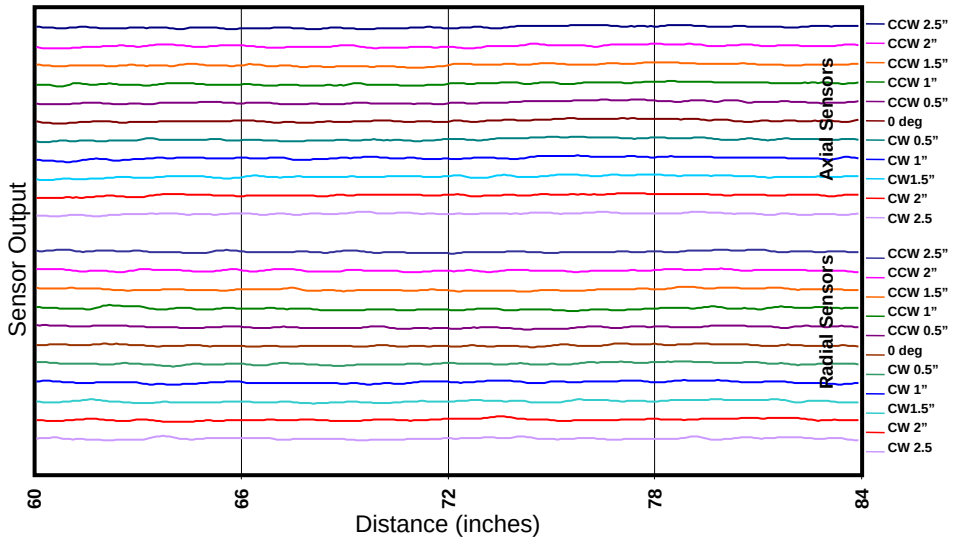
Sensor Output
Distance (inches)
60
66
72
78
84
Axial Sensors
Radial Sensors
CCW 2.5”
CCW 2”
CCW 1.5”
CCW 1”
CCW 0.5”
0 deg
CW 0.5”
CW 1”
CW1.5”
CW 2”
CW 2.5

P3-11

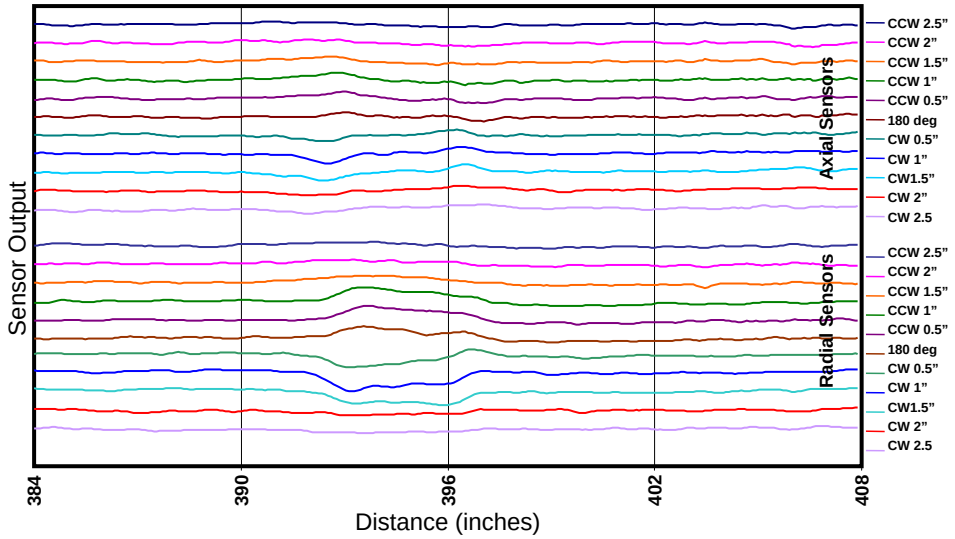
Sensor Output
Distance (inches)
384
390
396
402
408
Axial Sensors
Radial Sensors
CCW 2.5”
CCW 2”
CCW 1.5”
CCW 1”
CCW 0.5”
180 deg
CW 0.5”
CW 1”
CW1.5”
CW 2”
CW 2.5

P3-12

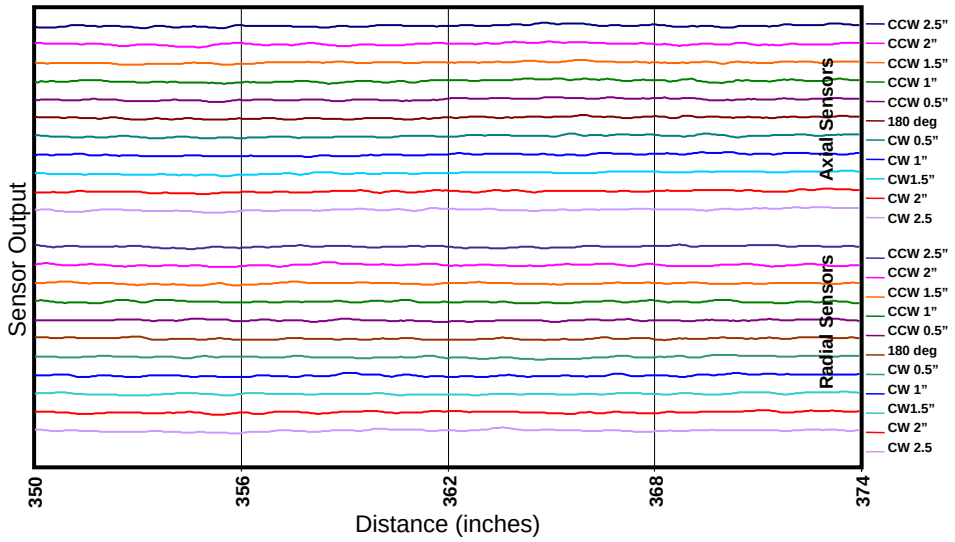
Sensor Output
Distance (inches)
350
356
362
368
374
Axial Sensors
Radial Sensors
CCW 2.5”
CCW 2”
CCW 1.5”
CCW 1”
CCW 0.5”
180 deg
CW 0.5”
CW 1”
CW1.5”
CW 2”
CW 2.5

P3-13

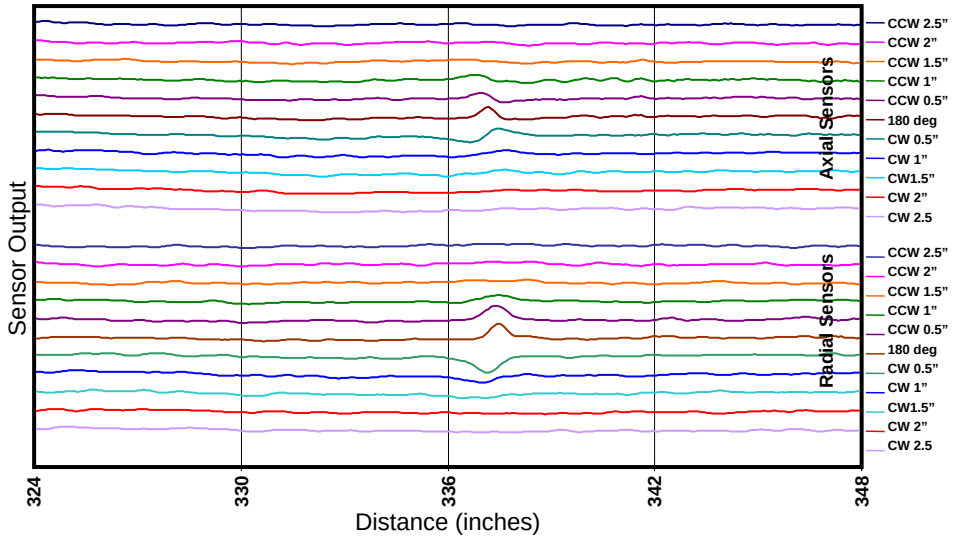
Sensor Output
Distance (inches)
324
330
336
342
348
Axial Sensors
Radial Sensors
CCW 2.5”
CCW 2”
CCW 1.5”
CCW 1”
CCW 0.5”
180 deg
CW 0.5”
CW 1”
CW1.5”
CW 2”
CW 2.5

P3-14

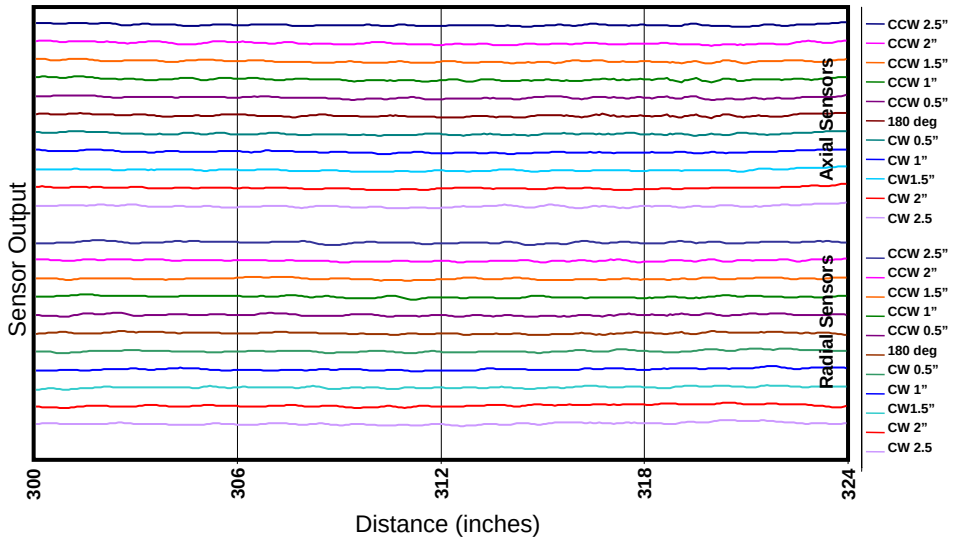
Sensor Output
Distance (inches)
300
306
312
318
324
Axial Sensors
Radial Sensors
CCW 2.5”
CCW 2”
CCW 1.5”
CCW 1”
CCW 0.5”
180 deg
CW 0.5”
CW 1”
CW1.5”
CW 2”
CW 2.5

P3-15

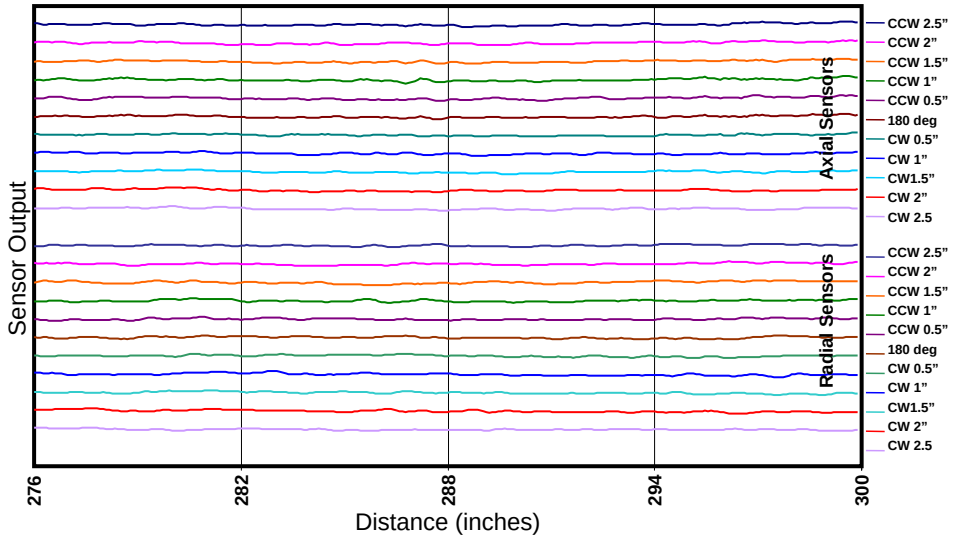
Sensor Output
276
282
288
294
300
Distance (inches)
Axial Sensors
Radial Sensors
CCW 2.5”
CCW 2”
CCW 1.5”
CCW 1”
CCW 0.5”
180 deg
CW 0.5”
CW 1”
CW1.5”
CW 2”
CW 2.5

P3-16

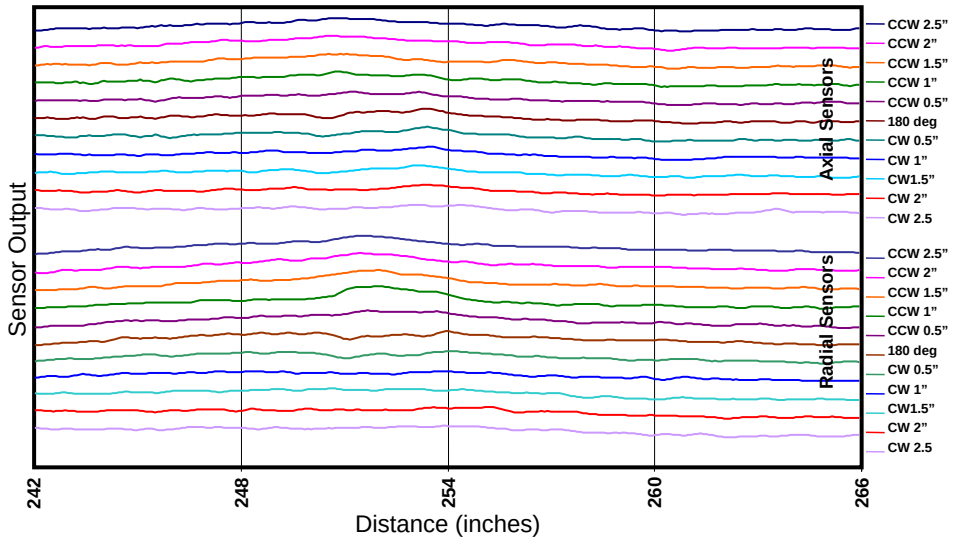
Sensor Output
242
248
254
260
266
Distance (inches)
Axial Sensors
Radial Sensors
CCW 2.5”
CCW 2”
CCW 1.5”
CCW 1”
CCW 0.5”
180 deg
CW 0.5”
CW 1”
CW1.5”
CW 2”
CW 2.5

P3-17

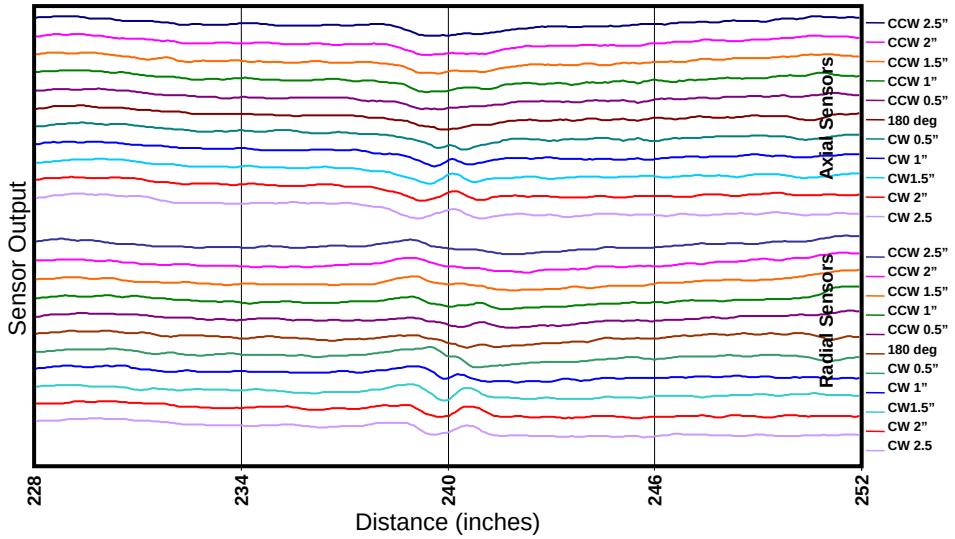
Sensor Output
Distance (inches)
228
234
240
246
252
Axial Sensors
Radial Sensors
CCW 2.5”
CCW 2”
CCW 1.5”
CCW 1”
CCW 0.5”
180 deg
CW 0.5”
CW 1”
CW1.5”
CW 2”
CW 2.5

P3-Weld

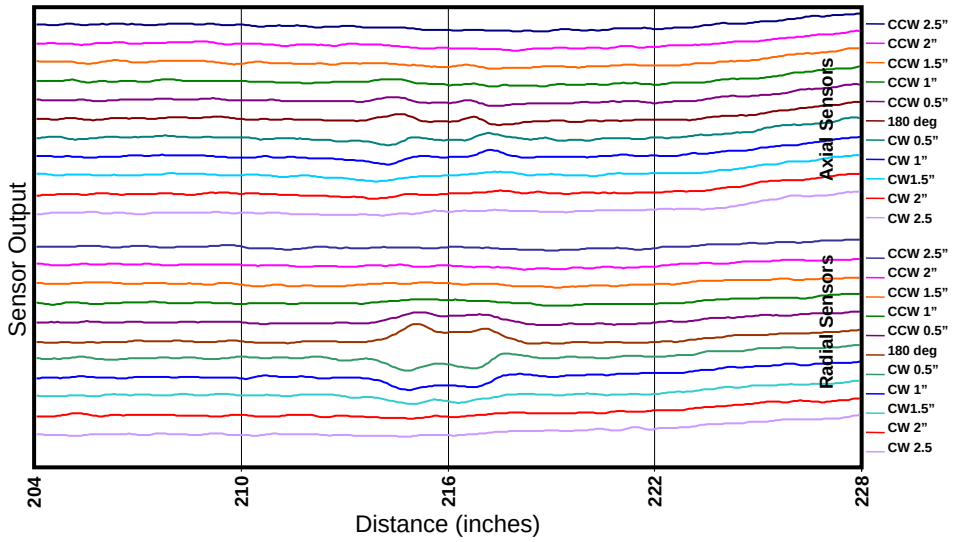
Sensor Output
Distance (inches)
204
210
216
222
228
Axial Sensors
Radial Sensors
CCW 2.5”
CCW 2”
CCW 1.5”
CCW 1”
CCW 0.5”
180 deg
CW 0.5”
CW 1”
CW1.5”
CW 2”
CW 2.5

P3-18

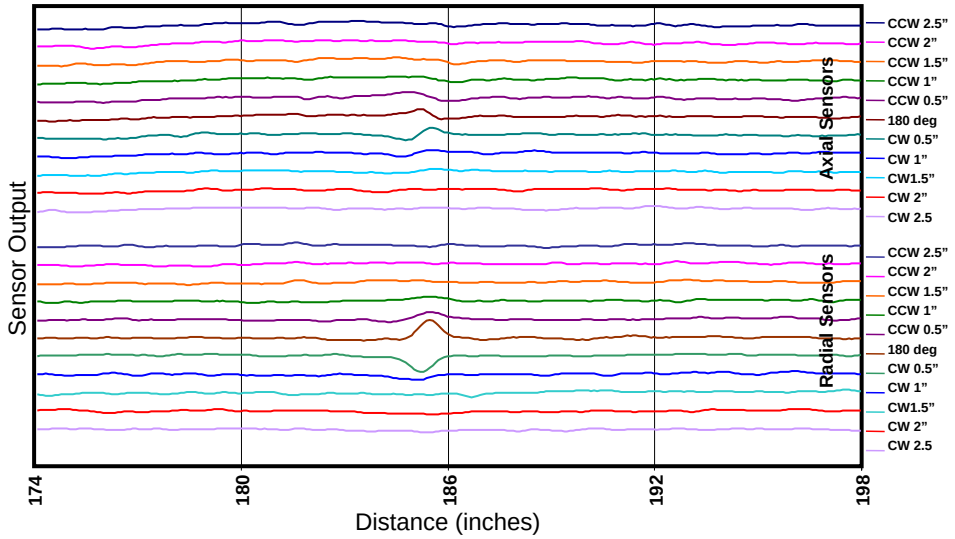
Sensor Output
Distance (inches)
174
180
186
192
198
Axial Sensors
Radial Sensors
CCW 2.5”
CCW 2”
CCW 1.5”
CCW 1”
CCW 0.5”
180 deg
CW 0.5”
CW 1”
CW1.5”
CW 2”
CW 2.5

P3-19

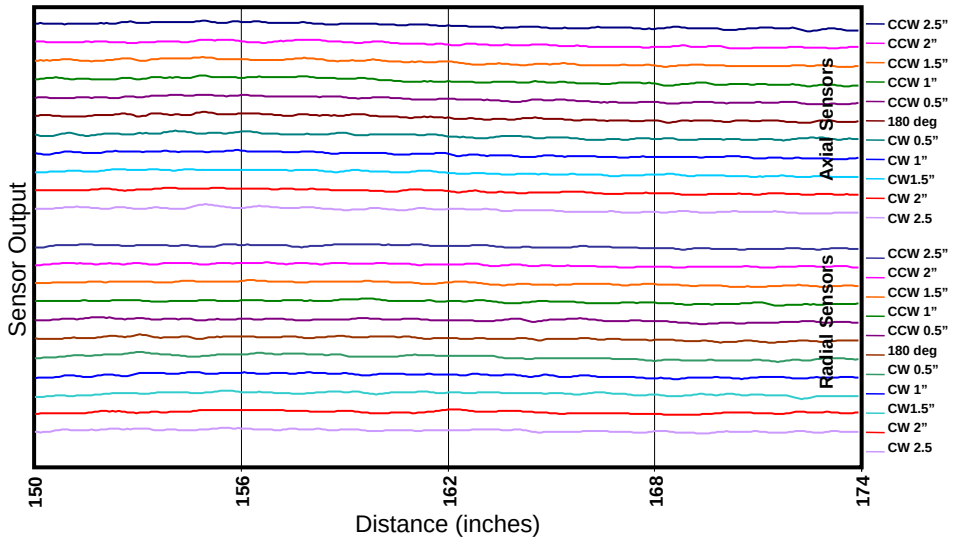
Sensor Output
Distance (inches)
150
156
162
168
174
Axial Sensors
Radial Sensors
CCW 2.5”
CCW 2”
CCW 1.5”
CCW 1”
CCW 0.5”
180 deg
CW 0.5”
CW 1”
CW1.5”
CW 2”
CW 2.5

P3-20

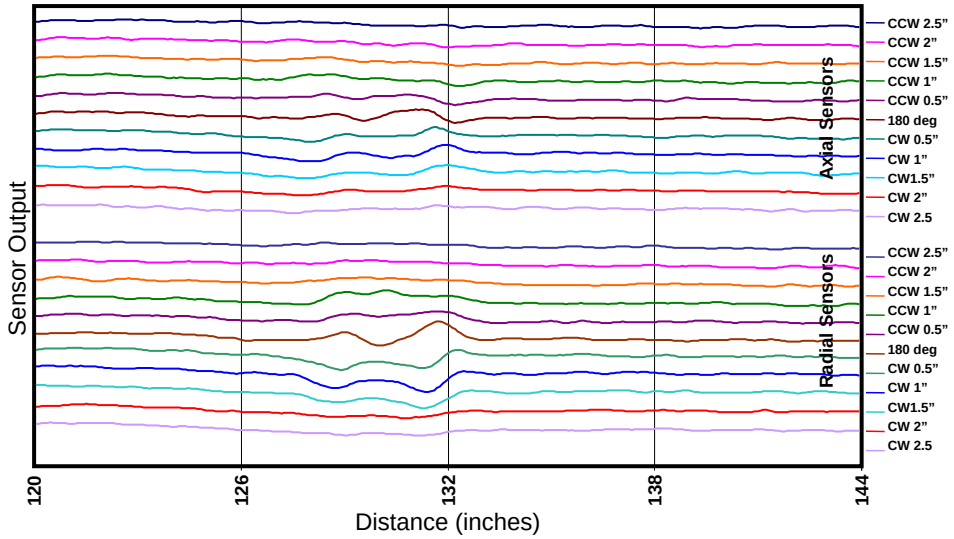
Sensor Output
Distance (inches)
120
126
132
138
144
Axial Sensors
Radial Sensors
CCW 2.5”
CCW 2”
CCW 1.5”
CCW 1”
CCW 0.5”
180 deg
CW 0.5”
CW 1”
CW1.5”
CW 2”
CW 2.5

P3-21

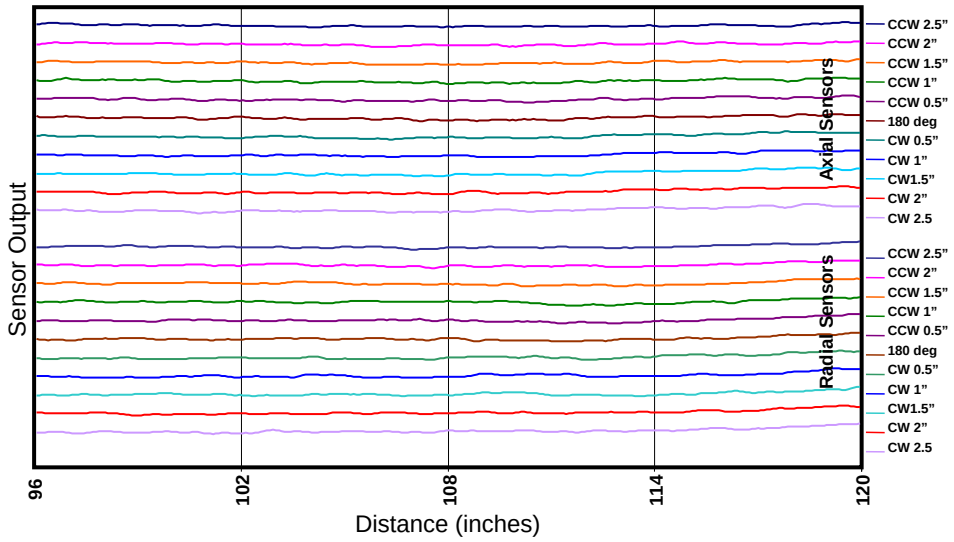
Sensor Output
Distance (inches)
96
102
108
114
120
Axial Sensors
Radial Sensors
CCW 2.5”
CCW 2”
CCW 1.5”
CCW 1”
CCW 0.5”
180 deg
CW 0.5”
CW 1”
CW1.5”
CW 2”
CW 2.5

P3-22

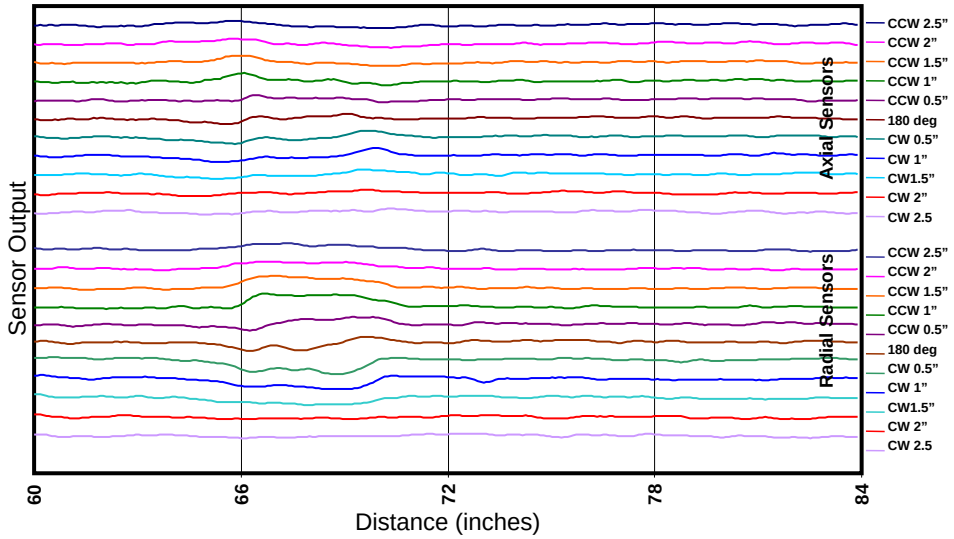
Sensor Output
60
66
72
78
84
Distance (inches)
Axial Sensors
CCW 2.5”
CCW 2”
CCW 1.5”
CCW 1”
CCW 0.5”
180 deg
CW 0.5”
CW 1”
CW1.5”
CW 2”
CW 2.5
Radial Sensors
CCW 2.5”
CCW 2”
CCW 1.5”
CCW 1”
CCW 0.5”
180 deg
CW 0.5”
CW 1”
CW1.5”
CW 2”
CW 2.5

P3-23

This page intentionally blank.

PACIFIC NORTHWEST NATIONAL LABORATORY (PNNL) DEMONSTRATION TEST DATA

This page intentionally blank.

Benchmarking of Inspection Technologies
Detection of Mechanical Damage - Page 1

Name:	Paul D. Panetta
Date:	27-Jan-06
Company:	Pacific Northwest National Laboratory
Sensor Design:	Electromagnetic Acoustic Transducer (EMAT) Stress and strain measurements

CALIBRATION DATA

	Dent Locations	Total Length of Dent Region	Maximum Depth of Dent Region	Relative Dent Severity	Comments
	inches from end A to center of dents	inches	Depth measured with deformation sensor (in)	0 = No damage 1 = Least Severe 2 = Moderately Severe 3 = Severe 4 = Most Severe	Dent severity is relative to the pipe sample being evaluated. Do NOT interpret dent severity between Pipe Sample 1 and Pipe Sample 2; only evaluate the relative severity between dents in the same pipe sample.
Mechanical Damage Pipe SAMPLE 1 (~28 feet)					
Calibration Dent P06dTH1:	1' 8"	20	-.025"	0	
	1' 11"	20	.075"	1	
	2' 2"	20	.325"	3	
	2' 5"	20	.150"	2	
	2' 8"	20	.200"	3	
	2' 11"	20	0	0	
	3' 2"	20	.325"	3	
	3' 5"	20	0.75"	1	
Mechanical Damage Pipe SAMPLE 2 (40' 1.5")					
Calibration Dent R01:	42.25"	3.5	1.2%	1	
Calibration Dent R02:	73.25"	8.5	0.8%	2	

TEST DATA

Pipe Sample:	**SAMPLE 1**
Defect Set:	24" Diameter Pipe with Mechanical Damage; Length =~28'

Defect Number	Search Region (Distance from End A to Center of Dent)	Dent Severity	Comments
	feet & inches	0 = No damage 1 = Least Severe 2 = Moderately Severe 3 = Severe 4 = Most Severe	The multiple dents and the non-circular nature of the pipe from the three rows of dents created a significant amount of background de
D1	5' 4.5"	4	dent start at 63.5" end at 66.5", length 3"
D2	5' 8.5"	2	dent start at 67" end at 70", length 3"
D3	6' 5.5"	1	dent start at 77.3" end at 78.1", length 0.9"
D4	8' 9"	2.5	long dent along the axis dent start at 99.9" end at 110.4", length 10.5"
D5	9' 6"	2.5	long dent along the axis dent start at 113.8" end at 119.9", length 6.1"
WELD	10' 5.5"		Weld detected at 10' 5.5", length approximately 0.8"- material properties of pipes change on each side of weld.
D6	13' 6"	GOUGE NOT PART OF DEMONSTRATION	detected, damage looks as significant as a 3 or 4, length approximately 6 inches long or two dents approximately 2 inches long separ
	195.5"		damage detected damage looks as significant as a 3, (1 defect approximately 7 inches long or 2 defects, one 4 inches long and a second 2 inches long separated by approximately 1 inch)
D7	19' 2"	3	dent start at 228.1" end at 234.7", length 6.7"
D8	20'	2	dent start at 236.4" end at 242.1 length 5.7"
D9	20' 6"	0.5	dent start at 245.7" end at 246.2", length 0.5"
D10	22' 3.5"	4	similar to calibration defects dent start at 264" end at 270.1", length 6.1"
D11	22' 10"	4	similar to calibration defects dent start at 271" end at 276.1 length 5.1"
D12	23' 4.5"	4	similar to calibration defects dent start at 277.3" end at 282.6", length 5.3"
D13	25' 5.5"	not reported	out of scan range
D14	25' 10"	not reported	out of scan range
D15	26' 1"	not reported	out of scan range

This page intentionally blank.

Benchmarking of Inspection Technologies Detection of Mechanical Damage - Page 2	
Name:	Paul D. Panetta
Date:	27-Jan-06
Company:	Pacific Northwest National Laboratory
Sensor Design:	Electromagnetic Acoustic Transducer (EMAT) Stress and strain measurements

TEST DATA	
Pipe Sample:	**SAMPLE 2**
Defect Set:	24" Diameter Pipe with Mechanical Damage; Length = 40' 1.5"

Defect Number	Search Region (Distance from End A to Center of Dent)	Dent Severity	Comments
	inches	0 = No damage 1 = Least Severe 2 = Moderate Severity 3 = Most Severe	
R03	109.25"	1	small degree of damage, start of dent 107" end 110" length 3"
R04	144"	2	moderate damage, start of dent 140.25" end 147.5", length 7.25"
R05	183"	3	significant damage, start of dent 178.75" end 187.25, length 8.5
R06	217"	1	small degree of localized damage, start of dent 215.5" end 220, length 4.5"
R07	253"	2	moderate damage, start of dent 250.5" end 258.5, length 8"
R08	289.5"	3	significant damage, start of dent 286.75 end 295.25, length 8.5"
R09	325"	2	moderate damage, start of dent 323" end 331", length 8"
R10	360.5"	3	significant damage, start of dent 359" end 367", length 8"
R11	397"	0	no dent

PNNL Ultrasonic measurements along the axis on Pipe 2, R Defects, at 15 degrees (approximately 3") from TDC

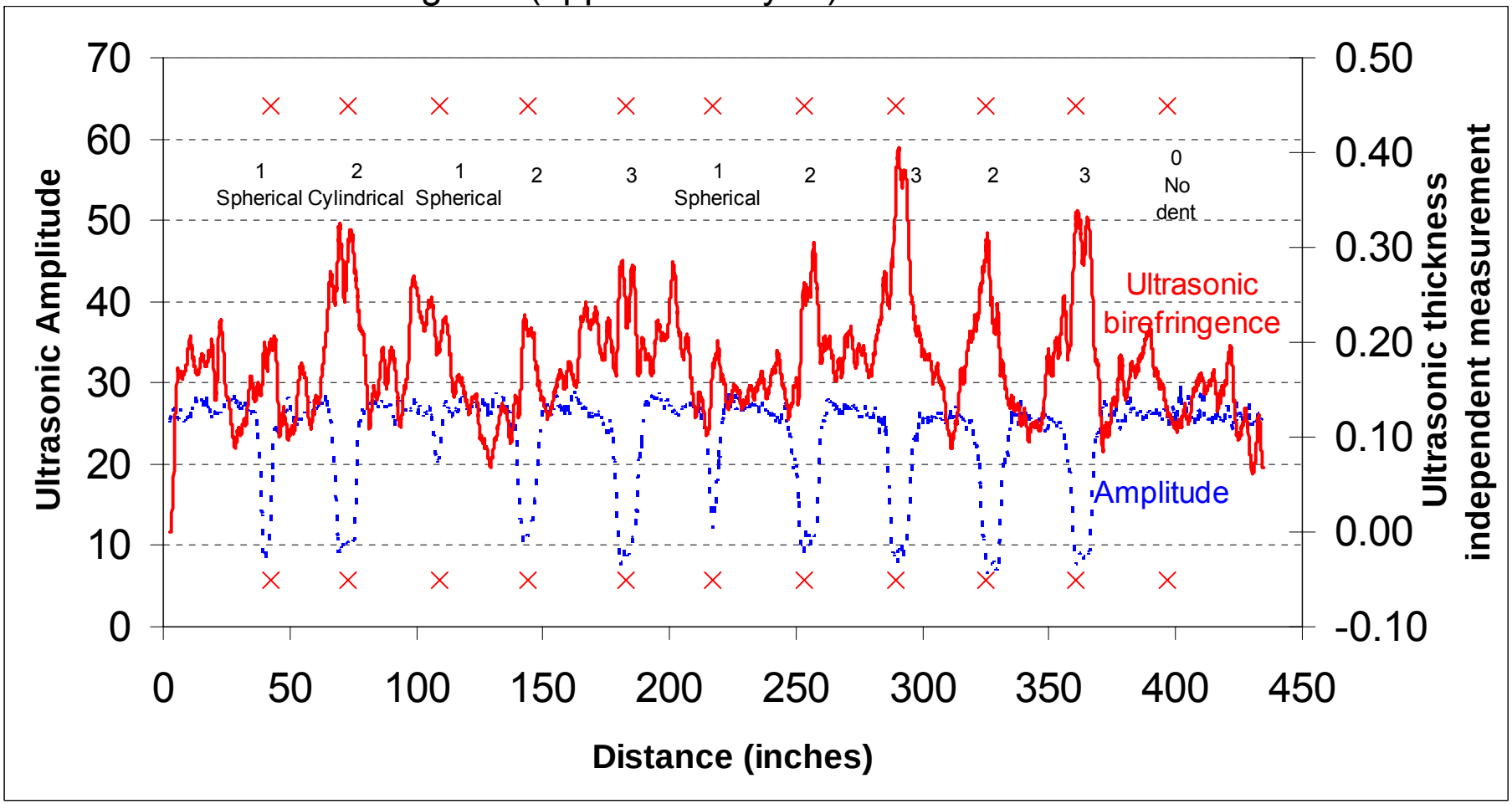

OAKRIDGE NATIONAL LABORATORY (ORNL)
DEMONSTRATION TEST DATA

This page intentionally blank.

Benchmarking of Inspection Technologies Detection of SCC - Page 1	
Name:	Venugopal K. Varma, Austion Albrught, and Philip Bingham
Date:	1/27/2006
Company:	Oak Ridge National Laboratory
Sensor Design:	EMAT shear Horizontal wave design

CALIBRATION DATA

Pipe Sample: 993	Calibration Crack Location	Length	Depth	Measured Length	Measured Depth	Comments
	inches from end B	inches	% wall thickness			
1	186.4	2.5				multiple cracks; max = ~3/4"
2	58.7	5				multiple cracks; max = ~1/4"
3	86.4	5				multiple cracks; max = ~3 1/4"
4	82.4	2.5				multiple cracks; max = ~1/2"
5	44.4	3				multiple cracks; max = ~1/2"
Blank Area:						

TEST DATA

Pipe Sample:	**893**
Defect Set:	26" Diameter Pipe with Stress Corrosion Cracks; Length = 27 feet
	TEST LINE 1

Defect Number	Search Region (Distance from End B)	Start of Crack Region from Side B	End of Crack Region from Side B	Type of SCC	Comments
	inches	inches	inches		
SCC5	140" to 152"	145"	148"	☐ Isolated Crack ☑ Colony of Cracks ☐ None	Another isolated at 142"
SCC4	175" to 187"			☐ Isolated Crack ☐ Colony of Cracks ☑ None	
SCC3	210" to 222"	214"	216"	☑ Isolated Crack ☐ Colony of Cracks ☐ None	
SCC2	226" to 242"			☐ Isolated Crack ☐ Colony of Cracks ☑ None	
SCC1	242" to 254"			☐ Isolated Crack ☐ Colony of Cracks ☑ None	

Benchmarking of Inspection Technologies
Detection of SCC - Page 2

Name:	Venugopal K. Varma, Austion Albrught, and Philip Bingham
Date:	1/27/2006
Company:	Oak Ridge National Laboratory
Sensor Design:	EMAT shear Horizontal wave design

TEST DATA

Pipe Sample:	**893**
Defect Set:	26" Diameter Pipe with Stress Corrosion Cracks; Length = 27 feet

TEST LINE 2

Defect Number	Search Region (Distance from End B)	Start of Crack Region from Side B	End of Crack Region from Side B	Type of SCC		Comments
	inches	inches	inches			
SCC10	140" to 152"	144"	149"	☐	Isolated Crack	Looks like a gap in the middle.
				☑	Colony of Cracks	May be two sets separated by 1".
				☐	None	
SCC9	188" to 200"	194"	196"	☐	Isolated Crack	
				☑	Colony of Cracks	
				☐	None	
SCC8	210" to 222"	210"	211"	☑	Isolated Crack	
				☐	Colony of Cracks	
				☐	None	
SCC7	234" to 246"	236"	237"	☑	Isolated Crack	
				☐	Colony of Cracks	
				☐	None	
SCC6	246" to 258"			☐	Isolated Crack	
				☐	Colony of Cracks	
				☑	None	

Benchmarking of Inspection Technologies Detection of SCC - Page 3						
Name:	Venugopal K. Varma, Austion Albrught, and Philip Bingham					
Date:	1/27/2006					
Company:	Oak Ridge National Laboratory					
Sensor Design:	EMAT shear Horizontal wave design					
TEST DATA						
Pipe Sample:	**893**					
Defect Set:	26" Diameter Pipe with Stress Corrosion Cracks; Length = 27 feet					
	TEST LINE 3					
Defect Number	Search Region (Distance from End B)	Start of Crack Region from Side B	End of Crack Region from Side B	Type of SCC		Comments
	inches	inches	inches			
SCC14	140" to 152"	139	141	☑	Isolated Crack	
				☐	Colony of Cracks	
				☐	None	
SCC13	188" to 200"			☐	Isolated Crack	
				☐	Colony of Cracks	
				☑	None	
SCC12	210" to 222"			☐	Isolated Crack	
				☐	Colony of Cracks	
				☑	None	
SCC11	225" to 245"	237	239	☑	Isolated Crack	After scanning, we documented large dirt patches along line 3
				☐	Colony of Cracks	We believe EMATs lifted off the surface due to dirt inside pipe.
				☐	None	Reliability of data in this area is low

This page intentionally blank.

Calibration Note

For calibration of SCC, a 26” pipe was provided with five SCC’s. These were located using liquid fluorescent magnetic particle inspection method. During the week of the testing we used the liquid fluorescent magnetic particle inspection to relocate the defects and had a hard time locating them. SCC 4 and SCC 5 could not be located and SCC3 and SCC 2 were indistinguishable from the scratches surrounding them. We could make out something SCC 2 &# area, but could not be confirmed. We cleaned the area using a wire brush and cleaner, but could not definitely identify the region having SCC. Only SCC1 could easily be identifiable, but this is more likely a manufacturing defect than an SCC. Due to lack of credible calibration data on 26 “ pipe, we had to base all algorithms on a previous 30” diameter training set.

Venu, Philip, and Austin

1/27/2006

This page intentionally blank.

NATIONAL ENERGY TECHNOLOGY LABORATORY (NETL)
DEMONSTRATION TEST DATA

This page intentionally blank.

Benchmarking of Inspection Technologies Detection of Plastic Pipe Defects - Page 1	
Name:	Jim Spenik, Chris Condon, Bill Fincham, Travis Kirby
Date:	Submitted 01/23/06
Company:	NETL
Sensor Design:	Capacitive sensor for Polyethylene Pipe Inspection

CALIBRATION DATA

Defect	Calibration Defect Location	Volume of Defect	Depth of Defect	Diameter of Defect	Comments
	inches from end A	cubic inches	inches	inches	
C1:	18	0.028	0.25	0.375	

TEST DATA

Pipe Sample:	**PLASTIC PIPE SAMPLE**
Pipe Parameters:	6" Diameter, 0.5" Wall Thickness Pipe Sample, ~13' in length
	LINE 1

Defect Number	Search Region (Distance from End A)	Location of Defect Region from Side A	Significance of Defect (Output/Calibration Output)	Volume of Defect (in^3) (provided to participant after defect signif reported)	Depth of Defect (in) (provided to participant after defect signif reported)	Comments
	inches	inches		cubic inches	inches	
D1	18" to 28"	18.14 & 25.06	18.14" = 1, 25.06"=1.38			For significance: defect calibration hole @ 18" = 1 Vol @ 18" = 0.028 , Vol @ 25.06 = 0.039
D2	28" to 34"	None				
D3	34" to 42"	None				
D4	42" to 48"	45.62	0.99			Volume = 0.028
D5	48" to 56"	52.55	1.31			Volume= 0.037
D6	56" to 62"	None				
D7	62" to 70"	66.36	1.15			Volume = 0.033
D8	70" to 76"	None				
D9	76" to 84"	None				
D10	84" to 90"	87.15	0.43			Volume = 0.012
D11	90" to 98"	None				
D12	98" to 104"	101.03	1.61			Volume = 0.045
D13	104" to 112"	107.84	0.71			Volume = 0.02
D14	112" to 118"	114.75	0.57			Volume = 0.016
D15	118" to 126"	121.89	0.74			Volume = 0.020
D16	126" to 132"	None ?				We have indications that a consistant amount of material may have been removed along the entire length
D17	132" to 138"	None ?				We have indications that a consistant amount of material may have been removed along the entire length
D18	138" to 144"	138.3	1.13			Volume = 0.032
D19	144" to 150"	146.76	0.71			Volume = 0.020

This page intentionally blank.

APPENDIX C – DEVELOPER COMMENTS

SOUTHWEST RESEARCH INSTITUTE (SWRI)
COMMENTS ON PIPELINE INSPECTION TECHNOLOGIES DEMONSTRATION REPORT

This page intentionally blank

Final Comments on

"PIPELINE INSPECTION TECHNOLOGIES DEMONSTRATION REPORT"

APPLICATION OF REMOTE-FIELD EDDY CURRENT (RFEC) TESTING TO INSPECTION OF UNPIGGABLE PIPELINES

OTHER TRANSACTION AGREEMENT DTRS56-02-T-0001
SwRI® PROJECT 14.06162
PIPELINE AND HAZARDOUS MATERIALS SAFETY ADMNISTRATION
U.S. DEPARTMENT OF TRANSPORTATION

SOUTHWEST RESEARCH INSTITUTE®

February 2006

Southwest Research Institute (SwRI) believes that the results of the demonstration testing indicate that the SwRI RFEC system is very promising as an inspection tool that can accurately detect and characterize wall-loss defects in pipelines. The report showed a comparison of predicted vs. measured defect parameters with error bands of ±10% of wall thickness for defect depth and ±0.5 inch for defect length and depth. For the SwRI data, 68% of the predicted depths, 88% of the predicted lengths, and 88% of the predicted widths were within those error bands. If the error band is increased to ±20%, then 91% of the predicted depths would be within the band. The depth prediction had a systematic error in that the predicted depths were generally less than the measured ones. If corrections are made to the SwRI depth prediction algorithm to reduce the systematic error (for example, by using the demonstration test defect responses to correct the calibration approach), then even better results can be obtained.

It is emphasized that the SwRI RFEC tool was designed to meet the specifications and constraints of the Explorer II robot under development by Carnegie Mellon University (as discussed in the SwRI comments on page B–4 of this report). The demonstration tests were thus conducted with sensors, instrumentation, data processing, scan speeds, etc. that are very representative of a field inspection system as integrated with Explorer II. SwRI therefore expects that results similar to those obtained in this demonstration would be obtained with an actual inspection system and that no degradation in performance would be experienced by transitioning to field hardware and inspection conditions.

Additional Information on the SwRI Remote Field Eddy Current Technology and Design as Integrated with the Explorer II Robotic Platform

SwRI Remote-Field Eddy Current – Through funding support from PHMSA/OPS, Southwest Research Institute® has developed a remote-field eddy current (RFEC) technology to be used in unpiggable lines. The SwRI RFEC tool is capable of detecting corrosion on the inside or outside pipe surface. Since a large percentage of pipelines cannot be inspected using "smart pig" techniques because of diameter restrictions, pipe bends, and valves, a concept for a collapsible excitation coil was developed but found unnecessary for the pipe sizes and materials of interest in this demonstration. A breadboard system that meets the size, power, and communication requirements for integration into the Carnegie Mellon Explorer II robot was developed and used in the demonstration tests. This system is shown in Figure 1. The demonstration system incorporates eight detectors, and data from all eight channels are acquired and processed simultaneously as the system is scanned along the pipe at speeds up to 4 inch/sec. All of the instrumentation, except for a DC power supply and a laptop computer (used for storage of the processed data), is located on the tool. Figure 2 shows the system design as integrated with the Explorer II robot under development by Carnegie Mellon University. The RFEC system can expand to inspect 6- or 8-inch-diameter pipe and can retract to 4 inches to pass through obstructions.

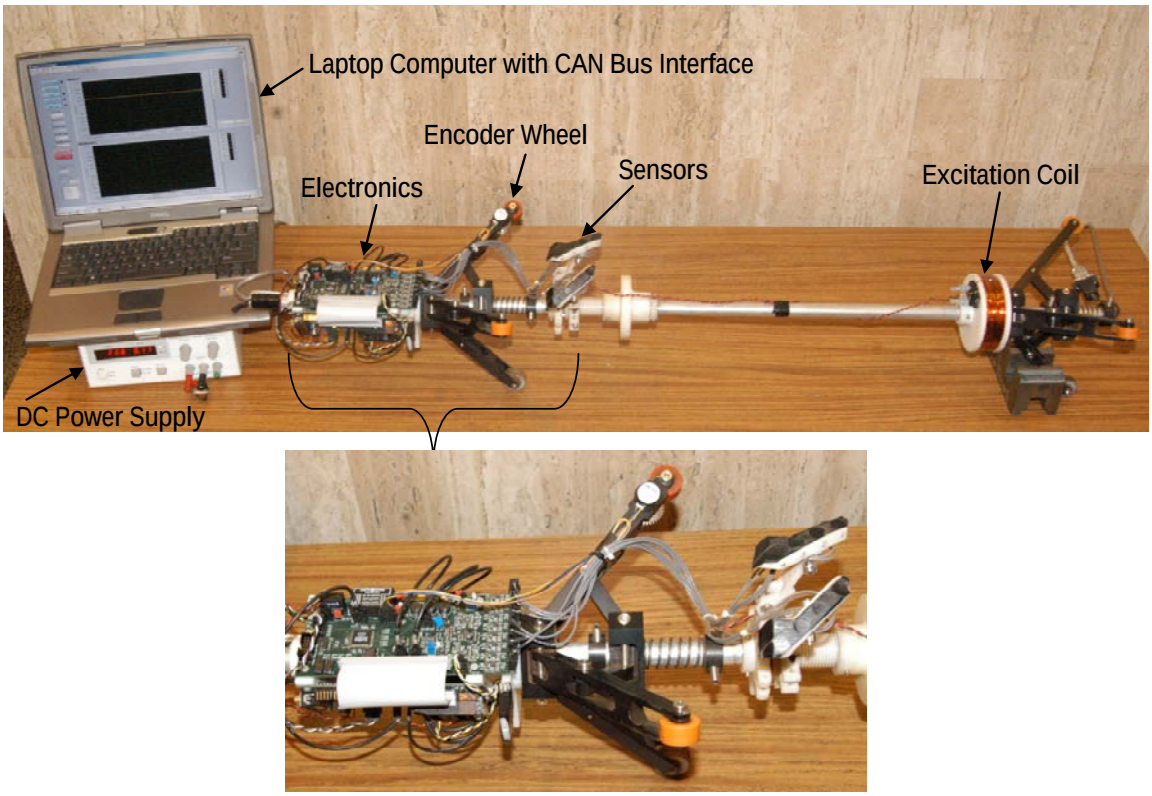

Figure 1. SwRI RFEC tool used in demonstration tests

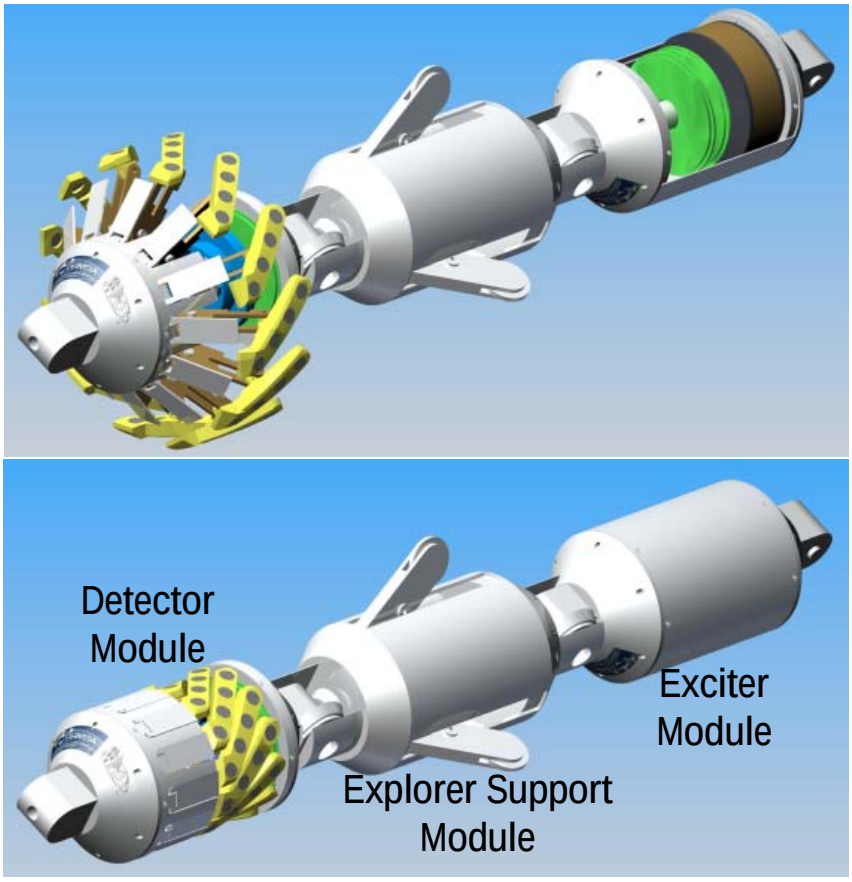

Figure 2. SwRI RFEC tool design as integrated with Explorer II robot: Top–Expanded for inspection with cover removed from exciter module, Bottom–Retracted to pass through restricted areas.

This page intentionally blank

GAS TECHNOLOGY INSTITUTE (GTI)
COMMENTS ON PIPELINE INSPECTION TECHNOLOGIES DEMONSTRATION REPORT

This page intentionally blank.

Comments on the Comparison of Benchmarks and GTI Results

Albert Teitsma, Julie Maupin, and Paul Shuttleworth

Gas Technology Institute
1700 S. Mount Prospect Rd.
Des Plaines, IL 60018

25 October 2004

Introduction

During the week of 9 January 2006, GTI staff came to the West Jefferson facility of Battelle Labs in Columbus, OH to test a prototype RFEC inspection vehicle in 3 sections of 8 inch pipe. We reported on our test results in a previous document.[6] In this document we comment on the benchmarks reported in "Pipeline Inspection Technologies Demonstration Report" by Stephanie A. Flamberg and Robert C. Gertler.

Comparison of Benchmarks and GTI Results

Table 1 below compares GTI results to the benchmark data. There are two types of error in these results, systematic and random. The systematic errors are the average readings in Table 1, while scatter gives the random error. A different researcher analyzed the data from each pipe and the subjective components of the data analysis do show. All three underestimated the defect lengths, in one case by half an inch with a scatter of .4 inches. Particularly for small deep defects, this is too large an error, but the table also shows that proper analysis does give an acceptable precision (average=-0.139", scatter=0.133). Precision in the circumferential direction was not as good, but as pointed out in a previous report, remaining strength calculation such as B31G or RSTRENG do not use circumferential extent in the calculations.

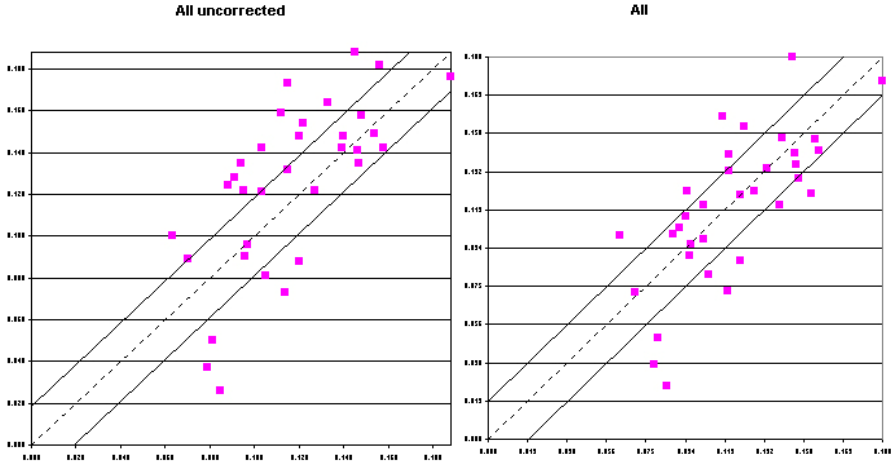

Figure 1. Data with Pipe 3 corrected for calibration error.

There was a serious depth calibration error for pipe three, which made the scatter for the GTI results look worse than it was. Figure 1 shows the improvement with recalibrated data. GTI expected that the anticipated error would be about +/- 10% of the full wallthickness, as indicated by the lines in Figure1. Table 1 shows that more experienced analysts can achieve that, the scatter for Pipe 1 being 10%, while that for Pipe 3 was a mere 7%.

GTI's sizing of the natural corrosion areas was excellent.

[6] "Analysis of Sensor Benchmarking Tests: Remote Field Eddy Current Technique", Julie Maupin, Albert Teitsma, and Paul Shuttleworth.

Time to Take the Data

Since time to take the data has become an issue, GTI has included results from its run with Russell NDE Systems, Inc. equipment, which GTI plans to use in its modules, in this report.

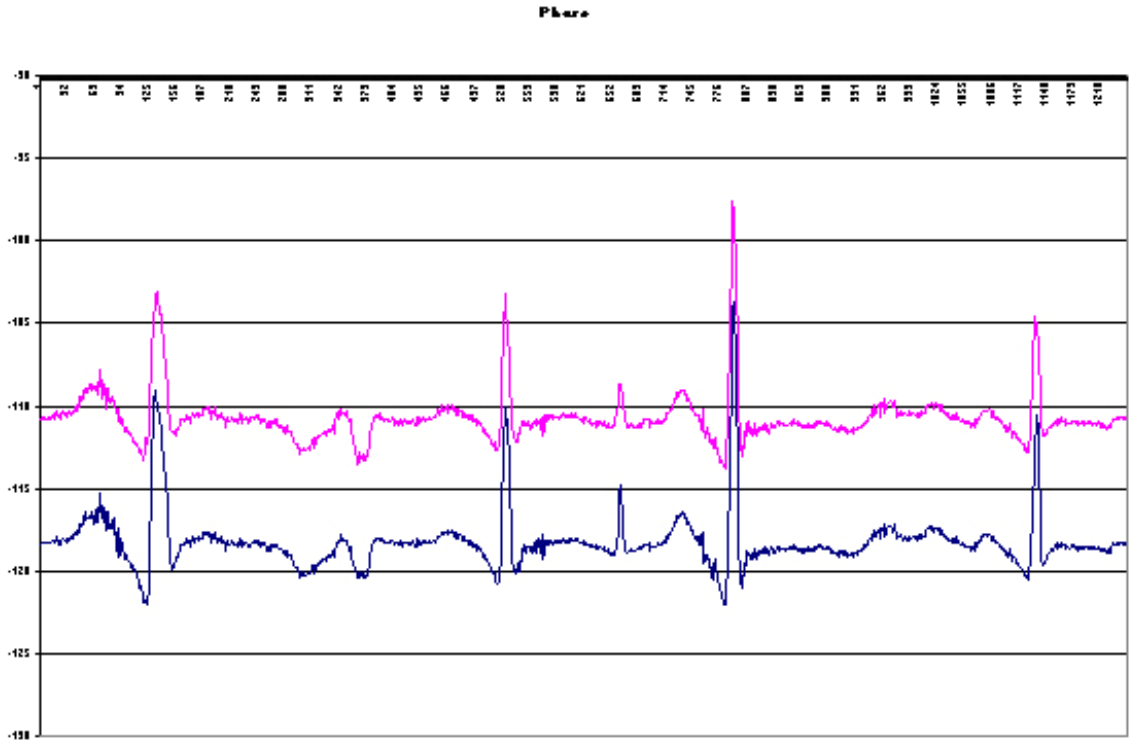

Figure 2. A faster run using Russell NDE Systems, Inc. instrumentation.

GTI inspected 23’ of Pipe 3 in 7 minutes using this instrumentation, which GTI brought along for demonstration purposes only. The speed was limited by the speed of our tow motor. The instrumentation can easily handle the 4” per second specified for Explorer II. The unfiltered data in Figure 2 is a little noisier than that obtained from the laboratory lock-in amplifier, but more than good enough for the size of the signals obtained during the benchmark tests. GTI concentrated on maximizing signal strength and minimizing power consumption. Speed at the very low speeds used by Explorer II was never an issue.

For most of the measurements, it took GTI a little over half a day per run in Pipes 1 and 5, and a little longer in Pipe 3 using a single lock-in amplifier to measure all sixteen channels. To ensure superior data quality the lock-in was allowed to settle nearly a second before reading the data from a sensing coil.

C-Scans

C-scans obtained with the RFEC inspection do not have the resolution of the benchmark scans, but the correlation between them are excellent. Figure 3 compares the natural corrosion defect, P1-23. Similar results are obtained for the other defects.

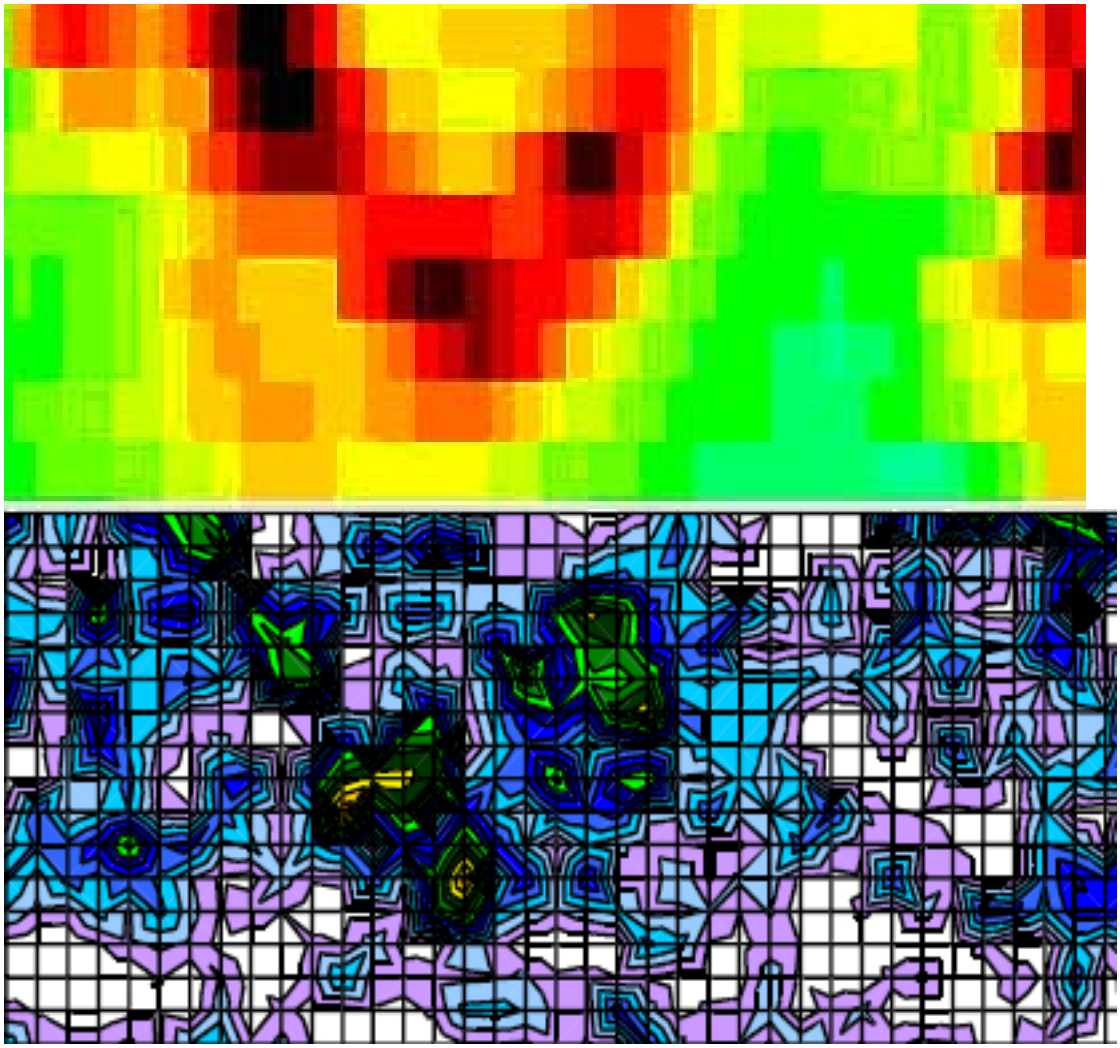

Figure 3. Excellent correlation between the RFEC results and the natural corrosion benchmark data.

Conclusion

The results clearly demonstrate that the RFEC technique is eminently suited for inspecting transmission and distribution piping. The measurements had excellent quality. However GTI's analysis indicates that it takes experienced analysts to translate the measurements into precise defect severity estimates. Although most of the results were not obtained at inspection speeds, the short run with more realistic field equipment showed that inspection at Explorer II speeds will not reduce the quality of the defect severity measurements.

Defect Number	Search Region (Distance from End B)	Length of Defect	Length of Defect	Diff Length		Width of Defect	Width of Defect	Diff Width		Maximum Depth of Defect	Maximum Depth of Defect	Diff Depth	Diff Loss % WT
	inches	GTI	inches	inches		GTI	inches	inches		GTI	inches	inches	%
P1-12	52" to 64"	2.875	4.125	-1.250		1.84	2	-0.160		0.154	0.122	0.032	13.3
P1-9	120" to 144"	14.25	20.25	-6.000		FC	FC			0.141	0.146	-0.005	6.4
P1-7	184" to 196"	1.625	2.125	-0.500		1.5	2	-0.500		0.135	0.147	-0.012	10.1
P1-5	232" to 244"	3.75	3	0.750		3	1	2.000		0.07	0.081	-0.011	9.6
P1-4	256" to 268"	3.375	4	-0.625		3	2	1.000		0.1	0.063	0.037	16.0
P1-3	280" to 292"	2.875	3.125	-0.250		1.5	2	-0.500		0.09	0.096	-0.006	6.9
P1-23	74" to 86"	2.875	4	-1.125		2.25	2	0.250		0.096	0.097	-0.001	4.3
P1-22	98" to 110"	1.625	2	-0.375		1.5	2	-0.500		0.088	0.12	-0.032	20.7
P1-21	120" to 144"	14.25	20.75	-6.500		FC	FC			0.122	0.127	-0.005	6.4
P1-18	210" to 222"	3.25	4.25	-1.000		2	2	0.000		0.188	0.145	0.043	19.1
P1-14	306" to 318"	2.875	3.125	-0.250		1.5	1	0.500		0.132	0.115	0.017	5.3
P1-13	330" to 342"	3	3.875	-0.875		1.75	1.75	0.000		0.122	0.095	0.027	10.6
			average	-0.550			average	0.209			average	0.007	
			scatter	0.425			scatter	0.583			scatter	0.020	10.7
P2-10	78" to 90"	3.75	4.375	-0.625		2.5	2	-0.500		0.188	0.147	-0.041	27.6
P2-9	102" to 114"	4	4.125	-0.125		1.5	2	0.500		0.142	0.158	0.016	2.7
P2-7	150" to 162"	3	3.25	-0.250		2	1	-1.000		0.026	0.085	0.059	25.6
P2-6	174" to 186"	3.25	3.125	0.125		1	1	0.000		0.073	0.114	0.041	16.0
P2-4	222" to 234"	2.25	2.125	0.125		2	2	0.000		0.037	0.079	0.042	16.5
P2-20	54" to 66"	3	3.125	-0.125		1.5	1	-0.500		0.176	0.188	0.012	0.6
P2-17	126" to 138"	4	4.125	-0.125		2	2	0.000		0.159	0.112	-0.047	30.8
P2-14	198" to 210"	3	3.125	-0.125		1.5	1	-0.500		0.081	0.105	0.024	7.0
P2-12	246" to 258"	2	2.125	-0.125		1.5	2	0.500		0.148	0.14	-0.008	10.0
			average	-0.139			average	-0.167			average	0.011	
			scatter	0.133			scatter	0.500			scatter	0.036	15.2
P3-03	330" to 342"	2	2.25	-0.250		1.5	2	-0.500		0.164	0.133	0.031	2.5
P3-04	300" to 312"	1.25	0.75	0.500		1	0.75	0.250		0.158	0.148	0.010	8.6
P3-05	270" to 282"	2	2.25	-0.250		2	2	0.000		0.142	0.103	0.039	6.8
P3-07	186" to 198"	3.5	4.125	-0.625		2	2	0.000		0.173	0.115	0.058	16.9
P3-09	138" to 150"	1.25	0.67	0.580		1	0.67	0.330		0.148	0.12	0.028	0.9
P3-10	102" to 114"	3	3.25	-0.250		2	1	1.000		0.182	0.156	0.026	0.1
P3-12	390" to 402"	3	4.125	-1.125		2.5	2	0.500		0.135	0.094	0.041	7.9
P3-14	330" to 342"	1	0.75	0.250		1	0.75	0.250		0.149	0.154	-0.005	16.6
P3-17	248" to 260"	2.75	3.125	-0.375		1.5	1	0.500		0.089	0.07	0.019	3.8
P3-18	210" to 222"	2.75	3.125	-0.375		1.5	1	0.500		0.128	0.091	0.037	5.7
P3-19	180" to 192"	1	0.72	0.280		1	0.72	0.280		0.142	0.139	0.003	12.4
P3-21	126" to 138"	3.5	4.125	-0.625		2	2	0.000		0.121	0.103	0.018	4.4
P3-23	66" to 78"	3.75	4.125	-0.375		2	2	0.000		0.124	0.088	0.036	5.2
			average	-0.203			average	0.373			average	0.026	
			scatter	0.373			scatter	0.289			scatter	0.013	7.1

BATTELLE
COMMENTS ON PIPELINE INSPECTION TECHNOLOGIES DEMONSTRATION REPORT

This page intentionally blank

Comments on Demonstration Results for the

ROTATING PERMANENT MAGNET INSPECTION TOOL

Prepared by Battelle

February 17, 2006

Theory of Operation

The rotating permanent magnet inspection method employed by Battelle at the Pipeline Inspection Technologies Demonstration is an alternative to the common concentric coil methods to induce low-frequency eddy currents in ferromagnetic pipe and tubes. Battelle's technology consists of a pair of permanent magnets that rotate around a central axis in proximity to the inner surface of the pipe sample. The rotating permanent magnet pairs are used to induce high current densities in the material undergoing inspection. Following fundamental laws of electrical induction, rotating permanent magnet pairs inside a pipe along its longitudinal axis establishes an alternating electrical current in the wall of the pipe. Figure 1, a cutaway drawing showing the rotating permanent magnet exciter, illustrates this concept. The current flows in an elliptical path around the magnets. When the magnetizer is vertical, strong currents flow axially along the top and bottom of the pipe and circumferentially at the sides. When the magnetizer is horizontal, strong currents flow circumferentially at the sides of the pipe and axially at the top and the bottom. Finite element modeling shows that a two-pole magnetizer produces strong current densities at distances reasonably far away from the magnetizer. Although the current is complex at the magnet poles (where it is strongest), at distances of a pipe diameter or more away from the magnetizer it is uniform and sinusoidal. With this uniform energy induced in the pipe, simple magnetic field sensors can be used to detect the change in current densities in the pipe wall and thus pinpoint the location of defects and anomalies.

The development of this technology began in fall 2003 and is sponsored by The U.S. Department of Energy's National Energy Technology Laboratory with cofunding from the Pipeline Research Council International. The first known use of this inspection method to detect corrosion was performed in September 2004.

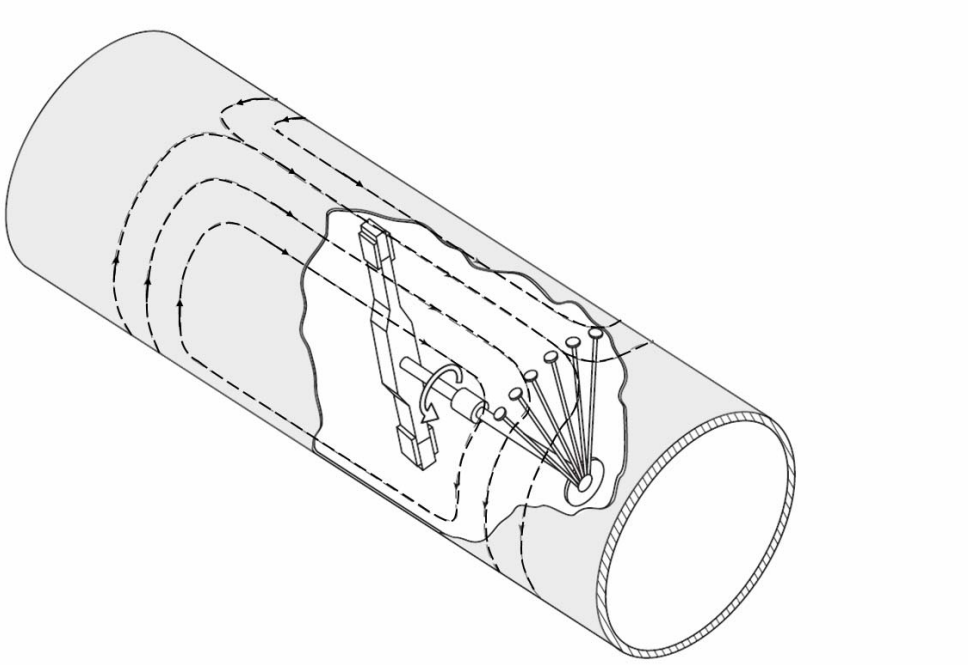

Figure 2. Illustration of the rotating permanent magnet exciter and sensor location

System Configuration as Demonstrated

Figure 2 shows the prototype used for the 8 inch corrosion inspection benchmark demonstration. A pair of NdFeB magnets is mounted on a steel core machined from 1018 steel. The magnets are 2 inches long, 1 inch wide, and 0.5 inch thick; the magnet strength is 38 MegaGauss-Oersted. While the strong holding force secures the magnets on the steel core, copper covers keep the magnets precisely aligned. The air gap between the magnet and the pipe wall is 0.5 inch. Wheeled support plates keep the magnet centered in the pipe. A variable speed direct current motor is used to rotate the magnetizing assembly. The rotational speed used in this demonstration was 300 rpm or 5 Hz. The power required to rotate the magnets at this speed was about 70 watts. While this is above the available power of 50 watts budgeted by Explorer II, this power requirement is significantly better than the 200 watts required in prior designs. Three pairs of axial and a radial Hall Effect sensors were mounted in 4 sensor shoes designed to ride on the ID of the pipe. While sensor to magnet spacing of 8 to 10 inches provides stronger signal changes from corrosion anomalies, the distance from the magnet to the sensor was 13 inches to meet EXPLORER II specifications. To continuously monitor rotational speed, a small magnet was attached to the shaft and an additional Hall Effect sensor was used to produce a synchronous signal.

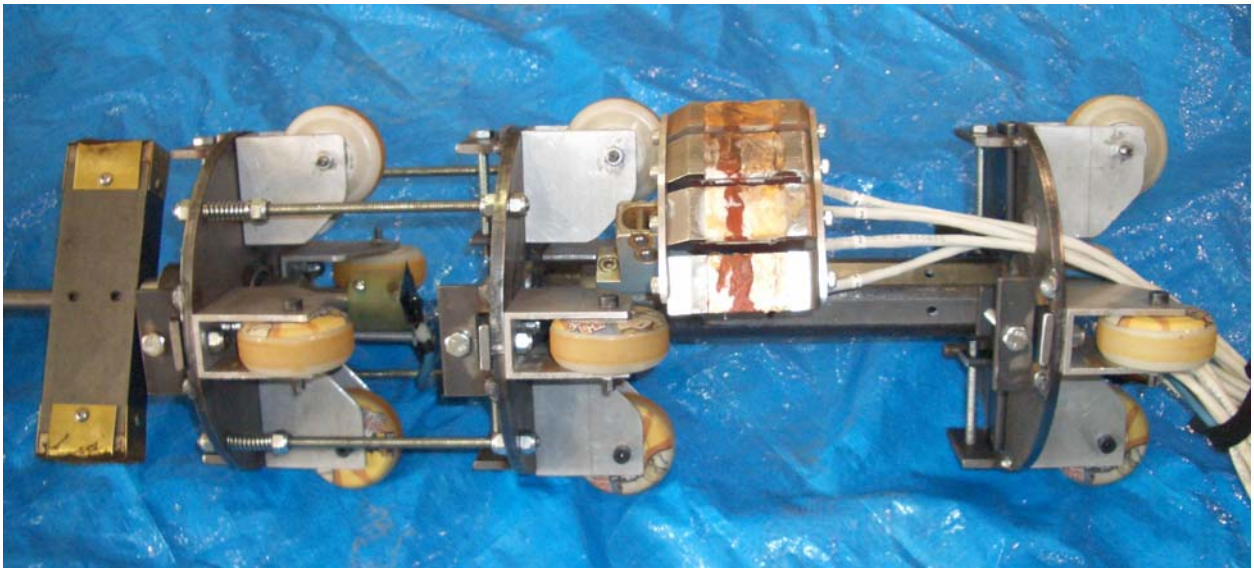

Figure 3. Rotating permanent Magnet Inspection system as configured for the technology demonstration

A 24 channel real-time data recorder system was implemented and fundamental experiments were conducted to provide data to aid in the design of the rotating magnetizer. A system was designed to simultaneously record and process 11 sensor pairs, the sync signal and one open channel. The block diagram of the data recorder system is shown in Figure 3. The heart of the recorder is the National Instruments PXI-4472, an eight-channel dynamic signal acquisition module for making high-accuracy frequency-domain measurements. The eight NI PXI-4472 input channels simultaneously digitize input signals over a bandwidth from 0.5 Hz to 45 kHz. Three PXI-4472 modules were synchronized to provide 24 channel input using the PXI chassis and a star trigger bus. The PXI chassis communicates with a desktop computer using a fiber optic link. The desktop computer is used to analyze the signals using a lock-in amplifier approach, as described in a previous DOE semiannual report. LabVIEW software modules for lock-in amplifier measurements were used in the development of a custom data acquisition and display program.

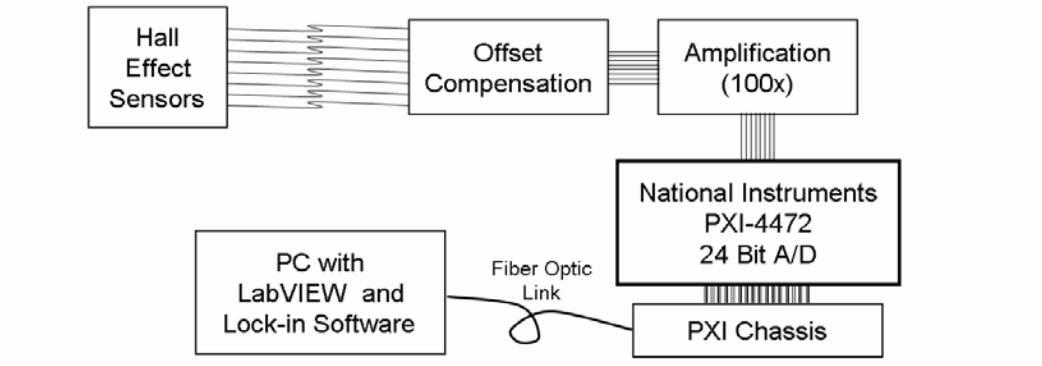

Figure 3. The block diagram of the data acquisition system

Display of results

The data acquisition and processing hardware and software processed signals and displayed data in real time during the demonstration. A typical output of the data recording package is shown in Figure 4. In real time display mode, the data scrolls along the monitor as the inspection tool traverses the pipe. The upper and lower graphs show the axial and radial sensors respectively using a stacked line plotting routine, a format familiar to pigging vendors and users of pipeline inspection technologies. In this figure, the signal from an axially short, circumferentially wide metal loss anomaly can be seen in the middle channels of each sensor type.

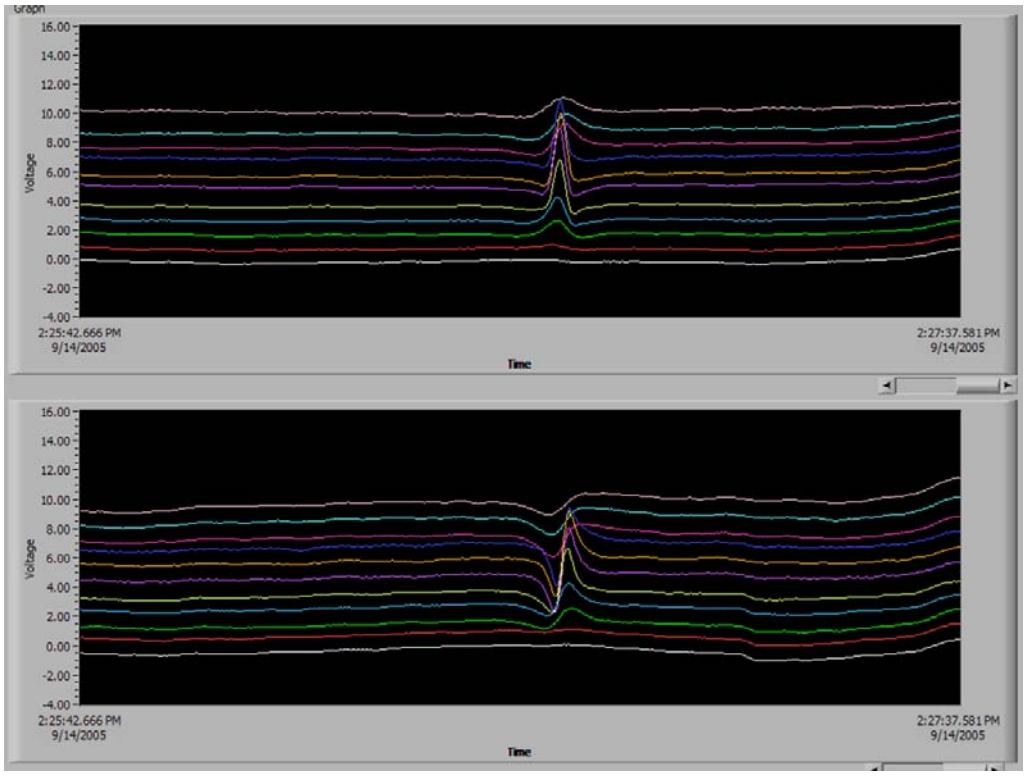

Figure 4. Screen capture of custom LabVIEW data acquisition and display program

The results submitted by Battelle on January 26, 2006 (contained in appendix B) included signals from each reporting area in a uniform format. An example signal is shown in Figure 5 for pipe sample 2, search area 10. The upper and lower stacked graphs show the signals from the axial and radial sensors respectively; the color codes repeat so that sensor pairs can be correlated. Since only about 70 degrees of the pipe was instrumented, the center sensor was positioned so that it traversed the centerline of the defect. In some of the graphs in appendix B it is evident that the tool rotated slightly as it was pulled through the pipe because some of the corrosion signals are greater in other sensors. The signals provided with the report were plotted on the same scale for quick visual comparison. For detection and assessment, signals were amplified so that smaller corrosion areas could be more easily detected and assessed. Other graphical representations, including plotting axial versus radial signals, are proving to be useful in assessing corrosion. A scaled topographical map of the corrosion depth is included at the bottom of Figure 5 after it was flipped (the tool was pulled from right to left). The two humps in the stacked graphs correspond to the two pits in the image. In the reported results, the presence of single or multiple pits was indicated in the comment section. The depth assessment was based on the largest signal since the data reporting form specifically requested maximum depth.

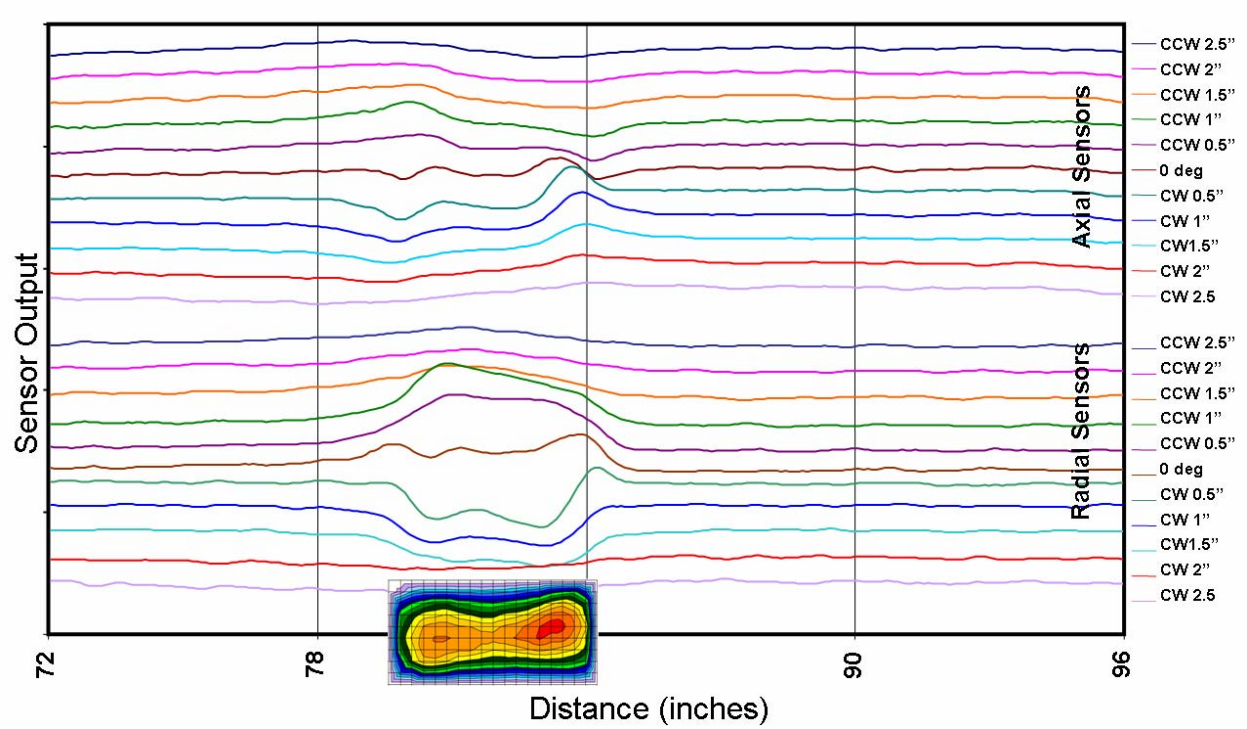

Figure 5. Signal from pipe sample 2, search area 10

Comments on Results

The results presented in the main section of the demonstration report are representative of the current capability of the rotating permanent magnet tool. This comparatively new inspection methodology is in its third year of development. Specific comments on detection and sizing results are provided next.

Detection. The results of the demonstration showed that all corrosion anomalies were detected and one additional anomaly was falsely detected. The false call anomaly was assessed as small and not detected in all pulls. The spacing between sensors (sensor pitch) of the demonstration configuration was 0.5 inches. For corrosion with shallow depth and a width and length nominally the same as the sensor pitch, a detectable signal may only be produced by a sensor traveling directly underneath the anomaly. Two sensors straddling the same anomaly may not produce a signal. Future implementations may need a finer sensor pitch to improve results.

Corrosion sizing. A corrosion anomaly locally increases the density of the currents that are induced by the rotating magnetizer. The local change in current density is also influenced by the length and width. The algorithm for estimating the depth of the corrosion anomaly includes these three measures, in a manner similar to magnetic flux leakage data analysis methods. Data from the calibration anomalies and the first benchmark demonstration were used to establish the sizing algorithm. The unity plot shown in the main report indicates a good correlation between measured and predicted values, however there is a general tendency to under-call the depth. This was the first algorithm developed for corrosion anomaly depth assessment. Additional data and algorithm refinement should help improve results.

Natural Corrosion Sample. The natural corrosion sample was difficult to assess because of the unexpected weld. In hindsight, the signals were quite clear. Figures 6 and 7 show the reported raw data with new annotations for lines 1 and 2 respectively. In the results reported on January 27, 2006 for these lines Battelle discussed:

- Line 1 - A large area of general corrosion of variable depth that spans the entire sensor width. The corrosion is close to the weld, altering both signals. A large wide corrosion area at 128"
- Line 2 - An area of general corrosion of variable depth that spans most sensors. A large wide corrosion area at 128"

The signal 128 inches from the end was the unexpected weld signal. The general corrosion on either side of the weld corresponds to the measured results; however the close welds caused interference and sizing was not attempted at this time. While the natural corrosion pipe was complex, it is only one of many unique challenges that must be faced when implementing inspection technology and the experience will be valuable in future developments.

Summary

The benchmarking results are a representative assessment of the current state of development of the rotating permanent magnet inspection system. The planned improvements of this technology should advance the capability of this inspection system. Battelle is currently working on reducing magnetizer size, increasing rotation speed, and increasing the separation distance between the magnet and the pipe. Separations of over an inch appear to be practical, which will aid in the implementation of this technology. The rapid advances of this new inspection technology should make this methodology useful for unpigable pipeline applications in the near future.

Acknowledgement

The U.S. Department of Energy’s National Energy Technology Laboratory is sponsoring this development with cofunding from the Pipeline Research Council International. However, any opinions, findings, conclusions, or recommendations expressed herein are those of the authors and do not necessarily reflect the views of these sponsors.

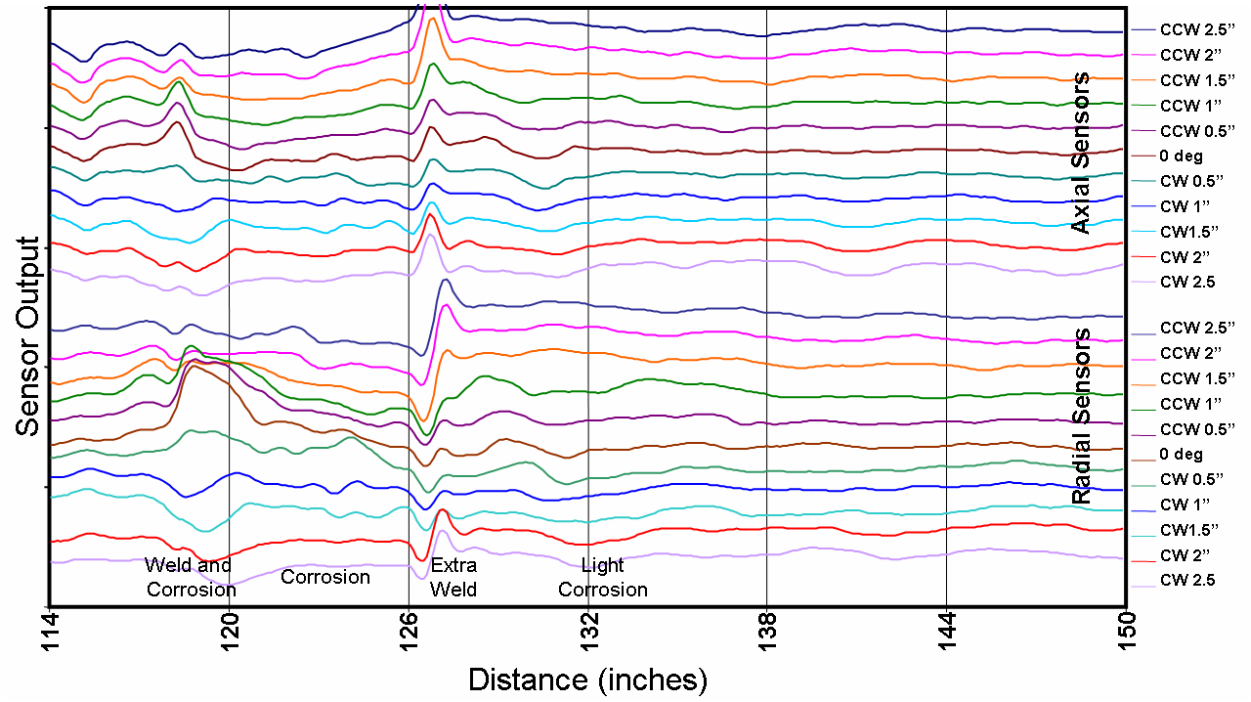

Figure 6. Natural corrosion results line 1

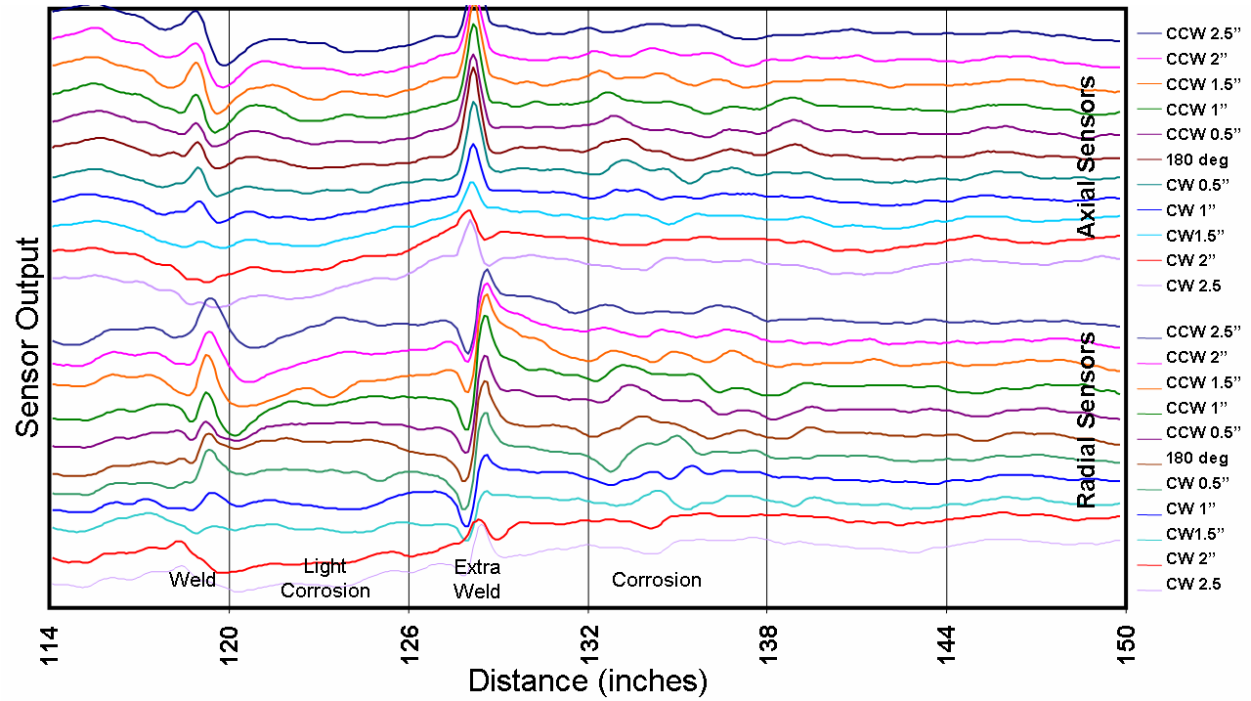

Figure 7. Natural corrosion results, line 2

This page intentionally blank

PACIFIC NORTHWEST NATIONAL LABORATORY (PNNL) COMMENTS ON PIPELINE INSPECTION TECHNOLOGIES DEMONSTRATION REPORT

This page intentionally blank

Comments on NETL and Pipeline & Hazardous Materials Safety Administration pipeline inspection technologies demonstration

Submitted by: Paul D. Panetta
Pacific Northwest National Laboratory
Richland, WA 99352
paul.panetta@pnl.gov
(509) 372-6107

The Pacific Northwest National Laboratory (PNNL) participated in the Pipeline Inspection Technologies Demonstration during the week of January 9, 2006. The main focus of the demonstration was to rank the severity of dents based on ultrasonic measurements of the mechanical properties and the presence of plastic strain. This approach is dramatically different than the current assessment based solely on dimensional measurements. The advantage of this approach is that the reliability of the pipeline can be determined based on material properties and how they change with time and damage, rather than the size and shape of a dent.

Measurements were performed on two 24 inch diameter pipes containing dents and dents with gouges. Pipe 1 contained 3 rows of dents from a track how with a very small separation distance, on the order of a few inches in some cases. The total number of dents exceeded 40 dents. The operation of creating these dents and dents with gouges created a significant amount of distortion to the pipe and ovalization of the pipe. In-service pipelines with the amount of denting are highly unlikely and this pipe does not represent a realistic pipeline operating scenario. Despite this significant distortion results were promising. Pipe 2 contained 10 dents and 11 reporting locations. All dents were successfully detected and estimates of the size were provided. The ultrasonic strain measurement correctly ranked 7 out of the 9 reporting locations for 100% detectability and 77% accuracy on ranking severity.

The sensor was a non contact electromagnetic acoustic transducer (EMAT) that was scanned along the axis of the pipe at several distances from the dents placed at top dead center. The sensor and cart are shown in Figure 1. Figure 2 shows the amplitude and ultrasonic measurements along pipe 2 with the sensor placed 15 degrees from top dead center. The amplitude clears shows a deviation at each reporting location with a dent and no deviation where there is no dent. The ultrasonic shear wave birefringence is independent of thickness which is critical for characterizing mechanical properties due to deformation because a simple thickness measurement is NOT an accurate assessment of strain.

The inspection speed was as fast as 5 inches per second and the electronics can operate as fast as 4 or 5 feet per second (~3 MPH). The measurements were performed in a 24 inch pipe and are amenable to pipes as small as 4 inches in diameter. The technology proved to be very sensitive to mechanical damage due to dents and is also ideal for application where pipelines are bent due to subsidence or other earth movement. This technology is ready for incorporation onto robotics platforms and for field testing and subsequent commercialization for specific applications.

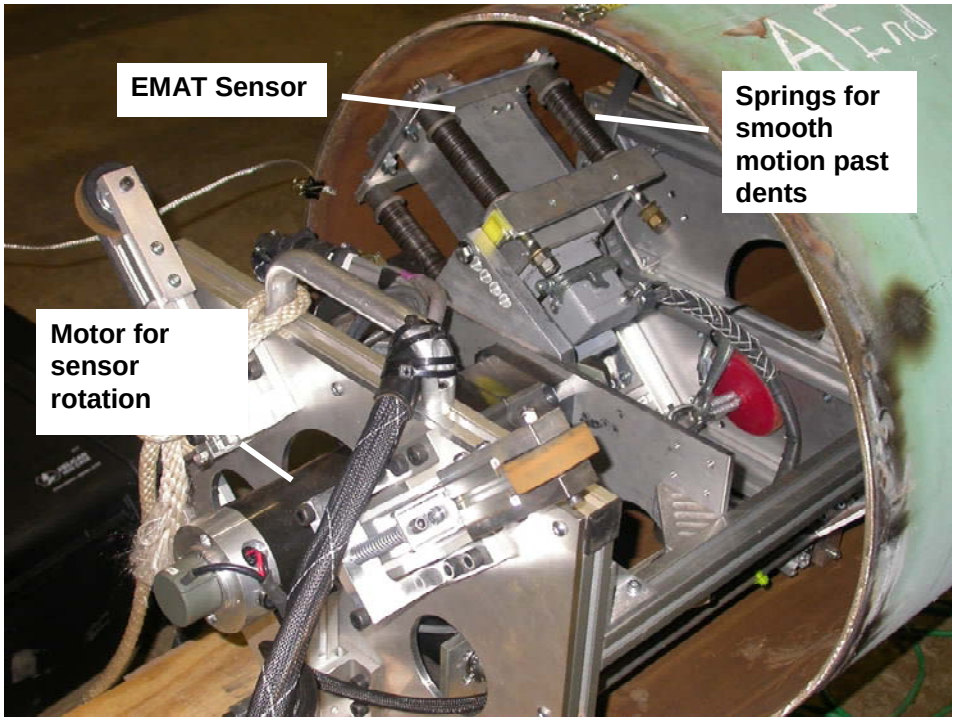

Figure 1. Photo of the ultrasonic sensor and scanning cart.

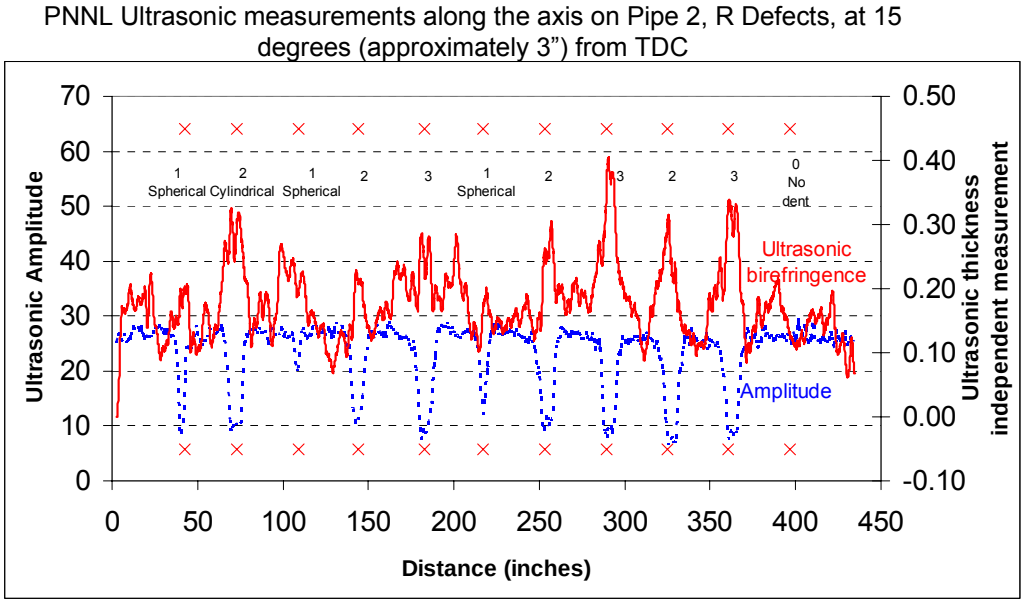

Figure 2. Amplitude and ultrasonic birefringence as a function of distance along pipe 2.

OAKRIDGE NATIONAL LABORATORY (ORNL)
COMMENTS ON PIPELINE INSPECTION TECHNOLOGIES DEMONSTRATION REPORT

This page intentionally blank

SCC detection using Shear Horizontal EMAT

Based on the results, we feel that the ORNL SCC detection system using shear horizontal wave EMAT detection has performed very well for the test conditions. In this response, we address areas pertaining to: training data issues, lack of data on SCC depth, additional defects along test line 1, and false positives. With these comments concentrating on issues where the results are in question, we would like to emphasis that the system performed very well for the test and addressing these issues will only improve or better clarify the results.

Training Data:

The current ORNL set-up for detecting SCCs with the shear horizontal wave EMAT uses transmitted signals to assess the presence of a crack. The signals from '*no-flaw'* regions are compared to the signals from *'flaw'* regions to identify cracks. The key issue in performing this measurement is the determination of features, derived from the response signals that separate *flawed* regions from those with *no flaws*. In the current algorithm, wavelet based features from both '*flaw'* and '*no-flaw'* regions are used to establish classes (SCC, no-flaw, other anomaly). Since this technology requires training data of known defect and no-defect regions, a 26" training pipe was provided in addition to the test pipe during our visit to the test facility. Unfortunately, we were unable to generate a proper training set from this test pipe due to the quality and the discrepancy in the location of the flaws. Instead, previous data collected from a 30" pipe for training were used. Although the mode frequencies were different for the 26" and 30" pipe due to change in wall thickness and pipe diameter the results were still satisfactory. This indicates a robustness of the training sets across pipe diameters and thicknesses. The system performance would have only improved had we used a training set generated out of similar pipe geometry.

SCC Depth Data:

Defect sizes were given in terms of length and area of crack on the pipe with no depth information. Liquid fluorescent magnetic particle inspection for detecting SCCs does not contain any information on the depth of the crack, while the EMAT based approach has a direct dependence on it. Hence, some very small cracks detected by magnetic particle method may not be detected by EMAT due to their depth being small. This is a possible reason for SSC2 not being detected. With the knowledge of SCC depth, we could have determined how well the system is able to detect the severity of the crack.

Additional Known Defects in Test Line 1:

In testing, we were instructed to test along three different lines of the test pipe to determine the presence of defects over particular spans along each line. Figure 1 shows the pipe layout for the test. Each test box (blue boxes labeled SCC1 – SCC14) along with every defect previously identified on the pipe (pink boxes labeled 4-9, 15-20) are pictured. The dashed lines represent the three scan lines. As mentioned in the results, the SCC defect we were to locate in SCC3 is defect 8 (far left side of box). However, we positioned this defect to the right by several inches. Since the EMATs scans an arc of ~12 inches around the circumference of the pipe, the SCC boxes within the figure have been drawn with 12 inch height to show the area covered by the sensor. From the figure, we see that defects 17, 18, and 19 are all on the upper edge of SCC3.

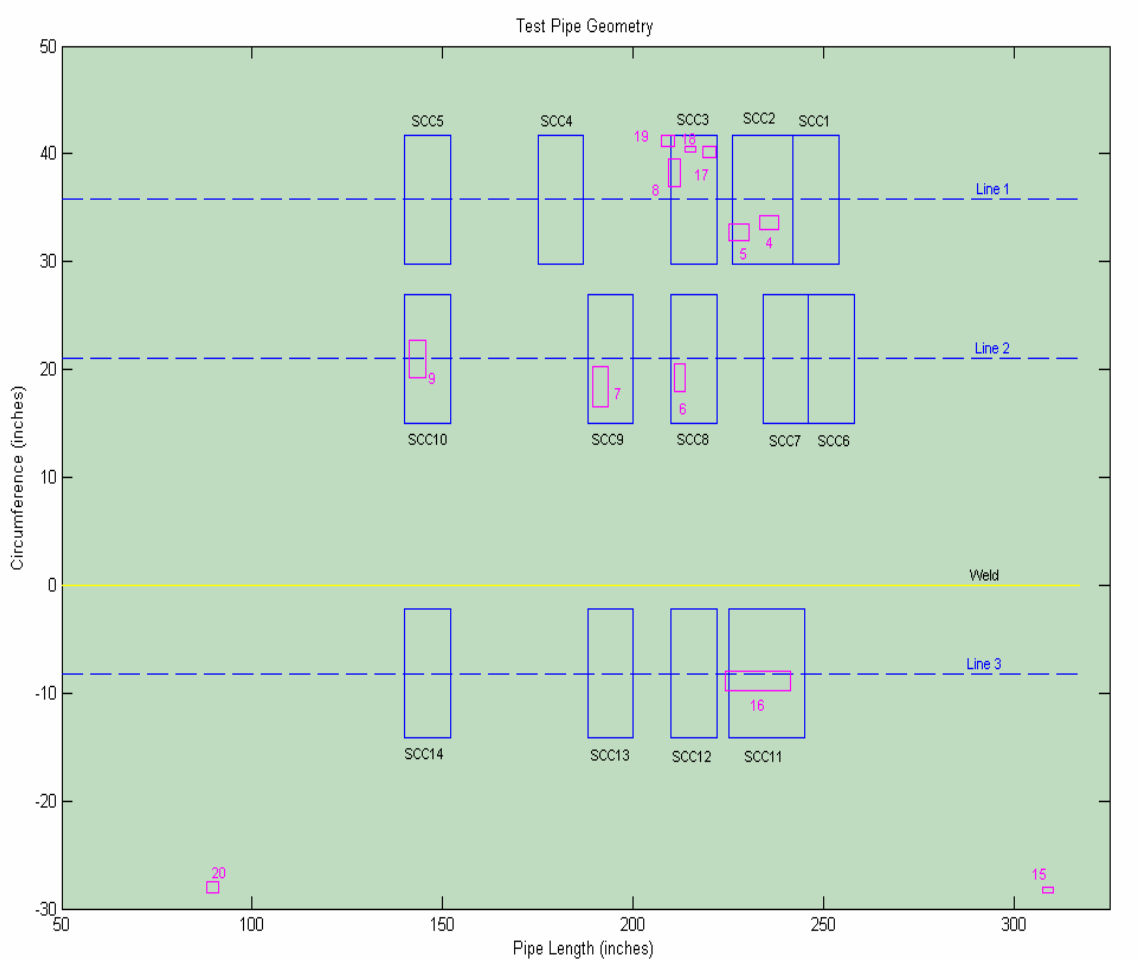

Figure 4. Test setup.

Our defect detection signal is essentially a distance measurement from the no-defect class within our feature space. This distance is pictured in Figure 2 for the SCC3 region. Red lines show boundary of box SCC3 and the approximate locations of defects 8, 17, 18, and 19 are shown in pink text. In our response to the test, we listed the defect in the SCC3 box based on the large signal that appears to correspond to defect 18 (a fairly large inclusion). From the signal, we do feel that we are seeing the intended defect 8 as well but did not list it due to its location straddling the boundary of the SCC3 region.

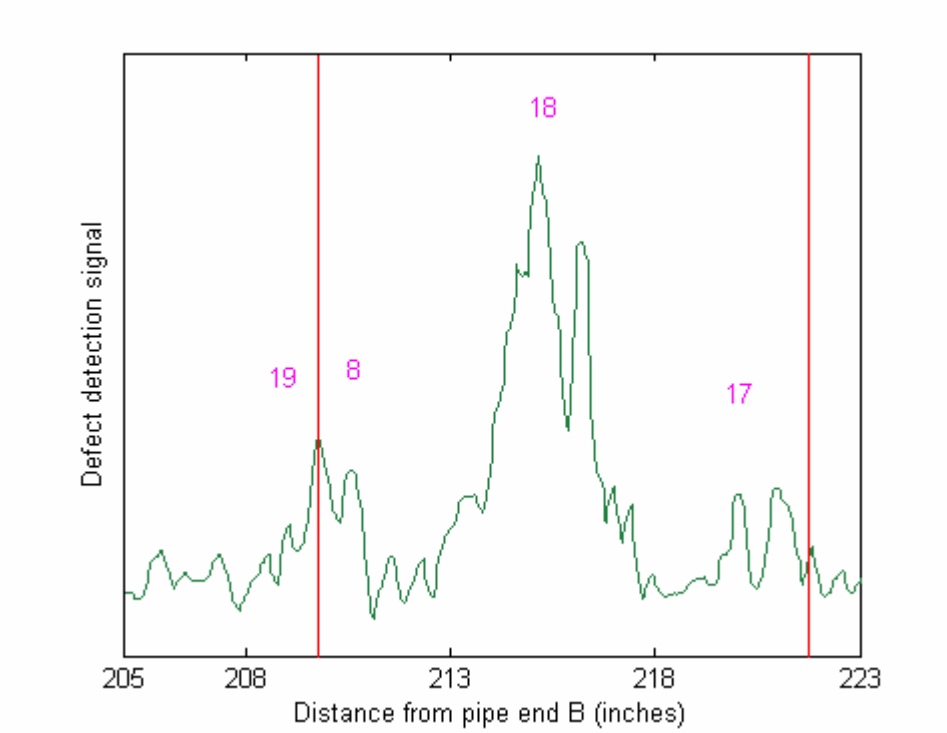

Figure 5. Defect response signal for SCC3 area.

False Positives:

As mentioned in the results, we also identified a false positive on each scan line. The EMATs did indicate flaws in areas where they were none, and this could be the result of not having the baseline data or the algorithm needing further refinement. Lack of good natural SCC data has been one of the difficulties we faced while developing this technology. We have created synthetic SCCs using electrical discharge machining (EDM), however, EDM machined SCCs do not give a signature truly characteristic of a natural SCC. Figure 3 shows the signals returned for the three false positives that have peaks similar to our previous experience with SCC signatures. Red lines delineate the regions of interest. The false positive on line 1 (Figure 3a) shows a series of peaks each similar in shape to an SCC response. The false positive in line 2 (Figure 3b) shows a well-isolated peak typical of an SCC response. The false positive in line 3 (Figure 3c) shows an SCC type response on the right side of SCC14 box. Similar bumps also can be seen near 160" mark but were not marked as SCCs due to the low dome shape of the response.

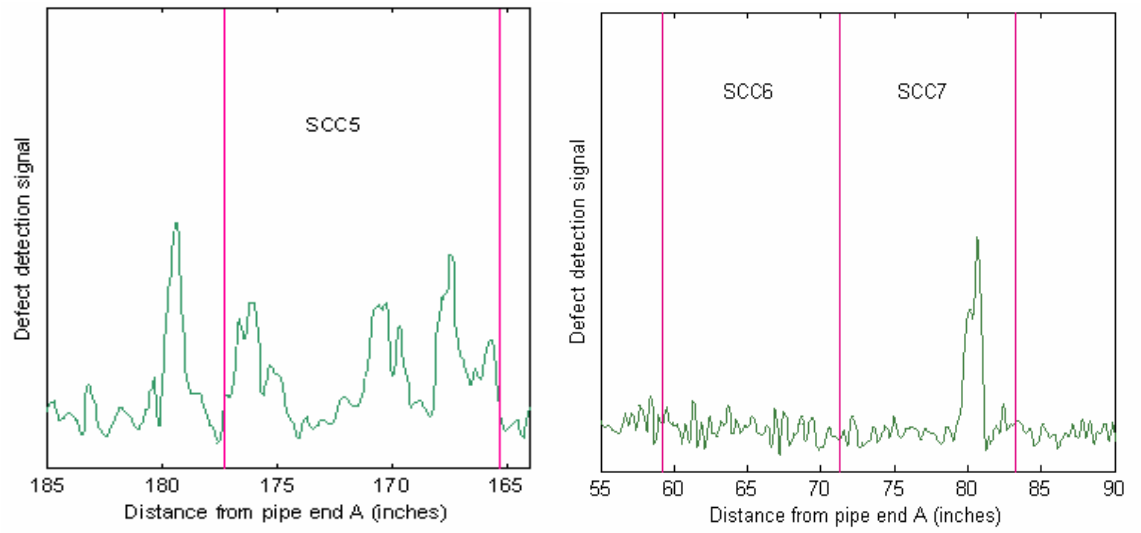

(a) **(b)**

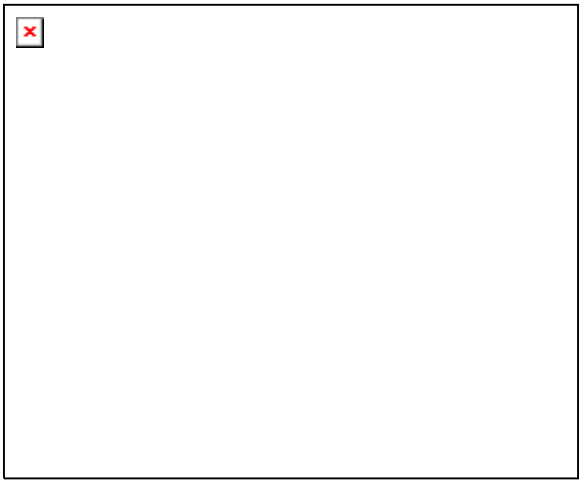

(c)

Figure 6. False positive signals for scan lines 1, 2 and 3 are shown in (a), (b) and (c) respectively

Conclusion:

As mentioned earlier, we feel the ORNL SCC detection system performed well in this test. Lessons learned from the tests are: 1) Training data may not be necessary for each pipe geometry being investigated, and 2) Information on SCC depth is needed to fully characterize the system performance. We feel that the system performance will continue to improve as more training data from natural SCCs are collected and used to train the algorithm.

NATIONAL ENERGY TECHNOLOGY LABORATORY (NETL) COMMENTS ON PIPELINE INSPECTION TECHNOLOGIES DEMONSTRATION REPORT

This page intentionally blank

Analysis of Sensor Benchmark Tests

Capacitive Sensor for Polyethylene Pipe Inspection

Prepared by:
James Spenik, Chris Condon, Bill Fincham, Travis Kirby
National Energy Technology Laboratory
3610 Collins Ferry Road
Morgantown, WV 26505

February, 15, 2006

This page intentionally blank

Introduction:

Representatives from the National Energy Technology Laboratory demonstrated polyethylene pipe inspection technology at Battelle's West Jefferson Pipeline Simulation Facility near Columbus, OH. The technology was demonstrated January 10 – 12, 2006 by James Spenik (REM), Chris Condon (REM), Bill Fincham (Parsons) and Travis Kirby (WVU).

Battelle provided a 13-foot length of 6-inch nominal diameter, 0.5-inch wall thickness polyethylene pipe. Holes and saw cuts were placed into the top outer surface of the pipe along an axial line. Twelve defects were placed within nineteen 6-inch long search regions. Eight of the regions did not contain a defect, one region contained two defects. The line of defects was covered thus the experimenters did not know their location when data was collected. However, a calibration defect was available whose characteristics and location was known to the experimenters.

The probe was able to identify the defect in every search region without false positives.

Technique:

Abnormalities in the pipe wall are determined by changes in the dielectric properties of the wall material. An electric field is projected through the pipe wall by the probe head (Fig. 1). The wall material behaves as the dielectric component of a capacitor. This arrangement formed the probe head of the sensor device. Since the dielectric constant of polyethylene is greater than that of air (or natural gas) an absence of material within the electric field will manifest itself as a decrease in capacitance.

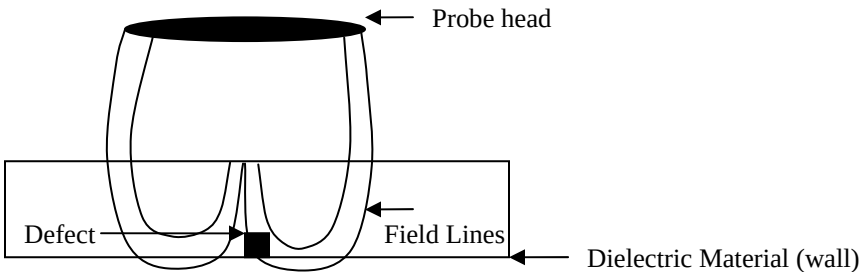

Figure 1 Projection of Electric Field through Pipe Wall

The probe head and associated electronics were mounted on a platform designed for this particular test (Fig. 2). The probe head was mounted 5.5 inches from the back circular disk of the 9.25-inch long platform. A 5.5 inch diameter disk was mounted at each end of the platform. In future use, the probe could be incorporated on existing platforms.

The platform was propelled through the pipe using a stationary stepper motor and nylon filament. An optical encoder was used to determine probe position within the pipe. Data were transmitted using RF transmission via Bluetooth technology. Another option would be to store the data onboard and retrieved at a later time. Power was supplied using an on-board 9-volt

battery. The data transmission rate for this particular demonstration was controlled by the optical encoder and stepper motor. Capacitance data were to be transmitted every forty counts of the optical encoder (0.09 inch axial movement) but this value may have varied a few counts. The stepper motor moved the platform at a rate of approximately 0.09 in/s. The sampling rate was approximately 1 Hz for this configuration due to the constraints previously mentioned. Thus the transit time through the pipe was approximately 15 minutes. However, the electronics package used is capable of transmission rates of between 45 – 90 Hz and modifications to the package would allow transmission rates in the MHz range.

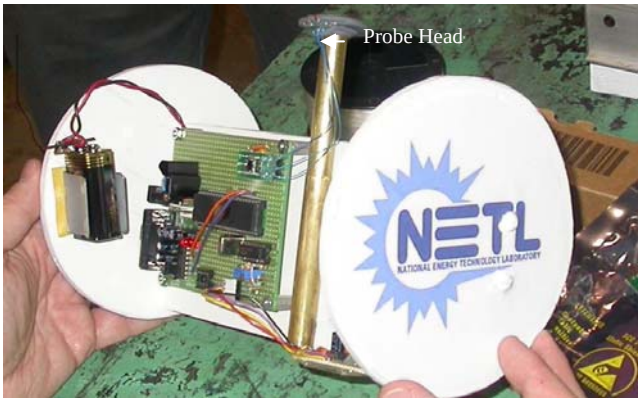

Figure 2 Platform with Probe Electronics

Data collection/analysis:

Twenty traverses were performed during the three days of data acquisition. The first ten were preliminary to identify problems. These difficulties were not related to the function of the pipe defect sensor but rather sensor movement. Initially, the optical encoder did not react to movement along the surface of the yellow polyethylene pipe. This was an unforeseen problem since, in an earlier test, the encoder reacted in black polyethylene pipe. The problem was resolved by placing a strip of material visible to the encoder on the interior lower surface of the pipe. Movement of the platform would be halted due to a slightly underpowered stepper motor. The edges of the platform disks were lubricated with graphite which minimized the problem. The deviation of the probe head from a linear path was minimized using guide line attached to the bottom of the pipe and through the bottom of both platform disks. These problems were identified and solved during the first ten traverses. Data from the second set of ten traverses were useful and provided data for statistical analysis.

Tests commenced with the rear disk approximately 1.5 inch from the “B” end of the pipe placing the sensor head at the 149 inch position of the 156 inch (13 foot) pipe (Fig. 3). Tests concluded with the probe head at the 7 inch position. Run11 – Run 20 were compiled to determine the position of anomalies within the polyethylene pipe.

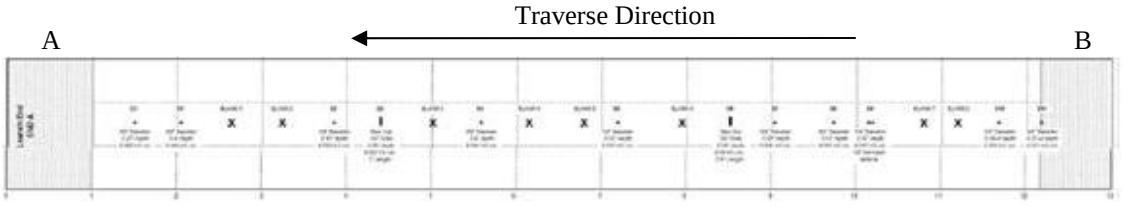

Figure 3 Path of Probe Through Pipe

The average number of data points accumulated for each run was 1619 points corresponding to a measurement for each 0.0877 inches of travel. However, this number varied between runs with a standard deviation of 46. These discrepancies can be attributed to either binding of the stepper motor or variations in the triggering level of the optical sensor. The focus of the research was creation of the probe; the platform was designed only after conformation of the teams' participation in the demonstration was received. Data were post processed to determine the exact position of each defect within each search region in the following manner:

1. Data were aligned so the minimum capacitance for each run near the calibration hole coincided. (Minimum capacitance corresponds to the center of the anomaly)

2. Since the total length of the traverse and the total number of data points were known, the ratio of these numbers yielded an initial estimate of step size for each run.

3. The data for each run was separated by search region.

4. The position and value of the minimum capacitance value within the search region for each run was determined.

5. The average position of the minimum within the region was determined.

6. Each run was realigned within the region so the minimum was located at the average minimum position.

This method was effective; however, cumulative error caused the position of the anomaly within a search region to be progressively misinterpreted. The measured position and actual position of the defect in search area D1 was at 25 inch, however, the actual position of the defect in search area D19 was 148" and the measured position was 146.8" Again, this is not due to sensor error but rather due to positioning error. All defects were identified with the exception of a binary defect (two holes separated by 0.5 inch on centers) located at position D15 which we identified as a single entity. The probe in its current configuration was not designed to separate binary anomalies separated by less than an inch.

Although it was not part of the benchmarking demonstration, an attempt was made to provide a comparative value of volume of material removed by the defect. Only moderate success was achieved in this endeavor. The reason that definitive volumetric values could not be determined was because the defects presented in the pipe could be considered to have three variables: diameter, depth and type (round hole or saw cut). Due to the nature of the electric field produced

by the probe, the depth and diameter cannot be combined into the single variable volume. Since the electric field strength diminishes as a function of distance from the probe head, a smaller volume closer to the probe head is seen as equivalent to a larger volume further away. The output from the current probe design yields two values: capacitance and change in capacitance with respect to axial position. Therefore there were three unknowns and only two equations and thus the volume of material removed was indeterminate. A future design of the probe allowing circumferential measurements will allow the development of an algorithm to define defect volume.

Figures 4 through 7 illustrate the typical probe response when a defect was encountered. Each figure compiles the ten runs taken within an eight-inch long region of interest. The abscissa is the variation from minimum capacitance within the region and the ordinate is the linear position. Figure 4 shows the calibration defect and the probe response. Figure 5 shows a typical response to a round defect and Figure 6 indicates the response to a saw cut. Figure 7 indicates the probe response in a region with no known defects. The presence of an anomaly typically produced a variation of 4000 aF. Variations in a region without defined anomalies were typically 500 aF.

Conclusion:

The probe successfully identified the position of all defects within the search regions and had no false positive results. Deviations from the precise position of the defects within the search region can be attributed to the means of locomotion and position identification procedures. The data acquisition rate can be markedly increased with a superior locomotion scheme. Further devlopment to this technology will produce a device that can be inserted into in situ natural gas pipelines and determine their integrity.

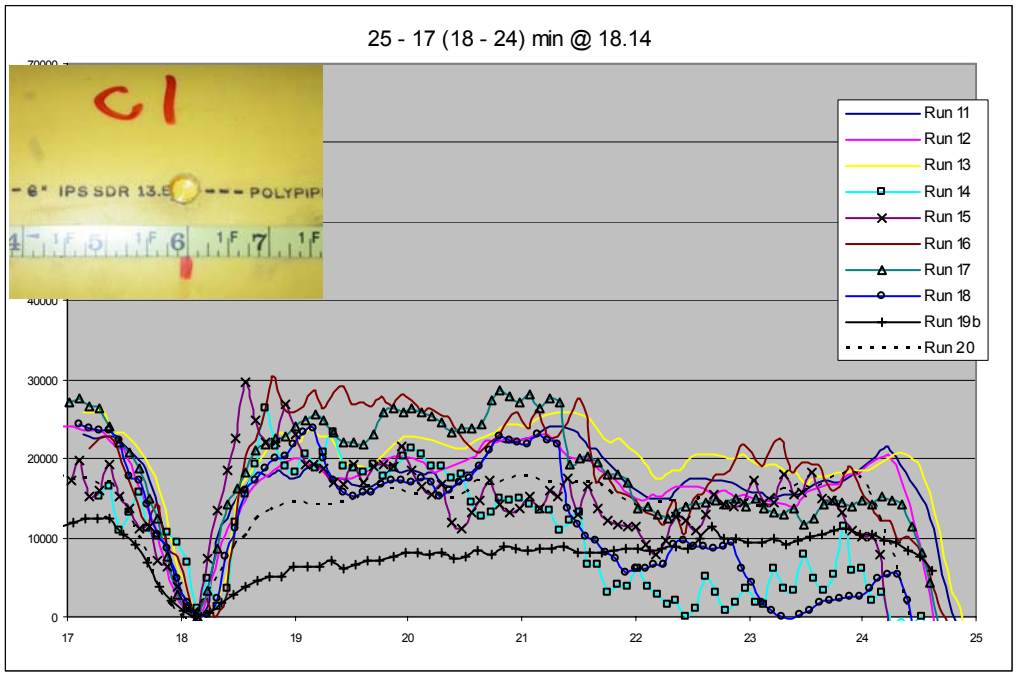

Figure 4 Calibration Hole and Probe Response (18” position)

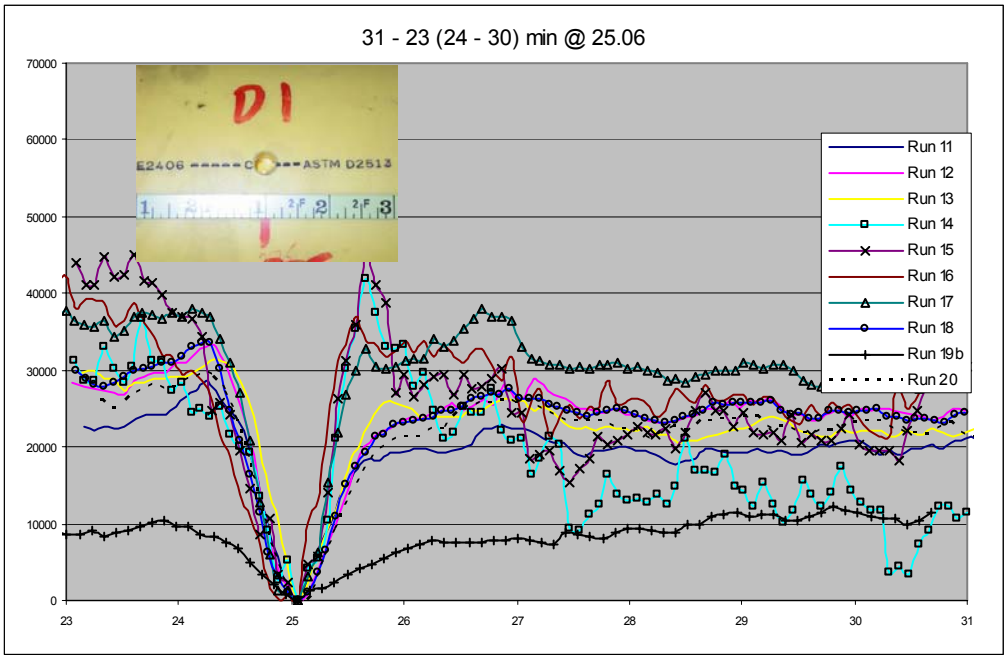

Figure 5 Round Hole Defect and Probe Response (25” position)

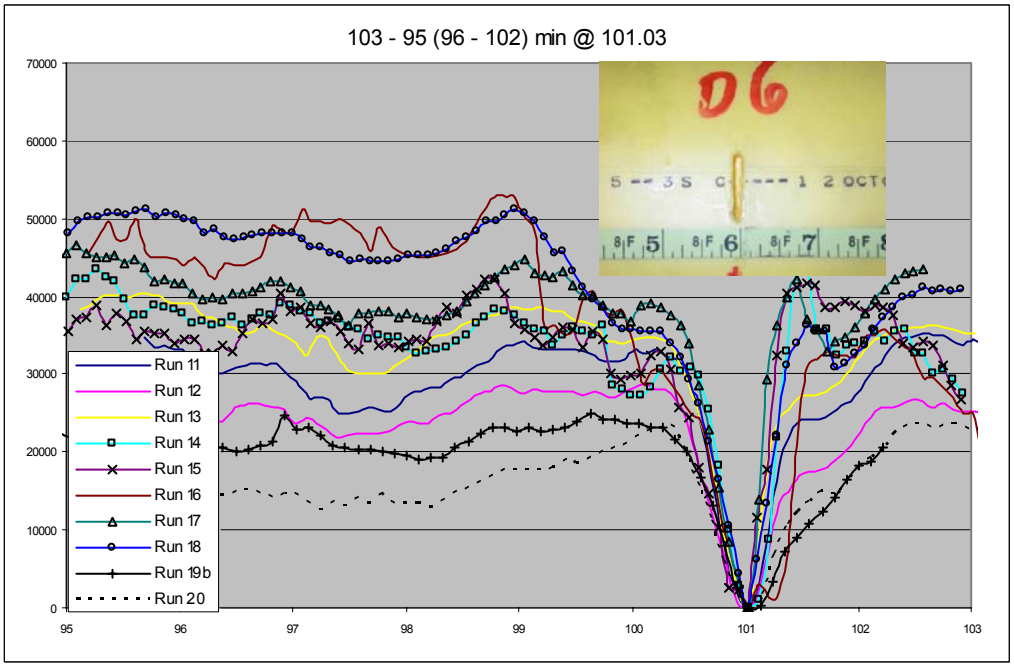

Figure 6 Saw Cut Defect and Probe Response (102” position)

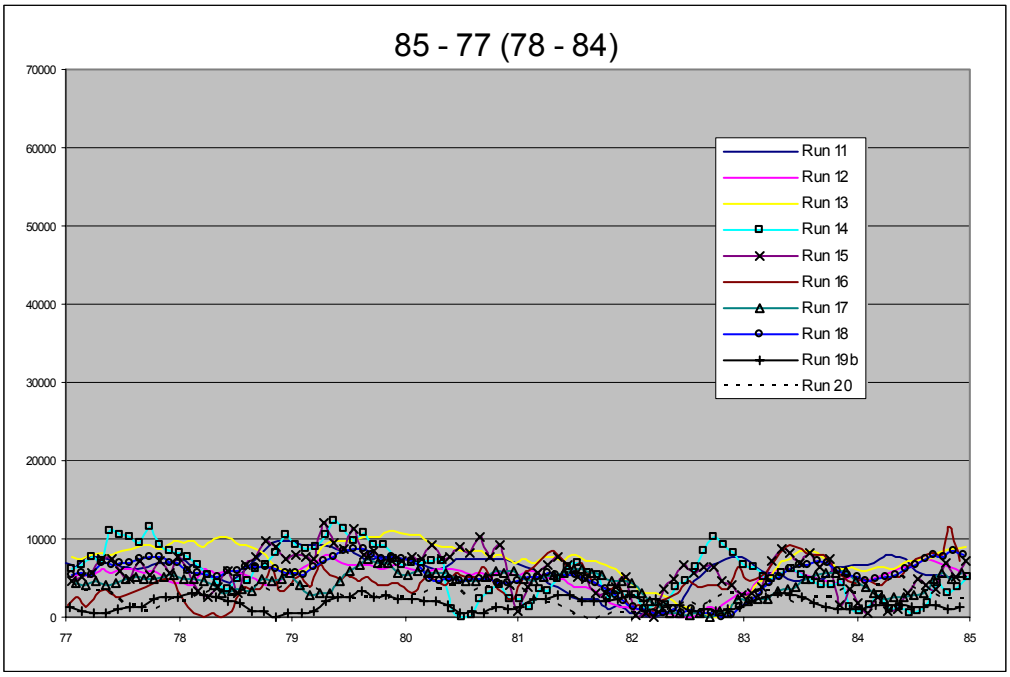

Figure 7 Probe Response with no Defect (102” position)